ROCK GLACIERS AND WATER SUPPLIES IN THE HIMALAYA

Submitted by Darren Brian Jones to the University of Exeter as a thesis for the degree of Doctor of Philosophy in Physical Geography, November 2019.

I certify that all material in this thesis which is not my own work has been identified and that any material that has previously been submitted and approved for the award of a degree by this or any other University has been acknowledged.

Signature: .....

For Katrina & Florence

ABSTRACT

The high-mountain cryosphere forms water towers that are important for ecosystem services provision, supplying large populations living in mountains and the surrounding lowlands and producing potable water resources, and water for agriculture, industry and hydropower generation. However, continued glacier recession and mass loss is projected throughout the twenty-first century, and this raises major concerns regarding the future sustainability of cryospheric water resources. While glacier meltwater represents an essential drought-resilient freshwater resource in vulnerable drought-prone regions, little research has focused on the contribution made by runoff from rock glaciers. These are located widely throughout the high-mountain cryosphere and estimates of rock glacier water volume equivalent (WVEQ) vs glaciers suggests that the former may constitute increasingly important long-term water stores. Owing to the insulating effects of thick supraglacial debris cover, rock glaciers are climatically more resilient than glaciers; therefore, their relative importance versus glaciers may increase under future climate warming. Yet, while the hydrological role of debris-free glaciers and debris-covered glaciers has been the subject of much research, that of rock glaciers has received comparatively little attention. Given the need for strong climate adaptation in many of the world's mountain regions, it is clear that a more comprehensive understanding of all components of the hydrological cycle in the high-mountain cryosphere is required.

In this thesis, I develop the scientific understanding of rock glacier significance in deglacierizing mountains across a range of spatial scales (local, national, regional and global), with a specific focus on High Mountain Asia (HMA). The review chapter critically assesses the state of current scientific knowledge regarding the hydrological role of rock glaciers in high mountain systems and serves to form the context for the empirical chapters. The thesis has three key themes to which the empirical chapters are aligned: (1) the distribution and hydrological significance of rock glaciers at global scales, (2) the distribution and hydrological significance of rock glaciers at regional and national spatial scales (Himalaya and Nepalese Himalaya), and (3) advancing rock glacier evolutionary theory.

(1) the thesis created a meta-analysis of existing systematic rock glacier inventories and compiled the first near-global rock glacier database (RGDB). The RGDB presented here includes >73,000 rock glaciers (intact = ~39,500, relict = ~33,500), which contain a WVEQ of 83.7 ± 16.7 Gt [~69–102 trillion litres]. Furthermore, the estimated ratio of rock glacier: glacier WVEQ is 1:456 globally.

(2) the results of the meta-analysis described in (1) show that only ~9% of studies included in the RGDB cover the Hindu Kush Himalaya (HKH); therefore, I produced the first systematic rock glacier inventory for the (i) Nepalese Himalaya (national-scale), and (ii) Himalaya (regional-scale). In the former (i) I inventoried >6,000 rock glaciers, and these are estimated to contain a WVEQ of 20.90 ± 4.18 km^3 (19.16 ± 3.83 Gt). For the Nepalese Himalaya estimated rock glacier: glacier WVEQ ratio is 1:9. In the latter (ii) ~25,000 rock glaciers have been inventoried. The total WVEQ is 51.80 ± 10.36 km^3 (47.48 ± 9.50 Gt) with an estimated rock glacier: glacier WVEQ ratio of 1:24. The results of Theme 1 and 2 indicate that rock glaciers form considerable long-term water stores, which may become increasingly important as climatically-driven glacier recession and mass loss continues throughout the twenty-first century and beyond.

(3) in order to understand debris-free glacier transition to rock glaciers I use *in situ* sedimentological data and kite aerial photography (KAP) data and develop a conceptual hypothesis to explain the key drivers of this process. The thesis suggests that sediment connectivity (i.e. the strength of the link between sediment sources and downslope landforms) is one such driver of these transition processes. As a consequence, I hypothesise that the presence of well-developed lateral moraines along glacier margins serves to reduce this connectivity, and thus reduce the likelihood of glacier-to-rock glacier transition occurring. The corelationships between rock glaciers and glacial, periglacial and paraglacial processes are also evaluated in the context of rock glacier origin and the changing influence these processes have upon rock glacier evolution through their lifecycle.

Collectively, this research has shaped the understanding of the current and potential future role of rock glaciers in mountain hydrology and is the first to comprehend the distribution and hydrological significance of rock glaciers globally and in the Himalaya.

LIST OF CONTENTS

LIST OF FIGURES

LIST OF TABLES

DECLARATION OF AUTHORSHIP

Chapters 4, 5, 6, 7, 8, and 9 have been published or written for publication as co-authored academic papers.

Published Papers

Chapter 4: Stephan Harrison (SH) conceived the concept for this chapter. The manuscript was based on a decade-old draft (research letter) written by SH and W. Brian Whalley (WBW). I led the writing of the manuscript and developed it using comments from SH, Karen Anderson (KA) and WBW.

Paper published as *Jones, D.B., Harrison, S., Anderson, K. and Whalley, W.B., 2019. Rock glaciers and mountain hydrology: A review. Earth-Science Reviews, 193: 66–90.*

Chapter 5: SH and KA conceived the concept for this chapter. I developed the methodology, conducted the meta-analysis to construct the RGDB, and analysed the data. I led the writing of the manuscript and developed it using comments from SH and KA. Richard Betts (RAB) commented on the final version.

Paper published as *Jones, D.B., Harrison, S., Anderson, K. and Betts, R.A., 2018. Mountain rock glaciers contain globally significant water stores. Scientific Reports, 8(1): 2834.*

Chapter 6: SH and KA conceived the concept for this chapter. I developed the methodology, compiled the rock glacier inventory and processed and analysed the data. Heather Selley digitised the randomly selected rock glacier sample. Joanne Wood prepared Figure 6.4–Figure 6.7. I led the writing of the manuscript and developed it using comments from SH and KA. RAB commented on the final version.

Paper published as *Jones, D.B., Harrison, S., Anderson, K., Selley, H.L., Wood, J.L. and Betts, R.A., 2018. The distribution and hydrological significance of rock glaciers in the Nepalese Himalaya. Global and Planetary Change, 160(Supplement C): 123-142.*

Chapter 8: Jasper Knight (JK) and SH conceived the concept for this chapter. JK led the writing of the manuscript. I contributed significantly to section 8.5 – *"Rock glaciers in the Himalayas: their classification and evolution"*. I designed all the fieldwork and processed and analysed the *in situ* data with advice from SH, and prepared Figure 8.2–Figure 8.6. The manuscript was further developed using comments from all authors.

Paper published as *Knight, J., Harrison, S. and Jones, D.B., 2019. Rock glaciers and the geomorphological evolution of deglacierizing mountains. Geomorphology, 324: 14-24.*

Chapter 9: SH conceived the concept for this chapter. I designed all the fieldwork with advice from SH and KA. I led the fieldwork campaigns with assistance from SH and KA. I processed and analysed the *in situ* data with guidance from SH and KA. I led the writing of the manuscript and developed it using comments from SH and KA.

Paper published as *Jones, D.B., Harrison, S. and Anderson, K., 2019. Mountain glacier-to-rock glacier transition. Global and Planetary Change, 181: 102999.*

Unpublished Papers

Chapter 7: SH and I conceived the concept for this chapter. I developed the methodology and created the systematic rock glacier inventory. I also processed and analysed the data. Figure 7.1 was kindly provided by Dr Sarah Shannon (University of Bristol). I led the writing of the manuscript and developed it using comments from SH and KA. N.B. this manuscript is currently being prepared for journal submission.

Additional Papers

I have contributed to other publications during my PhD research, in recognition of which I have been included as a co-author. These publications do not form part of this thesis but are related to my understanding of human-induced climate change impacts on high mountain systems in the study region (Anderson et al., 2019; Shannon et al., 2019; Parry et al., 2020), and are therefore listed below.

*Shannon, S., Smith, R., Wiltshire, A., Payne, T., Huss, M., Betts, R., Caesar, J., Koutroulis, A., **Jones, D.** and Harrison, S., 2019. Global glacier volume projections under high-end climate change scenarios. The Cryosphere, 13(1): 325-350.*

*Parry, L., Harrison, S., Betts, R., Shannon, S., **Jones, D.B.** and Knight, J., 2020. Impacts of climate change on Himalayan glaciers: processes, predictions and uncertainties. In: A.P. Dimri, B. Bookhagen, M. Stoffel and T. Yasunari (Editors), Himalayan Weather and Climate and their Impact on the Environment. Springer International Publishing, Cham, pp. 331–349.*

*Anderson, K., Fawcett, D., Cugulliere, A., Benford, S., **Jones, D.** and Leng, R., 2019. Vegetation expansion in the subnival Hindu Kush Himalaya. Global Change Biology: 1-18.*

ACKNOWLEDGEMENTS

I would firstly like to thank my supervisors Stephan Harrison and Karen Anderson for all their fantastic support, encouragement and guidance throughout my PhD. Your patience, stimulating discussions and good humour, even whilst suffering the effects of altitude (!), have made undertaking this PhD a genuinely enjoyable and hugely rewarding experience. A special thank you to Karen and Jamie Shutler for your friendship and support outside of PhD life, particularly when we welcomed Florence into the world. Hugely appreciated. I am grateful to both Liam Reinhardt and Neil Glasser for conducting my *viva voce*; your encouraging discussion, thoughtful questions and comments made for an interesting and enjoyable experience.

I would like to thank my friends across the Penryn campus for making this PhD experience all the more enjoyable. In particular, I owe huge thanks to James Duffy for your great friendship inside and outside the academic bubble. Your generosity with your time and knowledge, without which I would not have achieved as much during these last 4 years, is greatly appreciated. Your great company has helped to keep the PhD fun! I am also immensely thankful for the continued friendship of Jo Wood and Jon Bennie. The (numerous) coffee breaks, pub visits, beach trips, BBQs and general 'banter' has kept me sane during this PhD.

Dhananjay Regmi and the team at Himalayan Research Expeditions Ltd. are greatly thanked for providing organisational support during the fieldwork campaigns in Nepal. Mahesh Magar, Laxmi Kumar Kulung and Shankar Natshiring are especially thanked for their expert guidance, invaluable field assistance during data collection and friendly company. Thanks also to Scott Watson and Owen King for showing me the ropes and being excellent company during the first fieldwork season. The hospitality of countless others I met in Nepal is greatly appreciated.

I would like to acknowledge the Natural Environment Research Council (NERC GW4+ DTP) for funding my studentship. Also, thanks to the Royal Geographical Society (with IBG) for providing additional funds to support fieldwork.

I would like to thank my family for their continued love and support.

Finally, throughout this PhD I have had the unwavering support, patience and encouragement of my best friend. To Katrina, thank you for sharing this adventure with me.

TABLE OF ABBREVIATIONS

AL	Active layer
ANOVA	Analysis of variance
ARD	Acid rock drainage
DDA	Discrete debris accumulation
DEM	Digital elevation model
DSM	Digital surface model
EC	Electrical conductivity
ERT	Electrical resistivity tomography
GCP	Ground control point
GIS	Geographic Information System
GLIMS	Global Land Ice Measurements from Space
GPR	Ground-penetrating radar
HKH	Hindu Kush Himalaya
HMA	High Mountain Asia
I-DL	Ice-debris landform
InSAR	Interferometric Synthetic Aperture Radar
IQ	Insufficient quality
KAP	Kite aerial photography
KML	Keyhole Markup Language
LIA	Little Ice Age
MAAT	Mean annual air temperature
MaxE	Maximum elevation of the landform
MEF	Minimum elevation at the front
NSIDC	National Snow and Ice Data Center
PR	Permafrost region
PZI	Permafrost Zonation Index
RCP	Representative Concentration Pathway
RGDB	Rock glacier database
RGI	Randolph Glacier Inventory
RMSE	Root mean square error
RSF	Rock-slope failure
SfM-MVS	Structure-from-motion multi-view stereo
SLE	Sea-level equivalent
SNP	Sagarmatha National Park
SRTM	Shuttle Radar Topography Mission
SSC	Suspended sediment concentrations
TDS	Total dissolved solids
TU	Tritium Units
WVEQ	Water volume equivalent

1 INTRODUCTION AND RESEARCH CONTEXT

1.1 INTRODUCTION

The world's high-mountain cryosphere (i.e. snow, ice and permafrost) form natural 'water towers' that may constitute an important source of freshwater for downstream regions, particularly in arid and semi-arid zones (Messerli et al., 2004; Viviroli et al., 2007). Glacier- and snowpack-derived meltwaters contribute to streamflow in otherwise low-flow conditions during drier months and thus buffer hydrological seasonality (e.g., Kaser et al., 2010). Furthermore, in vulnerable drought-prone regions, glacial meltwater represents a uniquely drought-resilient water source (Bolch, 2017; Pritchard, 2019). In this context, the high-mountain cryosphere is crucial for ecosystem services provision (Grêt-Regamey et al., 2012), supplying multiple societal needs in mountain regions and the surrounding lowlands – potable water supplies, hydropower generation, industry and agriculture, for example (Immerzeel et al., 2010; Viviroli et al., 2011).

However, continued climate-induced glacier recession [and mass loss] throughout the twenty-first century is projected under a range of plausible emissions scenarios (Representative Concentration Pathways [RCPs]) (e.g., Kraaijenbrink et al., 2017; Hock et al., 2019a; Shannon et al., 2019) (**Figure 1.1**). A reasonable assumption considering elevation-dependent warming – rates of warming are amplified with increasing elevation – follows that it is probable that the high-mountain cryosphere will experience comparatively faster warming rates than low-altitude mountain ranges, particularly at low-latitudes (Vuille et al., 2008; Mountain Research Initiative, 2015). Indeed, Rabatel et al. (2013) report the complete loss of glaciers within certain low-latitude mountain ranges.

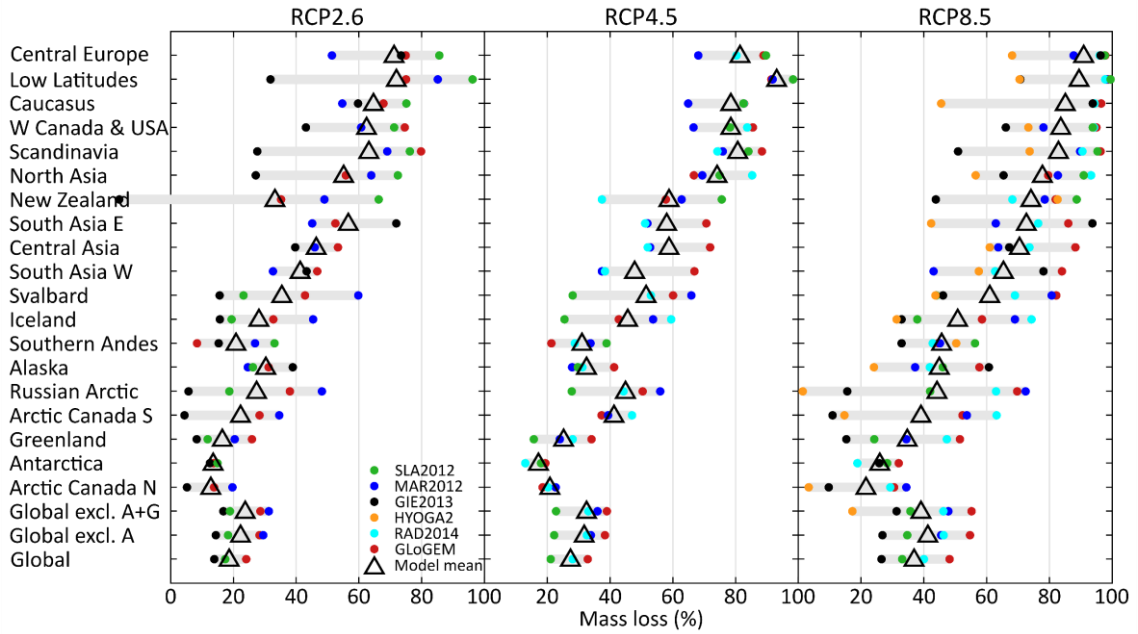

Figure 1.1. Projected glacier mass losses by 2100 (%) as a proportion of recorded glacier mass (reference year: 2015) for 19 Randolph Glacier Inventory (RGI) regions. Results were derived from six glacier models under three RCP emissions scenarios. Dots reflect the multi-GCM (General Circulation Model) means for each glacier model. Grey bars reflect the range of these results, and triangles show their arithmetic mean. Here, regional results are sorted according to the mean mass loss under RCP8.5. Furthermore, results are shown for (i) all regions combined (Global), (ii) all regions combined excluding the Antarctic periphery (A) and (iii) all regions combined excluding the Antarctic and Greenland periphery (A+G). N.B. not all glacier models compute all regions nor use all three emission scenarios. Figure after Hock et al. (2019a).

In the short-term, annual water release from long-term glacial storage increases; however, beyond 'peak water' enhanced melt rates are overwhelmed by glacier shrinkage, and projected glacier runoff gradually declines (Gleick and Palaniappan, 2010). Notably, recent global-scale projections for a number of glacierised macroscale (>5,000 km²) basins suggest that peak water has already been exceeded (Huss and Hock, 2018). A key message, therefore, is that glaciers are finite water stores (Jansson et al., 2003). Additionally, possible increases in the rain-to-snow fraction (Berghuijs et al., 2014), reductions in snow cover extent and/or longevity (Brown and Mote, 2009; Bavay et al., 2013; Zhou et al., 2017; Smith and Bookhagen, 2018), seasonal runoff maxima shifts towards earlier in the year (Hanzer et al., 2018; Huss and Hock, 2018) and widespread permafrost degradation (Haeberli, 2013; Biskaborn et al., 2019) will further diminish long-term runoff in snowmelt- and icemelt-dominated basins.

The anticipated effects of the above-described future decline of the high-mountain cryosphere may have severe implications for freshwater resources and their effective management (for summary see Beniston, 2003; Barnett et al., 2005; Bolch et al., 2012; Huss et al., 2017; Milner et al., 2017; Beniston et al., 2018). In consideration of climate change adaptation

strategies, a comprehensive understanding of all components of the hydrological cycle in the high-mountain cryosphere is vital. Yet, whilst the hydrological role of debris-free glaciers (see Fountain and Walder, 1998; Jansson et al., 2003; Irvine-Fynn et al., 2011) and debris-covered glaciers (Fyffe et al., 2019, and references therein) have been the subject of much research, that of rock glaciers – lobate or tongue-shaped landforms comprising a continuous, thick seasonally frozen debris layer (known as the active layer [AL]) covering ice-supersaturated debris or pure ice, which slowly creep downslope (see Martin and Whalley, 1987; Barsch, 1996; Haeberli et al., 2006; Berthling, 2011) – has received comparatively little attention (Duguay et al., 2015).

Found ubiquitously throughout the high-mountain cryosphere worldwide (Harrison et al., 2008), estimated rock glacier WVEQ vs glaciers suggests they may constitute non-negligible long-term water stores, notably in arid and semi-arid zones where glaciers have limited presence or are absent (e.g., Azócar and Brenning, 2010; Rangecroft et al., 2015; Munroe, 2018; Schaffer et al., 2019). A considerable number of published rock glacier inventories have been compiled in various mountain ranges (see Chapter 3). Yet, no global-scale (complete) inventory has been constructed to date, despite being described as the "most pressing need" in rock glacier research (Janke et al., 2013). In response, significant recent research efforts have greatly elaborated inventory coverage in the succeeding years, for example in South America (Falaschi et al., 2014; Rangecroft et al., 2014; Falaschi et al., 2015; Falaschi et al., 2016; Azócar et al., 2017; Barcaza et al., 2017; Esper Angillieri, 2017; García et al., 2017; Janke et al., 2017; IANIGLA-CONICET, 2018; Selley et al., 2018), North America (Charbonneau and Smith, 2018; Munroe, 2018), Central Europe (Colucci et al., 2016; Kellerer-Pirklbauer et al., 2016; Roudnitska et al., 2016; Salvador-Franch et al., 2016; Triglav-Čekada et al., 2016; Winkler et al., 2016a; Onaca et al., 2017; Palma et al., 2017; Uxa and Mida, 2017; Fernandes et al., 2018; Popescu, 2018; Boccali et al., 2019), Asia (incorporating Central Asia, South Asia [East], South Asia [West] and North Asia) (Bolch and Gorbunov, 2014; Schmid et al., 2015; Lytkin and Galanin, 2016; Galanin, 2017; Wang et al., 2017; Ran and Liu, 2018; Blöthe et al., 2019; Pandey, 2019; Baral et al., in press), Antarctic and Subantarctic (Rudolph et al., 2018) and New Zealand (Sattler et al., 2016). Notably, however, relatively few systematic rock glacier inventory publications estimate WVEQ. Furthermore, notwithstanding improved systematic rock glacier inventory coverage (cited above), data-deficient regions remain evident within the world's high-mountain cryosphere (e.g., Central Asia). The aforementioned knowledge gaps

prevent the full assessment of rock glacier frequency, distribution and morphometric characteristics, and thus their fundamental hydrological value (WVEQ).

While rock glacier-related research has accelerated during the recent decades (see **section 4.2**), the role of these landforms in the (i) hydrology and (ii) morphological evolution of deglacierizing mountains has hitherto not been fully recognised (Knight et al., 2019).

Regarding (i), owing to the insulating effect of the AL, rock glaciers have retarded ice melt as their internal thermal regimes are at least partially decoupled from external micro- and meso-climates during the summer months (Juliussen and Humlum, 2008; Millar et al., 2013). It is, therefore, reasonable to assume that rock glaciers are comparatively climatically-resilient vs debris-free glaciers [and debris-covered glaciers to a lesser extent] (Anderson et al., 2018), and prolong long-term water storage in the high-mountain cryosphere. Notably, rock glaciers, therefore, are long-term water stores and thus may not constitute a readily available potable supply (Duguay et al., 2015; Rangecroft et al., 2015). At decadal and longer timescales under climate warming, however, it is anticipated that the hydrological contribution from rock glaciers to alpine streamflow will increase considerably (Thies et al., 2013; Geiger et al., 2014; Brighenti et al., 2019). Of note, a general lack of consensus concerning the present and future hydrological significance of rock glaciers pervades the literature (Duguay et al., 2015). With regards to rock glacier-catchment interactions, published studies suggest that rock glaciers may become increasingly important in shaping the properties of water bodies located downstream and alpine streams; discharge (timing, magnitude and duration) (Mateo and Daniels, 2019, and references therein), hydrochemistry (Colombo et al., 2018b, and references therein) and hydroecology, for example (Brighenti et al., 2019, and references therein). Importantly, the degree of activity of rock glaciers influences considerably their water storage and release behaviours – *active rock glaciers* contain ice and display movement, *inactive rock glaciers* contain ice but no longer display movement, and *relict rock glaciers* no longer contain ice nor display movement (Haeberli, 1985; Barsch, 1996). Indeed, as a consequence of degradation of ice subjacent to the AL, rock glacier feature porosity and thus storage capacity may potentially increase. In turn, this will promote changes in the rock glacier discharge pattern and influence runoff generation strongly in alpine catchments (e.g., Wagner et al., 2016; Winkler et al., 2016b; Rogger et al., 2017).

Regarding (ii), glacier recession in response to climate warming elicits a paraglacial (i.e. landscape relaxation) response whereby glaciers are undergoing a transition to rock glaciers (e.g.,

Monnier and Kinnard, 2015b; Seppi et al., 2015; Monnier and Kinnard, 2017). Considering the above-described insulative and damping effects of debris cover (i.e. an AL), glacier-rock glacier interactions – e.g., large glacier-rock glacier composite features, that comprise debris-covered glaciers and rock glaciers in their upper and lower parts, respectively – arguably have important hydrological implications for high mountain systems and the surrounding lowlands. Further, throughout the twenty-first century, moreover, continued climate-driven deglaciation and the associated shift from glacial- to paraglacial-dominated process regimes is likely to increase the frequency with which glacier-to-rock glacier transition occurs (Knight et al., 2019). Importantly, however, significant unknowns remain regarding: (1) how glacier-to-rock glacier transition occurs and how quickly, (2) which glaciers are liable to undergo this transition, (3) the factors (geomorphic, climatic etc.) driving this process and (4) the consequential water supply implications. Furthermore, a long-standing academic debate regarding rock glacier origin pervades the literature (see Barsch, 1977, 1987, 1996; Whalley and Martin, 1992; Hamilton and Whalley, 1995; Clark et al., 1998; Whalley and Azizi, 2003; Haeberli et al., 2006; Berthling, 2011) (see **section 4.3.2**) and forms the backdrop for this research focus.

1.2 REGIONAL SETTING

In this thesis, rock glaciers are investigated at global, regional (Himalaya), national (Nepalese Himalaya) and local (Khumbu Valley, Sagarmatha National Park [SNP], Nepal) spatial scales (**Figure 1.2**). In spite of improved systematic rock glacier inventory coverage (**section 1.1**), the Himalaya region remains comparatively data-deficient. No complete systematic rock glacier inventory exists within the study region. Across HMA[1], with the exceptions of Blöthe et al. (2019), Pandey (2019) and Baral et al. (in press), rock glacier-related research has been conducted at relatively small spatial scales or are incomplete inventories (e.g., Gorbunov et al., 1992; Jakob, 1992; Barsch and Jakob, 1998; Gorbunov et al., 1998; Owen and England, 1998; Shroder et al., 2000; Ishikawa et al., 2001; Regmi, 2008; Bolch and Gorbunov, 2014; Schmid et al., 2015). The hydrological role of rock glaciers in the study region, therefore, is largely unknown.

[1] The HMA region includes the Central Asia, South Asia East and South Asia West RGI regions (see **Supplementary Figure 12.2**).

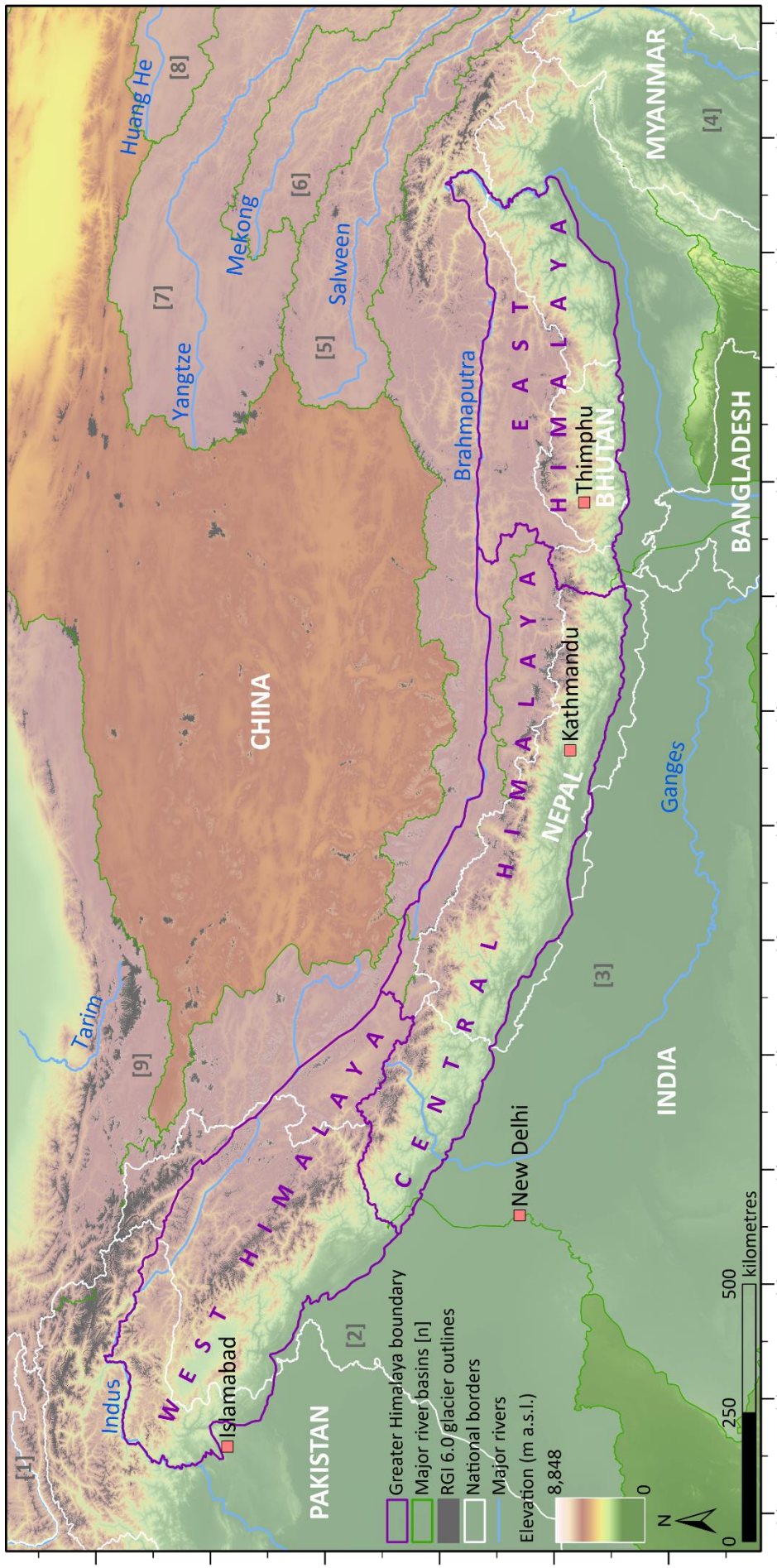

Figure 1.2. Topographic map of the Himalaya region showing the major river basin boundaries: [1] Amu Darya; [2] Indus; [3] Ganges; [4] Brahmaputra; [5] Salween; [6] Mekong; [7] Yangtze; [8] Yellow; and [9] Tarim. N.B. definitions of the extent of sub-regions (i.e. West, Central and East Himalaya) are taken from Bolch et al. (2012).

1.2.1 THE HIMALAYA

The Himalaya form a north-west to south-east arc across latitudes from ~26°N to ~37°N, stretching some 2,500 km through northern Pakistan, northern India, Nepal, Bhutan and China. Forming part of the "Asian Water Towers" (Immerzeel et al., 2010), this region contains a glacierised area of ~22,800 km² (Bolch et al., 2012). The Himalaya are divided into three overarching regions – the West Himalaya, Central Himalaya and East Himalaya (ibid.). Within the catchments of the Indus, Ganges and Brahmaputra rivers ~900 million people depend upon glacier and snowpack meltwater to varying degrees, particularly during dry seasons and in mountain valleys (Center for International Earth Science Information Network - CIESIN - Columbia University, 2018). Furthermore, ecosystem services (e.g., water, food, energy) provided by the Himalaya directly sustain the livelihoods of >200 million people residing in the mountains and foothills (Sharma et al., 2019).

The climate of the Himalaya is strongly influenced by the varying dominance of the East Asian and Indian monsoon systems and winds from the west (Bookhagen and Burbank, 2010; Scott et al., 2019). In the eastern Himalaya, monsoon-derived precipitation falls predominantly (>80%) between June to September (Bookhagen and Burbank, 2010). Precipitation in the north-western Himalaya is dominated by westerlies, where much of the annual high-altitude precipitation occurs during the winter months (ibid.). In excess of 50% of the total annual precipitation in the Karakoram and western Himalaya is delivered by fewer than ten extratropical cyclones (winter westerly disturbances [see Dimri et al., 2015]) that propagate eastwards each winter season (Lang and Barros, 2004; Barlow et al., 2005; Bookhagen and Burbank, 2010; Cannon et al., 2015). A strong south to north precipitation gradient exists across the Himalaya, from the Ganges plains and Himalayan foothills to the Tibetan Plateau (Kansakar et al., 2004; Bookhagen and Burbank, 2006, 2010). As a consequence, total precipitation ranges between 2,000–5,000 mm yr^{-1} in the Arunachal Pradesh region of India (south-eastern Himalaya) (Dhar and Nandargi, 2004) to >100 mm yr^{-1} in the Ladakh region (north-western Himalaya) (Schmidt and Nüsser, 2012). In the latter (north-western Himalaya), therefore, glacier meltwaters are important for reliable water supplies, particularly during drought summers (Pritchard, 2019).

Recent estimates of glacier ice volume across the Himalaya range between 1,237 and 1,909 km³ (Frey et al., 2014). Across HMA, glaciers have predominantly experienced mass loss (Bajracharya et al., 2015), with estimated glacial mass change rates of -26 ± 12 Gt yr^{-1} (2003–2009) (Gardner et al., 2013). Further considerable glacier mass loss in HMA throughout the

twenty-first century is projected under a range of plausible emissions scenarios (e.g., Huss and Hock, 2015; Kraaijenbrink et al., 2017; Hock et al., 2019a; Shannon et al., 2019). Notably, changes within HMA are not confined to glaciers-only; an overall decrease in snow water equivalent has been reported, particularly during spring (MAM) and summer (JJA), for a number of catchments in HMA (Smith and Bookhagen, 2018). The ongoing decline of HMA's cryosphere may have strong implications for downstream water supply (Immerzeel et al., 2010; Bolch et al., 2012; Lutz et al., 2014; Pritchard, 2019), particularly following peak water. For the mid-range emissions scenario (RCP4.5), most basins fed by HMA glaciers are projected to reach peak water by ~2050 – 2045 ± 17 years (Indus), 2044 ± 21 years (Ganges) and 2049 ± 18 years (Brahmaputra), for example (Huss and Hock, 2018).

1.2.2 THE NEPALESE HIMALAYA

Positioned within the Himalaya, Nepal is situated between the latitudes of 26°22' to 30°27' N and longitudes of 80°04' to 88°12' E and extends some 800 km east to west and an average ~140 km north to south. Encompassing an area of 147,181 km², Nepal is divided into five principal physiographical regions: Terai Plain, Siwalik Hills, Middle mountains, High mountains (inclusive of the Main Himalayas and the Inner Himalayan valleys), and the High Himalaya (see Shrestha and Aryal, 2011). In this thesis, research was primarily confined to the High Himalaya as this is where the majority of the permafrost region is found. Encompassing the area ≥4,000 m a.s.l., this region is characterised by extremely rugged terrain and is home to eight of the ten highest peaks in the world. Furthermore, ~3,800 glaciers covering ~3,900 km² (~3%) of the total area of Nepal are primarily situated within this physiographic region (Bajracharya and Shrestha, 2011). The snowline altitude is ~5,000 m a.s.l. (Shrestha and Joshi, 2011) with ~14,200 km² (~10%) of the total area of Nepal located above this elevation.

Due to the topographical extremes of the High mountains and High Himalaya, the climate type ranges from subtropical in the south to arctic in the north. The Asian summer monsoon dominates the climate of Nepal, providing most of the precipitation during June–September (Shrestha and Aryal, 2011); dependent on the location, ~80% of annual precipitation may occur within this period (Shrestha, 2000). Winter and spring precipitation predominantly falls as snow, forming snowpack stores that provide critical meltwater during the dry season (February–April). Alongside snowpack melt, glacier-derived meltwater contributions are important for maintaining the perennial flow of the major rivers in Nepal and also the Ganges in India (Shrestha and Aryal, 2011). Consequently, projected reductions in glacial coverage under

climate change, compounded by poor infrastructure and high population growth (Udmale et al., 2016), will have regional consequences for water resource availability (Shrestha and Aryal, 2011).

1.2.3 THE KHUMBU VALLEY

Located in the SNP, north-western Nepal, the Khumbu Valley (27°56'N, 86°49'E) encompasses some of the world's most striking peaks – Mount Everest (8,848 m a.s.l.), Mount Lhotse (8,516 m a.s.l.) and Mount Nuptse (7,861 m a.s.l.). This study region contains a number of landforms from across the spectrum of the glacial-paraglacial-periglacial landscape continuum within a relatively small spatial area. Dominating the Khumbu Valley, the ~15.7 km long Khumbu Glacier emerges from the Western Cwm and flows between the aforementioned peaks via the Khumbu Icefall, terminating at ~4,900 m a.s.l. The lowermost ~8 km of the glacier is debris-mantled, with debris thickness increasing towards the glacier terminus and reaching several metres (Nakawo et al., 1986). The debris-covered glacier tongue is characterised by a very low gradient, with the lowermost 3–4 km believed to be flowing at velocities <10 m a^{-1} (i.e. stagnant) (Hambrey et al., 2008; Quincey et al., 2009), and a pair of prominent lateral moraines dating from the Little Ice Age (LIA) (Rowan, 2017). Lobuche Glacier on the western side of Khumbu Glacier is smaller and encompasses a relic debris-mantled ablation zone ~1 km in length that is disconnected from the clean-ice accumulation zone (Watson et al., 2018). The eastern valley side (Pokalde Massif) is characterised by a number of rock glaciers, two of which – Lingten and Pokalde – are investigated in this thesis. Chola Glacier, believed to be a glacier-rock glacier composite landform (Knight et al., 2019), is located beyond the terminus of Khumbu Glacier beneath Mount Taboche (6,542 m a.s.l.) and Mount Cholatse (6,440 m a.s.l.) and flows ~3 km to ~4,400 m a.s.l.

The regional climate is dominated by the East Asian and Indian monsoon systems, with data from the PYRAMID Observatory Laboratory (hereafter: PYRAMID) near Lobuche (5035 m a.s.l.) indicating that 90% of annual precipitation falls during June-September (Bollasina et al., 2002; Salerno et al., 2015). Also, instrumental records reflect a topographically-driven steep precipitation gradient, with pronounced south (Chaurikharka [~2,600 m a.s.l.]: 2,418 mm yr^{-1}) to north (PYRAMID: 449 mm yr^{-1}) reduction in precipitation within the SNP (Salerno et al., 2015). Mean annual air temperature (MAAT) at the PYRAMID (1994–2012) was -2.4 °C, and mean temperature above 5,000 m a.s.l. is increasing by 0.044 °C yr^{-1} (ibid.). Seismic refraction studies conducted on four rock glaciers in the study region indicate that the regional lower

limit of discontinuous permafrost is situated at ≃5,000–5,300 m a.s.l. (Jakob, 1992); The detailed bedrock geology of the Everest Massif has been described (see Searle et al., 2003).

2 RESEARCH AIMS

This thesis aims primarily to review and extend scientific knowledge of the role of rock glaciers in mountain hydrology through advancing the understanding of their frequency, spatial distribution, hydrological importance and evolutionary pathways (e.g., glacier-to-rock glacier transition). This aim is addressed through three interrelated themes:

Theme 1. The hydrological role and importance of rock glaciers globally.

For high mountain systems at the global-scale, characterise

i. The hydrological role played by rock glaciers, and

ii. The water equivalent volume (WVEQ) stored in rock glaciers

Theme 2. Rock glacier distribution and hydrological significance in the Nepalese and Himalaya.

Address the paucity of data regarding the distribution and hydrological significance of rock glaciers at

i. A national spatial scale – The Nepalese Himalaya, and

ii. A regional spatial scale – The Himalaya

Theme 3. Advancing rock glacier evolutionary theory.

Advance the understanding of rock glacier evolution, particularly in deglacierizing mountains, by

i. Considering firstly the evolution of rock glaciers over time and space, and secondly their relationships with other mountain landforms, and

ii. Developing a conceptual hypothesis for glacier-to-rock glacier transition

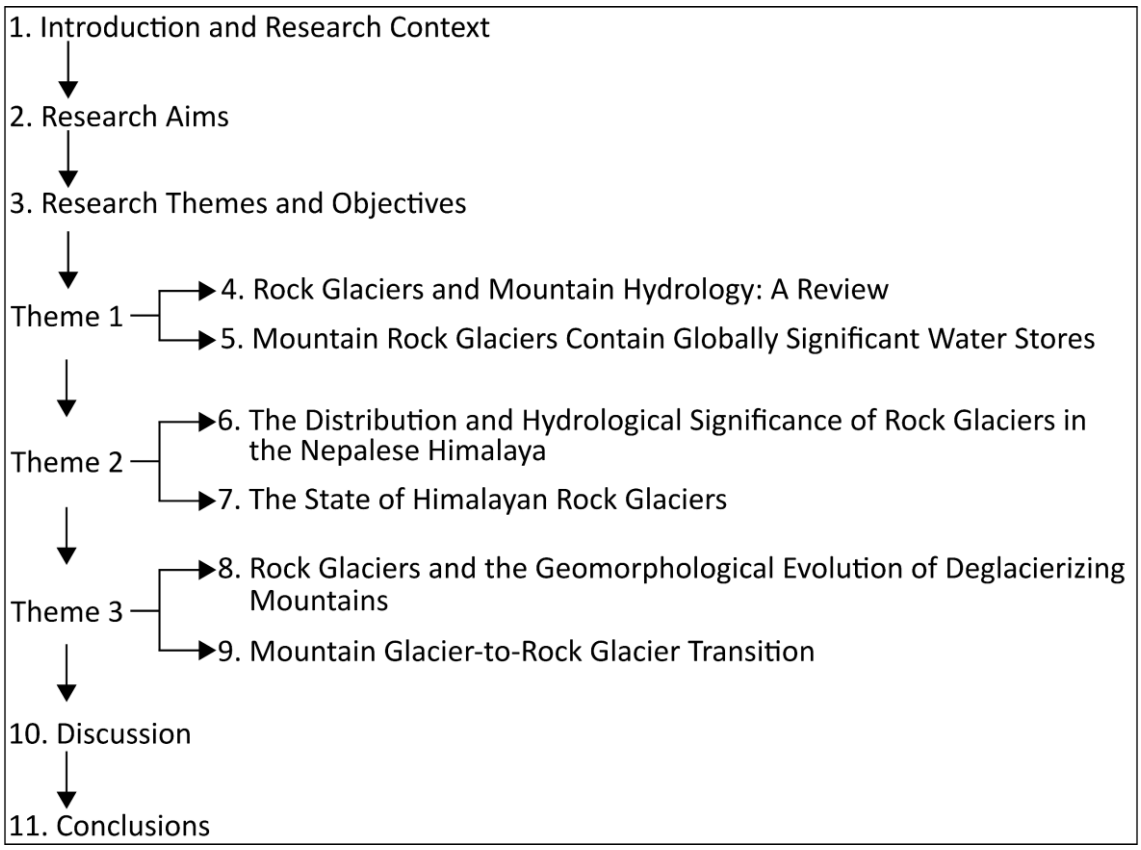

Figure 2.1. Schematic of the thesis structure (numbers correspond to the thesis chapters).

3 RESEARCH THEMES AND OBJECTIVES

3.1 THEME 1: RATIONALE AND OBJECTIVES

The high-mountain cryosphere forms an integral element of global high mountain systems, within which ~10% (671 million people) of the global population reside. Human-induced climate change threatens these natural 'water towers', affecting human systems in mountains and the surrounding lowlands (see Beniston, 2003; Huss et al., 2017; Milner et al., 2017). Rock glaciers are reportedly climatically more resilient than debris-covered glaciers and glaciers and contain potentially hydrologically valuable ice volumes, and yet to date have received considerably less research attention (Duguay et al., 2015). There exists a need, therefore, to synthesise and evaluate published articles regarding the hydrological role of rock glaciers in high mountain systems. In this thesis, Chapter 4 serves as a detailed literature review.

Objectives [Chapter 4]

- Review and assess the state of current scientific knowledge about the hydrological role and contribution of rock glaciers in mountain regions, and signpost towards critical future directions for rock glacier hydrological research.

Key to understanding the global and regional hydrological implications of rock glaciers is quantifying their WVEQ at the global and regional spatial scales. Considerable recent research efforts have greatly elaborated the spatial coverage of systematic rock glacier inventories; however, as yet no global-scale (complete) inventory has been compiled, despite previously being described as the "most pressing need" in rock glacier research (Janke et al., 2013). Furthermore, few existing published articles have assessed the WVEQ of rock glaciers.

Objectives [Chapter 5]

- Conduct a meta-analysis of existing systematic rock glacier inventories globally and compile the first global-scale rock glacier database (RGDB), in order to
  i. Calculate the WVEQ stored in rock glaciers at global and regional spatial scales.
  ii. Assess rock glacier and glacier WVEQ at global and regional spatial scales.
  iii. Identify key data-deficient regions as future research priorities.
- Make the RGDB open-access to encourage further data sharing and inventory standardisation within the rock glacier research community*.

*N.B. this objective feeds directly into the objectives of the International Permafrost Association Action Group (2018–2020) – *Rock Glacier Inventories and Kinematics* (for further information see https://www3.unifr.ch/geo/geomorphology/en/research/ipa-action-group-rock-glacier/).

3.2 THEME 2: RATIONALE AND OBJECTIVES

In HMA, continued climate-induced glacier recession [and mass loss] throughout the twenty-first century is projected under a range of RCPs (e.g., Kraaijenbrink et al., 2017; Hock et al., 2019a; Shannon et al., 2019). For the 800 million people dependent at least in part on meltwater from them (Pritchard, 2019), the anticipated effects of continued glacier recession will have serious implications (see Beniston, 2003; Huss et al., 2017; Milner et al., 2017). Bolch et al. 's (2012) review – "The State and Fate of Himalayan Glaciers" – and (2019b) assessment – "Status and Change of the Cryosphere in the Extended Hindu Kush Himalaya Region" – synthesise and evaluate the state of knowledge regarding changes in the high-mountain cryosphere; however, in these publications rock glaciers are not or only briefly mentioned, respectively. Existing research from other mountainous regions suggests that rock glaciers may constitute hydrologically valuable water stores, particularly in semi-arid and arid zones where glaciers are absent or have limited presence (e.g., Azócar and Brenning, 2010; Rangecroft et al., 2015; Janke et al., 2017). Yet, across HMA rock glacier-related research has been conducted at relatively small spatial scales. Research that has been undertaken (i.e. rock glacier inventories) at national or regional spatial scales is generally incomplete (e.g., Regmi, 2008; Schmid et al., 2015). In deglacierizing mountains, the relative hydrological value and influence of rock glaciers could potentially increase; therefore, a spatially explicit understanding of the distribution and WVEQ of rock glaciers within this region is necessary. Furthermore, the results of Theme 2 will provide a unique scientific baseline from which rock glacier response to current and future climate change can be assessed.

Objectives [Chapter 6]

- For the Nepalese Himalaya, compile the first systematic inventory of rock glaciers, in order to
  - i. Characterise rock glacier frequency, spatial distribution, dynamic status and morphometric characteristics.
  - ii. Improve understanding of the geomorphic conditions necessary for rock glacier formation and persistence within the study region.

iii. Calculate rock glacier WVEQ.

iv. Assess rock glacier and glacier WVEQ across a range of spatial scales.

Objectives [Chapter 7]

- For the Himalaya, compile the first systematic inventory of rock glaciers using the methodology developed in Chapter 6, in order to

  i. Characterise rock glacier frequency, spatial distribution, dynamic status and morphometric characteristics.

  ii. Calculate rock glacier WVEQ.

  iii. Assess rock glacier and glacier WVEQ across a range of spatial scales.

3.3 THEME 3: RATIONALE AND OBJECTIVES

In deglacierizing high mountain systems, climatically-driven glacier recession is accompanied by a paraglacial (i.e. landscape relaxation) response whereby glaciers are undergoing a transition to rock glaciers (Knight and Harrison, 2014b). It is hypothesised that glacier-to-rock glacier transition has important implications for the climatic resilience of the high-mountain cryosphere given that rock glaciers are: (i) reportedly climatically more resilient than glaciers; and (ii) may have a long residence time in the landscape dissimilar to many other glacially influenced mountain landforms. Yet, little is known in terms of (i) the relationships of rock glaciers to glacial, periglacial and paraglacial environments and processes, and the implications of rock glacier development on long-term mountain landscape evolution; and (ii) the glacier-to-rock glacier transitional process – how this transition occurs and how quickly, which glaciers are liable to transition, the factors driving this process and the water supply implications that follow.

Objectives [Chapter 8]

- Consider the morphodynamic significance of rock glaciers in deglacierizing mountains, by

  i. Considering the relationships of rock glaciers to glacial, periglacial and paraglacial environments and processes.

  ii. Characterising specific examples of rock glaciers at local spatial-scales (Khumbu Valley, SNP, Nepal) across a range of geomorphic settings.

  iii. Propose a genetic classification model to describe the corelationships between different controls on rock glacier origin and evolution through their lifecycle using the findings of (i) and (ii).

Objectives [Chapter 9]

- (1) Produce a fine spatial-scale 3-D-model of a landform potentially undergoing glacier-to-rock glacier transition; and (2) characterise the sedimentology of six landsystems on the evolutionary spectrum from glaciers to rock glaciers, in order to
  i. Assess the surface geomorphic features of a potentially transitional landform.
  ii. Assess the textural properties of the features investigated.
  iii. Develop a conceptual hypothesis for glacier-to-rock glacier transition using the findings of (i) and (ii).

4 ROCK GLACIERS AND MOUNTAIN HYDROLOGY: A REVIEW

4.1 ABSTRACT

In mountainous regions, climate change threatens cryospheric water resources, and understanding all components of the hydrological cycle is necessary for effective water resource management. Rock glaciers are climatically more resilient than glaciers and contain potentially hydrologically valuable ice volumes, and yet have received less attention, even though rock glacier hydrological importance may increase under future climate warming. In synthesising data from a range of global studies, we provide the first comprehensive evaluation of the hydrological role played by rock glaciers. We evaluate hydrological significance over a range of temporal and spatial scales, alongside the complex multiple hydrological processes with which rock glaciers can interact diurnally, seasonally, annually, decadally and both at local and regional extents. We report that although no global-extent, complete inventory for rock glaciers exists currently, recent research efforts have greatly elaborated spatial coverage. Using these research papers, we synthesise information on rock glacier spatial distribution, morphometric characteristics, surface and subsurface features, ice-storage and hydrological flow dynamics, water chemistry, and future resilience, from which we provide the first comprehensive evaluation of their hydrological contribution. We identify and discuss long-, intermediate- and short-term timescales for rock glacier storage, allowing a more balanced assessment of the contrasting perspectives regarding the relative significance of rock glacier-derived hydrological contributions compared to other water sources. We show that further empirical observations are required to gain a deeper hydrological understanding of rock glaciers, in terms of (i) their genesis and geomorphological dynamics (ii) total ice/water volume; (iii) water discharge; and (iv) water quality. Lastly, we hypothesise that at decadal and longer timescales, under future climate warming, degradation of ice within rock glaciers may represent an increasing hydrological contribution to downstream regions, and thus increased hydrological significance while rock glacier water stores persist.

4.2 INTRODUCTION

Glacierised high mountain systems worldwide form natural ‘water towers’ that constitute a significant freshwater source for downstream regions, particularly in arid and semi-arid zones (Messerli et al., 2004; Viviroli et al., 2007). Here, glacial- and snowpack-derived meltwaters buffer hydrological seasonality, contributing to streamflow in otherwise low-flow conditions during drier months (e.g., Kaser et al., 2010). In this context, the mountain cryosphere (snow,

ice and permafrost) is important for ecosystem services provision (Grêt-Regamey et al., 2012), supplying multiple societal needs within mountains and the surrounding lowlands – potable water supplies, energy generation (hydropower) and agriculture, for example (Immerzeel et al., 2010; Viviroli et al., 2011). In vulnerable drought-prone regions, particularly, glaciers represent an important drought-resilient water source (Bolch, 2017). This has been illustrated for several high-altitude cities located in the Andes (Wouter et al., 2017) (**Table 4.1**).

Table 4.1. Relative contribution of glacial melt (%) to the water supply of selected cities under different meteorological conditions. Values in square brackets indicate the uncertainty ranges of the estimates. After Wouter et al. (2017).

	Quito (Ecuador)	La Paz (Bolivia)	Huaraz (Peru)
[NY] Annual average	2.2 [0.9–5.0]	14.8 [5.9–26.8]	19.0 [7.5–35.4]
[NY] Monthly maximum	5.3 [2.3–11.1]	61.1 [37.8–77.1]	67.3 [41.9–82.8]
[DY] Annual average	3.7 [1.5–8.0]	15.9 [6.4–29.4]	27.2 [11.6–46.7]
[DY] Monthly maximum	15.4 [7.3–27.6]	85.7 [74.1–91.5]	91.1 [78.1–96.0]

NY = Normal Year
DY = Drought Year

The rapid near-global retreat of mountain glaciers, predominantly attributed to anthropogenic causes (Marzeion et al., 2014), has previously been reported (Gardner et al., 2013) and glacial retreat and mass loss is projected to continue throughout the twenty-first century (Marzeion et al., 2012; Radić et al., 2014; Huss and Hock, 2015). Furthermore, under high-end climate change scenarios (RCP8.5) Shannon et al. (2019) project global ensemble mean glacier volume loss to be -64 ± 5% (excluding glaciers situated on the periphery of the Antarctic ice sheet) towards the end of the century, with particular regions experiencing mass losses exceeding 75%, including Central Europe, Caucasus, HMA and Southern Andes. Even under conservative projections – limiting global warming to 1.5 °C above pre-industrial levels (Paris Agreement) – substantial glacier mass loss occurs; e.g., ~36% reductions in glacier mass by 2100 in HMA (Kraaijenbrink et al., 2017). Elevation-dependent warming, i.e. rates of warming are amplified with increasing elevation, suggests high-altitude environments will likely experience comparatively faster warming rates than those at lower elevations, particularly at low-latitudes (Vuille et al., 2008; Mountain Research Initiative EDW Working Group, 2015). Indeed, within certain low-latitude mountain ranges, complete loss of glaciers has already occurred (Rabatel et al., 2013). Therefore, long-term glacial stores are finite (Jansson et al., 2003).

In the short-term, annual water release from long-term glacial storage increases; however, beyond 'peak water' enhanced melt rates are overwhelmed by glacier shrinkage, and

projected glacier runoff gradually declines. For example, recent global-scale projections encompassing 56 glacierised macroscale (>5,000 km²) basins suggests that to date (2017) peak water has been reached in 45% of the 56 studied basins, increasing to 78% by 2050 (RCP4.5) (Huss and Hock, 2018). Critically, by 2100 Huss and Hock (2018) report glacier runoff reductions exceeding 10% during at least one month of the melt season for one-third of the studied basins; the largest of which occur in Central Asian and Andean basins. These findings are corroborated across a range of spatial scales (e.g., Baraer et al., 2012; Sorg et al., 2014a; Frans et al., 2016; Hanzer et al., 2018). Importantly, accompanying glacier mass loss, the potential occurrence of increased rain-to-snow fraction (Berghuijs et al., 2014), reductions in snow cover extent and/or duration (Brown and Mote, 2009; Bavay et al., 2013; Zhou et al., 2017), seasonal runoff maxima shifts towards earlier in the year (Hanzer et al., 2018; Huss and Hock, 2018) and widespread permafrost degradation (Haeberli, 2013; Biskaborn et al., 2019) will further reduce long-term runoff in snowmelt- and icemelt-dominated basins.

The anticipated effects of the future decline of the mountain cryosphere pose far-reaching challenges for effective freshwater resource management. Several studies have previously summarised and discussed such impacts on anthropogenic and ecologic systems (see Beniston, 2003; Barnett et al., 2005; Bolch et al., 2012; Huss et al., 2017; Milner et al., 2017; Beniston et al., 2018), and we refer interested readers to those manuscripts for details. In terms of climate change adaptation strategies, an understanding of all components of the hydrological cycle in high mountain systems is vital (Jones et al., 2018a). However, whilst much has been written on the hydrological role of debris-free glaciers (see Fountain and Walder, 1998; Jansson et al., 2003; Irvine-Fynn et al., 2011) and increasingly on debris-covered glaciers (Fyffe et al., 2019, and references therein), that of rock glaciers has received comparatively less attention (Duguay et al., 2015).

Rock glaciers are landforms consisting of a continuous, thick seasonally frozen debris layer (i.e. the AL) covering ice-supersaturated debris or pure ice (Berthling, 2011; Bonnaventure and Lamoureux, 2013). They are formed by gravity-driven creep as a consequence of internal ice deformation. Intact rock glaciers (i.e. those features within which ice presence is expected beneath the AL [Barsch, 1996]) are thought to contain ice volumes of significant value (Azócar and Brenning, 2010; Rangecroft et al., 2015; Jones et al., 2018b; Munroe, 2018). Critically, due to the insulating effect of the AL, internal thermal regimes are at least partially decoupled from external micro- and meso-climates in summer (Juliussen and Humlum, 2008; Millar et al.,

2013). As a result, rock glaciers are reasonably assumed to have retarded ice melt, which suggests these landforms may prolong long-term water storage in high mountain systems and buffer losses from alternative sources (Millar et al., 2013; Rangecroft et al., 2015; Bosson and Lambiel, 2016; Jones et al., 2018b). Furthermore, rock glacier presence and abundance affects the amount and properties of runoff from high mountain watersheds. The potential hydrological value of rock glaciers, and thus their importance in terms of hydrological research, was first noted by Corte (1976). Yet, despite an acceleration of rock glacier-related research during recent decades – searches within Scopus using 'Article title, Abstract, Keywords' for all spelling variants of *rock glacier(s)* generated 973 peer-reviewed articles and reviews to date[2], 390 (40%) of which have been published since 2010 – research focusing upon their hydrological role remains limited. For example, Duguay et al. (2015) report that searches of both ISI Web of Science™ and Geobase™ resulted in just 28 papers with an appropriate discussion on rock glacier hydrology. Therefore, despite the near-ubiquitous nature of rock glaciers in high mountain systems (Jones et al., 2018a), there remains a need to understand the state-of-knowledge regarding the hydrological role of rock glaciers. The rationale and aim of this manuscript is thus to describe the state of current scientific knowledge about the hydrological role and contribution of rock glaciers in mountain regions.

4.3 ROCK GLACIERS

4.3.1 ROCK GLACIER CHARACTERISTICS

Rock glaciers are lobate or tongue-shaped assemblages of poorly sorted, angular-rock debris and ice (ice-cored or ice-cemented [see **section 4.3.2**]) commonly found in high mountain environments, which move as a consequence of the deformation of internal ice (Giardino and Vitek, 1988; Barsch, 1996). Previously, rock glaciers have been classified according to their ice content and dynamic behaviour (**Figure 4.1**); *active rock glaciers* contain ice and display movement, *inactive rock glaciers* contain ice and no longer display movement and *fossil rock glaciers* do not contain ice and no longer move, and are referred to regularly as *relict* (Haeberli, 1985; Barsch, 1996). Importantly, Kääb (2013) notes that "this classification is a theoretical concept. The transition between the three stages is actually continuous".

Active rock glaciers display rates of movement in the order of centimetres to a few decimetres per year (see Table 3 in Janke et al., 2013), although cases have been reported with surface

[2] March 2019.

velocities of several metres per year (Gorbunov et al., 1992; Kääb et al., 2003; Delaloye et al., 2013; Sorg et al., 2015; Hartl et al., 2016b; Eriksen et al., 2018). They are characterised by distinctive flow-like morphometric features reflecting their visco-plastic properties; spatially organised longitudinal or transverse ridge-and-furrow assemblages, steep (~>30–35°) and sharp-crested front and lateral slopes that typically rise 15–70 m above adjacent terrain, light-coloured (i.e. little weathered) frontal slope in contrast to the dark-coloured rock-varnished (i.e. greatly weathered) uppermost surface, a swollen, noticeably longitudinally convex appearance of the rock glacier body, and an absence of vegetation and/or lichen cover (Wahrhaftig and Cox, 1959; Martin and Whalley, 1987; Baroni et al., 2004; Haeberli et al., 2006; Harrison et al., 2008).

Inactive rock glaciers still contain ice but are immobile. Two types of inactivity can be defined: *climatically inactive*, where the ice has melted; and *dynamically inactive* where there is reduced nourishment of talus and/or ice as the rock glacier extends too far from the headwall (e.g., Kellerer-Pirklbauer and Rieckh, 2016), are cited as possible causes for this behaviour (see Barsch, 1996, p. 8–10). In comparison to active rock glaciers, the surface micro-topography of inactive features is relatively subdued. They generally have gentler, dark-coloured rock-varnished frontal slopes with partial to full vegetation and/or lichen cover (Ikeda and Matsuoka, 2002). As a consequence of the difficulty of differentiating between active and inactive forms, particularly through photogeomorphology, active and inactive rock glaciers are often collectively termed *intact*.

Relict rock glaciers, defined as former rock glaciers, no longer contain any ice and are characterised by subdued surface micro–topography. They often exhibit surface collapse features including thermokarst ponds, i.e. water-filled depressions resulting from melting of stagnant glacial ice, and have gentler (~ < 30°) and round-crested front and lateral slopes, a dark-coloured rock-varnished frontal slope, and extensive vegetation and/or lichen cover (Martin and Whalley, 1987; Barsch, 1996; Baroni et al., 2004; Harrison et al., 2008).

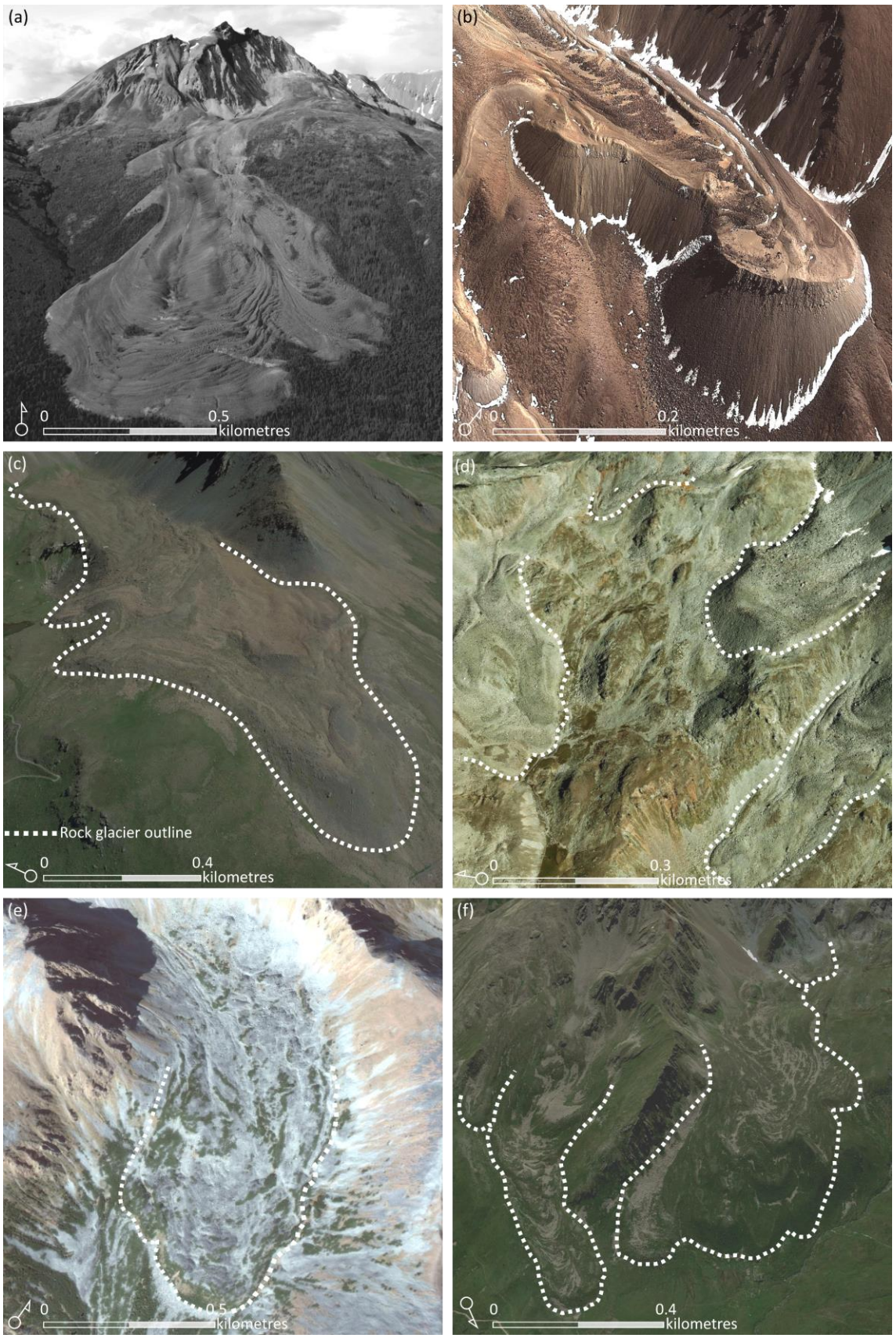

Figure 4.1. Typical examples of active [a, b], inactive [c, d] and relict [e, f] rock glaciers from around the world: (a) Sourdough rock glacier, Wrangell Mountains, AK, USA (61°23'N, 142°44'W). Note the steep headwall that serves as a source of snow avalanches and rockfall; (b) Caquella rock glacier, Bolivian Andes of South Lipez, Bolivia (21°29'S, 67°55'W); (c) Liapey d'Enfer rock glacier, Hérens valley, Swiss Alps, Switzerland (46°05'N, 7°32'E); (d) rock

glaciers in the Niggelingtälli, Turtmann Valley, Swiss Alps, Switzerland (46°13'N, 7°45'E); (e) Hoelltal rock glacier, Niedere Tauern Range, Central Eastern Alps, Austria (47°22'N, 14°39'E); (f) rock glaciers beneath Le Mourin mountain, Valais, Swiss Alps, Switzerland (45°56'N, 7°10'E). On the photographs, dashed lines correspond to the approximate rock glacier boundary. Images [a] modified after Anderson et al. (2018) and [b–f] from Google Earth.

It is important to note that recognition, delineation and classification (in terms of their activity) is not a trivial undertaking both from *in situ* surveys, or from analysis of remote sensing/photographic data, particularly where: (i) the "characteristic" surface morphology is not evident (Whalley et al., 1986), and/or (ii) rock glaciers form multi-lobed complexes with lobes of different activity types superimposed and embedded onto/into one another, forming a cascading form with active lobes at higher elevations and relict lobes at lower elevations (Roer and Nyenhuis, 2007). Regardless, identifying and establishing the activity status of rock glaciers represents an important initial step in determining their potential hydrological significance.

4.3.2 ROCK GLACIER ORIGIN AND EVOLUTION

A long-standing academic debate regarding rock glacier origin pervades the literature (see Barsch, 1977, 1987, 1996; Whalley and Martin, 1992; Hamilton and Whalley, 1995; Clark et al., 1998; Whalley and Azizi, 2003; Haeberli et al., 2006; Berthling, 2011). Specifically, the rock glacier controversy can be framed as the permafrost model where internal ice is assumed to be of a dominantly periglacial/permafrost origin (Haeberli, 1985) vs the glacier ice core model where a dominant glacial origin is assumed. In reality, within deglacierizing mountains rock glaciers are equifinal inasmuch as they can arise from separate or combined periglacial, glacial and paraglacial (i.e. landscape relaxation) processes (Knight et al., 2019). Indeed, glaciological vs slope vs climatic controls on the evolution of rock glaciers may vary through the rock glacier life cycle (ibid.). Here, we do not seek to contribute to this debate (this is beyond the scope of this paper) – several papers have already discussed the arguments for and against the different positions (see Whalley and Martin, 1992; Barsch, 1996; Haeberli et al., 2006; Berthling, 2011, for reviews); rather, we adopt the dispassionate view that rock glaciers can be derived through either model (as per Berthling, 2011) and proceed to describe these hypotheses in further detail below.

The permafrost model for rock glacier genesis follows Wahrhaftig and Cox (1959) where interstitial ice (pore-ice) or segregated ice (ice lenses), primarily derived from either the freezing of rain and meltwater percolating through the rock glacier matrix, the freezing of groundwater, and/or the burial of snow and ice accumulations (Burger et al., 1999; Haeberli, 2000; Haeberli et al., 2006), produces creep (Wahrhaftig and Cox, 1959; Barsch, 1977, 1987, 1988,

1996; Haeberli, 1985). Rock glaciers of periglacial origin are often called *talus-derived rock glaciers* (Humlum, 1996) or *ice-cemented rock glaciers* (Wayne, 1981). Of note is the occurrence of rock glaciers in nonglacial, periglacial environments; therefore, past or present glaciation is not a prerequisite for their formation (Haeberli, 1985; Giardino and Vitek, 1988; Hamilton and Whalley, 1995). Proponents of this model suggest that little evidence exists to support the glacier ice core model (see Berthling, 2011, for detailed discussion), although they acknowledge the possibility of incorporation of glacier (sedimentary) ice in permafrost (e.g., Haeberli, 1989; Haeberli and Vonder Mühll, 1996; Kääb et al., 1997; Haeberli et al., 2006). In such cases, it is argued that the long-term existence of these rock glaciers requires permafrost conditions (Harris and Murton, 2005; Berthling, 2011; Kääb, 2013).

Based on *in situ* data, other authors have presented evidence that supports a glacigenic origin (i.e. glacier ice core model) for certain rock glaciers (Outcalt and Benedict, 1965; Potter, 1972; Whalley, 1974; White, 1976; Whalley et al., 1994; Humlum, 1996; Potter et al., 1998; Ishikawa et al., 2001; Monnier et al., 2013; Petersen et al., 2016; Guglielmin et al., 2018). This model involves the creep of a thin (typically <50 m) ice body, which has been buried and preserved by an insulating weathered rock debris layer (Whalley and Martin, 1992; Whalley and Azizi, 2003). Recently, Anderson et al. (2018) showed that rock glaciers of glacigenic origin represent a plausible end-member response that is captured in numerical models of debris-free glaciers. Rock glaciers of this type are also referred to as *moraine-derived rock glaciers* (Harrison et al., 2008)*, ice-cored rock glaciers* (Potter, 1972)*, glacier ice-cored rock glaciers* (Johnson, 1978) or *glacier-derived rock glaciers* (Humlum, 1996). **Figure 4.2** represents a simplified perspective of rock glacier composition for features derived from either the permafrost or glacier ice core model as outlined by Martin and Whalley (1987).

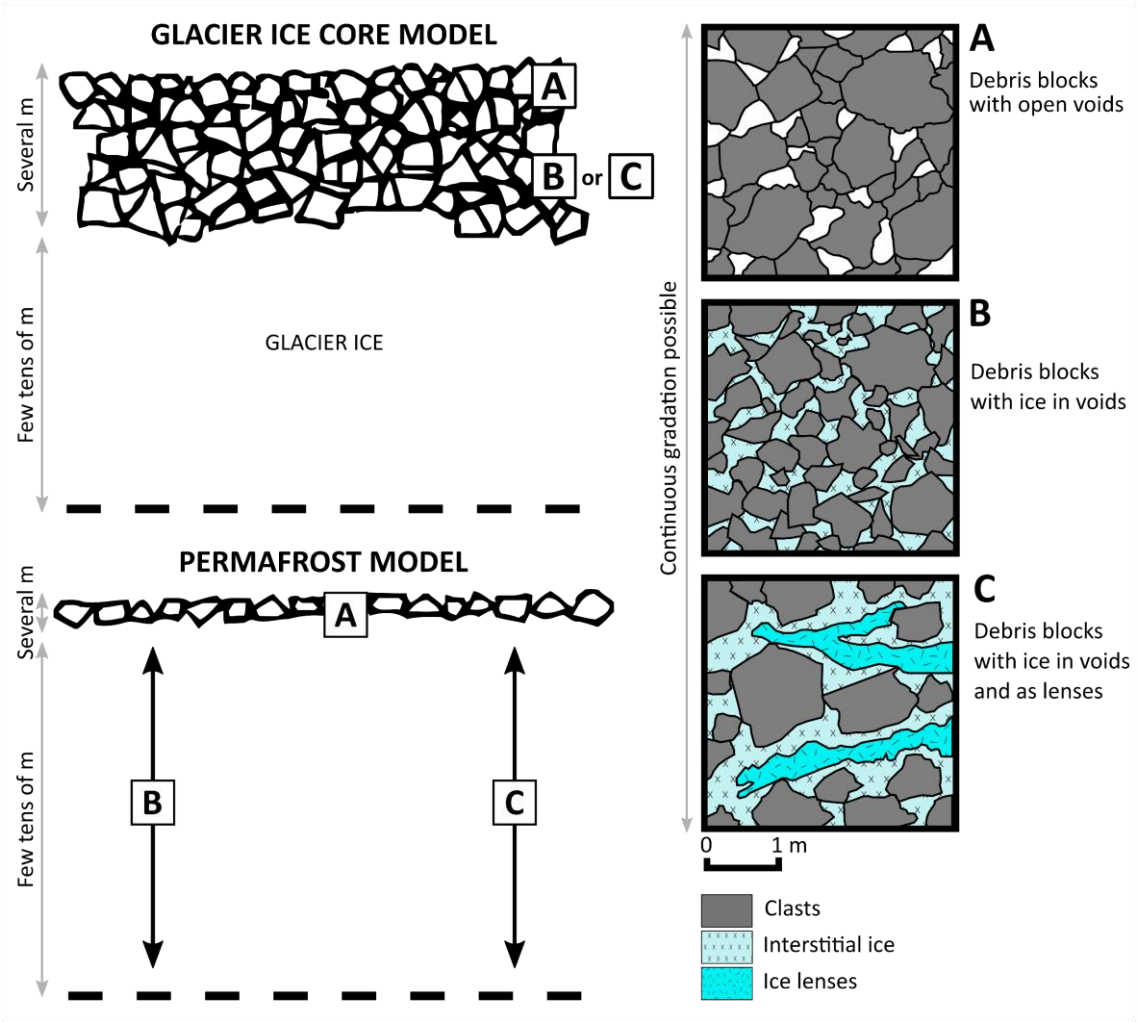

Figure 4.2. A basic representation of rock glacier internal composition associated with the glacier ice-core and permafrost models. Modified after Martin and Whalley (1987).

Proponents of the two competing concepts of rock glacier formation generally focus on already well-developed landforms (Monnier and Kinnard, 2015b). Yet, there are striking examples of large glacier-rock glacier composite features where the lowermost parts of debris-covered glaciers are *currently developing* into rock glaciers. Cases of glacier-to-rock glacier transition within relatively short timescales have been reported; for example, within ca. 50 years at Sachen Glacier, Nanga Parbat, Pakistan (Shroder et al., 2000) and ca. 60 years at Presenteseracae debris-covered glacier, central Andes, Chile (Monnier and Kinnard, 2015b). Nevertheless, studies of glacier-rock glacier interactions are rarely orientated towards such examples (Monnier and Kinnard, 2015b), in spite of their potential to elucidate the drivers behind which glaciers will fully transition into rock glaciers and those which will downwaste.

Here, it is important to distinguish between rock glaciers (cf. **section 4.3.1**) and debris-covered glaciers (Hambrey et al., 2008; Benn and Evans, 2010; Cogley et al., 2011; Jiskoot, 2011; Kirkbride, 2011), particularly when reviewing the hydrological significance of the former;

grouping these features would incorrectly inflate the hydrological significance of rock glaciers. Debris-covered glaciers are glaciers in which the ablation zone is partly or wholly covered with thin (typically less than several-decimetres thick) supraglacial debris (Kirkbride, 2011). There are critical differences between rock glaciers and debris-covered glaciers: rock glacier movement is governed by internal deformation, the majority of which occurs in a shear zone at depth within the feature (Arenson et al., 2002; Buchli et al., 2013, 2018; Krainer et al., 2015; Kenner et al., 2017a); debris-covered glacier motion may occur due to internal deformation, basal sliding, and soft bed deformation. Importantly, basal sliding is generally non-occurring or very limited for cold-based debris-covered glaciers (i.e. glaciers frozen to their beds), and only debris-covered glaciers underlain by a soft deformable substrate (i.e. unlithified sediments or poorly consolidated sedimentary rocks) exhibit soft bed deformation. The surface of debris-covered glaciers is complex topographically, consisting of a spatially-chaotic mosaic of features such as hummocks, depressions, supraglacial melt ponds and ice cliffs; the surficial instability and discontinuity of the debris-covered glacier debris layer mean that such ice exposures are frequently visible. Contrastingly, rock glacier surfaces are characterised by spatially coherent flow-like topography (**section 4.3.1**), and surficial ice-exposures are infrequent.

Monnier and Kinnard (2017) identify three types of glacier-rock glacier dynamic relationships within the literature: (i) the re-advance of glaciers or debris-covered glaciers overriding older permafrost bodies and coalescing (Lugon et al., 2004; Haeberli, 2005; Ribolini et al., 2007, 2010; Monnier et al., 2013; Dusik et al., 2015; Bosson and Lambiel, 2016; Kellerer-Pirklbauer and Kaufmann, 2018; Kenner, 2019). Such glacier-rock glacier interactions are defined by the permafrost model; (ii) the continuous emergence of a rock glacier from a debris-covered glacier, as indicated by the evolution of the surface morphology, together with the creep of a massive and continuous ice body that has been buried and preserved (Potter, 1972; Potter et al., 1998; Humlum, 2000; Krainer and Mostler, 2000). These types of glacier-rock glacier interactions are described by the glacier ice core model; (iii) debris-covered glacier-to-rock glacier transition through the evolution of the surface morphology and the internal structure, i.e. the development of a perennially frozen ice-rock mixture resulting from the incorporation of surface-derived debris and periglacial ice and fragmentation of the initial massive and continuous ice body (Monnier and Kinnard, 2015b, 2017; Seppi et al., 2015). Monnier and Kinnard (2015b) describe this as an alternative to the dichotomous debate between a periglacial or glacial origin. Regarding (ii) and (iii), the emerging rock glacier and debris-covered glacier morphology are in complete continuity, suggesting a continuum between debris-free glaciers and rock

glaciers where debris-covered glaciers form an intermediate stage (Giardino and Vitek, 1988; Ackert, 1998).

With continued climate-driven deglaciation, high mountain systems are transitioning from glacial to paraglacial dominated process regimes (Harrison, 2009). Ballantyne et al. (2014) note that formerly glacierised high mountain systems "are characterised by a high spatial density of large-scale post-glacial rock-slope failures (RSFs) such as major rockfalls, rockslides, rock avalanches and deep-seated gravitational slope deformations". RSFs occur in response to debuttressing or deglacial unloading that follows the exposure of glacially steepened rockwalls by glacier downwastage and retreat (Ballantyne, 2002b; Fischer et al., 2006). In the context of current and future climatic conditions, enhanced paraglacial processes (i.e. RSFs) driven by continuing deglaciation could increase supraglacial debris accumulation upon glacial forms, and thus limit ablation of the underlying ice (**section 4.4**) (Lambrecht et al., 2011; Pellicciotti et al., 2014; Lardeux et al., 2016). Thick supraglacial debris cover (i.e. decimetres to metres) influences glacier dynamics significantly, as inefficient sediment evacuation processes encourage glacier-rock glacier interactions (Shroder et al., 2000). Recent numerical model simulations report that under significant warming (+2.5 °C) debris-covered glacier-to-rock glacier transition can occur rapidly (~100 years) (Anderson et al., 2018). Therefore, glacier-rock glacier interactions could enhance the resilience of the mountain cryosphere, preserving frozen water stores as glaciers transition to rock glacier forms. Importantly, however, these landform assemblages are not included in glacio-hydrological modelling, which usually focuses solely on glaciers (Bolch et al., 2019a, and references therein). As such, an improved understanding of glacier-rock glacier dynamic relationships is critically important in the context of future water resources management. We further argue that of particular importance are empirical studies that seek to elucidate the drivers behind which glaciers will fully transition into rock glaciers and those which will simply downwaste.

4.3.3 ROCK GLACIER WATER STORAGE

Rock glacier water storage occurs as ice, snow and water at *long-term*, *intermediate-term* and *short-term* timescales (Jones et al., 2018b) (**Figure 4.3**), similar to glacier storage (cf. Jansson et al., 2003). Long-term storage concerns ice storage below the AL of rock glaciers on multi-annual to centennial and millennial timescales (e.g., Clark et al., 1996; Krainer et al., 2015). Recent research concludes that rock glaciers constitute non-negligible long-term water stores, particularly in deglacierizing/deglacierized semi-arid and arid regions (**section 4.5**). In addition,

this storage also includes the release of these water stores through degradation of the internal ice body. Intermediate-term storage encompasses the storage and release of snowmelt and AL thaw-derived runoff on a seasonal timescale (**section 4.6**). Short-term storage includes diurnal drainage of en- and sub[rock]glacial water through the rock glacier (**section 4.6**). In this context, intermediate-term and short-term storage can strongly influence catchment runoff characteristics, especially in catchments where rock glaciers are more abundant than glaciers. In addition, event storage and releases (i.e. singular storage releases), which have irregular occurrences and/or irregular intervals, are also types of rock glacier storage; for example, intermittent thermokarst ponds (Giardino et al., 1992; Haeberli et al., 2001; Kääb and Haeberli, 2001) or rock glacier-dammed lakes formed as a consequence of river channel disruption (Hewitt, 2014; Rosenwinkel, 2018; Blöthe et al., 2019). Detailed knowledge of the timescales and forms of rock glacier water storage represents critical information for the management of such resources but is currently lacking.

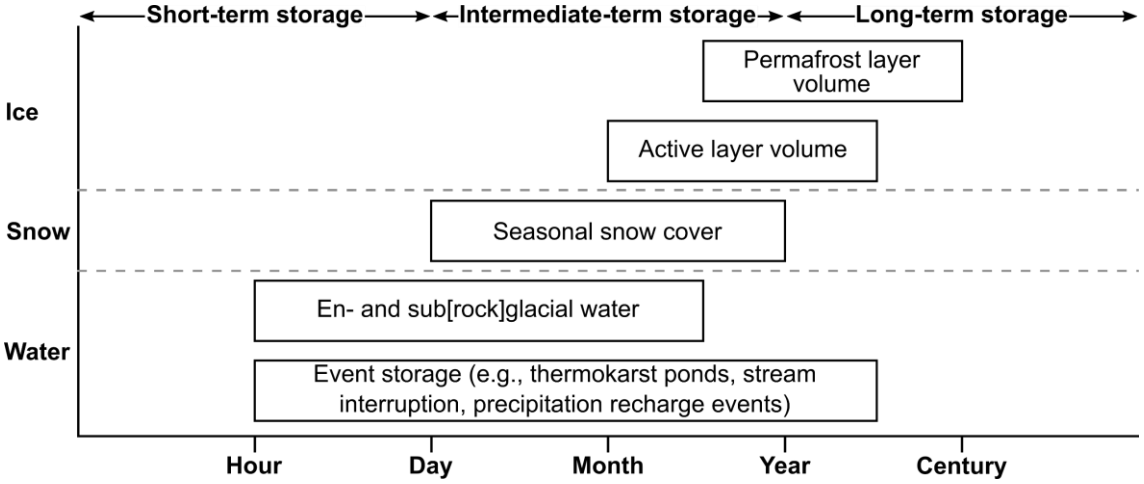

Figure 4.3. Schematic diagram showing the different forms of rock glacier storage and their associated timescales. Figure adapted from Jansson et al. (2003).

4.4 ICE PRESERVATION

Active rock glacier internal structure consists of two basic units: firstly, the AL, which is typically a few decimetres to a few metres in thickness and secondly, underlying the AL, a core of ice-supersaturated debris (i.e. nonglacial) or pure ice (i.e. glacial) (Ballantyne, 2018, p. 243). The AL typically comprises coarse blocky clasts ~0.2–5.0 m in length (Humlum, 1997) (**Figure 4.4a**), although boulders exceeding 5 m in length are sometimes present (**Figure 4.4b**).

Figure 4.4. Ground-based views of the lowermost part of the Chola Glacier (Khumbu Himal, Nepalese Himalaya, May 2017), an ongoing glacier-rock glacier interaction, including: (a) the coarse-blocky openwork debris that is characteristic of rock glacier AL surfaces. Field sampling of the visible clasts suggests mean grain size ~1.9 m (b-axis); (b) the variability of grain size (i.e. >5 m blocks) visible at rock glacier surfaces. The grain size variability reflects the diversity of processes (e.g., rockfalls, snow avalanches, etc.) by which debris is transferred to the rock glacier surface (Haeberli et al., 2006). Researcher for scale. Photos: Darren B. Jones.

Complex internal thermal regimes are generated within the coarse-blocky openwork structure of the AL, such that the AL acts as a thermal filter between the surface energy balance and the subjacent frozen rock glacier core (Humlum, 1997; Hanson and Hoelzle, 2004). Indeed, Gruber and Hoelzle (2008) illustrate that both the temperature beneath the seasonal snow cover and mean annual ground temperatures at greater depth can be considerably reduced due solely to the low thermal conductivity of the openwork blocky debris according to a simple and purely conductive model. Consequently, the thermal regime within coarse-blocky openwork debris is different to the surrounding environment leading to the development of cooler ground temperatures when compared to fine-grained or bedrock surfaces in similar settings (Harris and Pedersen, 1998; Juliussen and Humlum, 2008) and MAATs (Gorbunov et al., 2004; Millar et al., 2013). This leads to the continued persistence of buried ice at elevations where MAAT exceeds 0 °C, i.e. elevations where permafrost persistence

outside of rock glaciers and similar landforms is highly improbable (e.g., Baroni et al., 2004; Popescu et al., 2017), occasionally reaching below the tree line (e.g., Sorg et al., 2015; Charbonneau and Smith, 2018) (**Figure 4.1a**).

It is probable that a number of non-conductive (i.e. convective and advective heat flow) and conductive processes are responsible for the cooling influence of openwork blocky debris in relation to rock glaciers, talus slopes and blockfields (Harris and Pedersen, 1998). These processes include: (i) the Balch effect; (ii) the chimney effect; (iii) continuous air exchange with the atmosphere; (iv) summer-time evaporation or sublimation of water and/or ice; and (v) conductive heat loss via boulder protrusion. At different times of the year all of these mechanisms could feasibly be operating, but under different circumstances governed by the duration, depth and permeability of seasonal snow cover, local topography (i.e. slope length and gradient) and openwork blocky debris thickness (Ballantyne, 2018, p. 51). Each is summarised below.

- *The Balch effect (or Balch ventilation):* This is defined as the insulating effect of air-filled voids within the openwork blocky debris (Thompson, 1962; Barsch, 1996, p. 238). During periods of low wind speeds and no or little snow cover, density-induced cooling occurs as comparatively cold air masses penetrate the openwork blocky debris and displace warmer air masses. In contrast to this, warmer air masses at the surface are prevented from penetrating into the openwork blocky debris by cold air trapped within inter-clast voids. Consequently, heat transfer is conductive only, thus warming of the openwork blocky debris at depth is sluggish, whereas density-induced non-convective processes (e.g., Balch ventilation) take place much more rapidly, particularly at night (e.g., Humlum, 1997). Importantly, wind pumping produced by high winds, however, may upset the above-described pattern and even dynamically displace trapped cold air as comparatively warmer and less dense near-surface air masses are driven into the openwork blocky debris by means of forced ventilation (Humlum, 1997). Of note, Ballantyne (2018, p. 50) notes that most investigators reject this explanation of negative temperature anomalies within openwork blocky debris as it fails to explain seasonal temperature variations at depth.
- *The chimney effect:* First proposed by von Wakonigg (1996), this theory concerns a seasonally switching air circulation mechanism that produces ascending warm air in winter and descending cold air in summer. Consequently, a positive and negative thermal

anomaly develops in the upper and lower parts of the slope, respectively. Specifically, in winter, warmer air masses move upslope through the openwork blocky debris under thick seasonal snow cover, exiting through warm funnels in the upper parts of the slope. As a result, the concomitant aspiration of cold air into the lower parts of the slope occurs. This process is most efficient during particularly cold periods leading to the build-up of a cold reservoir in the lower parts of the slope. In summer, this mechanism is reversed, with a gravity discharge of cold air through the openwork blocky debris, exiting at the foot of the slope (Harris and Pedersen, 1998; Delaloye and Lambiel, 2005). This process is frequently perceptible as a persistent breeze towards the base of rock glacier frontal slopes during the summer (Delaloye and Lambiel, 2005). Importantly, the chimney effect, therefore, facilitates the preservation of ice in openwork blocky debris on slopes >1,000 m below the regional limit of discontinuous permafrost, where MAAT is > + 5 °C (Delaloye and Lambiel, 2005). In addition, the results of recent 2-D numerical modelling (cf. Wicky and Huack, 2017) successfully replicate the above-described mechanism, placing further emphasis on its importance for the preservation of frozen ground under future climate warming.

- *Continuous air exchange with the atmosphere:* Proposed by Harris and Pedersen (1998), this theory is a simple extension of the chimney effect in areas where continuous snow cover is lacking. In its absence, continuous air exchange with the atmosphere occurs over the entirety of the openwork blocky debris; therefore, in response to changes in air temperature, almost instantaneous warming and cooling of the openwork blocky debris to a considerable depth occurs. This process is most effective in windy situations on steep slopes.
- *Summer-time evaporation or sublimation of water and/or ice:* Latent heat absorbed from block surfaces in these processes may cool the blocks in the upper layers of the openwork blocky debris (von Wakonigg, 1996). This process is most effective in regions with relatively dry summer air (Harris and Pedersen, 1998).
- *Conductive heat loss via boulder protrusion:* Boulders protruding into and through the seasonal snow cover act as “efficient heat bridges”, thermally coupling the openwork blocky debris and the surface air in winter and thereby enhancing conduction (Juliussen and Humlum, 2008). In block fields (Elgåhogna and Sølen Mountains, central-eastern Norway), Juliussen and Humlum (2008) recorded mean annual ground temperatures 1.3–2.0 °C lower than nearby till and bedrock.

In addition to the above-described processes, ice subjacent to the AL can 'self-preserve' as it increases the heat capacity, thermal conductivity and emissivity of the ground relative to unfrozen ground within which the pore spaces are air-filled. It may act as an effective heat sink, rapidly absorbing, emitting and distributing heat without undergoing high amounts of melt (Kenner et al., 2017b). Critically, therefore, rock glaciers have retarded melt as the ice underlying the AL is thermally decoupled from external macro- and meso-climates. Indeed, long-term ice preservation is feasible within rock glaciers previously considered morphologically inactive or relict (**section 4.3.1**) (e.g., Scapozza et al., 2011; Harrington et al., 2018; Colucci et al., 2019), as the lower ice content potentially increases AL porosity [and potentially void-interconnectedness], which improves internal air circulation (Delaloye and Lambiel, 2005). For example, field investigations at the inactive Helen Creek rock glacier (Banff National Park, Alberta, Canada) indicate the presence of isolated patches of subsurface ice where the AL is most coarse (clasts often >1 m b-axis) (Harrington et al., 2018). As a consequence, the response of rock glaciers to present-day and future climate warming may occur at comparatively longer timescales than glaciers (Giardino et al., 2011; Kenner and Magnusson, 2017; Anderson et al., 2018; Jones et al., 2018a). Indeed, Janke et al. (2013) note that "[u]nlike glaciers that are sensitive to extreme fluctuations on a shorter timescale, a strong climatic signal must exist to produce change in a rock glacier system". On this basis, it is reasonable to conclude that the hydrological role of rock glaciers (i.e. long-term storage) will likely become increasingly important with continued glacier recession (Bolch and Marchenko, 2006; Millar and Westfall, 2008), at least until the rock glaciers themselves become relict.

Of note, however, are emerging observations of increased rock glacier surface velocities potentially in response to recent climate warming at both decadal (Kääb et al., 2007; Kaufmann and Ladstädter, 2007; Delaloye et al., 2008; Bodin et al., 2009; Scapozza et al., 2014; Nickus et al., 2015; Sorg et al., 2015) and seasonal (Kääb et al., 2003; Perruchoud and Delaloye, 2007; Delaloye et al., 2010; Liu et al., 2013; Wirz et al., 2016) timescales. In the European Alps, for example, annual terrestrial geodetic surveys conducted at 16 rock glacier lobes suggest that relative to the respective previous year, mean surface velocity increase was ~ +52% during the reporting period (2010–2014) with most rock glaciers reaching new surface velocity maxima in 2014 (PERMOS, 2016). Elsewhere, striking examples of rapid rock glacier movement (i.e. several metres annually) (Delaloye et al., 2013; Hartl et al., 2016b; Eriksen et al., 2018) and partial rock glacier collapse (Bodin et al., 2017) have been explained, at least in part, by climatic factors. Furthermore, the synchronous kinematic behaviour recorded at multiple rock glaciers

with considerably different local conditions (e.g., elevation, topographical conditions, lithology), has been attributed to external drivers (i.e. climate warming) (Kääb et al., 2007; Delaloye et al., 2008, 2010; Kellerer-Pirklbauer and Kaufmann, 2012; Sorg et al., 2015; Kellerer-Pirklbauer et al., 2018). In explanation, increased rock glacier surface velocities are potentially due to modification of the rheological behaviour of warming ice (i.e. increased internal deformation) (Kääb et al., 2007) and/or hydrological effects (i.e. increased water content) within the frozen rock glacier core (i.e. higher pore pressure) or at the base (i.e. possibly basal sliding) (Ikeda et al., 2008; Roer et al., 2008; Buchli et al., 2013, 2018; Kenner et al., 2017a).

Rock glaciers with ground temperatures close to 0 °C are reported to have higher thermal responsiveness and creep faster in general than colder features (Kääb et al., 2007; Müller et al., 2016), and thus are likely to be more vulnerable to future climate warming. Numerical flow modelling of the Huhh1 and Murtèl rock glaciers (Swiss Alps, Switzerland) by Müller et al. (2016) indicate that an immediate 1 °C increase in rock glacier temperature considerably affects rock glacier horizontal velocity and surface geometry (**Figure 4.5**) – features with temperatures closest to 0 °C are most impacted. Further, Marcer et al. (2019) modelled the destabilisation susceptibility of rock glaciers (see section 'Reaction Typology' in Schoeneich et al., 2015), reporting that occurrence of this phenomenon is more likely in elevations near the 0 °C isotherm, north-facing aspects, steep slopes (25–30°) and flat to slightly convex topographies. Indeed, they identify significant evidence of destabilisation (e.g., crevasses and scarps) at 46 active rock glaciers in the French Alps – 10% of all active rock glaciers in this region. Research considering the implications of future climate warming on rock glaciers is therefore much required, yet it remains in its infancy (Rangecroft et al., 2016). In one of the few studies to date, Rangecroft et al. (2016) modelled future MAAT projections at intact rock glacier sites in the Bolivian Andes. Assuming a conservative rock glacier activity threshold of +2 °C (MAAT), the authors conclude that >98% of currently intact inventoried landforms will become relict by 2080. Similarly, within the Argentinian Andes >50% of currently active rock glaciers will terminate below the mean annual 0 °C isotherm by 2050 under RCP2.6 (i.e. best-case climate scenario) (Drewes et al., 2018). Under RCP8.5 (i.e. worst-case climate scenario) the majority will terminate below the mean annual 0 °C isotherm by 2070, e.g., 92.6% (~4,120 of 4,449 currently active rock glaciers) in the Central Andes sub-region (ibid.). While no allowances were made for a lagged response of rock glaciers to the modelled temperature shifts (see Rangecroft et al., 2016; Drewes et al., 2018), considering the above-described emerging

observations, in a changing climate the hydrological significance of rock glaciers as long-term stores is questionable.

Importantly, however, establishing statistically significant correlations between meteorological variables (e.g., MAAT, snow cover [depth, duration, timing], summer temperature, positive degree days etc.) and rock glacier response mechanisms can prove challenging (Roer et al., 2005; Kellerer-Pirklbauer and Kaufmann, 2012; Hartl et al., 2016b; Scotti et al., 2017). As a consequence, it is highly likely that rock glacier kinematic behaviour and surface geometry are determined by a complex combination of geomorphic (e.g., rock glacier internal structure, underlying topography [slope angle, slope convexity]), environmental (e.g., short and long-term temperature change, snow cover – including depth, duration and timing, rainfall events) and paraglacial processes (e.g., landslide and/or rockfall driven debris overload of the rooting zone) (Krainer and Mostler, 2006; Bodin et al., 2009, 2017; Delaloye et al., 2013; Schoeneich et al., 2015; Hartl et al., 2016b; Wirz et al., 2016; Scotti et al., 2017; Buchli et al., 2018; Eriksen et al., 2018). Here, it is important to stress that some rock glaciers yet to exhibit a climatically-forced response have been reported (Potter et al., 1998; Janke, 2005a). Nevertheless, in the context of projected climatic warming, clearly, further research is required to critically quantify and assess rock glacier-climate relations and the associated implications for future water resources. To this end, research focused upon the response of rock glaciers to past environmental conditions could provide key information for validating projected responses to future climate warming; however, there is currently a paucity of such studies (Sorg et al., 2015).

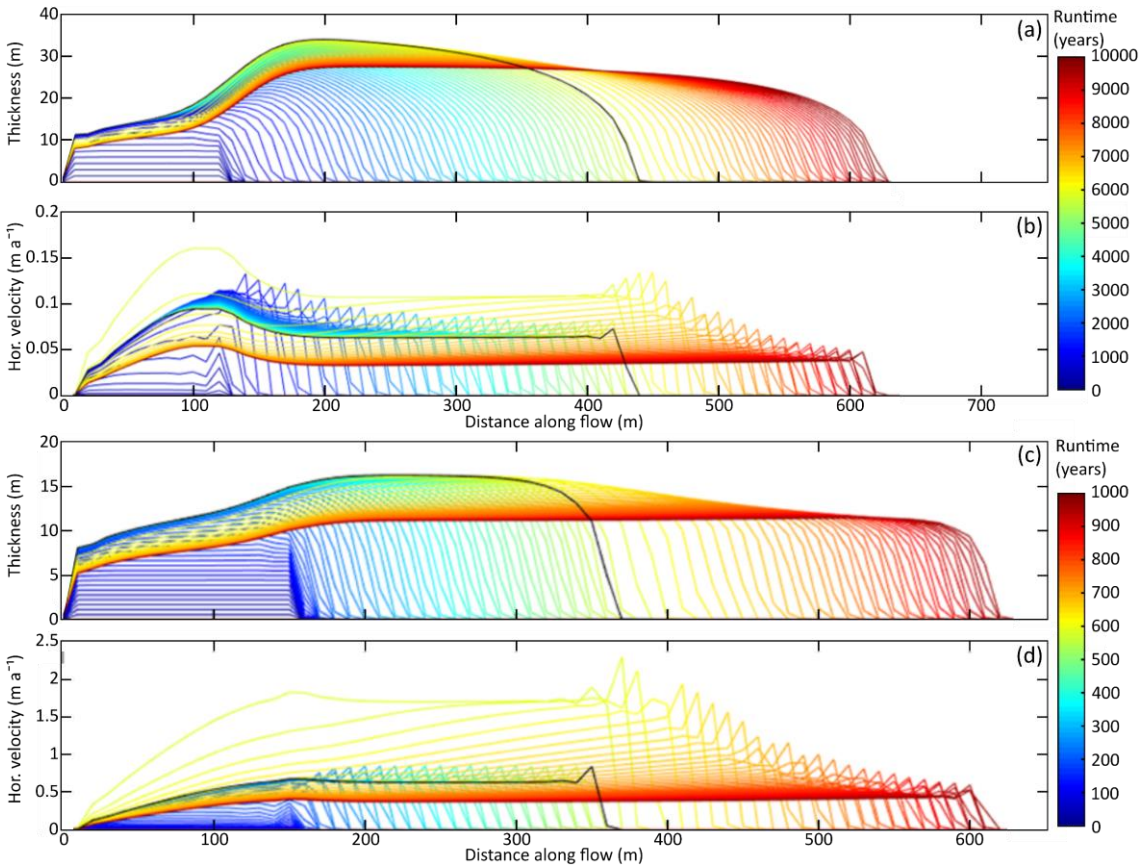

Figure 4.5. Modelled evolution of absolute thickness and horizontal velocities along the central flow line of the Murtèl [a, b] and Huhh1 rock glaciers [c, d] introducing a 1 °C temperature increase to the entire rock glacier body and 40% of the original material input following rock glacier build-up (Murtèl = 6,000 years, Huhh1 = 600 years [black lines]). The black lines reflect the pre-perturbation state of the rock glaciers. A reference rock glacier temperature of -1.5 °C was used; thus, the 1 °C temperature increase corresponds to a rate factor [referring to the material softness] increase by a factor of 1.7. The lines are plotted in 100 a steps [a, b] and 10 a steps [c, d]. Modified after Müller et al. (2016).

4.5 ROCK GLACIER DISTRIBUTION AND STORAGE

A considerable number of rock glacier inventories have been compiled in various mountain ranges (see Jones et al., 2018a). However, as yet no global-scale (complete) inventory has been compiled, despite being described as the "most pressing need" in rock glacier research (Janke et al., 2013). It should be noted that significant recent research efforts have greatly elaborated inventory coverage in the succeeding years, for example in South America (Falaschi et al., 2014; Rangecroft et al., 2014; Falaschi et al., 2015; Falaschi et al., 2016; Azócar et al., 2017; Barcaza et al., 2017; Esper Angillieri, 2017; García et al., 2017; Janke et al., 2017; IANIGLA-CONICET, 2018; Selley et al., 2018), North America (Charbonneau and Smith, 2018; Munroe, 2018), Central Europe (Colucci et al., 2016; Kellerer-Pirklbauer et al., 2016; Roudnitska et al., 2016; Salvador-Franch et al., 2016; Triglav-Čekada et al., 2016; Winkler et al., 2016a; Onaca et al., 2017; Palma et al., 2017; Uxa and Mida, 2017; Fernandes et al., 2018;

Popescu, 2018), Asia (incorporating Central Asia, South Asia [East], South Asia [West] and North Asia) (Bolch and Gorbunov, 2014; Schmid et al., 2015; Lytkin and Galanin, 2016; Galanin, 2017; Wang et al., 2017; Jones et al., 2018b; Ran and Liu, 2018; Blöthe et al., 2019), Antarctic and Subantarctic (Rudolph et al., 2018) and New Zealand (Sattler et al., 2016). Recently, Jones et al. (2018a) presented a near-global database containing >73,000 rock glaciers (intact = ~39,500, relict = ~33,500). The authors provide an approximate estimate of the WVEQ stored within these rock glaciers as being 83.7 ± 16.7 Gt, equivalent to ~68–102 trillion litres (**Figure 4.6**). Furthermore, excluding the Antarctic and Subantarctic and Greenland Periphery Randolph Glacier Inventory (RGI; Pfeffer et al., 2014) regions, along with RGI regions within which no systematic rock glacier inventories have been undertaken, the estimated ratio of rock glacier-to-glacier WVEQ is 1:456 globally, implying that glaciers store a volume of water 456 times larger than rock glaciers currently, a ratio that will change under a warming climate due to the differential wasting rates of glaciers vs rock glaciers, as previously discussed.

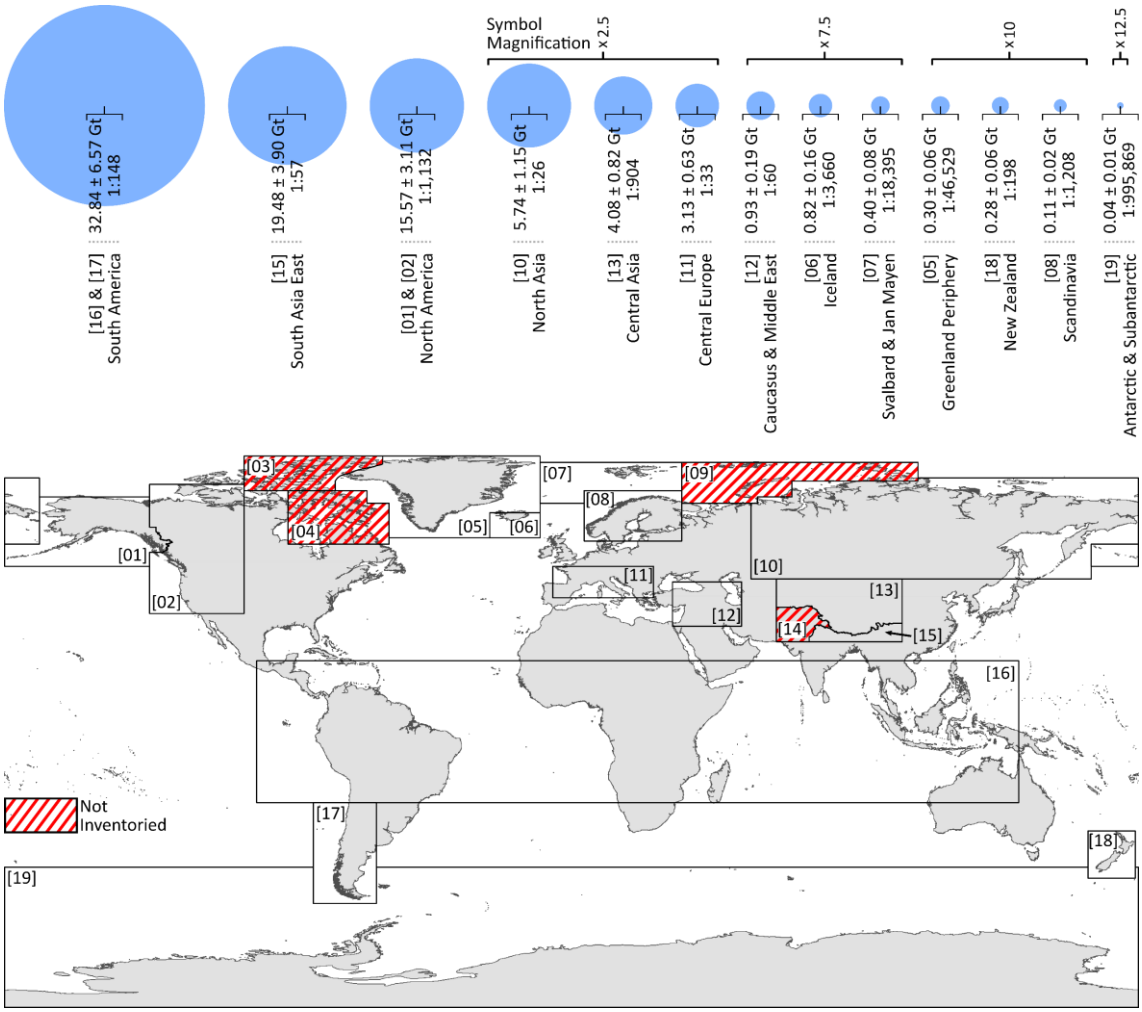

Figure 4.6. Near-global rock glacier WVEQ (Gt) and ratios of rock glacier-to-glacier WVEQ. Rock glacier WVEQs (blue circles) are sized proportionately to the whole. Rock glacier WVEQs reflect 50 ± 10% ice content by volume. The data are organised into the first-order RGI regions, which are reflected in the accompanying world map. No

systematic rock glacier inventory studies have been undertaken in RGI regions *03* (Arctic Canada North), *04* (Arctic Canada South), *09* (Russian Arctic), and *14* (South Asia West). Data are derived from Jones et al. (2018a).

Importantly, near-global- and RGI-regional-scale ratios (**Figure 4.6**) suggest that rock glaciers form considerable water stores; however, arguably the abovementioned ratios mask the potential hydrological value of rock glaciers at a national and regional level, particularly in semi-arid and arid zones where glacier presence is limited/absent. For example, rock glacier-to-glacier WVEQ ratios of 3:1 in parts of the Chilean Andes (29°–32° S) suggests that rock glaciers collectively contain more water than glaciers (Azócar and Brenning, 2010). Furthermore, Janke et al. (2017) conclude that rock glaciers constitute ~50% of surface water storage in the Aconcagua River Basin, further south in Chile. Elsewhere, studies in Bolivia estimate rock glacier-to-glacier WVEQ ratios to be 1:7 (Sajama region) (Rangecroft et al., 2015) and as high as 1:3 in the West region of Nepal (Jones et al., 2018b). This emphasises the importance of rock glaciers as non-negligible water stores. Indeed, the recently adopted National Glacier Law of Argentina[3] protects glaciers and rock glaciers as strategic water reserves, prohibiting detrimental human activities (e.g., mining and oil and gas activities) in their vicinity, recognising the potential hydrological value of such features. Nonetheless, although a small number of national-scale glacier inventories include rock glaciers, such as the Inventario Nacional de Glaciares of Argentina (Zalazar et al., 2017; IANIGLA-CONICET, 2018), they are omitted from global-scale glacier databases, e.g., the RGI (Pfeffer et al., 2014) or glacier outlines available from Global Land Ice Measurements from Space (GLIMS) glacier inventory (www.glims.org) – it is conceivable that in their absence, rock glaciers could be considered as hydrologically insignificant by the wider scientific community and decisionmakers. In addition, while rock glacier inventory density is high in certain areas (e.g., Central Europe [Jones et al., 2018a]) further inventories are required to better understand the hydrological significance of rock glaciers, particularly where future climate warming will likely considerably impact freshwater resources in the long-term (e.g., Andes, Hindu Kush, etc.). With this in mind, it is important to provide an overview of the techniques to assess both rock glacier distribution (**section 4.5.1**) and subsurface characteristics (**section 4.5.2**).

[3] Law No. 26.639, "Minimum Standards Regime for Preservation of Glaciers and Periglacial Environment". Available to view online (in Spanish): http://servicios.infoleg.gob.ar/infolegInternet/anexos/170000-174999/174117/norma.htm.

4.5.1 APPROACHES FOR ASSESSING ROCK GLACIER DISTRIBUTION

Whereas debris-free glaciers can feasibly be mapped/monitored through the application of semi-automated and automated remote sensing classification techniques applied to optical satellite data (e.g., Bolch et al., 2010; Guo et al., 2015), the continuous debris-layer that characterises rock glaciers confounds such approaches. In explanation, rock glacier – and debris-covered glacier – surficial debris and debris from the surrounding slopes share a mutual origin; thus their spectral similarity "render[s] them mutually indistinguishable" (Shukla et al., 2010) using spectral properties alone. Accordingly, combined methodologies have been developed to identify debris-covered glaciers (Paul et al., 2016), for example using multispectral [optical and thermal] satellite data (e.g., Shukla et al., 2010); however, such approaches are generally unsuitable for mapping rock glaciers or heavily debris-covered glaciers (e.g., Brenning, 2009). Consequently, rock glacier inventory compilation by means of manual-recognition, -delineation and -classification (i.e. dynamic behaviour) using representative rock glacier features (**section 4.3.1**; **Figure 4.1**) (e.g., Scotti et al., 2013; Schmid et al., 2015) arguably remains the optimum approach. As such, rock glacier inventories are inherently subjective (see Scotti et al., 2013; Schmid et al., 2015; Jones et al., 2018b), influenced as they are by the expertise and field knowledge of the mapper. In particular, this is evident in the case of ongoing glacier-rock glacier interactions (cf. Monnier and Kinnard, 2015b) (**section 4.3.2**) where defining the divide between rock glaciers and debris-covered glaciers can prove challenging, especially where rock glaciers are not well-developed (i.e. lacking their characteristic surface features) (e.g., Mölg et al., 2018). These ongoing glacier-rock glacier interactions are commonly not included in either glacier, e.g., the RGI (Pfeffer et al., 2014) or GLIMS, or rock glacier inventories in spite of their potential future hydrological value and we argue their inclusion is of critical importance.

Of further influence on rock glacier inventory accuracy are the resolution and quality of both the terrain (i.e. digital elevation model [DEM] and maps) and optical (i.e. aerial or satellite imagery) data used. The increased availability of spatial data with high repeat frequency in recent years has enabled existing rock glacier inventories to be updated, so the global picture is becoming more complete (e.g., Kellerer-Pirklbauer et al., 2012; Janke et al., 2017). Additionally, open-source and new types of data have provided enhanced opportunities for rock glacier mapping and monitoring, with: (i) fine spatial resolution optical data (e.g., QuickBird, WorldView-1 and 2, IKONOS) accessible freely through Google Earth enabling large-scale rock glacier inventories to be compiled (e.g., Rangecroft et al., 2014; Schmid et al., 2015; Jones et

al., 2018b); (ii) finer than 1 m resolution LiDAR (light detection and ranging [i.e. airborne laser scanning]) data enabling heavily vegetated relict rock glaciers, which can significantly influence catchment hydrology (Winkler et al., 2016b) (see **section 4.6.3**), to be mapped (e.g., Colucci et al., 2016); and (iii) InSAR (Interferometric Synthetic Aperture Radar) data (e.g., ESA Sentinel-1) enabling both rock glacier mapping and accurate classification of activity type through the investigation of surficial kinematics, such as feature displacement (Kenyi and Kaufmann, 2003; Strozzi et al., 2004; Lambiel et al., 2008; Echelard et al., 2013; Liu et al., 2013; Barboux et al., 2014; Wang et al., 2017; Imaizumi et al., 2018; Villarroel et al., 2018).

We argue that further research addressing the controls on rock glacier distribution and development (see Johnson et al., 2007; Forte et al., 2016; Kenner and Magnusson, 2017) could further exploit the abovementioned data to identify suitable "habitats" for rock glaciers, thereby encouraging more efficient inventory compilation in rock glacier data-deficient regions. Research efforts with respect to this, for instance, using statistical estimation techniques and generalised additive modelling with terrain/optical data (e.g., Brenning et al., 2007; Azócar and Brenning, 2010; Brenning and Azócar, 2010), have already been undertaken. Further improvements within this research area may enable semi-automated or automated identification and mapping of rock glaciers over larger spatial scales in the future, although this would demand the use of new datasets, e.g., time-series of SAR interferometry data for distinguishing sedimentary areas experiencing ground deformation (rock glaciers) vs static features. Critically, better knowledge of rock glacier distribution and more accurate classification of activity type and temporal dynamics will facilitate an informed assessment of future water supplies with respect to rock glaciers. Furthermore, inventories are time-static, and an ongoing concern should be regular monitoring of rock glaciers using up-to-date satellite data, to determine rates of change and wastage over large extents. With new satellite systems in orbit, such as the Sentinel-1 SAR constellation, we are entering a time where routine regular observations can be used to update inventories (e.g., Villarroel et al., 2018), and as Paul et al. (2016) explain this could "considerably improve over previous capabilities, thanks to increased spatial resolution and dynamic range, a wider swath width and more frequent coverage". Rock glacier scientists should also explore the capabilities offered by cloud-based image processing on Google Earth Engine, which could enhance the efficiency with which such large volumes of data can be processed in the future (Gorelick et al., 2017).

4.5.2 APPROACHES FOR ASSESSING ROCK GLACIER SUBSURFACE CHARACTERISTICS

4.5.2.1 INTERNAL STRUCTURE

Information concerning the number, spatial distribution and morphometric characteristics of rock glaciers is useful; nevertheless, complementary subsurface data (i.e. internal structure: origin, thickness and proportional ice content, hydrological flowpaths) are required to better understand the hydrological role of rock glaciers. Knowledge of the subsurface properties of rock glaciers is derived predominantly from geophysical techniques such as ground-penetrating radar (GPR), electrical resistivity tomography (ERT) and seismic refraction tomography (for reviews see: Scott et al., 1990; Maurer and Huack, 2007; Kneisel et al., 2008; Hauck, 2013). Geophysical investigations suggest that rock glacier internal structure comprises four general layers: (i) a debris mantle (i.e. AL) with a thickness in the order of meters; (ii) an ice-rich (i.e. high ice content [vol%]) frozen layer a few tens of metres thick; (iii) ice-poor (i.e. low ice content) or ice-free sediments underlying the ice-rich layer; and (iv) the surface of the bedrock. For example, the Ölgrube and Kaiserberg rock glaciers (Ötztal Alps, Austria) each comprise a 4–6 m thick AL that is underlain by ice-rich permafrost 20–30 m in thickness, then 10–15 m of ice-free sediments (Hausmann et al., 2012). The above-described subsurface composition has been confirmed through geophysical investigations at a number of other rock glaciers (e.g., Isaksen et al., 2000; Fabrot et al., 2005; Hausmann et al., 2007; Bodin et al., 2009). Furthermore, information from boreholes drilled through the well-studied Murtèl-Corvatsch and Muragl rock glaciers (Haeberli et al., 1998; Arenson et al., 2002) also support the general rock glacier internal structure as earlier described (Kääb, 2013). Importantly, rock glacier subsurface characteristics (e.g., AL thickness, multiple ice origins [i.e. freezing of sub- and supra-groundwater, seasonal snow accumulation, avalanching and buried glacial ice], volumetric ice content, permafrost table topography, rock debris abundance, etc.) within and between rock glaciers can be highly heterogeneous (Haeberli et al., 2006) (**Figure 4.7**). Two cores drilled on the Lazaun rock glacier in the southern Ötztal Alps, Italy, further demonstrate the horizontal and vertical heterogeneity of rock glacier subsurface structure and ice content (Krainer et al., 2015) (**Figure 4.8**). This spatial heterogeneity is also reported at the Las Liebres rock glacier (Chilean Andes, Chile) where ice content markedly varies along a longitudinal GPR profile (22–83%) (Monnier and Kinnard, 2015a).

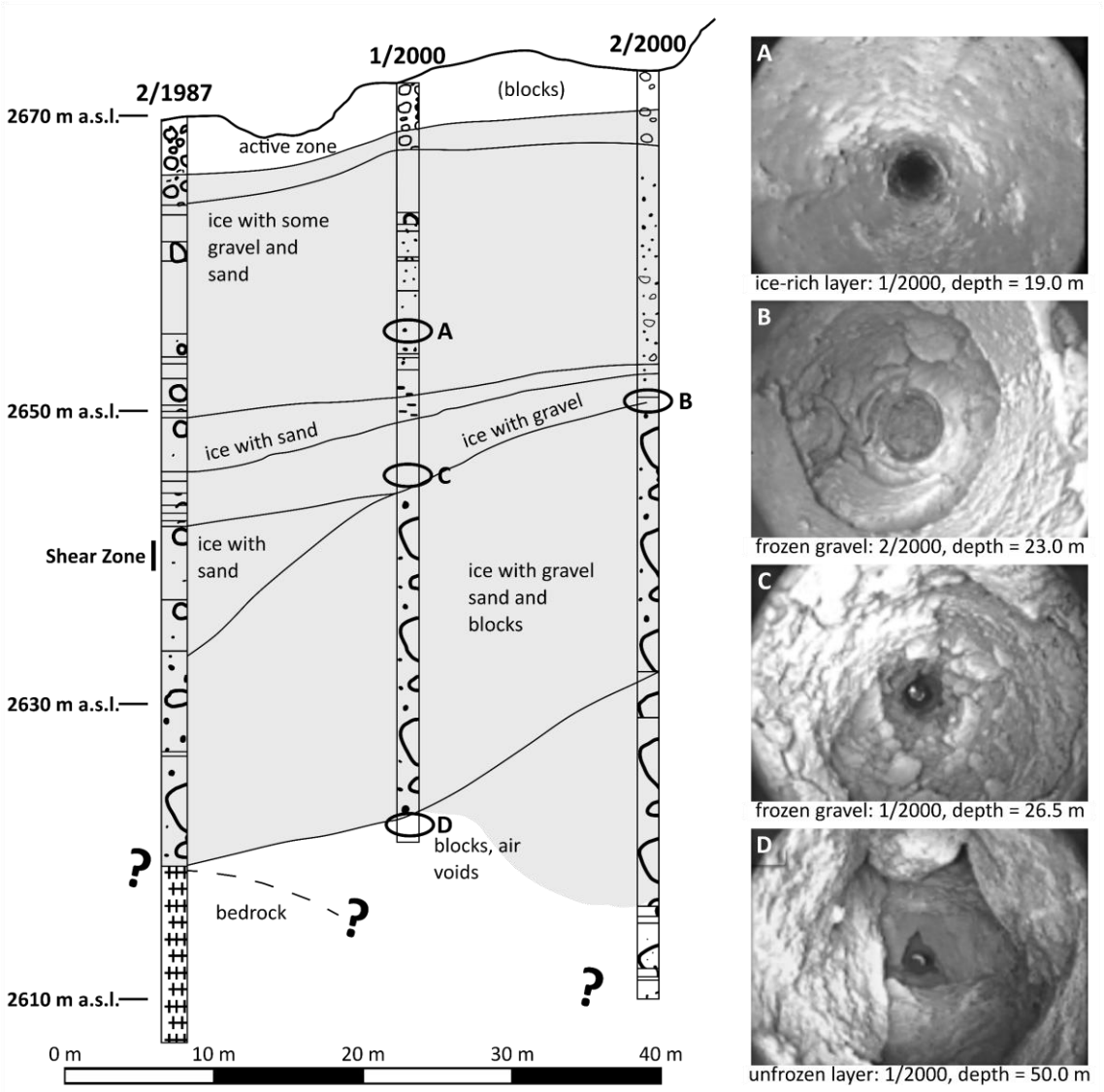

Figure 4.7. Detailed stratigraphy of the Murtèl-Corvatsch rock glacier through three boreholes (BH 2/1987, BH 1/2000 and BH 2/2000) (Arenson et al., 2002). Photographs A-D from a borehole camera reflect the stratigraphy of the rock glacier at 19.0 m, 23.0 m, 26.5 m and 50.0 m depths. These subsurface investigations demonstrate the heterogeneity of rock glaciers, with zones of massive and interstitial ice present. Modified after Springman et al. (2012).

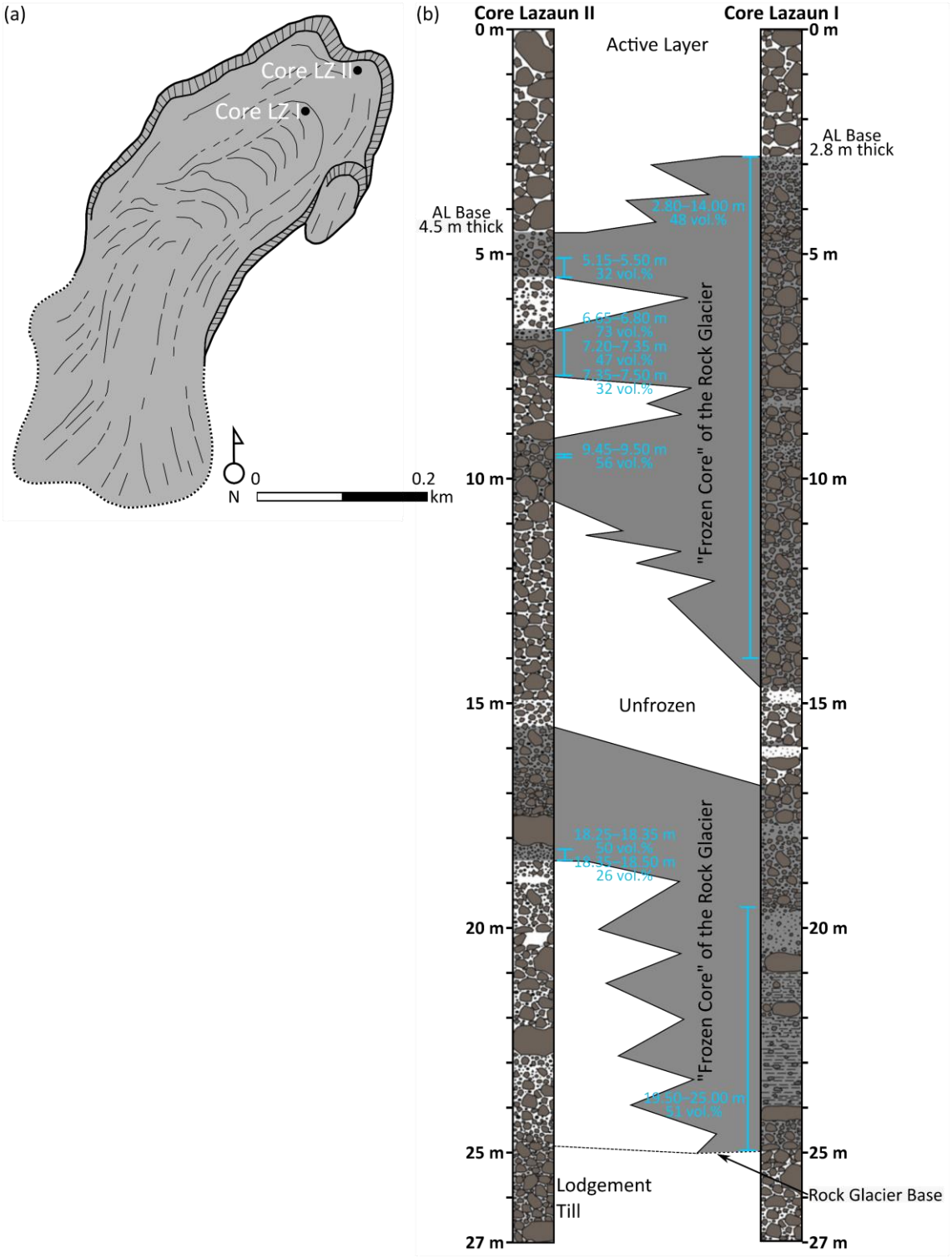

Figure 4.8. (a) Map of the Lazaun rock glacier including the locations of core Lazaun I and II; (b) the rock glacier internal structure from core Lazaun I and II. The average ice content of core Lazaun I is 43 vol%, varying between 0 and 98 vol% and core Lazaun II is 22 vol%, varying between < 2–73%. Examples of higher ice content within the cores are shown. Note the presence of intra-permafrost taliks (particularly in core Lazuan II), the formation of which has been attributed to advective and conductive heating by infiltrating water and circulating air (Luethi et al., 2017). Modified after Krainer et al. (2015).

While significant progress has been made regarding scientific knowledge of the interior characteristics of rock glaciers, such understanding is derived from a relatively small number of

features due to the formidable logistical challenges of fieldwork in such environments (e.g., government restrictions on sampling and/or equipment use, field location accessibility, presence of large boulders and megaclasts [i.e. b-axis > 4.1 m] at the surface [**Figure 4.4b**]) that would require considerable expense and time to overcome, particularly drilling (Degenhardt Jr and Giardino, 2003; Janke et al., 2013). Indeed, very few rock glaciers have been drilled (see Table 3 in Haeberli et al., 2006). Therefore, although non- or minimally invasive geophysical techniques can rapidly provide 2-D subsurface data over extended survey areas, in contrast to 1-D information provided by drilling (Haeberli et al., 2010), geophysical investigations have rarely been validated by direct measurements (Degenhardt Jr and Giardino, 2003; Hauck and Kneisel, 2008). As a consequence, where detailed information on the density and composition of rock glaciers are unavailable, and geophysical data quality is variable, significant uncertainties in the interpretation of geophysical data can occur due to ambiguities in relating subsurface data to material properties within the rock glacier (e.g., differentiating between rock and ice) (Hauck et al., 2011; Hauck, 2013).

In response, innovative, alternative methodologies have been developed; for example, at the Äußeres Hochebenkar rock glacier (Ötztal Alps, Austria), feature thickness was calculated using a simple creep model based on high-resolution surface displacement and slope data derived from multitemporal DEMs. Comparison of model results and GPR data proved helpful in fine-tuning the analysis of the latter (Hartl et al., 2016a). Also, where multitemporal high-resolution DEMs are available, rock glacier thickness and volume could be estimated with this method (Hartl et al., 2016a). As the modelling approach of Hartl et al. (2016a) accounts for individual rock glacier-specificities (i.e. rock glacier dynamics and local topography), estimated rock glacier thickness and volume will be more accurate than those generated using more general approaches, such as empirical power-law relations (**section 4.5.2.2**).

Of further note, improved geophysical techniques will provide opportunities to improve understanding of rock glacier internal structure and ice content. For example, helicopter-mounted quasi-3-D GPR was recently successfully used to investigate the internal structure of Furggwanghorn rock glacier, Swiss Alps (Merz et al., 2015a; Merz et al., 2015b), overcoming some of the logistical challenges associated with detailed *in situ* geophysical surveys. Emmert and Kneisel (2017) found that quasi-3-D ERT enables the mapping and monitoring of spatial variations within the rock glacier internal structure, with considerable potential to deliver new insights into surface and subsurface process-linkages. Additionally, the geophysically based 4-

phase model (see Hauck et al., 2011) combines ERT and refraction seismic tomography measurements to obtain volumetric proportions and characterise the lateral and vertical distribution of the rock glacier constituents: air, water, ice, and rock. The model has already been successfully applied to rock glaciers for this purpose (e.g., Hauck et al., 2011; Schneider et al., 2013). Furthermore, Mewes et al. (2017) demonstrate the suitability of the 4-phase model for detecting interannual and seasonal phase change between liquid water and ice in rock glaciers; therefore, this model is a valuable tool for monitoring degradation of the internal ice body (**section 4.4**). These new techniques will provide a platform to better understand the internal structure, dynamics and response of rock glaciers to future warming. In particular, more detailed geophysical investigations may enable volume and WVEQ estimation for glacier-rock glacier transitional forms (**section 4.3.2**), for which simplified geomorphometric approaches (**section 4.5.2.2**) are not suitable due to the internal complexity of such features (Bolch et al., 2019a).

4.5.2.2 VOLUME AND WVEQ

Since detailed subsurface information is available for only a limited number of rock glaciers, 2-D-area-related statistics have enabled first-order approximations of thickness and volume of unmeasured rock glaciers. In particular, *empirical thickness-area (H-S) relations* have been applied to predict rock glacier thicknesses and derive rock glacier volume (e.g., Brenning, 2005a; Azócar and Brenning, 2010; Bodin et al., 2010; Perucca and Esper Angillieri, 2011; Rangecroft et al., 2015; Janke et al., 2017; Jones et al., 2018a, 2018b). Empirical H-S relations can be expressed as $\bar{h} = c \cdot S^{\beta}$, where mean rock glacier thickness $\bar{h}$ (m) is calculated as a function of surface area *S* (km²) and a scaling parameter *c* (50) and scaling exponent *β* (0.2) (Brenning, 2005a). Rock glacier volumes were determined by $V = \bar{h} \cdot S$. Rock glacier WVEQ was subsequently estimated through the multiplication of *V* and estimated ice content (% by vol.) and assuming an ice density conversion factor of 900 kg m^{-3} (Paterson, 1994).

To our knowledge, no study has evaluated empirical power-law relations (i.e. H-S and V-S [volume-area] scaling relations) for their suitability to approximate rock glacier thickness and volume. Empirical power-law relations have been evaluated in relation to glaciers (see Frey et al., 2014; Bahr et al., 2015), upon which they have more commonly been used to predict regional- and global-scale glacier thickness and volume (e.g., Chen and Ohmura, 1990; Bahr et al., 1997; Radić and Hock, 2010; Grinsted, 2013; Andreassen et al., 2015). Frey et al. (2014) demonstrate that considerable uncertainty is associated with the application of power-law relationships for

this purpose. It is reasonable to assume that shortcomings experienced when applying these approaches to glaciers and rock glaciers are similar. Regarding V-S scaling relations (i.e. $V = c \cdot S^{\gamma}$ [where γ is $\beta + 1$]) for glaciers, the scaling exponent γ is considered a constant (Bahr et al., 1997, 2015) whereas the scaling parameter c should be considered as a variable determined by several parameters that vary between glaciers (e.g., basal topography, sliding parameters, ice-flow parameters) (Bahr et al., 2015). Further, several researchers have suggested different, region-specific values for both c and γ from the regression of the available data (see Grinsted, 2013). Brenning's (2005a) empirical power-law relation was developed from morphometric field measurements at 19 rock glaciers in the Andes of Santiago, Chile (Bodin et al., 2010). As such, this approach cannot account for regional specificities of rock glaciers around the world (e.g., dominant ice origin, local climatic parameters, local topography, etc.) (Jones et al., 2018a) that could reasonably be expected to influence the value of scaling parameter c, as described above. To date, a constant scaling parameter c and scaling exponent β have thus been used in rock glacier studies applying Brenning's (2005a) empirical power-law relation (e.g., Brenning, 2005a; Azócar and Brenning, 2010; Bodin et al., 2010; Perucca and Esper Angillieri, 2011; Rangecroft et al., 2015; Janke et al., 2017; Jones et al., 2018a, 2018b). Therefore, use of such methods with respect to rock glaciers requires careful and critical evaluation. To improve the effectiveness of empirical power-law relations for rock glaciers requires that (i) the physics (i.e. dynamics) of rock glaciers are better understood, (ii) the sample size used to constrain the scaling parameter c and choose the value for β needs to be increased, and (iii) the scaling parameter c is localised.

Previous studies predicting rock glacier WVEQ have assumed a 'typical' volumetric rock glacier ice content of 50% (Brenning, 2005b; Azócar and Brenning, 2010; Perucca and Esper Angillieri, 2011) – WVEQ values for 40–60% vol. (i.e. lower [40%], mean [50%] and upper [60%] estimates) are sometimes provided to account for uncertainty (Brenning, 2005a; Bodin et al., 2010; Rangecroft et al., 2015; Jones et al., 2018a, 2018b) – consistent with *in situ* data derived from different climatic regions worldwide (e.g., Elconin and LaChapelle, 1997: >50%; Arenson et al., 2002: 40–70%; Croce and Milana, 2002: ~55%; Hausmann et al., 2007: 45–60%; Hausmann et al., 2012: 40–60%). Importantly, studies that have used Brenning's (2005a) empirical power-law relation – excluding Janke et al. (2017) – have considered intact rock glaciers (i.e. active and inactive rock glaciers treated collectively). Yet, Arenson and Jakob (2010) suggest that the application of the abovementioned statistical model should better differentiate between the volumetric ice content of active and inactive rock glaciers. Indeed, a classification

system for debris-covered glaciers and rock glaciers divides the latter into three subclasses: (i) "Class 4: Proper" (i.e. active), ice content = 25–45%; (ii) "Class 5: Transitional" (i.e. inactive), ice content = 10–25%; and (iii) "Class 6: Glacier of rock" (i.e. relict), ice content ≤ 10% (Janke et al., 2015). As a consequence, large uncertainties will be introduced to rock glacier WVEQ predictions by the typically lower volumetric ice content of inactive rock glaciers (Brenning, 2010). In addition, existing rock glacier WVEQ estimations have not considered volumetric air content, reported to be up to 25% in intact rock glaciers (Arenson and Springman, 2005), that would further reduce predicted WVEQ (Arenson and Jakob, 2010). Nonetheless, existing rock glacier WVEQ estimations provide a much-needed first approximation that should stimulate further research and gain the attention of policymakers.

4.6 ROCK GLACIER WATER DISCHARGE

4.6.1 CHARACTERISTICS OF ROCK GLACIER DISCHARGE

To date, only very few studies have investigated the hydrological aspects of rock glacier water discharge, in spite of recent research reporting that rock glaciers constitute non-negligible long-term water stores (**section 4.5**). Besides the above-stated formidable logistical challenges of rock glacier-related fieldwork (**section 4.5.2.1**), this is because water discharge measurements are challenging or virtually impossible to conduct for rock glaciers (i) with multiple, often inaccessible springs (Krainer et al., 2012), (ii) with no spring(s), i.e. the water drains within the debris (Krainer and Mostler, 2002), (iii) that grade into downslope landforms, and (iv) that terminate in lakes or ponds (Colombo et al., 2018c). Based on the few available measurements, the discharge from springs of intact rock glaciers is estimated to range from <1 to >1,000 L s^{-1} during the melt season (**Table 4.2**).

Table 4.2. Discharge from intact rock glaciers during the melt season.

Rock Glacier Name	Location	Discharge (L s^{-1})	Reference
Gruben	Swiss Alps, Switzerland	2–50	(Haeberli, 1985)
Hilda	Rocky Mts., Alberta, Canada	90–270*	(Gardner and Bajewsky, 1987)
Dos Lenguas	Central Andes, Argentina	5–8	(Schrott, 1991, 1996)
East Slims River	St. Elias Mts., Yukon, Canada	0.7–3.7	(Harris et al., 1994)
Morenas Coloradas	Central Andes, Argentina	230–1,000	(Trombotto et al., 1997)
Reichenkar	Stubai Alps, Austria	20–375	(Krainer and Mostler, 2002)
Gößnitz	Hohe Tauern Mts., Austria	5–310	(Krainer and Mostler, 2002)
Innere Ölgrube	Ötztal Alps, Austria	30–1,000	(Berger et al., 2004)
Kaiserberg	Ötztal Alps, Austria	25–600	(Krainer et al., 2007)
Reichenkar	Stubai Alps, Austria	20–450	(Krainer et al., 2007)
Mt. Tukuhnikivatz	La Sal Mts., Utah, USA	0.1–25.2	(Geiger et al., 2014)
Lazaun	Southern Ötztal Alps, Italy	9–140	(Krainer et al., 2015)
Äußeres Hochebenkar	Ötztal Alps, Austria	10–300	(Nickus et al., 2015)

* The Hilda rock glacier has been classified as an inactive rock glacier (Luckman and Crockett, 1978). Furthermore, Harris et al. (1994) note that the rock glacier spring " is actually a groundwater spring mantled by the rock glacier" , and thus the results may not reflect only rock glacier discharge.

Intact rock glacier discharge patterns are characterised by strong seasonal and diurnal variability, primarily determined by local weather conditions, the thermal conditions within the AL, and the physical mechanisms that control meltwater flow through the rock glacier (Krainer and Mostler, 2002; Berger et al., 2004; Krainer et al., 2007, 2015). The water released from intact rock glaciers is derived from (i) melting of the winter snowpack, (ii) melting of glacier ice, (iii) melting of rock glacier ice, (iv) rainfall, particularly during summer thunderstorms with heavy rainfall, and (v) groundwater (Krainer and Mostler, 2002). The contribution to intact rock glacier discharge of the abovementioned water sources changes considerably during the melt season. Typically, discharge rates are highest during the spring/early summer snowmelt and gradually decline through summer and autumn to low or zero flow in the winter months. In addition, rock glacier discharge fluctuates strongly in response to rainfall events and periods of colder weather with snowfall (Johnson, 1981; Blumstengel and Harris, 1988; Krainer and Mostler, 2002; Berger et al., 2004; Krainer et al., 2007) (**Figure 4.9**). Further, intense melting of the winter snowpack during periods of warm weather produce marked diurnal runoff cycles, with low discharge at noon and peak discharge towards late evening (Krainer and Mostler, 2002). In this respect, generally, rock glacier discharge patterns mimic those of glaciers, although at considerably lower magnitude (Krainer and Mostler, 2002; Geiger et al., 2014). Additionally, various authors suggest that rock glacier discharge fluctuates less than glaciers (Potter, 1972; Corte, 1976, 1987; Gardner and Bajewsky, 1987), at least on diurnal timescales (Haeberli, 1985; Pourrier et al., 2014); however, few have demonstrated this empirically.

Isotopic analyses of rock glacier springs, alongside discharge and electrical conductivity sampling (EC) data, support the above-described seasonal evolution of intact rock glacier discharge composition (Krainer and Mostler, 2002; Berger et al., 2004; Williams et al., 2006; Krainer et al., 2007). For example, Krainer et al. (2007) report that rock glacier discharge in the Stubai and Ötztal Alps, Austria, exhibits: (i) intermediate $\delta^{18}O$ values at the beginning of the melt season, reflecting the mixed origin of runoff from re-frozen meltwater from the preceding autumn (high $\delta^{18}O$) and snowmelt (low $\delta^{18}O$); (ii) significantly reduced $\delta^{18}O$ and EC values following the onset of spring discharge, with runoff predominantly derived from snowmelt; and (iii) gradually increasing $\delta^{18}O$ and EC values during the melt season, which reflect the continued depletion of the winter snowpack and increased icemelt (i.e. melting of the frozen rock glacier core) and groundwater contributions. Intermittent sharp peaks in rock glacier discharge, $\delta^{18}O$ values and concomitant depressions of EC suggest that outflows temporarily

derive predominantly from summer rainfall events (which have higher $\delta^{18}O$ values and are EC-depleted) (Krainer et al., 2007) (**Figure 4.9**).

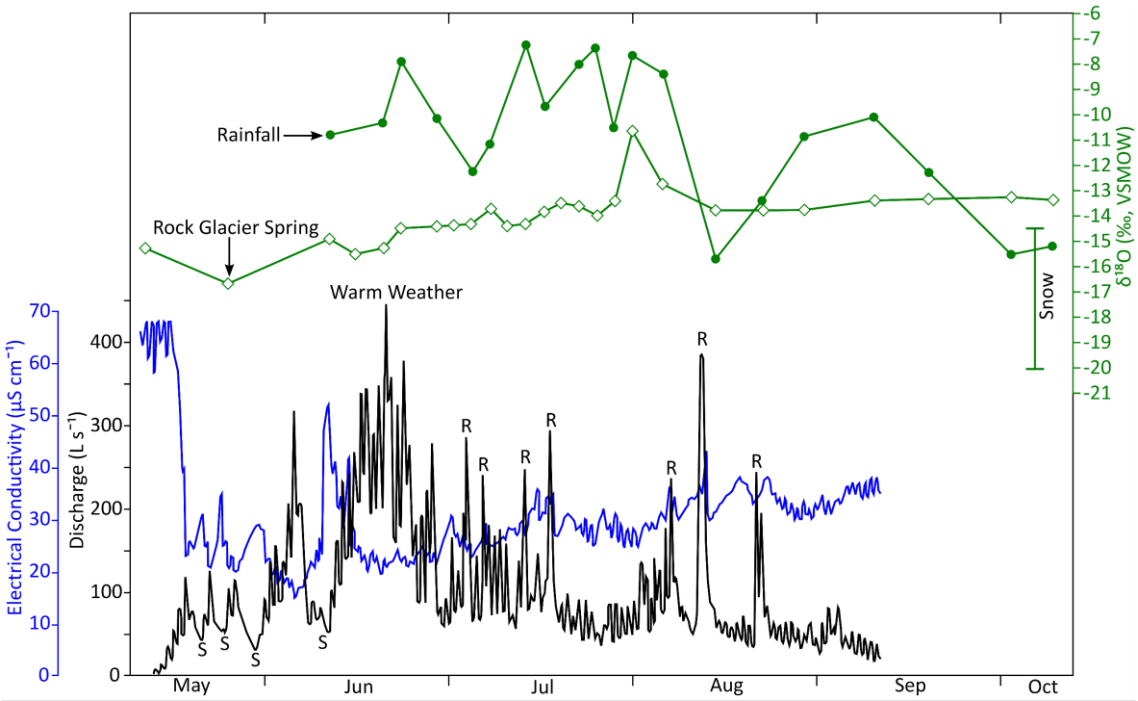

Figure 4.9. Hydrograph of the meltwater stream at the Reichenkar rock glacier and EC between mid-May and mid-September 2002. Major snowfall (S) and rainfall (R) events vs Oxygen isotope composition ($\delta^{18}O_{water}$) of the rock glacier spring and rain precipitation is also depicted for the period from mid-May to mid-October 2002. The snow profile was sampled in April 2002. Of note, $\delta^{18}O$ values of the frozen rock glacier core (not depicted) are similar to those of the rock glacier spring. Modified after Krainer et al. (2007).

Of note, previous studies have primarily investigated the temporal evolution of $\delta^{18}O$ in conjunction with discharge and EC data to ascertain the origins of rock glacier outflows. Yet hitherto very few attempts have been made to determine the proportional contribution to rock glacier discharge of different sources. Williams et al. (2006) analysed the outflow components of the Green Lake 5 rock glacier (Colorado Front Range, USA) through geochemical and stable isotopic analyses in combination with end-member mixing analysis: 30% was snowmelt, 32% was soil water, and 38% was baseflow – the latter includes icemelt. Notably, studies have not successfully isolated the contribution of icemelt to rock glacier discharge (Krainer et al., 2007); however, seasonal discharge, $\delta^{18}O$ and EC data, as prior discussed, suggest water released from rock glaciers principally derives from snowmelt, glacial meltwater and intermittent rainfall events, with negligible or non-measurable contributions derived from icemelt (Croce and Milana, 2002; Krainer and Mostler, 2002; Krainer et al., 2007). Minimal icemelt contributions are predominantly due to the insulative effects of the AL, which prevents substantial melt rates (**section 4.4**). For instance, Krainer et al. (2015) estimate that melting of the frozen rock

glacier core contributed ~0.6 L s^{-1} or ~2.3% of the total annual mean discharge of ~26 L s^{-1} during the melt season at the Lazaun rock glacier. At the Helen Creek rock glacier (Banff National Park, Alberta, Canada) – an inactive feature – minimal icemelt contributions (3–5% [July-August]) support these findings (Harrington et al., 2018). Elsewhere, using radioisotope analysis, Cecil et al. (1998) compared tritium concentrations in rock glacier outflows (9.2–13.2 TU [Tritium Units]) to those in an ice core at the same location (-1.3–0.2 TU). They conclude that frozen rock glacier core formation pre-dates the peak of above-ground nuclear weapons testing (1950s/1960s), whereas rock glacier outflows primarily derive from modern precipitation (i.e. minor contributions from icemelt).

Notably, rock glacier-catchment hydrology interactions remain poorly understood, and opinions regarding the hydrological contributions of rock glaciers diverge. Indeed, a number of studies have suggested that rock glacier hydrological contributions to downstream runoff are significant; however, the majority of these conclusions are based upon non-quantitative data (for summary see Duguay et al., 2015). It is important to note that investigations focused upon rock glacier hydrology generally consider present as opposed to future rock glacier hydrological contributions. Therefore, thus far the hydrological significance of rock glaciers has been defined according to a restricted timescale. Critically, while rock glaciers form long-term water stores and thus may not constitute a readily available water resource (Duguay et al., 2015; Rangecroft et al., 2015), at decadal and longer timescales, under climate warming, degradation of the frozen rock glacier core may represent an increasing hydrological contribution to streamflow (Thies et al., 2013; Geiger et al., 2014).

4.6.2 CHARACTERISATION OF ROCK GLACIER HYDROLOGICAL FLOWPATHS

Importantly, as well as rock glacier hydrological contributions, rock glacier-catchment hydrology interactions should be considered with respect to discharge timing. In addition to the seasonal availability of different water sources (**section 4.6.1**), rock glacier discharge timing is determined by spatially- and temporally-variable, convoluted subsurface flowpaths (Burger et al., 1999). Based upon the following information, a model of the hydrological flowpaths within rock glaciers of periglacial and glacial origin was constructed (**Figure 4.10**).

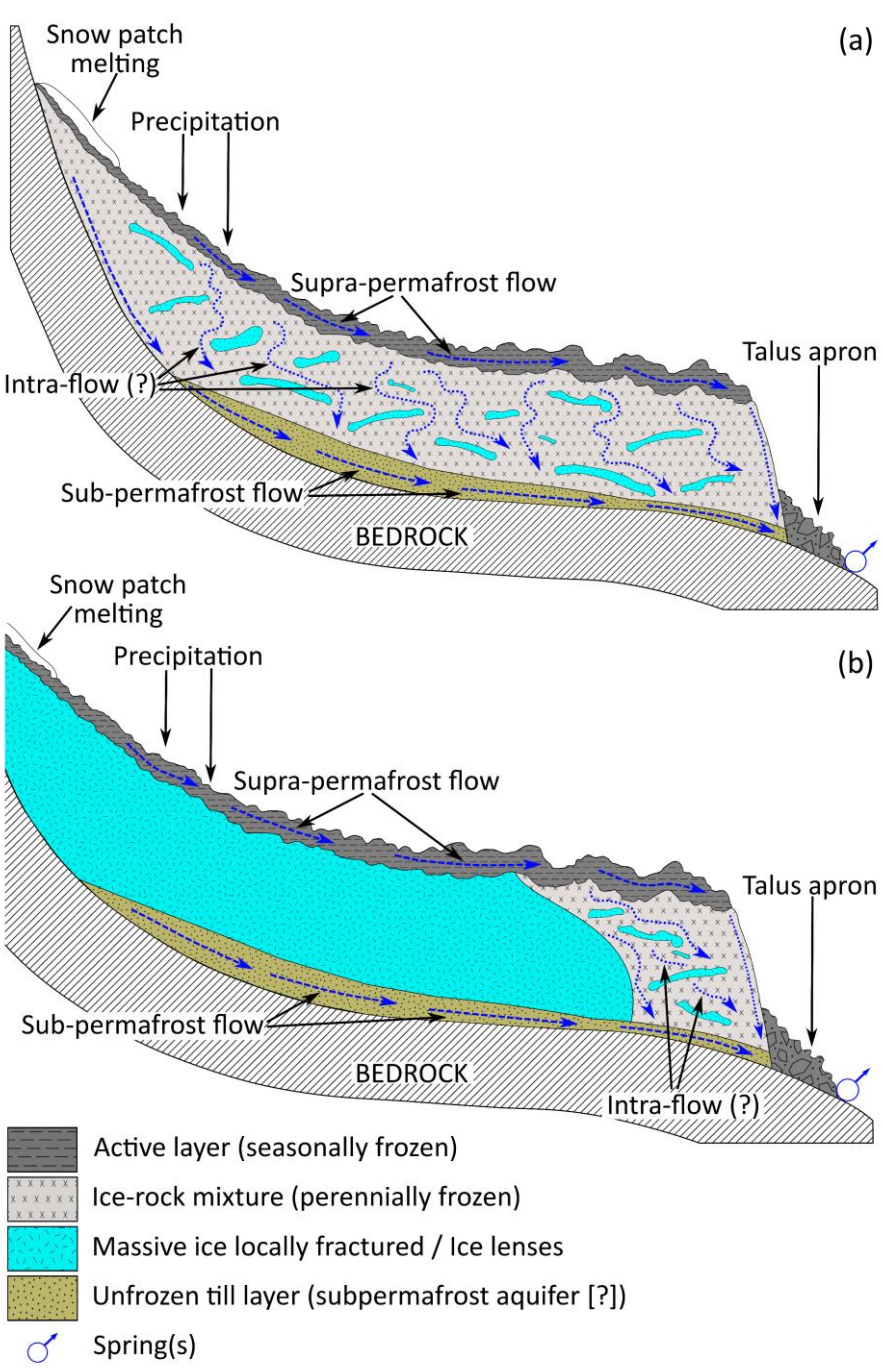

Figure 4.10. A simplified hypothetical model of hydrological flowpaths through an active rock glacier of (a) periglacial origin, and (b) glacial origin. N.B. hydrological flowpath terminology was maintained for [a] and [b] for consistency (i.e. supra-*permafrost*, intra-*permafrost*, and sub-*permafrost* flow), regardless of the dominant ice origin. Arrows depict the flowpath direction.

Conceptual models of rock glacier hydrology suggest that subsurface water movement occurs along two flowpath types: *supra-permafrost flow* and *sub-permafrost flow* atop and below an impermeable frozen rock glacier core, respectively (Giardino et al., 1992). This is consistent with the conclusions of Krainer and Mostler (2002) who identified two storage reservoirs, the "quickflow reservoir" (herein *quickflow*) and "baseflow reservoir" (herein *baseflow*), which correspond to supra-permafrost flow and sub-permafrost flow, respectively. Rock glacier

hydrographs, dye tracer tests and EC values demonstrate that quickflow and baseflow have significantly different characteristics of water storage and release (Krainer and Mostler, 2002). These characteristics are likely determined by the AL thickness (i.e. depth of the 0 °C isotherm), hydraulic connectivity, sedimentological characteristics, and the degree of rock glacier activity (i.e. volumetric ice content [% by vol.]) (Tenthorey, 1992; Harris et al., 1994; Krainer and Mostler, 2002; Williams et al., 2006; Buchli et al., 2013).

Dye tracer test results reported in Tenthorey (1992) and Krainer and Mostler (2002) indicate flow velocities of 54–327 m h^{-1}, demonstrating that the coarse-blocky openwork structure of the AL promotes quickflow. Elsewhere, the rapid temporal evolution of rock glacier discharge in conjunction with $\delta^{18}O$ and EC values suggests that waters derived from high-intensity weather events (i.e. intense snowmelt or summer rainfall events) are generally transmitted through active rock glaciers as quickflow with a lag time of a few hours (Krainer et al., 2007) (**Figure 4.9**). These results also show that quickflow occurs predominantly as channelised flow along a network of conduits eroded into the frozen rock glacier core (Krainer and Mostler, 2002). Occasionally, quickflow is visible and/or audible in the AL of intact rock glaciers (Tenthorey, 1992; Krainer and Mostler, 2002; Berger et al., 2004; Rogger et al., 2017).

Baseflow contributions are likely to form a relatively small proportion of water discharge and are characterised by high EC values, indicating that baseflow predominantly derives from slow diffuse groundwater flow transiting through unfrozen, fine-grained material at the base of the rock glacier (e.g., Krainer and Mostler, 2002). Investigations of the internal structure of active rock glaciers confirm the presence of ice-free, fine-grained sediments at the base of rock glaciers (**section 4.5.2.1**), supporting the presence of the baseflow reservoir. Water tracer tests indicate that baseflow exhibits highly variable residence times, ranging from several days to several months (e.g., Tenthorey, 1992; Harris et al., 1994). Following depletion of the snow cover, rock glacier hydrographs and EC data demonstrate that baseflow contributions increase (e.g., Krainer and Mostler, 2002).

A further subsurface flowpath in rock glaciers with low ice content, *intra-flow* (i.e. slow internal flow), was identified through dye-tracing experiments (Tenthorey, 1992, 1994). Intra-flow also includes water transiting through active rock glaciers by means of unfrozen drainage networks, i.e. *intra-permafrost flow* (Tenthorey, 1992, 1994; Krainer and Mostler, 2002). Intra-permafrost flow has been reported at depth in the frontal portions of active rock glaciers (e.g., Arenson et al., 2010). In explanation, Ikeda et al. (2008) suggested that networks of air voids

and fractures develop within the frozen rock glacier core as a result of fast deformation rates, based upon data from the Büz North rock glacier (Swiss Alps), and thus increased intra-permafrost flow throughout the landform. This has significant implications for rock glacier creep velocities and stability, including via the reduction of effective stress by infiltrated water (Krainer and Mostler, 2006; Perruchoud and Delaloye, 2007; Ikeda et al., 2008); however, these implications are not discussed here. Typically, intra-flow is released from the rock glacier as baseflow.

Importantly, geophysical methodologies, such as the 4-phase model (**section 4.5.2.1**), provide opportunities to estimate the liquid water content within the frozen rock glacier core and to identify preferential subsurface flowpaths (Mewes et al., 2017, and references therein). Limitations and required improvements within the 4-phase model are detailed in Hauck et al. (2011) and Mewes et al. (2017).

4.6.3 ROCK GLACIER-CATCHMENT HYDROLOGY INTERACTIONS

Very few systematic studies of catchment-scale geomorphic drivers of streamflow regimes (i.e. timing, magnitude and duration of discharge) have conducted comparative assessments of the hydrological response between alpine catchments. Physical catchment parameters, including slope, elevation range, drainage area, and bedrock geology, have previously been used to assess inter- and intra-catchment variations in the hydrological response. Contrastingly, the hydrological influence of discrete debris accumulations (DDAs) and/or ice-debris landforms (I-DLs), e.g., talus slopes, protalus ramparts, protalus lobes, and rock glaciers, are largely neglected (Weekes et al., 2015). N.B. ground ice exists within I-DLs. Yet, recent research demonstrates that DDAs and I-DLs can modulate the hydrologic response (e.g., Clow et al., 2003; Geiger et al., 2014; Weekes et al., 2015; Rogger et al., 2017).

In the La Sal Mountains, Utah, a comparative assessment of a [active] rock glaciated vs non-rock glaciated catchment indicates that the presence of active rock glaciers had a pronounced influence upon catchment hydrology (Geiger et al., 2014). Hydrographs from the rock glaciated (i) and non-rock glaciated catchments (ii) are distinctly different. (i) In this catchment, flood peaks are delayed following the onset of precipitation, flood peaks are higher, and the proportion of precipitation leaving the catchment as stormflow is high. (ii) Contrastingly, in this catchment, flood peaks occur much more quickly and are short in duration, and the proportion of precipitation leaving the catchment as stormflow is significantly lower than in the rock glaciated catchment (see Table 2 in Geiger et al., 2014). This indicates that in non-rock

glaciated catchments, significant losses of precipitation to deep groundwater storage may occur. Importantly, rock glacier hydrographs have shown that rock glacier stormflow constitutes a significant proportion of total catchment runoff (15–30%). It appears that the proportion of rock glacier stormflow to catchment stormflow is determined by precipitation intensity rather than precipitation volume. For example, 37.6 mm of precipitation (1.21 mm h^{-1}) and 7.2 mm of precipitation (2.40 mm h^{-1}) derived from two different storms resulted in a 15% and 30% contribution to total catchment runoff, respectively. The above-described observations indicate that active rock glaciers act as impervious surfaces following high-intensity weather events, with the net effect of increasing runoff generation within rock glaciated catchments (Geiger et al., 2014). In the Krummgampen catchment, western Ötztal Alps, Austria, model simulations indicate that complete disappearance of permafrost will reduce flood peaks by ~17%, supporting the above-described findings (Rogger et al., 2017).

Notably, the characteristics of rock glacier water storage and release (i.e. storage behaviour) differ considerably between active, inactive, and relict features. Indeed, lessening of the degree of activity through degradation of the frozen rock glacier core may potentially increase feature porosity, and thus increase the storage capacity. In turn, this will cause changes in the rock glacier discharge pattern, and consequently influence runoff generation in alpine catchments (Rogger et al., 2017). In response, several scientific studies have considered rock glacier-catchment hydrology interactions in relation to relict features (e.g., Wagner et al., 2016; Winkler et al., 2016b; Rogger et al., 2017). Globally, relict rock glaciers are numerous (**section 4.5**), and under future climate warming, intact rock glaciers will transition towards relict activity status, and thus from quickflow to baseflow dominated landforms. In explanation, the coarse-blocky openwork structure of rock glaciers promotes rapid infiltration and transmission of water inputs to the groundwater system – i.e. relict rock glaciers constitute unconfined aquifers (Geiger et al., 2014). For example, research in the Niedere Tauern Range (Eastern Alps, Austria) has shown that subsequent to precipitation events, relict rock glaciers rapidly (within hours) contribute ~20% precipitation volume to discharge; the remaining ~80% is delayed considerably with a mean residence time of ~7 months. This large storage component facilitates large baseflow rates long after precipitation events (Winkler et al., 2016b). As a consequence, relict rock glacier water stores can maintain streamflow during summer baseflow periods (e.g., Wagner et al., 2016). In addition, a large proportion of the terrain >2,000 m a.s.l. drains through rock glaciers (e.g., Seckauer Tauern Range = 51% [Winkler et al., 2016a]); therefore, it is reasonable to assume that relict rock glaciers constitute significant water stores at

intermediate-term timescales. Notably, to date studies assessing rock glacier WVEQ (**section 4.5.2.2**) have not included relict rock glacier water stores; however, including these stores would introduce large uncertainties into WVEQ estimations, likely due to the difficulty of estimating such transient stores. Nevertheless, it is clear that this rock glacier type strongly influences both the water storage capabilities and discharge behaviour of alpine catchments.

Investigations of rock glacier-catchment hydrology interactions that consider large glacier-rock glacier composite features are sparse. At the Tapado catchment (Coquimbo region, Chile) – an assemblage of cascading cryospheric landforms (debris-free glacier, debris-covered glacier, rock glacier and moraine complexes) – Pourrier et al. (2014) found that the storage capacity and transmissive function of rock glaciers is considerably different to debris-covered glaciers. Pourrier et al. (2014) present a conceptual model that synthesises the hypothesised hydrological functioning of this glacier-rock glacier composite feature (**Figure 4.11**). Analysis of the flow dynamics shows rapid and concentrated or slow and diffuse hydrological transfers for the debris-covered glacier and rock glacier, respectively. In this study, the debris-covered glacier forms a weakly capacitive but highly transmissive medium, whereas the rock glacier forms a highly capacitive but weakly transmissive medium. The hydrological data suggest that rock glaciers exhibit: (i) a strong buffering effect on the daily-to-monthly variability of transferring glacier meltwater to downstream areas; and (ii) high storage capacity that partially delays glacier meltwater transfer to downstream areas (Pourrier et al., 2014). Therefore, catchment hydrology will be significantly influenced by glacier-rock glacier interactions, particularly where debris-covered glaciers are currently developing into rock glaciers. As a consequence of the transition from glacial to paraglacial process regimes, glacier-to-rock glacier transition in high mountain systems is increasingly likely (**section 4.3.2**); therefore, it is important to better understand the catchment hydrology implications of glacier-rock glacier interactions.

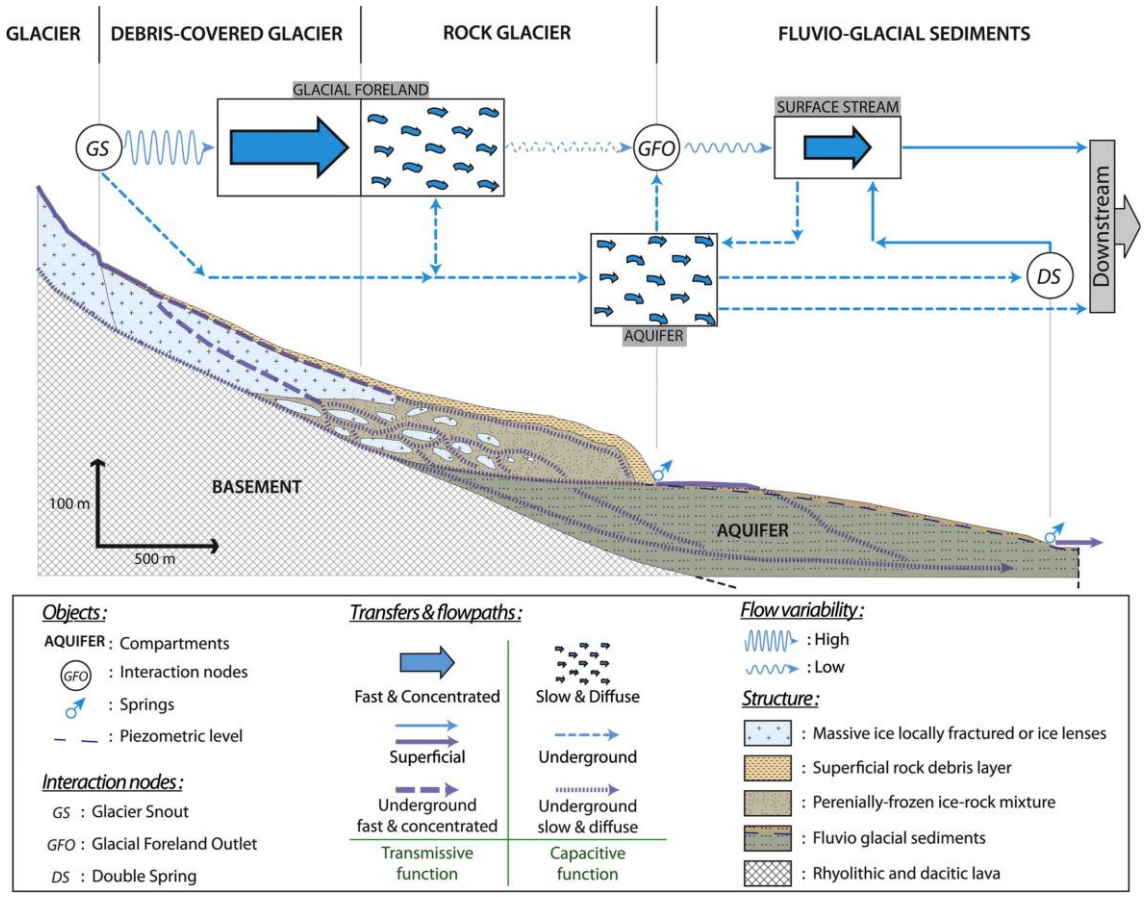

Figure 4.11. Schematic transect through the Tapado catchment synthesising the hypothesised hydrological interactions between the catchment components (i.e. debris-free glacier, debris-covered glacier, rock glacier, and fluvioglacial sediments). Figure after Pourrier et al. (2014).

4.7 ROCK GLACIER HYDROCHEMISTRY

Rock glacier water hydrochemistry is the focus of very few scientific investigations (see Table 1 in Colombo et al., 2018b). It is known that rock glaciers lose ice volume at slower rates than glaciers (**section 4.4**); therefore, the former potentially affect water hydrochemistry over longer timescales (Fegel et al., 2016). Indeed, work has shown that rock glacier thaw modifies the inorganic chemistry of both water bodies located downstream (Thies et al., 2007; Baron et al., 2009; Ilyashuk et al., 2014; Colombo et al., 2018a; Ilyashuk et al., 2018) and streams (Williams et al., 2006; Thies et al., 2013; Nickus et al., 2015; Fegel et al., 2016; Munroe, 2018). As a consequence, the water quality characteristics of rock glacier outflows should be a major focus of research, given their potential as potable water resources (Burger et al., 1999).

Previously, rock glacier outflow has been described as *clear* (i.e. predominantly sediment-free), containing comparatively lower *suspended sediment concentrations* (SSC) and higher *total dissolved solids* (TDS) relative to glacier-fed outflow (Gardner and Bajewsky, 1987). In addition, *total load* (i.e. SSC + TDS [excluding bedload transport]) within the latter are at least

one order of magnitude greater than that within rock glacier outflow (Gardner and Bajewsky, 1987). It is important to note that these conclusions are based on a small sample size, with just a small number of studies evidencing this. For example, SSC measurements from the Hilda rock glacier (Canadian Rocky Mountains, Canada) were generally low, ranging between 1 and 3 mg L^{-1} and reaching 20 mg L^{-1} only in response to precipitation events. As expected, increased rock glacier-derived discharge causes increases in SSC; however, a threshold value of ~150 L s^{-1} was reported after which SSC declines (Gardner and Bajewsky, 1987). SSC measurements reported for the Boundary glacier, situated ~1 km north of the Hilda rock glacier, ranged between 70 and 4,000 mg L^{-1} ($\bar{X}$ = 600–800 mg L^{-1}) during the same precipitation event (Gardner and Bajewsky, 1987), illustrating the potential filtering effect of rock glaciers on fine-grained sediment throughput. SSC measurements from the Reichenkar rock glacier (western Stubai Alps, Austria) reflect clear outflow associated with discharges <100 L s^{-1}, but SSC of 1,000 mg L^{-1} recorded at peak discharges of >300 L s^{-1} (Krainer and Mostler, 2002); SSC-discharge relationships are therefore unclear. TDS measurements of rock glacier outflow are generally low, although they have been shown to be significantly greater than those of glacier and snowmelt derived outflow. For instance, TDS values of 60–75 mg L^{-1} and 30–40 mg L^{-1} were reported for Hilda rock glacier and Boundary glacier outflow, respectively (Gardner and Bajewsky, 1987).

Rock glaciers characteristically have a higher debris fraction versus glaciers. Consequently, it is hypothesised that significant mineral surface area-ice contact promotes chemical weathering and leads to solute-enrichment of water contained within rock glaciers (Ilyashuk et al., 2014, 2018). This hypothesis is consistent with the results from Giardino et al. (1992) who reported that rock glacier outputs in the San Juan Mountains (Colorado, USA) had significantly higher TDS than rock glacier inputs. Rock glacier input pH levels (6.4–6.9) and output pH levels (7.3–8.4), further illustrate the solute-concentrating effect of rock glaciers (Ilyashuk et al., 2014). Giardino et al. (1992) recorded similar pH values for rock glacier inputs (6.4–7.0) and outputs (7.2–8.5) at three features in the Blanca Massif area of the Sangre de Cristo Mountain Range, Colorado, USA. Given that rock glacier thaw resulting from climate change could drive the export of enriched-solute fluxes, the analysis of EC, major ions (e.g., Ca^{2+}, Mg^{2+}, SO_4^{2-}, NO_3^-) and trace elements (e.g., Ni, Mn, Al, Hg, Pb) in rock glacier outflow has received increasing attention (for review see Colombo et al., 2018b).

In the American West (i.e. the Cascade Mountains, Rocky Mountains, Sierra Nevada), Fegel et al. (2016) report that rock glacier outflow samples exhibit higher pH and EC values and are also enriched in *weathering products* (i.e. SiO_2, Ca^{2+}, K^+, Mg^{2+} and Sr^{2+}) relative to glaciers. Similarly, Crespo et al. (2017) report higher EC values for rock glacier-derived waters ($\bar{x}$ = 1,201 µS cm^{-1}) compared to waters from debris-free glaciers ($\bar{x}$ = 32 µS cm^{-1}), snow-dominated streams ($\bar{x}$ = 159 µS cm^{-1}) and debris-covered glaciers ($\bar{x}$ = 805 µS cm^{-1}) in the Upper Mendoza River basin (Argentinian Andes). In addition, clear differences in the $\delta^{18}O$ signatures of glacier- (debris-free and debris-covered) vs rock glacier-derived waters are reported; depleted values (i.e. lower amount of heavy isotopes) and enriched values (i.e. higher abundance of heavy isotopes) are found in glacier- and rock glacier-derived waters, respectively (ibid.). To date, research directly comparing rock glacier- and glacier-derived meltwaters through hydrochemical and stable isotope analysis are few in number; most consider the hydrochemistry of rock glacier outflows over various timescales or relative to surface waters uninfluenced by rock glaciers (not explicitly of glacial origin). Long-term (1985–2005) increases in EC (by ~19-fold), Ca^{2+} (by ~13-fold), SO_4^{2-} (by ~26-fold) and Mg^{2+} (by ~68-fold) have been reported for the Rasass See alpine lake located beneath an active rock glacier in the Central Eastern Alps, Italy (Thies et al., 2007) (**Figure 4.12**). Increased enriched-solute fluxes related to rock glacier thaw are reflected in the strong seasonal variations found in outflow hydrochemistry. For instance, strong seasonal increases in SO_4^{2-} (by ~175-fold), Mg^{2+} (by ~30-fold), Ca^{2+} (by ~20-fold) and Na^+ (by ~4-fold) were recorded for Green Lake 5 rock glacier (Colorado Front Range, Rocky Mountains, USA) outflows in late summer/autumn compared with other surface waters during mid-summer (Williams et al., 2006). Such findings have been attributed to enhanced rock glacier thaw due to climate warming (Thies et al., 2007, 2013).

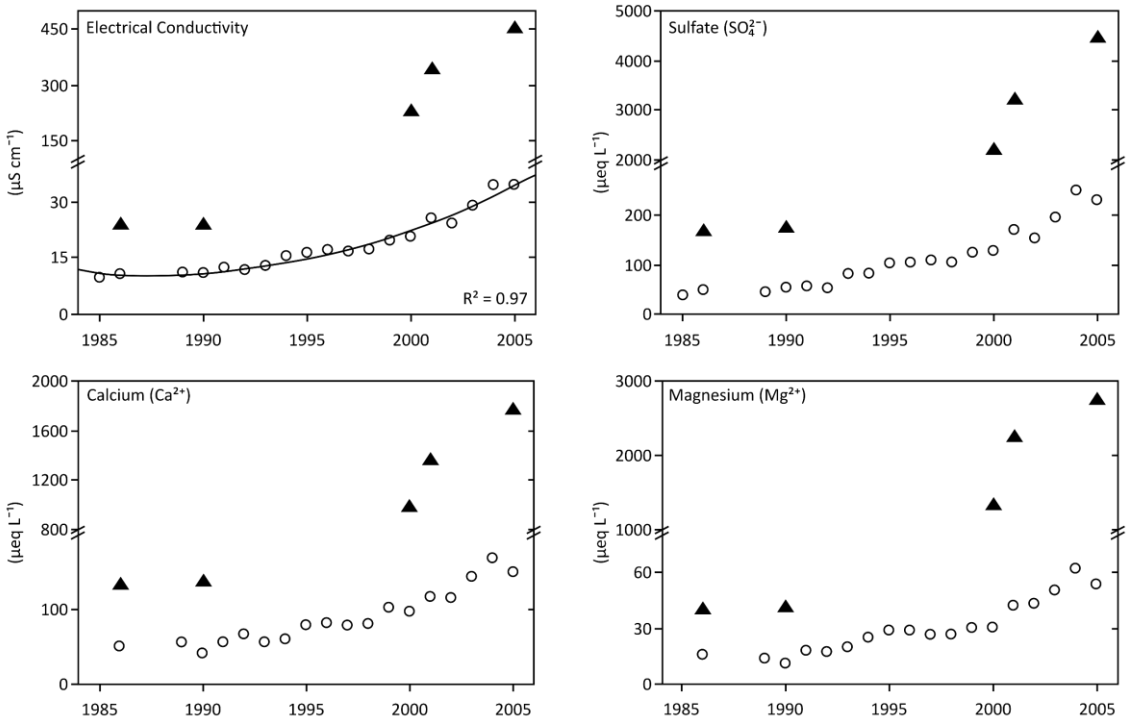

Figure 4.12. Long-term EC, sulfate (SO_4^{2-}), Calcium (Ca^{2+}) and magnesium (Mg^{2+}) concentrations in Rasass See (black triangles) and Schwarzsee ob Sölden (open circles) alpine lakes (1985–2005). Values for Rasass See and Schwarzsee ob Sölden represent mean values of four to seven discrete samples along the lake vertical profile taken during holomixis (i.e. compete mixing of the lake). Variability among single values is <5%. Diagonal lines on the y-axis depict scale breaks. Modified after Thies et al. (2007).

Elevated concentrations of trace elements in high-altitude alpine lakes, also attributed to the influence of rock glacier thaw (Thies et al., 2007), have been reported. For instance, natural *acid rock drainage* (ARD) can arise in mineralised catchments with sulfide-bearing lithologies following rock glacier thaw, as the exposure of sulfide-rich rocks to air and oxygenated water results in increased oxidation of sulfide minerals (Ilyashuk et al., 2014). ARD typically produces acid-sulfate waters enriched in metals; for example, high concentrations of Mn, Ni and Al in excess of EU maximum permissible levels in drinking water were recorded at Rasass See. Contrastingly, negligible concentrations were reported for the adjacent water body without a rock glacier in its catchment (Ilyashuk et al., 2014). In mineralised catchments with sulfide-bearing lithologies, under future climate warming, it is reasonable to expect enhanced ARD in response to increased AL thickness which permits atmospheric oxygen to penetrate to greater depths (Colombo et al., 2018b). Additionally, high-altitude mining operations may adversely affect rock glacier water quality as mining tailings – a source of ARD (Bellisario et al., 2013) – are piled onto rock glacier surfaces (Brenning, 2008; Bellisario et al., 2013). Of note, the origin(s) of high concentrations of trace elements in rock glacier ice often remains the subject of considerable uncertainty (Colombo et al., 2018b) and requires further study. For instance,

high heavy metal concentrations (Ni, Zn, Co, Cu, Fe and Mn) were determined in ice-cores drilled at Lazaun rock glacier, yet lithological analyses indicate the origin of these heavy metals is not the rocks of the catchment area of the rock glacier (Krainer, 2014; Krainer et al., 2015).

As described above, localised releases of enriched-solute fluxes following rock glacier thaw can alter significantly the inorganic chemistry of water surfaces downstream. Further, the increased export of enriched-solute fluxes can be expected under future climate warming. Therefore, an improved understanding of the meteorological drivers (i.e. air temperature, snowmelt and rainfall) responsible for the export of solute-enriched waters from rock glaciers is important for (i) determining causality for the hydrochemical response of water surfaces downstream and (ii) anticipating, monitoring and planning for future changes in downstream hydrochemistry (Colombo et al., 2018a). Three hypotheses are identified (Colombo et al., 2018b): (i) warmer air temperatures enhance rock glacier thaw, releasing solute-enriched waters (e.g., Krainer and Mostler, 2002; Berger et al., 2004; Williams et al., 2006; Krainer et al., 2007; Thies et al., 2013; Nickus et al., 2015; Colombo et al., 2018a); (ii) long-lasting snow cover delays rock glacier thaw thus soluble materials remain sequestered in rock glacier ice, while snowmelt also dilutes solute-enriched waters (Williams et al., 2006). Similarly, rainfall percolation through rock glaciers lowers solute concentrations in outflows (e.g., Krainer and Mostler, 2002; Berger et al., 2004; Krainer et al., 2007; Nickus et al., 2015); and (iii) rainwater percolating through rock glaciers flushes solute-enriched waters, particularly following snow cover depletion (e.g., Colombo et al., 2018a), in contrast to the effects described in hypothesis (ii). This lack of agreement likely stems from the limited availability of studies focused on meteorological variables, hydrologic processes and chemical characteristics of water surfaces downstream (Colombo et al., 2018a). Further, existing studies have predominantly been undertaken in the European Alps or North American mountain ranges (Colombo et al., 2018b). As such, it is evident that further scientific investigation is required, particularly an extension of research evidencing the suitability of water surfaces downstream of rock glaciers for use as safe, potable water sources to other regions worldwide.

4.8 CONCLUSIONS

In this contribution, we synthesise the available literature and present the first comprehensive evaluation of the hydrological role of rock glaciers over a range of spatial and temporal scales, considering globally-distributed published studies. Of note, rock glacier-related research has advanced considerably post-1970s, yet important gaps remain regarding the scientific

knowledge and understanding of rock glacier hydrology. A general lack of consensus concerning the present and future hydrological significance of rock glaciers pervades the literature.

Importantly, water storage within rock glaciers occurs over a range of timescales; yet, to date we identify those investigations focused upon rock glacier hydrological significance generally consider present as opposed to potential future rock glacier icemelt contributions – rock glacier hydrological significance has been defined according to a restricted timescale. A near-global first-order approximation of intact rock glacier WVEQ concludes that intact rock glaciers potentially constitute hydrologically valuable long-term stores (see **section 4.5**). Given that rock glaciers are climatically more resilient than glaciers (see **section 4.4**), we hypothesise that the relative importance of rock glacier hydrological contributions will increase as climate warming proceeds through the twenty-first century, particularly in semi-arid and arid regions. Furthermore, with continued climate-driven deglaciation and thus a transition from glacial- to paraglacial-dominated process regimes, glacier-to-rock glacier transition is likely to become increasingly common (see **section 4.3**). This may potentially enhance the resilience of the mountain cryosphere to future climate warming.

Thus far, rock glacier-related research has primarily defined the hydrological significance of rock glaciers according to the ice content/WVEQ and/or the proportional contribution to rock glacier discharge of icemelt. However, for the first time, we have synthesised published work to consider rock glacier "hydrological significance" as encompassing: (i) rock glacier-catchment hydrology interactions (i.e. total discharge volume, variability, and timing); and (ii) rock glacier effects upon the physical characteristics (i.e. hydrochemistry, temperature, etc.) of water inputs. Regarding (i), hydrographs from [active] rock glaciated and non-rock glaciated catchments have been reported to be distinctly different, and relict rock glaciers – regularly overlooked in rock glacier hydrology research – can also strongly influence alpine catchment hydrology (see **section 4.6**). In regard to (ii), hydrochemical analysis of rock glacier outflows indicates that rock glaciers may adversely affect the inorganic chemistry of water bodies located downstream and streams (see **section 4.7**).

4.9 ACKNOWLEDGEMENTS

This work was supported with a research grant by the Natural Environment Research Council (Grant No. NE/L002434/1) and the Royal Geographical Society (with IBG) through a Dudley Stamp Memorial Award. We thank the reviewers for their detailed and constructive comments.

5 MOUNTAIN ROCK GLACIERS CONTAIN GLOBALLY SIGNIFICANT WATER STORES

5.1 ABSTRACT

Glacier- and snowpack-derived meltwaters are threatened by climate change. Features such as rock glaciers are climatically more resilient than glaciers and potentially contain hydrologically valuable ice volumes. However, while the distribution and hydrological significance of glaciers are well studied, rock glaciers have received comparatively little attention. Here, we present the first near-global RGDB through an analysis of current inventories and this contains >73,000 rock glaciers. Using the RGDB, we identify key data-deficient regions as research priorities (e.g., Central Asia). We provide the first approximation of near-global rock glacier WVEQ, and this is 83.72 ± 16.74 Gt. Excluding the Antarctic and Subantarctic, Greenland, and regions lacking data, we estimate a near-global rock glacier to glacier WVEQ ratio of 1:456. Significant rock glacier water stores occur in arid and semi-arid regions (e.g., South Asia East, 1:57). These results represent a first-order approximation. Uncertainty in the water storage estimates includes errors within the RGDB, inherent flaws in the meta-analysis methodology, and rock glacier thickness estimation. Here, only errors associated with the assumption of rock glacier ice content are quantified, and overall uncertainty is likely larger than that quantified. We suggest that rock glacier water stores will become increasingly important under future climate warming.

5.2 INTRODUCTION

In semi-arid and arid high mountain systems glaciers and seasonal snowpack form natural buffers to hydrological seasonality, as seasonal meltwater contributions smooth the effects of highly variable summer precipitation and associated irregular runoff (Kaser et al., 2010; Viviroli et al., 2011; Beniston et al., 2014). Described as the world's natural "water towers" (Messerli et al., 2004), glacier- and snowpack-derived meltwater are critical to ecological, social and economic systems in these regions. Additionally, mountain water stores provide buffering capacity for surrounding lowlands (Pritchard, 2017). Elevation-dependent warming (i.e. an amplified rate of warming with altitude) suggests that high-altitude environments will likely experience comparatively faster warming than lower altitude areas (Mountain Research Initiative EDW Working Group, 2015). Furthermore, high-altitude hydrological resources are highly sensitive to environmental change (Viviroli and Weingartner, 2004; Beniston et al., 2014). Indeed, between 2003 to 2009, glacier volume loss globally was estimated to be -259 ± 28 Gt yr^{-1} (Gardner et al., 2013). With projected atmospheric warming, long-term glacier

and seasonal snowpack changes are expected to impact significantly hydrological resources stored within high mountain systems (Beniston, 2003). Small and low-lying glaciers are particularly likely to be sensitive to warming, with many disappearing (Ramírez et al., 2001; Francou et al., 2005; Vaughan et al., 2013). In the short-term glacier shrinkage results in increased runoff. However, following "peak non-renewable water" (Gleick and Palaniappan, 2010), summer runoff will significantly reduce in semi-arid and arid regions (Baraer et al., 2012; Sorg et al., 2014a). Additionally, a warming-induced precipitation shift from snowfall to rainfall (Berghuijs et al., 2014) combined with a temporal shift towards earlier snowpack melt (Barnett et al., 2005), will further lead to runoff reduction.

Consequently, effective water resource management in terms of climate change adaptation strategies is critical. However, this is hampered by an incomplete understanding of all components of the hydrological cycle in high mountain systems. Whilst much has been written on the hydrological role of glaciers (Vuille et al., 2008), that of rock glaciers has received comparatively little attention (Duguay et al., 2015). Rock glaciers are cryospheric landforms that are formed by the gravity-driven creep of accumulations of rock debris supersaturated with ice. They are characterised by a seasonally frozen, clastic-blocky surficial layer ~0.5 to 5 m thick that thaws each summer (known as the *AL*) (Bonnaventure and Lamoureux, 2013). Rock glaciers are described as active or inactive if they contain ice beneath the AL. These are described collectively as intact rock glaciers. Those containing no or minimal ice content are termed relict rock glaciers (Barsch, 1992). Rock glaciers are thermally decoupled from external micro- and meso-climates because of the insulating effect of the AL, which is shown to slow the rate of ice melt within rock glaciers (Bonnaventure and Lamoureux, 2013). Consequently, rock glaciers respond to climate change at comparatively longer time scales than glaciers (Haeberli et al., 2006). Therefore, rock glaciers are more climatically resilient than glaciers and form frozen water stores of potentially significant hydrological value (Rangecroft et al., 2016). Indeed, under future climate warming rock glaciers are expected to form a larger component of base flow to rivers and streams (Janke et al., 2015). Rock glaciers containing ice generally display slow movement rates (mm yr^{-1} to cm yr^{-1}) because of the gravity-driven creep of the ice-supersaturated rock glacier body. This movement creates distinctive morphometric characteristics that enable feature identification and activity classification (i.e. intact or relict) (**Figure 5.1**).

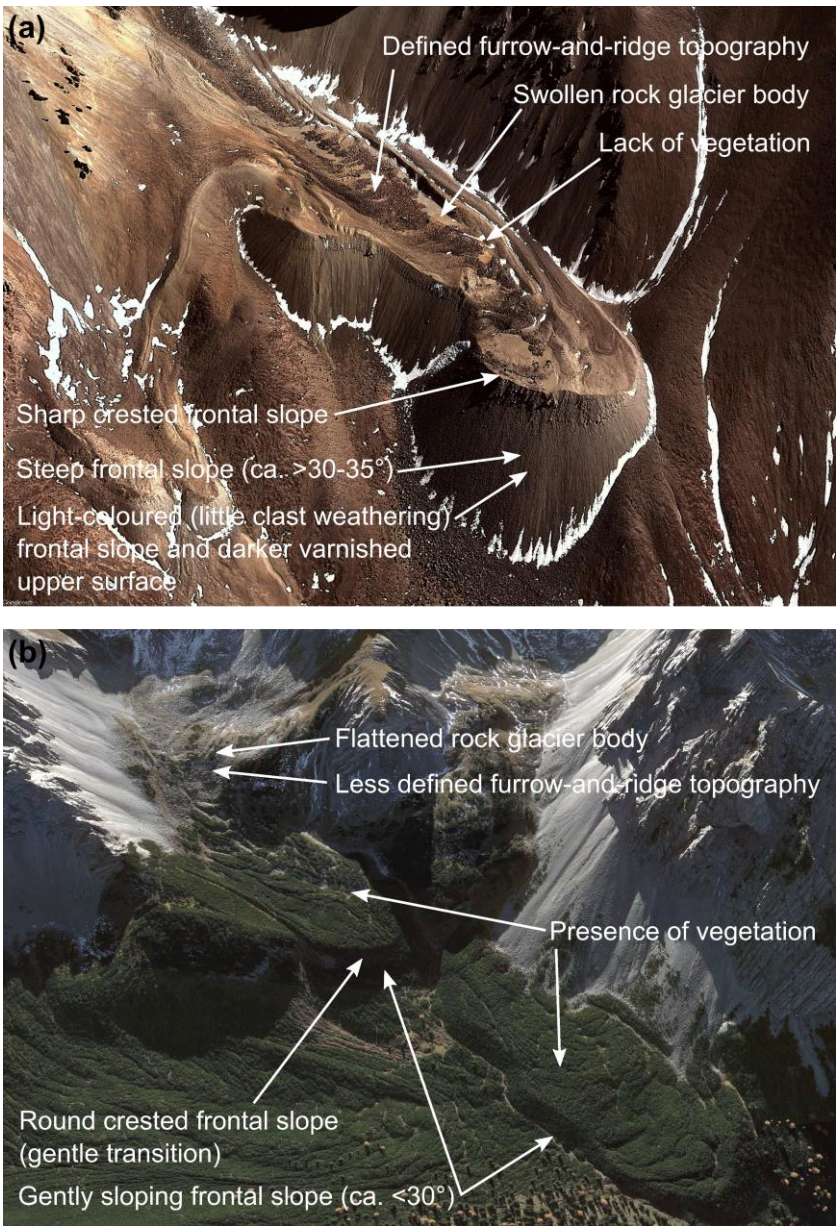

Figure 5.1. Annotated examples of rock glaciers: (a) the intact Caquella Rock Glacier, Bolivia (21°29'S, 67°55'W). Image data: Google Earth (version 7.1.5.1557, Google Inc., California, USA), DigitalGlobe; imagery date: 20 July 2010; (b) a relict rock glacier complex, Nördliche Kalkalpen (Northern Calcareous Alps), Austria (47°19'N, 11°23'E). Image data: Google Earth, DigitalGlobe; imagery date: 17 October 2017.

Ubiquitously distributed through the world's high mountain systems (Harrison et al., 2008), rock glaciers have been found in greater numbers than glaciers in certain regions, for example, the central Andes (Janke et al., 2015). Despite this, rock glaciers are not currently included in global-scale glacier databases such as the GLIMS glacier inventory. To date, rock glacier distribution has only been researched at regional scales (e.g., European Alps, PermaNET [Cremonese et al., 2011]). Although described as the "most pressing need" in rock glacier research, as yet no global-scale rock glacier inventory exists (Janke et al., 2013). This prevents

the full assessment of rock glacier distribution and their hydrological value as water stores, forming the motivation for this study.

5.3 BRIEF METHODS

As the primary objective of this study, we present the first near-global-scale RGDB. The RGDB is shared as a Microsoft Excel database available in the supplementary information online. We argue that data dissemination forms a positive step towards scientific transparency and open-access research, benefitting both the scientific and local/regional communities. The RGDB was developed through a meta-analysis of systematic inventory studies published prior to October 2017 (see **section 12.1.1**). In this study, 'systematic inventory studies' refer to the strategic and complete mapping of rock glacier features within a study area. We identified these using ISI Web of Science, Scopus, ProQuest Dissertations and Theses, Google Scholar, and National Snow and Ice Data Center (NSIDC) search tools (**Supplementary Table 12.1**). The meta-analysis resulted in 131 systematic inventory studies. To avoid duplicate data (i.e. overlapping study areas), some studies were excluded or partially excluded. Consequently, 76 studies form the RGDB.

Within this study, our secondary objective was to establish the relative hydrological contributions of glaciers and rock glaciers at a near-global scale. Therefore, it is important to be able to compare quantitatively the estimated WVEQ of rock glaciers vs glaciers. With regards to rock glaciers, thickness-area (H-S) scaling relations, i.e. $\bar{h} = c \cdot S^{\beta}$ where mean rock glacier thickness ($\bar{h}$) is calculated as a function of surface area (S) and two scaling parameters (c and β), were applied. The scaling parameters applied here were derived from the empirical rule established by Brenning (2005a) (see **Equation 3**). Rock glacier volume was estimated through the multiplication of ($\bar{h}$) and (S). Where complete rock glacier inventories were available, rock glacier surface area data were extracted for each individual feature for use in the H-S relationship. A three-step approach to determine rock glacier volume was used where inventory data was incomplete or unknown (see **section 12.1.1**; **Supplementary Figure 12.1**). By definition, rock glaciers do not contain 100% ice (i.e. ice content is spatially heterogeneous), but because few geophysical investigations of rock glaciers have been conducted, precisely estimating ice content is difficult. Here, we assumed ice content to be 40–60% by volume, enabling calculation of lower (40%), mean (50%), and upper (60%) estimates, following other studies (Barsch, 1996; Haeberli et al., 1998; Hausmann et al., 2012). Subsequently, WVEQ was calculated assuming an ice density conversion factor of 900 kg m^{-3}. With regards to glaciers, the RGI version

4.0 (herein RGIv4.0) released December 2014 (Consortium, 2014) "provides a globally complete set of outlines for all [ice- and debris-covered-] glaciers outside the two ice sheets Greenland and Antarctica" (Pfeffer et al., 2014). For each glacier of the RGIv4.0, Huss and Hock (2015) calculated glacier volume and ice thickness distribution through the application of an ice-thickness distributed model (Huss and Farinotti, 2012) (see **section 12.1.1**). These global-scale data were used in this study. To better enable regional assessment, the RGDB was divided into RGIv4.0 adapted regions (see **section 12.1.1**; **Supplementary Figure 12.2**; **Supplementary Table 12.2**). The above-described approaches have potentially large associated uncertainties as described in **section 5.4.4**. Therefore, the volumetric results presented here represent a first-order approximation. Nevertheless, we thought it prudent to include these results, as there exists a need to make significant advances in this research field in the context of continued climate change.

5.4 RESULTS AND DISCUSSION

5.4.1 RGDB META-ANALYSIS RESULTS

Searches of the ISI Web of Science, Scopus and ProQuest Dissertations and Theses generated 799, 1,023, and 357 studies, respectively (**Supplementary Table 12.1**). Excluding duplicates, peer-reviewed studies (i.e. ISI Web of Science and Scopus) published within the previous decade (2007–2017) totalled 579. In total, 131 systematic rock glacier inventory studies resulted from the categorisation of the available collated literature, of which ~72% were published post-2000 and ~63% during the last 10 years (2007–2017). This reflects, as in previous studies (Stine, 2013), an increased interest in rock glacier research in the last decade. After duplicate rock glacier data, i.e. overlapping study areas, were excluded, 76 studies formed the final RGDB. Systematic rock glacier inventories forming the RGDB were predominantly generated using expert photomorphic mapping from remote sensing image data, with landforms manually identified and digitised based upon geomorphic indicators (see **Figure 5.1**). Recent technological advancements in remote sensing science have:

(i) provided the opportunity for large-scale geomorphological surveys. For instance, fine spatial resolution satellite image data are accessible freely through Google Earth, including SPOT and DigitalGlobe (e.g., QuickBird, Worldview-1 and 2, and IKONOS). The RGDB includes studies that have used the Google Earth platform to compile systematic rock glacier inventories (Schmid et al., 2015; Jones et al., 2018b);

(ii) provided open-access to <1 m resolution airborne laser scanning (LiDAR) data, enabling relict rock glaciers covered by dense vegetation to be systematically mapped (Colucci et al., 2016). This is important as relict landforms strongly influence catchment hydrology (Winkler et al., 2016b); and

(iii) provided accessible InSAR data (e.g., ESA Sentinel-1). In the context of this study, InSAR has enabled systematic rock glacier mapping through the investigation of surficial kinematics (i.e. feature movement). Subsequently, activity status classification can be defined with greater accuracy (e.g., Liu et al., 2013).

5.4.2 RGDB COVERAGE

Our results from the meta-analysis suggest that the number of systematic rock glacier inventory studies is relatively strongly and significantly related to the total number of rock glaciers identified (r = 0.71, *p-value* = <0.01). Study density is highest in Central Europe (n = 27), followed by South America (n = 17) and North America (n = 7) (**Table 5.1**). These RGI regions account for ~67% of systematic rock glacier studies within the final RGDB. Therefore, we can use the RGDB to identify regions that have been the focus of far less scientific research. Significant gaps in the available data are evident. For example, no systematic rock glacier inventory studies have been compiled for Arctic Canada North, Arctic Canada South, Russian Arctic, and South Asia West RGI regions. Furthermore, only ~9% of studies contained within the RGDB cover the Hindu Kush-Himalayan range (Central Asia = 5, South Asia East = 2, South Asia West = 0), home to the largest ice volume outside of the polar regions and a region that the authors, amongst others, have found contains thousands of rock glaciers (Hewitt, 2014; Schmid et al., 2015; Jones et al., 2018b). The RGDB includes only data derived from the meta-analysis, with overall coverage determined by available systematic rock glacier inventory studies. Given the above-mentioned knowledge gaps, the RGDB presented here represents a 'near-global' resource.

5.4.3 GLACIER- AND ROCK GLACIER-HYDROLOGICAL VALUE

The RGDB presented here contains 73,045 rock glaciers (intact = 39,320, relict = 33,725) covering an estimated area of ~8,880 km². From this, we present a first-order approximation of volumetric ice content contained within intact rock glaciers. In total, we estimate that intact rock glaciers contain a total ice volume of ~93 Gt assuming 50% ice content by volume. Therefore, intact rock glaciers contain a total WVEQ of between 66.97 and 100.46 Gt, equivalent to ~68-102 trillion litres (**Table 5.1**), if a possible range of ice content between 40% and 60% is

considered. Regionally, intact rock glaciers located within South America (32.84 ± 6.57 Gt), South Asia East (19.48 ± 3.90 Gt), and North America (15.57 ± 3.12 Gt) likely contain the largest water stores (**Figure 4.6**). Conversely, WVEQs found within the Antarctic and Subantarctic, Greenland Periphery, New Zealand, and Scandinavia RGI regions are the smallest, with the upper estimate (i.e. 60% ice content by volume) containing <0.88 Gt combined. Importantly, long-term rock glacier water stores in arid and semi-arid regions are large (e.g., South America = 32.84 ± 6.57 Gt). This is particularly significant where glacial meltwater provides an important portion of potable water, for example in La Paz, Bolivia where future water scarcity due to the pressures of climate change, poor infrastructure and increasing population is likely (Rangecroft et al., 2013; Soruco et al., 2015).

Table 5.1. RGDB data reflecting total studies, rock glacier numbers, areas, and WVEQs at the regional (RGI regions) and near-global scale. The WVEQ calculations are associated with an estimated range of ice content by volume (%), with lower (40%), mean (50%), and upper (60%) estimates. Those RGI regions where no systematic rock glacier inventory studies have been undertaken (i.e. Arctic Canada North, Arctic Canada South, Russian Arctic, South Asia West, and Svalbard and Jan Mayen) are excluded from the table. See **Supplementary Figure 12.2** and **Supplementary Table 12.2** for details on the RGI regions. Values are reported to two decimal places.

RGI region	No. studies (n)	Rock glaciers (n)			Rock glacier area			WVEQ
		Total	Intact	Relict	Total	Intact	Relict	
	(-)	(-)	(-)	(-)	(km²)	(km²)	(km²)	(Gt)
Antarctic and Subantarctic	3	35	33	2	3.21	3.01	0.20	0.04 ± 0.01
Caucasus and Middle East	3	983	551	432	113.22	68.52	44.70	0.93 ± 0.19
Central Asia	5	2,187	1,991	196	291.61	290.35	17.24	4.08 ± 0.82
Central Europe	27	11,917	4,189	7,728	752.28	326.18	495.84	3.13 ± 0.63
Greenland Periphery	1	390	186	204	46.00	21.91	24.09	0.30 ± 0.06
Iceland	2	181	121	60	61.37	47.57	13.80	0.82 ± 0.16
New Zealand	1	386	166	220	42.56	20.47	22.09	0.28 ± 0.06
North America	7	13,833	7,874	5,959	1,710.67	1,131.08	628.73	15.57 ± 3.11
North Asia	5	7,207	3,431	3,776	801.51	422.77	378.73	5.74 ± 1.15
Scandinavia	2	248	67	181	26.44	8.26	18.18	0.11 ± 0.02
South America	17	28,665	16,117	12,548	3,557.69	2,307.60	1,299.40	32.84 ± 6.57
South Asia East	2	6,513	4,356	2,157	1,417.57	950.80	466.77	19.48 ± 3.90
Svalbard and Jan Mayen	1	500	238	262	55.66	29.36	26.30	0.40 ± 0.08
NEAR-GLOBAL	**76**	**73,045**	**39,320**	**33,725**	**8,879.79**	**5,627.89**	**3,436.06**	**83.72 ± 16.74**

The RGIv4.0 contains 197,654 digital glacier outlines covering an area of ~726,792 km² globally (Huss and Hock, 2015). Furthermore, Huss and Hock (2015) estimated glaciers to contain 138,074 Gt of ice, equating to an estimated WVEQ of 124,266 Gt (**Table 5.2**). As a result, the total ratio of rock glacier to glacier WVEQ is estimated to be 1:1,649 (**Table 5.2**). This implies that glaciers contain a store of water 1,649 larger than that of rock glaciers at the near-global scale.

Excluding those RGI regions where no systematic rock glacier inventory studies have been undertaken (i.e. Arctic Canada North, Arctic Canada South, Russian Arctic, and South Asia West), the estimated ratio of rock glacier to glacier WVEQ is 1:1,098. For completeness, we also excluded the Antarctic and Subantarctic and Greenland Periphery RGI regions, similar to other studies (Jacob et al., 2012), along with the aforementioned RGI regions where no systematic rock glacier inventories have been undertaken. The resulting estimated ratio of rock glacier to glacier WVEQ globally is 1:456. The ratio of rock glacier to glacier WVEQ varies greatly geographically, between 1:26 (North Asia) and 1:18,395 (Svalbard and Jan Mayen), excluding the Antarctic and Subantarctic and Greenland Periphery RGI regions. However, continental-extent ratios are not reflective of national-level or regional-level ratios. For example, rock glacier to glacier WVEQ ratios of 3:1 (semi-arid Chilean Andes [29°–32°]) (Azócar and Brenning, 2010) and 1:3 (West region, Nepal) (Jones et al., 2018b) have been reported.

A number of RGI regions are underrepresented within the RGDB (**Table 5.1**). Importantly, this includes RGI regions within which severe water stress will likely result from future climate warming, for example, those RGI regions encompassing the HKH (Central Asia, South Asia East, South Asia West). From this, we argue that the RGDB data set likely underestimates the potential hydrological value of rock glaciers as future water stores. Furthermore, with continued climate-driven deglaciation, high mountain systems are in the initial stages of transitioning from glacial- to paraglacial-dominated process regimes (Knight and Harrison, 2012). The term paraglacial is defined as "…nonglacial earth-surface processes, sediment accumulations, landforms, landsystems and landscapes that are directly conditioned by glaciation and deglaciation" (Ballantyne, 2002b). Modification of rock slopes (through rock slope failures [RSFs]) dominate the rock slope paraglacial system, as high mountain systems respond to deglacial unloading or debuttressing following the exposure of glacially steepened rockwalls by glacier downwastage and retreat (ibid.). This may subsequently increase glacier surface insulation through enhanced debris-supply. Therefore, frozen water store preservation may occur, as

glaciers transition to rock glacier forms (Knight and Harrison, 2014a). Sasaki et al. (2016) estimated global supraglacial debris-cover to be ~43,750 km² (~20,830 km² classified as thick) and also provided regional estimations. For example, significant debris-cover in Central Asia (13,965 km²), South Asia West (5,555 km²), and South Asia East (3,343 km²) suggest that potentially 'suitable habitats' for rock glacier development exist within these locations. We suggest, therefore, that these are priority regions for future systematic rock glacier inventory studies. Furthermore, given the global glacier volume loss projections of 25–48% between 2010–2100 (Huss and Hock, 2015), we further suggest that rock glaciers will play an increasingly important future role in regional water supply.

Table 5.2. Rock glacier and glacier total areas and WVEQs at the regional (RGI regions) and near-global scale. The ratios of rock glacier to glacier WVEQ is also given. Rock glacier WVEQ uses the average ice content by volume (50%). Values are reported to two decimal places.

RGI region	Rock glacier		Glacier		Ratio
	Area (km^2)	WVEQ (Gt)	Area (km^2)	WVEQ (Gt)	Rock glacier: glacier WVEQ
Antarctic and Subantarctic	3.21	0.04	132,867.00	39,834.76	1:995,869
Arctic Canada North	No Data	No Data	104,873.00	24,742.59	∞
Arctic Canada South	No Data	No Data	40,894.00	7,272.89	∞
Caucasus and Middle East	113.22	0.93	1,139.00	55.38	1:60
Central Asia	291.61	4.08	62,606.00	3,688.13	1:904
Central Europe	752.28	3.13	2,063.00	103.37	1:33
Greenland Periphery	46.00	0.30	89,721.00	13,958.78	1:46,529
Iceland	61.37	0.82	11,060.00	3,001.45	1:3,660
New Zealand	42.56	0.28	1,162.00	55.38	1:198
North America	1,710.67	15.57	101,274.00	17,628.45	1:1,132
North Asia	801.51	5.74	3,430.00	147.67	1:26
Russian Arctic	No Data	No Data	51,592.00	11,326.51	∞
Scandinavia	26.44	0.11	2,851.00	132.91	1:1,208
South America	3,557.69	32.84	31,679.00	4,873.21	1:148
South Asia East	1,417.57	19.48	21,799.00	1,103.85	1:57
South Asia West	No Data	No Data	33,859.00	2,791.02	∞
Svalbard and Jan Mayen	55.66	0.40	33,922.00	7,357.80	1:18,395
NEAR-GLOBAL	**8879.79**	**83.72**	**726,792.00**	**138,074.14**	**1:1,649**

5.4.4 STUDY UNCERTAINTY

It is important to acknowledge possible sources of uncertainty within this study, particularly given the necessity to generalise with regards to rock glacier ice volume and the associated WVEQ calculations. Possible sources of uncertainty are discussed below.

(1) *Inherited errors within the RGDB:* Whereas automated and semi-automated techniques have enabled the mapping and monitoring of clean-ice glaciers from optical satellite data (Shukla et al., 2010), these approaches are generally unsuitable for mapping debris-covered glaciers (e.g., Alifu et al., 2015). This is because both supraglacial-debris (upon the glacier) and debris at the glacier margins share a common source, and thus spectral similarity of features "render them mutually indistinguishable" (Shukla et al., 2010). This limitation is also applicable to rock glaciers (e.g., Brenning, 2009). Therefore, manual rock glacier identification and digitisation using geomorphic indicators (**Figure 5.1**) remains the optimal approach for inventory compilation. This approach is used by many studies included within the RGDB. However, this methodology is inherently subjective and introduces potential uncertainties (see Scotti et al., 2013; Jones et al., 2018b). Furthermore, Whalley et al. (1986) have previously highlighted the problem of mapping 'hidden' ice with respect to rock glaciers. The RGDB presented here includes only meta-analysis derived data from the available systematic rock glacier inventory studies. As such, any errors present (and where those errors are quantified or unquantified) in the original studies will be present here.

(2) *The meta-analysis methodology:* The RGDB was developed through a meta-analysis of systematic rock glacier inventory studies published prior to October 2017, using ISI Web of Science, Scopus, ProQuest Dissertations and Theses and NSIDC search tools. Therefore, the RGDB comprehensiveness is predominantly governed by the availability of openly accessible academic information on the topic. As such, studies outside of these research-bounds, in particular, those published in non-ISI indexed journals, may have been missed. Furthermore, integration of systematic rock glacier inventory data into the RGDB was hampered by (i) non-standardised inventory datasets (see Cremonese et al., 2011); (ii) non-English language writing; (iii) the absence of an accessible open-access database (only 43 studies in the full RGDB [~33%] had linked databases); and (iv) incomplete inventory data. With regards to (ii), we used Microsoft Translator/PROMT Translator to increase the accessibility of non-English manuscripts, and thus increased the

completeness of the RGDB. Studies where Microsoft Translator/PROMT Translator was used are noted as such within the RGDB files available in the supplementary information. Additionally, a possible source of error occurs in situations where systematic rock glacier inventory data are either incomplete or unknown ([iii] and [iv]). As previously mentioned, in these situations, we chose to implement a three-step approach to determine rock glacier activity status, area, and ice volume (**Supplementary Figure 12.1**). This three-step approach has potentially large associated uncertainties as we have, of necessity, to generalise.

(3) *Methodology for determining (a) glacier- and (b) rock glacier-hydrological stores:* Regarding (a), within this study, results provided in Huss and Hock (2015) were adopted. For each glacier of the RGIv4.0 Huss and Hock (2015) calculated glacier volume and ice-thickness distribution through the application of the model of Huss and Farinotti (2012) (herein HF-model), updating the previous results of Huss and Farinotti (2012) that relied upon RGIv2.0 data (released June 2012). "[T]he RGI is intended to be a snapshot of the world's glaciers as they were near the beginning of the 21st century (although in fact its range of dates is still substantial)" (Consortium, 2017). Indeed, within the RGIv4.0 released in December 2014 (Consortium, 2014), the average satellite acquisition date (± 1 standard deviation) of inventoried glacier outlines within each of the 19 first-order regions ranges from 1970 ± 19 (North Asia) to 2009 ± 2 (Alaska) (Huss and Hock, 2015). Given that glacier volume loss globally was estimated to be -259 ± 28 Gt yr^{-1} between 2003 to 2009 (Gardner et al., 2013), RGI-derived data may overestimate the glacier area. With regards to the HF-model, previously uncertainty assessments have been undertaken, the results of which have been summarised and discussed in detail (Huss and Farinotti, 2012; Frey et al., 2014). Lastly regarding (a), results within Huss and Hock (2015) were presented as sea-level equivalent (SLE) assuming an ice density of 900 kg m^{-3} and an ocean area of 3.625 x 108 km^2. For the purposes of this study, these results were converted from SLE to ice volume for each RGI first-order region. Converted ice volumes may slightly differ compared to the original dataset, as Huss and Hock (2015) reported SLE only to 2 decimal places.

With regards to (b), we acknowledge that the results presented here represent a first-order approximation. Although "[a] detailed examination of the surface features of a rock glacier [as used in many studies included in the RGDB] may also give a general

indication of the position, activity, and quantity of hidden ice" (Whalley et al., 1986), generally, rock glacier thickness and average ice content are unknown variables. Direct measurements of internal structure are limited due to the practicalities of field-based research (e.g., direct drilling, geophysical investigations) in largely remote locations (Janke et al., 2013). Indeed, regarding the paucity of such scientific investigations, it has been purported that "[m]embers of the mining community have had more opportunities to study rock glaciers internally than have geomorphologists" (Giardino and Vick, 1987). Furthermore, unless *in situ* internal structure data are spatially distributed with good coverage of the entire feature extent, the ice-thickness and ice-debris ratio at any location remains an assumption (Whalley and Azizi, 1994). Therefore, here H-S scaling relations, i.e. $H = cA^{\beta}$ (see **section 12.1.1**), were applied. Scaling parameters derived from the empirical rule established by Brenning (2005a) were used (**Equation 3**). According to this power-law relationship, a rock glacier sized 0.01 km² and 1 km² would contain an ice-debris layer 20 m and 50 m thick, respectively. This estimation of rock glacier thickness is based upon morphometric field measurements (Brenning, 2005a). However, this H-S scaling relationship was developed for rock glaciers in Central Chile. As such, this approach cannot account for regional specificities of rock glaciers around the globe, and thus we cannot be certain of the suitability of our approach to rock glaciers globally. As an alternative approach, it can be argued that a thickness of >~20 m is necessary for active rock glaciers to creep (Barsch, 1996; Whalley and Palmer, 1998). Indeed, some previous studies have adopted a consistent rock glacier permafrost thickness of 20 m for all rock glacier sites (Brenning et al., 2007). However, Burger et al. (1999) (cf. Table 4 in the journal paper) and Janke et al. (2013) detail examples where quantitative field measurements indicate rock glacier thicknesses far in excess of ~20 m. As such, the application of this alternate approach may significantly underestimate rock glacier thicknesses.

Further regarding (b), here we assume estimated ice volume is 40–60% by volume (Barsch, 1996; Haeberli and Beniston, 1998; Hausmann et al., 2012), enabling the calculation of lower (40%), average (50%), and upper (60%) estimates. Ice content within rock glaciers is spatially heterogeneous. Therefore, the volumetric ice content varies strongly within a rock glacier and between individual rock glaciers. "The average volumetric ice content of rock glaciers is widely accepted to vary between approximately 40 per cent and 70 per cent... (Barsch, 1996: 40–60%; Burger et al., 1999: 50–70%)" (Brenning, 2010). This percentage array is consistent with field data from different climatic regions

worldwide (Croce and Milana, 2002; Haeberli et al., 2006; Hausmann et al., 2012). In this context, the assumption of an average 50% ice content is reasonable. Within the RGDB, many studies assume rock glaciers contain 40–60% ice content by volume; adoption of the same percentage array in this study enables inter-study comparative assessment. Furthermore, within the RGDB numerous studies classify rock glaciers as intact, i.e. studies do not provide separate data for active and inactive rock glaciers. Related to this, potential bias may be introduced by the typically lower ice contents of inactive rock glaciers (Brenning, 2010). Additionally, information regarding rock glacier genesis, i.e. periglacial origin or glacigenic origin, is predominantly absent within the RGDB despite strongly influencing ice content. Therefore, we acknowledge that due to the nature of the RGDB and the methodology, we cannot comprehensively account for regional specificities. Further research related to ice-thickness and ice content by volume is certainly needed.

5.5 CONCLUSIONS

The significance of these results is fourfold. First, the systematic meta-analysis undertaken here has enabled the first near-global RGDB to be developed. This is based on the present state-of-knowledge of systematic rock glacier inventory studies. Second, this work focuses on RGDB coverage and therefore enables identification of priority regions for systematic rock glacier inventory studies, both at the RGI regional- and local- scales. Third, for the first time, we present an assessment of WVEQs contained in the world's observed rock glaciers. These indicate that rock glacier water stores are of potentially significant hydrological value (83.72 ± 16.74 Gt). In particular, our RGI regional approach indicates significant frozen water stores contained within rock glaciers in arid and semi-arid high mountain systems facing potential future water scarcity (e.g., South America). Fourth, the methodology presented here enable an approximate comparative assessment of the ratios of rock glacier to glacier WVEQs at RGI regional- and near-global-spatial scales. Finally, we acknowledge and discuss the uncertainty associated with the results presented here. These results represent a first-order approximation; uncertainty in the near-global rock glacier water storage estimates is due to several factors, e.g., inherited errors within the RGDB, inherent flaws in the meta-analysis methodology, and rock glacier thickness estimation, but here only errors associated with the assumption on rock glacier ice content are quantified. Therefore, overall uncertainty is likely larger than that quantified here. Importantly, a full understanding of all inputs to the high mountain system

hydrological cycle is critical for effective water resource management to mitigate or adapt to the impacts of climate change – this includes rock glaciers.

5.6 ACKNOWLEDGEMENTS

This work was supported by the Natural Environment Research Council (grant number: NE/L002434/1 to DBJ). SH and RAB received funding from the European Union Seventh Framework Programme FP7/2007–2013 under grant agreement no 603864 (HELIX: High-End cLimate Impacts and eXtremes; www.helixclimate.eu). The work of RAB forms part of the BEIS/Defra Met Office Hadley Centre Climate Programme GA01101.

6 THE DISTRIBUTION AND HYDROLOGICAL SIGNIFICANCE OF ROCK GLACIERS IN THE NEPALESE HIMALAYA

6.1 ABSTRACT

In the Nepalese Himalaya, there is little information on the number, spatial distribution and morphometric characteristics of rock glaciers, and this information is required if their hydrological contribution is to be understood. Based on freely available fine spatial resolution satellite data accessible through Google Earth, we produced the first comprehensive Nepalese rock glacier inventory, supported through statistical validation and field survey. The inventory includes the location of over 6,000 rock glaciers, with a mean specific density of 3.4%. This corresponds to an areal coverage of 1,371 km². Our approach sampled approximately 20% of the total identified rock glacier inventory (*n* = 1,137) and digitised their outlines so that quantitative and qualitative landform attributes could be extracted. Intact landforms (containing ice) accounted for 68% of the sample, and the remaining were classified as relict (not containing ice). The majority (56%) were found to have a northerly aspect (NE, N, and NW), and landforms situated within north- to west-aspects reside at lower elevations than those with south- to east-aspects. In Nepal, we show that rock glaciers are situated between 3,225 to 5,675 m a.s.l. (metres above sea level), with the mean MEF estimated to be 4,977 ± 280 m a.s.l. for intact landforms and 4,541 ± 346 m a.s.l. for relict landforms. The hydrological significance of rock glaciers in Nepal was then established by statistically upscaling the results from the sample to estimate that these cryospheric reserves store between 16.72 and 25.08 billion cubic metres of water. This study, for the first time, estimates rock glacier WVEQs and evaluates their relative hydrological importance in comparison to ice glaciers. Across the Nepalese Himalaya, rock glacier to ice glacier WVEQ is 1:9 and generally increases westwards (e.g., ratio = 1:3, West region). This inventory represents a preliminary step for understanding the spatial distribution and the geomorphic conditions necessary for rock glacier formation in the Himalaya. With continued climatically-driven ice glacier recession, the relative importance of rock glaciers in the Nepalese Himalaya will potentially increase.

6.2 INTRODUCTION

The HKH region contains ~54,000 glaciers covering an area of ~60,000 km² (Bajracharya and Shrestha, 2011), constituting the most extensive glacier coverage outside of the polar regions and forming the "Asian water towers" (Immerzeel et al., 2010). HKH-derived glacier and snowpack meltwater are important in sustaining seasonal water availability, and the food- and

water-security of millions (Viviroli et al., 2007; Immerzeel et al., 2010; Kohler et al., 2014). HKH glaciers have generally undergone mass loss between 1980–2010 (Bajracharya et al., 2015), with estimated glacial mass change rates of -26 ± 12 Gt yr^{-1} (2003–2009) (Gardner et al., 2013), while substantial further long-term glacial mass losses are projected under climate warming (Bolch et al., 2012; Jiménez Cisneros et al., 2014; Huss and Hock, 2015; Shrestha et al., 2015). The recession and, in some locations, loss of high-altitude frozen water stores may have significant consequences for downstream water supply (Immerzeel et al., 2010; Bolch et al., 2012), particularly following peak non-renewable water (Gleick and Palaniappan, 2010), with long-term decreased summer runoff projected (e.g., Sorg et al., 2014a, 2014b). However, more climatically resilient permafrost features, including intact rock glaciers, contain ground ice volumes of potentially significant hydrological value (e.g., Rangecroft et al., 2015).

Rock glaciers are cryospheric landforms formed by the gravity-driven creep of ice-supersaturated accumulations of rock debris, incorporating a perennially frozen mixture of poorly sorted angular-rock debris and ground ice (Haeberli et al., 2006). They are characterised by a seasonally frozen, clastic blocky surficial layer ~0.5 to 5 m thick that thaws each summer (Bonnaventure and Lamoureux, 2013; Pourrier et al., 2014). Critically, compared to clean-ice glaciers, the AL has been shown to slow melt of ground ice within rock glaciers (Humlum, 1997; Bonnaventure and Lamoureux, 2013; Gruber et al., 2016). Rock glaciers thus potentially form key hydrological stores in semi-arid and arid mountains, e.g., dry Andes, South America (Brenning, 2005b; Azócar and Brenning, 2010; Rangecroft et al., 2014), and are expected to form a larger component of base flow to rivers/streams under climate warming (Janke et al., 2015).

There have been a great number of inventories compiled for rock glacier distribution in various mountain ranges, for instance in central Europe (Chueca, 1992; Imhof, 1996; Guglielmin and Smiraglia, 1997; Baroni et al., 2004; Nyenhuis et al., 2005; Roer and Nyenhuis, 2007; Cremonese et al., 2011; Krainer and Ribis, 2012; Seppi et al., 2012; Bodin, 2013; Scotti et al., 2013; Colucci et al., 2016; Salvador-Franch et al., 2016; Triglav-Čekada et al., 2016; Winkler et al., 2016a; Onaca et al., 2017), Greenland and Scandinavia (Sollid and Sørbel, 1992; Humlum, 2000; Lilleøren and Etzelmüller, 2011), Iceland (Etzelmüller et al., 2007), North America (Ellis and Calkin, 1979; Janke, 2007; Johnson et al., 2007; Millar and Westfall, 2008; Page, 2009; Liu et al., 2013; Charbonneau, 2015; Legg, 2016), South America (Brenning, 2005b; Perucca and Esper Angillieri, 2008; Esper Angillieri, 2009; Azócar and Brenning, 2010; Perucca and Esper

Angillieri, 2011; Falaschi et al., 2014, 2015, 2016; Rangecroft et al., 2014; Azócar et al., 2017; Janke et al., 2017), Asia (Gorbunov et al., 1998; Ishikawa et al., 2001; Bolch and Marchenko, 2006; Regmi, 2008; Bolch and Gorbunov, 2014; Schmid et al., 2015; Wang et al., 2016) and New Zealand (Brazier et al., 1998; Allen et al., 2008; Sattler et al., 2016). However, rock glaciers in the HKH are comparatively less well studied, particularly within the Nepalese Himalaya where no inventory exists. Additionally, previous studies that have been carried out in the HKH were conducted at localised extents or are incomplete (e.g., Gorbunov et al., 1992; Jakob, 1992; Barsch and Jakob, 1998; Gorbunov et al., 1998; Owen and England, 1998; Shroder et al., 2000; Ishikawa et al., 2001; Regmi, 2008; Bolch and Gorbunov, 2014; Schmid et al., 2015). Thus, the hydrological contribution of these 'hidden ice' features to streamflow in the HKH is completely unknown. A full understanding of all inputs to the high-altitude hydrological cycle, including rock glaciers, is necessary for effective water resource management to mitigate or adapt to the impacts of climate change, particularly given that the HKH supplies water to millions of people.

In this context, the primary objectives of this study were to map the distribution of rock glaciers across the Nepalese Himalaya and assess their hydrological significance, compared to glaciers, at regional and national spatial scales. The genesis of rock glaciers remains contested; this controversy has been between the *permafrost school* (purely periglacial-origin) vs the *continuum school* (glacial- and periglacial-origin) and has previously been summarised and discussed in detail (see Berthling, 2011). Discussion of this is beyond the scope of this study; therefore, here we adopt the inclusive, and non-genetic, terms DDAs and I-DLs to incorporate rock glaciers, protalus lobes and protalus ramparts. Ground ice is present within I-DLs (Harrison et al., 2008; Jarman et al., 2013).

6.3 REGIONAL SETTING

Located within the HKH region, Nepal is situated between 26°22' to 30°27' N latitude and 80°04' to 88°12' E longitude extending ~800 km east to west and an average ~140 km north to south (**Figure 6.1**). Nepal encompasses an area of 147,181 km², divided into five principal physiographical regions: Terai Plain, Siwalik Hills, Middle mountains, High mountains (inclusive of the Main Himalayas and the Inner Himalayan valleys), and the High Himalaya (see Shrestha and Aryal, 2011). In this study, our work was primarily concerned with the High Himalaya as this is where the majority of the permafrost region is found. Encompassing the area ≥4,000 m a.s.l., this region is characterised by extremely rugged terrain and is home to

eight of the ten highest peaks in the world including Mount Everest (8,848 m a.s.l.). Furthermore, ~3,800 glaciers covering ~3,900 km² (~3%) of the total area of Nepal are primarily situated within this physiographic region (Bajracharya and Shrestha, 2011). The snowline altitude is ~5,000 m a.s.l. (Shrestha and Joshi, 2011) with ~14,200 km² (~10%) of the total area of Nepal located above this elevation.

Due to the topographical extremes of the High mountains and High Himalaya, the climate type ranges from subtropical in the south to arctic in the north. The Asian summer monsoon dominates the climate of Nepal, providing most of the precipitation during June–September (Shrestha and Aryal, 2011); dependent on the location, ~80% of annual precipitation may occur within this period (Shrestha, 2000). Winter and spring precipitation predominantly falls as snow, forming snowpack stores that provide critical meltwater during the dry season (February–April). Alongside snowpack melt, glacier-derived meltwater contributions are important for maintaining the perennial flow of the major rivers in Nepal and also the Ganges in India (Shrestha and Aryal, 2011). Consequently, projected reductions in glacial coverage under climate change, compounded by poor infrastructure and high population growth (Udmale et al., 2016), will have regional consequences for water resource availability (Shrestha and Aryal, 2011).

6.4 MATERIALS AND METHODS

6.4.1 COMPILATION OF THE INVENTORY

Whereas automated and semi-automated techniques have enabled mapping and monitoring of clean-ice glaciers from optical satellite image data (e.g., Bolch and Kamp, 2006; Bhambri and Bolch, 2009; Shukla et al., 2010), these approaches are generally unsuitable for mapping debris-covered glaciers (e.g., Alifu et al., 2015) and rock glaciers (e.g., Brenning, 2009). This is because both supraglacial-debris (upon the glacier) and debris along the glacier margins originate from surrounding valley rock, and thus the spectral similarity of features "render[s] them mutually indistinguishable" (Shukla et al., 2010; Shukla and Ali, 2016). Therefore, following the methodology used in other inventory studies (e.g., Baroni et al., 2004; Scotti et al., 2013; Falaschi et al., 2014; Rangecroft et al., 2014) manual feature identification and digitisation using geomorphic indicators was the optimal approach for DDA/I-DL inventory compilation.

6.4.1.1 REMOTE SENSING DATA

The inventory was generated using expert photomorphic mapping from fine spatial resolution satellite image data accessible freely through Google Earth (version 7.1.5.1557, Google Inc.,

California, USA), including SPOT and DigitalGlobe (e.g., QuickBird, Worldview-1 and 2 and IKONOS) (Schmid et al., 2015). Google Earth has been used previously as a platform for mapping in a wide range of research areas (see Yu and Gong, 2012), and is particularly useful for large-scale geomorphological surveys (e.g., Bishop et al., 2014; Rangecroft et al., 2014; Schmid et al., 2015). Additionally, Google Earth Pro incorporates user-friendly geographic information system (GIS) tools, enabling the creation of user-defined databases exportable as Keyhole Markup Language (KML) formatted files for further spatial analysis in a GIS environment (e.g., ArcGIS) or data dissemination (e.g., Cremonese et al., 2011; Liu et al., 2013; Schmid et al., 2015). In this study, inventory data are shared as an open-source geodatabase (see Supplementary Information), and we argue that data dissemination through KML formatted files for use with free platforms such as Google Earth, is a positive step towards scientific transparency, and open-access research, with advantages for both the scientific and local/regional communities.

Topographic data were derived from a ~30 m resolution DEM created from the NASA Version 3.0 Shuttle Radar Topography Mission (SRTM) Global 1 arc-second data (herein referred to as "SRTM30") (for further information see USGS, 2015). Freely available SRTM30 data permits topographic analysis of DDAs/I-DLs, where finer resolution products (e.g., WorldDEM™ [~12 m], AW3GTM [~5 m]) are prohibitively expensive (Watson et al., 2015); SRTM DEMs have been successfully used in previous inventory studies in mountain regions (e.g., Bolch and Gorbunov, 2014; Schmid et al., 2015).

6.4.1.2 LANDFORM DIGITISATION AND DATABASE COMPOSITION

DDAs and I-DLs were identified and 'pinned' within Google Earth Pro according to the presence of geomorphic indicators (**Table 6.1**). This resulted in an initial point-based inventory for Nepal. The pinning methodology relied on using a gridded search methodology to ensure that the digitisation was exhaustive. To create the grid, in ArcGIS, the study region was divided using a vector overlay of ~25 km² grid squares (**Figure 6.1**). Subsequently, the gridded overlay was imported into Google Earth Pro, and each grid square was visually surveyed on an individual basis. The study region was split into five geographic sectors of equal longitudinal-width, loosely adapted from the Nepalese Administrative Districts: (i) East region (86°34'–88°12'E); (ii) Central region (84°56'–86°34'E); (iii) Central-west region (83°18'–84°56'E); (iv) West region (81°40'–83°18'E); and (v) Far-west region (80°02'–81°40'E) (**Figure 6.1**).

Table 6.1. Geomorphic indicators used to identify DDAs/I-DLs and their activity status.

Geomorphic Indicator	Active	Relict
Surface Flow Structure	> Defined furrow-and-ridge topography (Kääb and Weber, 2004)	> Less defined furrow-and-ridge topography (Kääb and Weber, 2004)
Rock Glacier Body	> Swollen body (Baroni et al., 2004) > Surface ice exposures (e.g., Potter et al., 1998)	> Flattened body (Baroni et al., 2004) > Surface collapse features (Barsch and King, 1975 as cited in Janke et al., 2013)
Front Slope	> Steep (~ >30-35°) (Baroni et al., 2004) > Abrupt transition (i.e. sharp-crested) to the upper surface (Wahrhaftig and Cox, 1959) > Light-coloured (little clast weathering) frontal zone and a darker varnished upper surface (e.g., Bishop et al., 2014)	> Gently sloping (~ <30°) (Baroni et al., 2004) > Gentle transition (i.e. round crested) to the upper surface (Wahrhaftig and Cox, 1959)

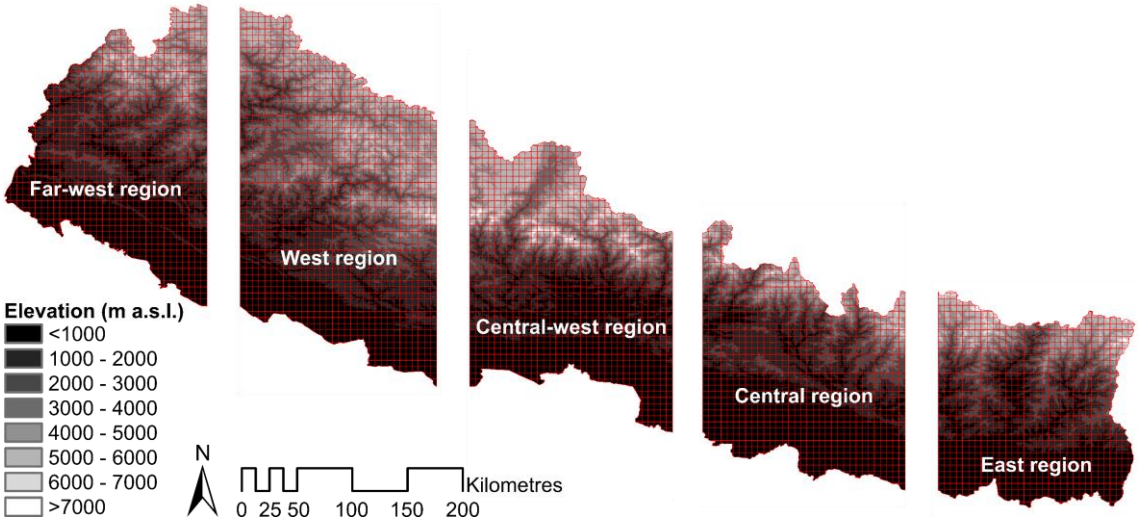

Figure 6.1. An overview map of Nepal, including the gridded overlay, overlaid on the SRTM30 DEM. Five geographic sectors were used in this research: Far-west region, West region, Central-west region, Central region and East region.

From the point-based inventory, a ~20% sample of the identified DDAs/I-DLs from each region were randomly selected using ArcGIS (version 10.3.1, ESRI, Redlands, CA, USA) and their geographic boundaries digitised within Google Earth Pro, forming a polygonised inventory within which more detailed spatial attributes were measured. The pseudo-3D viewer in Google Earth provided topographic context for landforms, and hence aided delineation of DDA/I-DL boundaries. Furthermore, the availability of multi-temporal satellite image data within Google Earth was critical for reducing the mapping uncertainty associated with poor quality image data (affected by, for instance, clouds, snow cover, and long cast shadows on steep-north facing slopes), enabling the generation of a more complete inventory.

The methodology of Scotti et al. (2013) was adopted for DDA/I-DL boundary digitisation. The outline of the entire landform surface, from the rooting zone to the base of the front slope (Barsch, 1996), was digitised for each of the randomly sampled subsets of DDAs/I-DLs. Some aspects of digitisation were challenging: delimitation of the upper boundary of DDAs/I-DLs through geomorphic mapping, is arbitrary (Krainer and Ribis, 2012); determining the upper boundary of I-DLs lacking prominent landforms (e.g., furrow-and-ridge topography) within the rooting zone, particularly in the absence of knowledge regarding landform kinematics (i.e. movement), is difficult (e.g., Roer and Nyenhuis, 2007); and delineation of individual polygons where multiple DDAs/I-DLs coalesce into a single body, is inherently subjective (e.g., Scotti et al., 2013; Schmid et al., 2015). Within this study, "when the frontal lobes of two (or more) rock glaciers originating from distinct source basins join downslope, we consider the two

components as separate bodies. Where the limits between lobes are unclear and the lobes share other morphological characteristics (e.g., degree of activity and vegetation cover), we classify the whole system as a unique rock glacier" (Scotti et al., 2013). Regarding cases where DDAs/I-DLs grade into upslope landforms (e.g., a rock glacier is gradually developing from a terminal/lateral moraine), "a clear distinction between the two landforms cannot be set and we delineated the whole body (i.e., moraine plus rock glacier)" (Scotti et al., 2013). Both quantitative and qualitative landform attributes were extracted and recorded for each digitised DDA/I-DL (**Table 6.2**).

Table 6.2. Inventory structure: attributes derived during DDA/I-DL mapping, with attribute explanation.

Attribute	Attribute Explanation
Name	[Region No.]Grid ID_Feature No._MMDDYYYY *(NB: MMDDYYYY refers to satellite image date)*
Region	[1] East [2] Central [3] Central-west [4] West [5] Far-west
DMSLon	Longitudinal coordinate of polygon centroid (DDD°MM'SS.sss [N|S])
DMSLat	Latitudinal coordinate of polygon centroid (DDD°MM'SS.sss [W|E])
MEF (m a.s.l.)	Minimum elevation at the front
MaxE (m a.s.l.)	Maximum elevation of the feature
Elevation_ (m a.s.l.)	Range | Mean
Area (km²)	/
Slope_ (°)	Maximum | Minimum | Range | Mean
Mean_Aspect (°)	0-359
Aspect_Class	N, NE, E, SE, S, SW, W, NW (e.g., 90° = E, 180° = S)
Max_Length (m)	/
Max_Width (m)	/
Mean_Width (m)	/
L:W_Ratio	Length: width ratio
Geometry_Type	Shape: Tongue-shaped, Lobate-shaped
Dynamic_Type	Active, Inactive, Relict
WVEQ_ (km³)	Water volume equivalent: 40% | 50% | 60%
Upslope_Boundary	Glacier, Slope
Index_Code	See Table 3
Certainty_Index	Medium_Certainty, High_Certainty, Virtual_Certainty

Within ArcGIS, a regional projected coordinate system, Nepal Nagarkot TM, was used for attribute extraction and DDA/I-DL polygons were reprojected into the WGS84 coordinate system for exportation to KML formatted files. The quantitative data (i.e. area, length, width) were directly calculated in ArcGIS. Lengths (parallel to the flow) were manually digitised within Google Earth Pro for each landform. Based on the methodology described by Frauenfelder et al. (2003), within ArcGIS widths (perpendicular to length) were digitised at ~50 m intervals, and mean width calculated in order to incorporate considerable width variation along the DDA/I-DL (**Figure 6.2**). Additionally, landforms were classified into *tongue-shaped* or *lobate-shaped*, where the length: width ratio is >1 or <1 respectfully (Guglielmin and Smiraglia, 1998; Harrison et al., 2008).

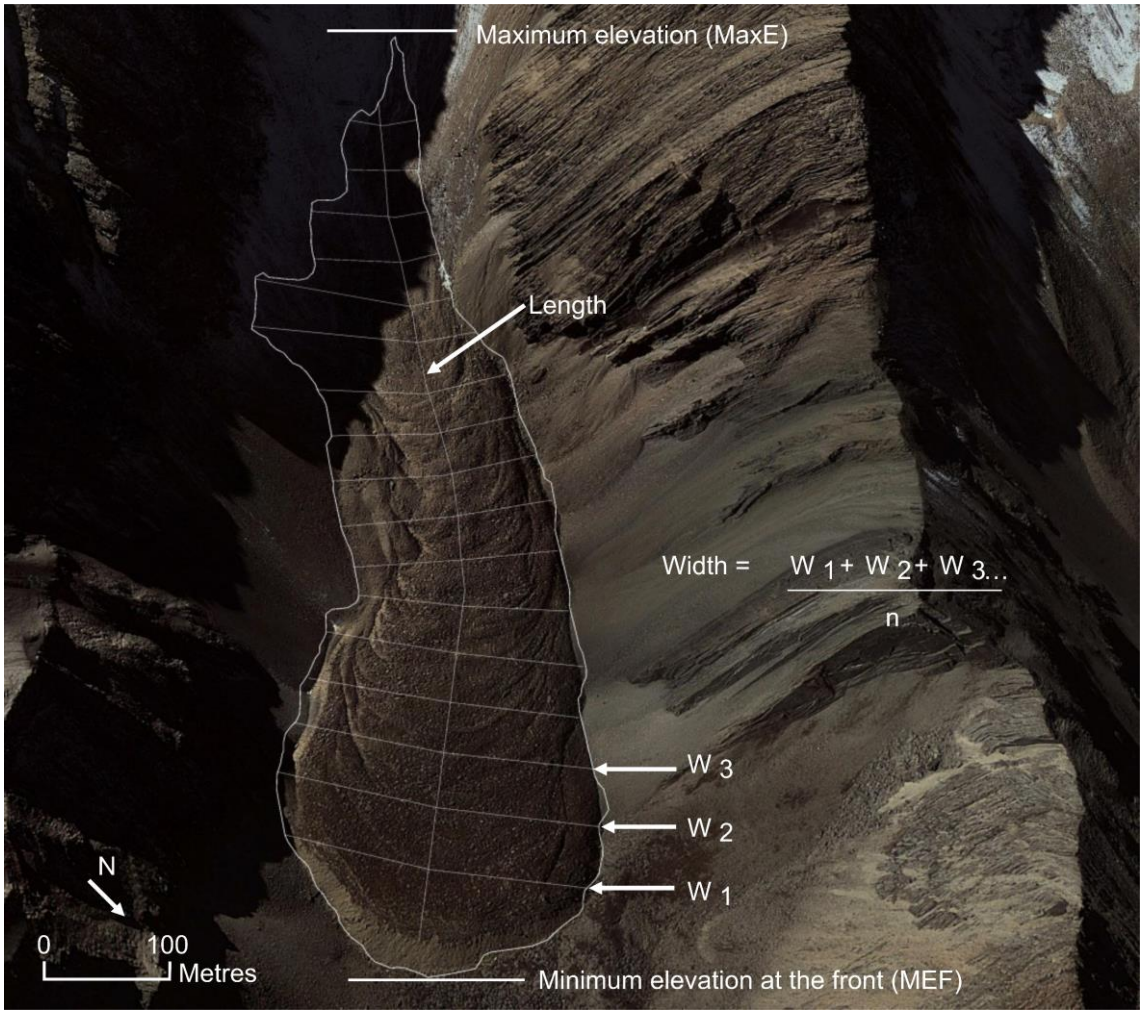

Figure 6.2. Annotated diagram of landform attributes on DDA/I-DL (Feature ID: [4]NEP1257_1_11052011), Nepal (29°06'20.36" N, 83°06'57.39" E). Image data: Google Earth, DigitalGlobe; imagery date: 05 November 2011.

Using ArcGIS surface raster functions, elevation, slope and aspect were calculated for the SRTM30 DEM. ArcGIS zonal statistics were used to overlay the polygonised DDAs/I-DLs onto SRTM30-derived raster surfaces to calculate minimum, maximum, range and mean elevation

and slope for each landform. The MEF for each DDA/I-DL was defined as the elevation at which the base of the front slope meets the slope downstream; the MaxE as the upper boundary (Scotti et al., 2013). As a circular parameter, mean aspect cannot be calculated using simple zonal statistics (i.e. the mean of 0° and 359° cannot be 180° [Davis, 1986 as cited in Janke, 2013]). The vector mean aspect ($\overline{\theta}$) was calculated in R (version 3.1.2, R Core Team, Vienna, Austria) using **Equation 1**:

Equation 1. $S = \sum \sin\theta, C = \sum \cos\theta \quad \overline{\theta} = \arctan\frac{S}{C}$

where *S* is the sum of sine values of aspect (θ) (based on individual pixels of the surface rasters), and *C* is the sum of cosine values of aspect (Paul et al., 2009; Janke, 2013). The mean aspect was then recoded into 8 classes (N, NE, E, SE, S, SW, W, NW).

The degree of activity was determined considering the presumed ice content and movement of DDAs/I-DLs, in accordance with the morphological classification by Barsch (1996), using morphological and geomorphological criteria from satellite image data interpretation. In our inventory, DDAs were categorised as *relict* (not containing ice, sometimes referred to as *fossil*) and I-DLs as *intact* (containing ice) (**Table 6.1**) (e.g., Cremonese et al., 2011; Scotti et al., 2013; Rangecroft et al., 2014; Onaca et al., 2017). The "intact" classification includes both *active* and *inactive* landforms.

Active landforms (I-DLs) are generally characterised by: distinctive surface micro-relief of furrow-and-ridge topography, predominantly the result of longitudinal compression (see Springman et al., 2012), gravity-driven viscous buckle folding (see Frehner et al., 2015) and/or the debris grain-size; steep lateral slopes; and steep frontal slopes near the angle of repose (Haeberli et al., 2006), all of which indicate ice presence (Barsch, 1996; Baroni et al., 2004). Inactive I-DLs also contain ice but are immobile. Barsch (1996) suggests two possibilities that may account for this inactivity: (i) melting of the upper layers within the frontal slope, such that "the unfrozen mantle at the top of the front slope is more than 10 m thick" (Barsch, 1973 as cited in Barsch, 1996). This type of I-DL inactivity is called *climatic inactive*; or (ii) I-DLs "extend so far from their source area that the tangential stress due to the slope, the thickness of the deposit [e.g., insufficient talus-nourishment rates to feature rooting zones (e.g., Kellerer-Pirklbauer and Rieckh, 2016)], its bulk density etc. decrease below the limit required for movement" (Barsch, 1996). This type of I-DL inactivity is called *dynamic inactive*. Relict landforms (DDAs), "formerly active landforms in which ice is vanished" (Scotti et al., 2013), are

characterised by surface collapse features (Barsch and King 1975 in Janke et al. 2013); subdued surface micro-relief; less steep front- and lateral-slope(s) (Barsch, 1996; Baroni et al., 2004), resulting from permafrost degradation; and often extensive vegetation cover (Scotti et al., 2013).

Finally, in order to account for subjectivity associated with the identification, digitisation and classification of landforms in the inventory, we detailed the degree of 'uncertainty' through the application of a *Certainty Index score*, adapted from Schmid et al. (2015), for each digitised DDA/I-DL (**Table 6.3**). Uncertainties in the definition of: (i) external boundaries (i.e. outline); (ii) snow coverage; (iii) longitudinal flow structure; (iv) transverse flow structure; and (v) frontal slope were all recorded. Critically, this approach enables more complete mapping of DDAs/I-DLs despite occasionally poor satellite image data quality; for example, Schmid et al. (2015) sampled 4,000 * ~30 km² grids in the HKH region, of which ~410 samples (~12,300 km²) were classified as insufficient quality (IQ), where IQ was defined as "poor image quality, excessive snow or cloud coverage *over any part of the sample*" and disregarded. Within this study, partially IQ grids are not disregarded; thus, previously unidentified DDAs/I-DLs are mapped within this inventory.

Table 6.3. Certainty index applied to each DDA/I-DL.

Parameter	Parameter Options (Index Code)		
	1 Point	**2 Points**	**3 Points**
External Boundary	None (ON)	Vague (OV)	Clear (OC)
Snow Coverage	Snow (SS)	Partial (SP)	None (SN)
Longitudinal Flow Structure	None (LN)	Vague (LV)	Clear (LC)
Transverse Flow Structure	None (TN)	Vague (TV)	Clear (TC)
Front Slope	Unclear (FU)	Gentle (FG)	Steep (FS)
Certainty Index Score	Medium Certainty (MC) ≤5	High Certainty (HC) 6 to 10	Virtual Certainty (VC) ≥11

6.4.2 ESTIMATING HYDROLOGICAL STORES

6.4.2.1 ICE-DEBRIS LANDFORMS

Estimations of I-DL water content (WVEQ [km³]) were calculated based on presumed ice volumes stored within intact I-DLs (Brenning, 2005b; Azócar and Brenning, 2010; Rangecroft et al., 2015). I-DL ice volume content was estimated through multiplying estimated I-DL thickness and I-DL surface area and then by estimated ice content. Within this study, I-DL thickness and average ice content are unknown variables; direct measurements of I-DL internal structure within the HKH are limited, due to practicalities of field-based research (e.g., boreholes,

geophysical investigations) in largely remote locations (Janke et al., 2013). Therefore, I-DL thickness was estimated through applying an empirical rule established by Brenning (2005a) (**Equation 3**), as applied in existing studies (e.g., Azócar and Brenning, 2010; Perucca and Esper Angillieri, 2011; Rangecroft et al., 2015; Janke et al., 2017); however, further research is needed to improve H-S relationships (Rangecroft et al., 2015).

By definition, I-DLs are ice-supersaturated accumulations of rock debris; thus, they do not contain 100% ice. Ice content within I-DLs is spatially heterogeneous; therefore, estimating WVEQ is challenging, due to difficulty in establishing I-DL genesis and subsequent ice depth and distribution (Seligman, 2009). Few geophysical investigations of I-DLs have been conducted within the HKH; those that have, focus on quantifying ice presence, opposed to ice content by volume (e.g., Jakob, 1992; Ishikawa et al., 2001). Therefore, here estimated ice volume is 40–60% by volume (Barsch, 1996; Haeberli et al., 1998; Hausmann et al., 2012), enabling lower (40%), average (50%), and upper (60%) estimates to be calculated. Finally, WVEQ was calculated assuming an ice density conversion factor of 0.9 g cm^{-3} (≡900 kg m^{-3}) (Paterson, 1994).

6.4.2.2 ICE GLACIERS

Within this study, we set out to establish the relative contributions of rock glaciers and ice glaciers in the Nepalese Himalaya. Therefore, it was important to be able to compare quantitatively the estimated WVEQs of rock glaciers vs ice glaciers. V-S scaling relations (e.g., Chen and Ohmura, 1990; Bahr et al., 1997), i.e. $V = cA^{\gamma}$ where glacier volume (V) is calculated as a function of surface area (A) and two scaling parameters (c and γ), are frequently used approaches for ice volume estimations (Frey et al., 2014). Indeed, V-S relations have previously been used within rock glacier – ice glacier comparative studies (e.g., Azócar and Brenning, 2010; Perucca and Esper Angillieri, 2011; Rangecroft et al., 2015). However, V-S relations, and H-S scaling relations (see Frey et al., 2014), are designed to estimate the ice volumes of large-sample ensembles (>20,000 minimum sample-limit [Cogley, 2011]); while suitable for global volumetric and/or thickness estimations (e.g., Huss and Farinotti, 2012; Marzeion et al., 2012; Grinsted, 2013), they are less so for smaller-samples or individual glaciers (Frey et al., 2014).

In the Himalayan-Karakoram region, Frey et al. (2014) report that V-S relations systematically overestimate ice volumes. Estimated ice volumes derived from the Glacier bed Topography ice-thickness distribution model (herein GlabTop2) (Frey et al., 2014), a new version of the GlabTop model (Linsbauer et al., 2009), are lower than results from V-S relations. Furthermore, direct comparison between GlabTop2 ice-thicknesses and local ice-thickness

measurements derived from GPR show good agreement; validation could not be undertaken for results from V-S relations (Frey et al., 2014). Therefore, here, we use ice-thickness results for Nepal derived from GlabTop2 (ibid.). The glacier outlines mapped by the International Centre for Integrated Mountain Development (Bajracharya and Shrestha, 2011) and the void-filled SRTM 3 arc-second data (~90 m resolution) were used for these calculations. Ice volumes were generated from the results following **Equation 2**:

Equation 2. $V = A * \sum H$

where *V* represents ice volume, *A* the glacier surface area, and *H* the ice-thicknesses derived from GlabTop2. Subsequently, we calculated the WVEQ of ice glaciers, assuming 100% ice content by volume and applying the aforementioned ice density conversion factor.

6.4.2.3 SPATIAL AND STATISTICAL INVENTORY ANALYSIS

Here, statistical analysis was performed in the statistical software R (bivariate statistics: one-way analysis of variance [ANOVA] and post hoc tests). One-way ANOVA and Tukey post hoc testing were used to investigate relationships and differences between independent qualitative variables (region, activity status, slope aspect class) and quantitative dependent variables (MEF, landform area, landform length) with the statistical significance evaluated at the $p = <0.05$ level. To satisfy the assumptions of ANOVA tests, i.e. normally distributed population, a logarithmic transformation was applied to landform area and length. ArcGIS and R were used to assess the relationship between landform slope aspect and hillslope aspect frequency for Nepalese mountain slopes.

6.5 RESULTS

6.5.1 INVENTORY ANALYSIS

In total, 6,239 DDAs/I-DLs were pinned across the Nepalese Himalaya. The upscaled estimates indicated that 4,226 and 2,013 landforms were classified as intact and relict, respectively (**Table 6.4**; **Supplementary Figure 12.3**). Estimated total upscaled DDA/I-DL area is 1,371 km², representing ~31% of the area covered by clean-ice glaciers in the same region (4,426 km²). Overall, 1,137 landforms were digitised (**Figure 6.3**; **Table 6.4**), and this detailed sample covered a total surface area of 249.83 km². Most of these landforms, 772 (68%), were classified as intact, covering 196.52 km², while the remaining 365 (32%) covered 53.31 km², and were classified as relict. Ninety-one per cent of DDAs/I-DLs were classified as tongue-shaped. Ninety per cent of DDAs/I-DLs were situated between ~4,200 and ~5,400 m a.s.l., with the calculated mean MEF of I-DLs (4,977 ± 280 m a.s.l.) at a higher altitude than that of DDAs (4,541 ± 346 m

a.s.l.) (**Table 6.4**). DDA/I-DL characteristics were analysed regionally and Nepal-wide. The open-source geodatabase within the supplementary information online provides detailed information for the sampled DDAs/I-DLs. Additionally, the Nepal inventory KML file of both the pinned landforms and the detailed sample are shared within the supplementary data.

Table 6.4. Key mean characteristics for intact and relict landforms.

Region	Activity	No. of land-forms	(%)	MEF (m a.s.l.)	MaxE (m a.s.l.)	Length (m)	Width (m)	Area (km²)	Aspect	No. of landforms (upscaled)
East	Intact	93	58	4,893	5,076	569	232	0.16	Northwest	492
(86°34'–88°12'E)	Relict	66	42	4,541	4,705	413	200	0.10	Northwest	349
Central	Intact	22	36	4,791	4,997	549	220	0.14	North	128
(84°56'–86°34'E)	Relict	39	64	4,480	4,631	417	206	0.11	Northwest	226
Central-west	Intact	199	88	5,141	5,405	743	280	0.25	West	1,081
(83°18'–84°56'E)	Relict	27	12	4,409	4,643	595	218	0.16	Northwest	147
West	Intact	347	64	4,947	5,192	829	272	0.29	West	1,951
(81°40'–83°18'E)	Relict	191	36	4,604	4,800	557	230	0.16	North	1,074
Far-west	Intact	111	73	4,880	5,109	807	262	0.27	Northeast	574
(80°02'–81°40'E)	Relict	42	27	4,394	4,666	662	228	0.18	Northwest	217
Total	Intact	772	68	4,977	5,215	765	266	0.25	West	4,226
	Relict	365	32	4,541	4,738	531	221	0.15	Northwest	2,013

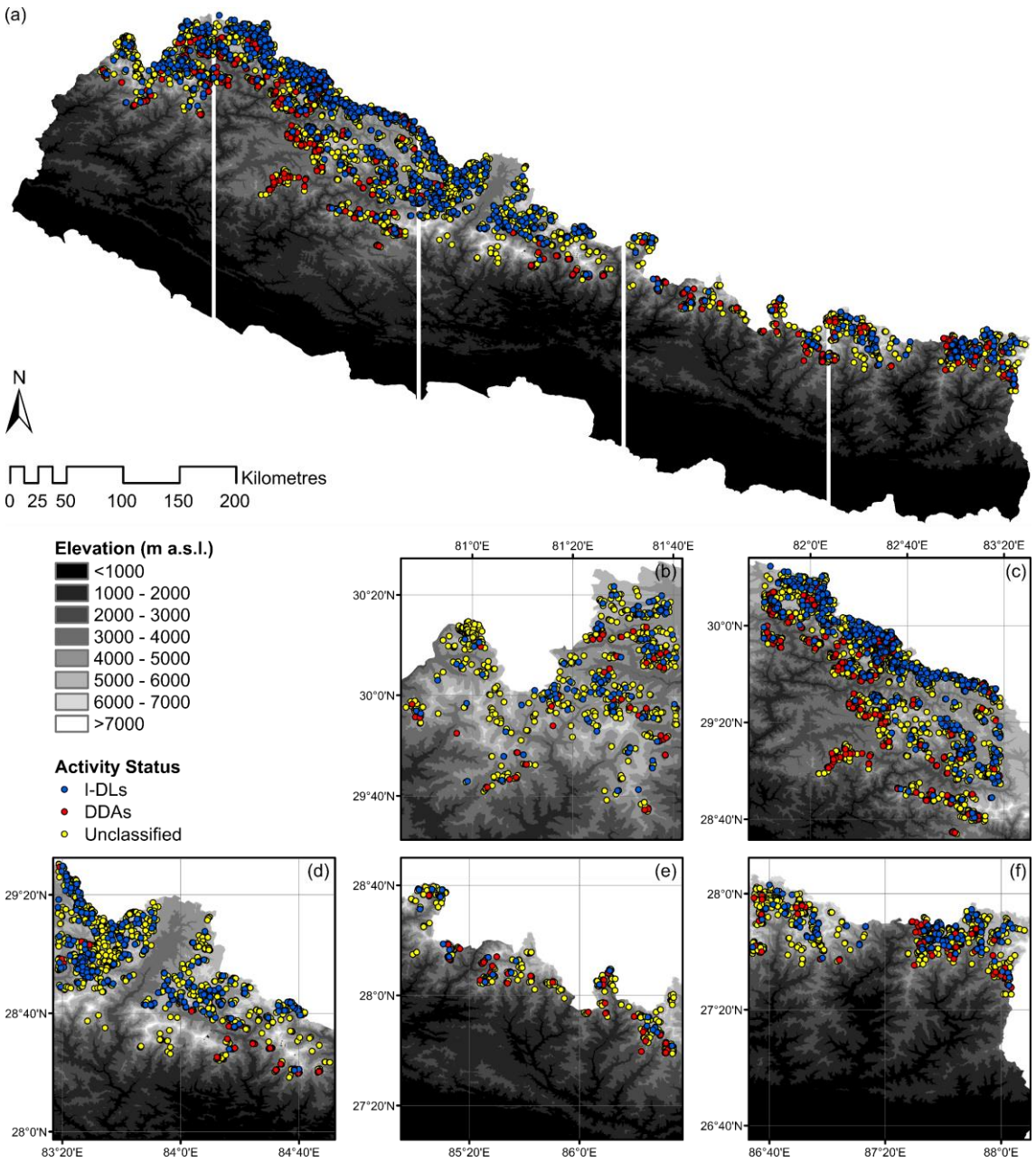

Figure 6.3. Distribution of DDAs and I-DLs overlaid on the SRTM30 DEM for the: (a) entirety of Nepal; (b) Far-west region; (c) West region; (d) Central-west region; (e) Central region; and (f) East region. Landforms with unclassified activity status (i.e. pinned rock glaciers that were not digitised) are depicted for completeness.

6.5.1.1 LANDFORM ELEVATION AND DISTRIBUTION

DDAs and I-DLs were situated within an elevation range of 3,225 to 5,675 m a.s.l. (**Figure 6.4**). Nationally, the mean MEF for DDAs/I-DLs was 4,837 ± 365 m a.s.l. Although the remotely-based classification of DDAs/I-DLs has associated limitations, the histogram and boxplots of MEFs across the regions provide an indirect qualitative validation of inventory reliability. Specifically, reported mean MEFs demonstrate that I-DLs consistently occurred at higher elevations than DDAs (**Figure 6.4**; **Figure 6.5**).

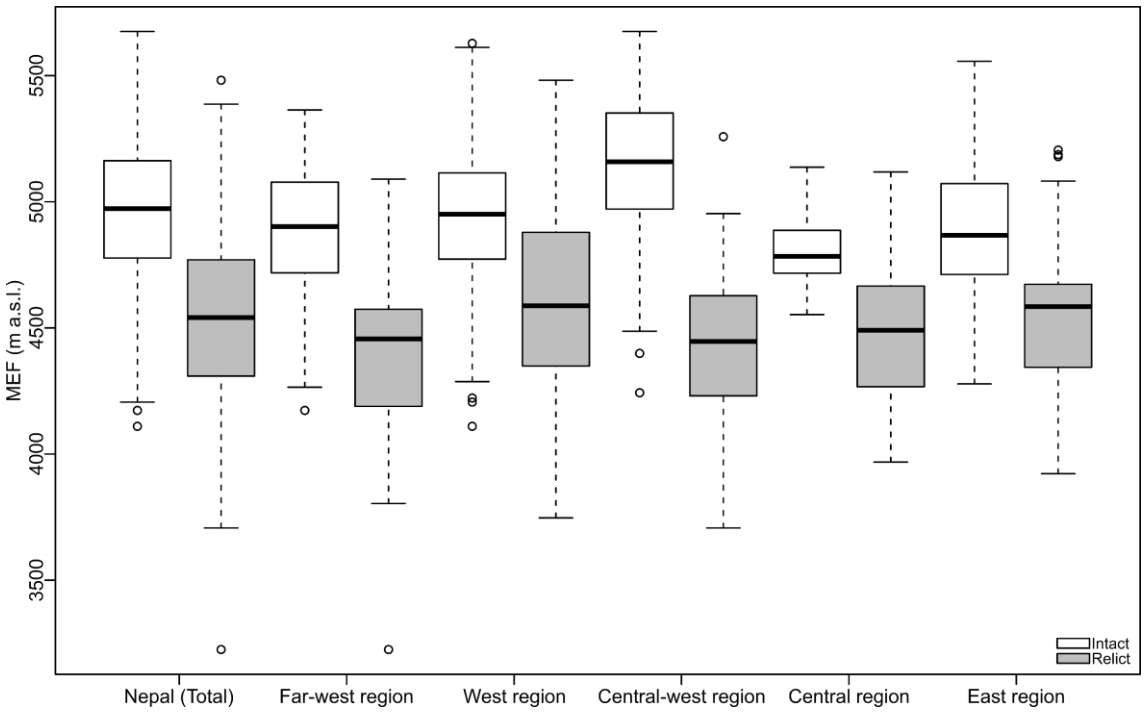

Figure 6.4. Boxplot showing the distribution of DDA/I-DL MEFs Nepal-wide (Total) and regionally from west to east. Here, the whiskers extend to either the minimum and maximum of the data or 1.5 times the interquartile range, whichever is smaller. The circles represent outliers.

The majority of I-DLs identified are located above 4,600 m a.s.l. (92%), with most situated within the 4,800–5,200 m a.s.l. (51%) elevation belt (**Figure 6.5**). DDAs cluster predominantly between 4,200 and 4,800 m a.s.l. (62%), and 4,400–4,800 m a.s.l. (43%) in particular (**Figure 6.5**). Nationally, the mean MEF for all I-DLs was 4,977 ± 280 m a.s.l. (**Table 6.4**), ranging between 4,110 and 5,675 m a.s.l. The highest I-DL was located in the Central-west region at 5,675 m a.s.l. ([3]NEP1186_1_10-25-2011). The mean MEF for all DDAs Nepal-wide was 436 m lower than that of I-DLs, at 4,541 ± 346 m a.s.l. (**Table 6.4**), with a range of 3,225 to 5,482 m a.s.l. The highest DDA was situated in the West region at 5,482 m a.s.l. ([4]NEP637_1_10-14-2010). I-DLs are located at statistically higher MEFs than DDAs at the national scale (ANOVA: F-value = 513.43, *df* within groups = 1, between groups = 1,135, p = <0.001); Tukey post hoc testing showed I-DLs were situated at statistically higher MEFs than DDAs in all sub-regions, with the greatest difference seen in the Central-west region (Diff = 732, p = <0.001) and smallest in the Central region (Diff = 310, p = <0.001). **Figure 6.4** shows that the largest MEF elevation spread of I-DLs occurs within the West region (4,110 to 5,628 m a.s.l., range = 1,518 m), while that of DDAs occurs within the Far-west region (3,225 to 5,090 m a.s.l., range = 1,865 m). The Central region had the smallest elevation range of both I-DLs (4,553 to 5,137 m a.s.l., range = 584 m) and DDAs (3,968 to 5,118 m a.s.l., range = 1,150 m).

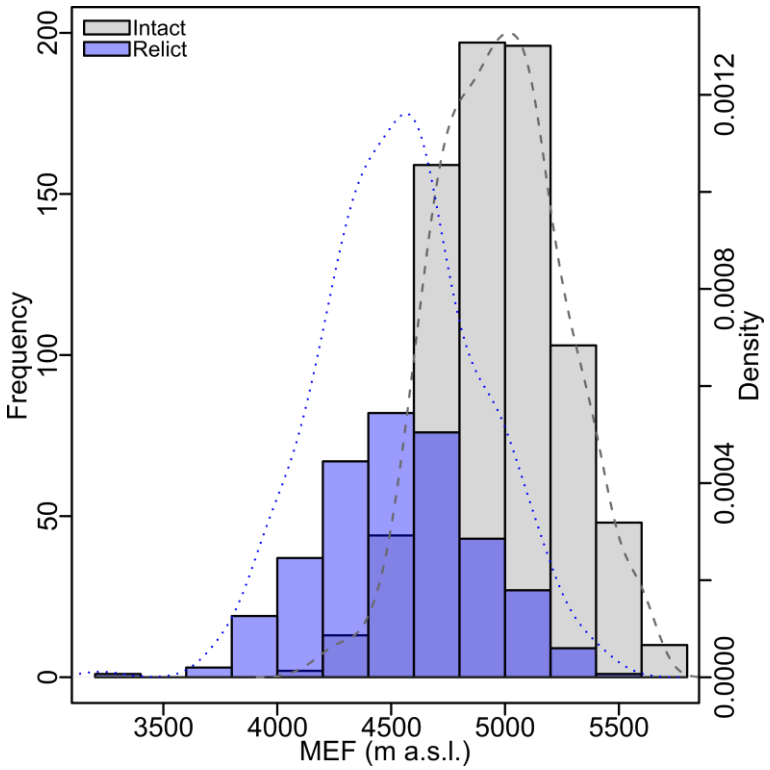

Figure 6.5. Nepal-wide frequency analysis of intact and relict landform MEF, grouped into classes of 200 m of elevation. The fitted lines represent a normal (Gaussian) distribution.

The spatial distribution of DDAs/I-DLs among the five sub-regions is also somewhat inhomogeneous; total landform numbers vary from 354 (~6%) in the Central region to 3,025 (~48%) in the West region (**Table 6.4**). Available suitable area, i.e. terrain ≥3,225 m a.s.l., appears to be key to DDA/I-DL development and sustainability in the Nepalese Himalaya. Mountainous terrain ≥3,225 m a.s.l. comprises ~43,500 km² (~27%) of Nepal; those regions with the largest proportional area ≥3,225 m a.s.l., correspondingly have the largest proportion of DDAs/I-DLs (**Table 6.5**). The overall mean density (*n* km^{-2}) of DDAs/I-DLs ranges between 0.09 (Central region) and 0.19 (West region), with an I-DL mean density of 0.10 and DDA mean density of 0.05 (**Table 6.5**). Considering the specific landform area ≥3,225 m a.s.l., values are greatest in the West region (4.69 ha km^{-2}) followed by the Far-west region (3.69 ha km^{-2}) and tend to decrease eastwards, with specific landform areas below the mean value (3.40 ha km^{-2}) in all remaining regions (**Table 6.5**).

Table 6.5. DDA/I-DL proportion, proportional area ≥3,225 m a.s.l., DDA/I-DL density and DDA/I-DL specific area across the sub-regions of Nepal. Where appropriate, values are reported to two decimal places.

	East (86°34'–88°12'E)	Central (84°56'–86°34'E)	Central-west (83°18'–84°56'E)	West (81°40'–83°18'E)	Far-west (80°02'–81°40'E)
DDA/I-DL proportion	13%	6%	20%	48%	13%
Proportional area ≥3,225 m a.s.l.	14%	10%	25%	39%	13%
Density (n km^{-2})*	0.15	0.09	0.12	0.19	0.15
Specific area (ha km^{-2})†	2.01	1.11	2.92	4.69	3.69

*Density (n km^{-2}) was calculated by considering the regional area ≥3,225 m a.s.l. (MEF of lowest observed landform).

†Specific area (ha km^{-2}) where 'ha' reflects DDA/I-DL area, was also calculated by considering the regional area ≥3,225 m a.s.l. The upscaled results were used within calculations of both density and specific area.

6.5.1.2 LANDFORM ASPECT

Generally, north-facing slopes dominate the development and formation of DDAs/I-DLs. Forty-four per cent of landforms are situated within north-facing aspects (NW, 15%; NE, 15%; N, 14%), while 17% have developed on west-facing slopes. Furthermore, taken as a whole, the mean aspect suggests DDAs/I-DLs are predominantly situated on north-western ($\bar{x} =$ 314°) slopes.

Activity classification of observed landforms shows that I-DLs are more evenly distributed across aspect classes, while DDAs are predominantly situated on north- (56%: NW, 21%; N, 19%; NE, 16%) and west-facing (17%) slopes, with 5 to 9% located in each of the remaining aspect classes (**Figure 6.6a**). I-DLs within the inventory show a mean aspect of 288°, with a circular variance of 0.13. Circular variance, defined as $CV = 1 - \bar{R}$ where the quantity $\bar{R}$ is the mean resultant length, indicates the dispersion of individual values around the mean, ranging between 0 and 1; values close to 1 suggest low dispersion (Davis, 2002, p. 321). DDAs show a mean aspect of 333°, with a circular variance of 0.34, therefore exhibit comparatively less dispersion than I-DLs. Regionally, with the exception of the Central-west region, a greater proportion (%) of I-DLs are situated within the northern- compared to the southern-quadrant (**Table 6.6**; **Figure 6.6b-f**). DDAs within all regions are predominantly situated within the northern quadrant (48 to 69%) compared to the southern quadrant (13 to 29%) (**Table 6.6**; **Figure 6.6b-f**).

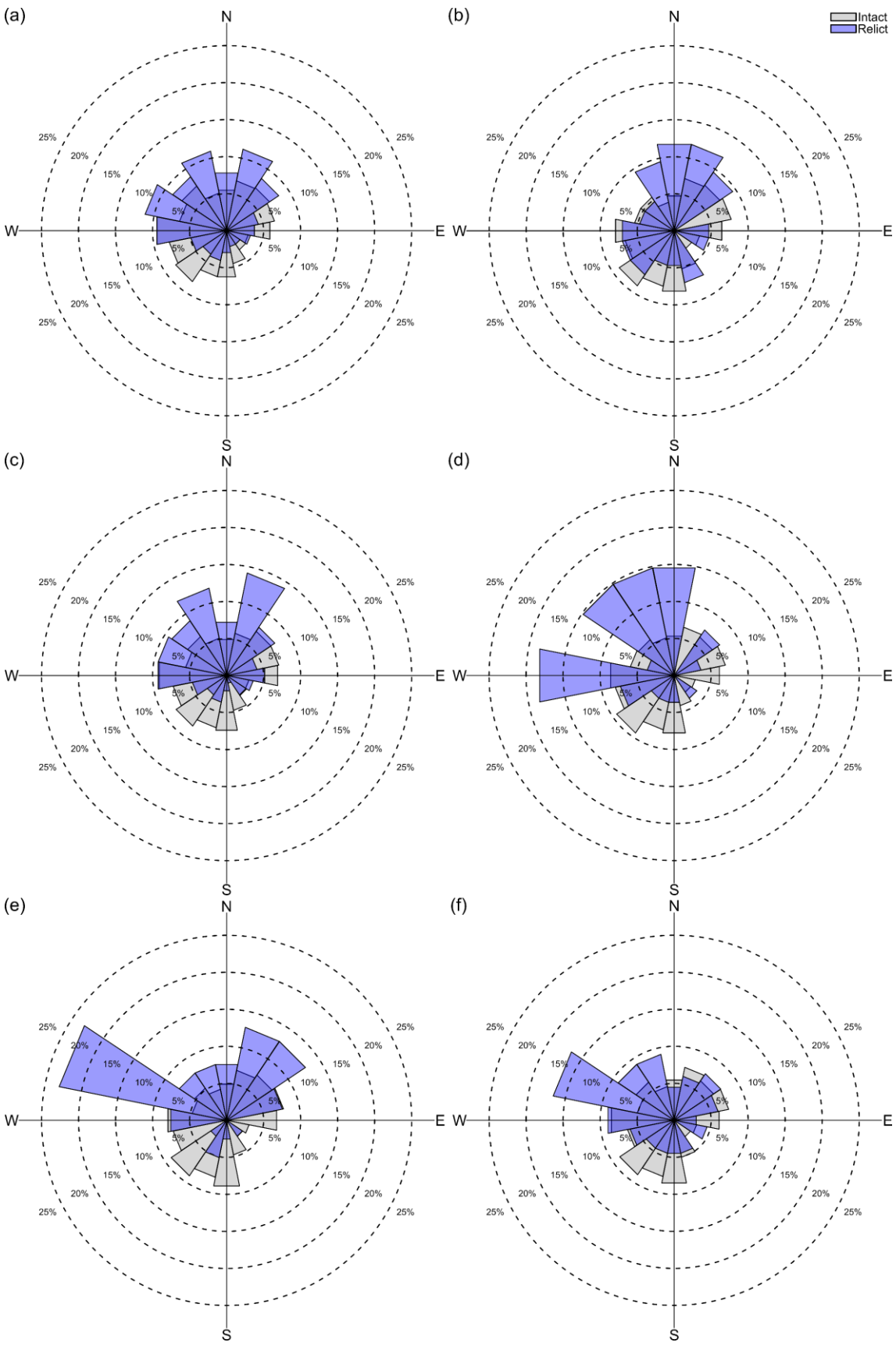

Figure 6.6. Rose plots showing the relative abundance (%) of intact and relict landforms across slope aspects within: (a) Nepal-wide (Total); (b) Far-west region; (c) West region; (d) Central-west region; (e) Central region; and (f) East region. The angular interval is 22.5°.

Table 6.6. Regional aspect classification of DDAs and I-DLs into north- (292.5 to 67.5°) and south- (112.5 to 247.5°) facing aspect quadrants.

Activity	Aspect Quadrant	Region				
		East (86°34'–88°12'E)	Central (84°56'–86°34'E)	Central-west (83°18'–84°56'E)	West (81°40'–83°18'E)	Far-west (80°02'–81°40'E)
Intact	North (NW, N, NE)	41%	55%	33%	39%	45%
	South (SW, S, SE)	35%	23%	39%	32%	29%
Relict	North (NW, N, NE)	48%	69%	56%	57%	52%
	South (SW, S, SE)	24%	13%	22%	17%	29%

Taken as a whole, landforms situated within the northern aspect quadrant occur at consistently lower elevations compared to DDAs/I-DLs located within the southern aspect quadrant (**Figure 6.7**; **Figure 6.8**; **Figure 6.9a**). This altitudinal mismatch ranges between 25 m (Far-west region) to 307 m (West region) ($\bar{x}$ = 240 m), and is reflected within both I-DLs and DDAs at $\bar{x}$ = 166 m and $\bar{x}$ = 152 m, respectively. Regionally, with the exception of the Far-west region where both I-DLs ($\bar{x}$ = 5 m) and DDAs ($\bar{x}$ = 81 m) situated within the southern quadrant occur at lower elevations, all regions reflect this observation.

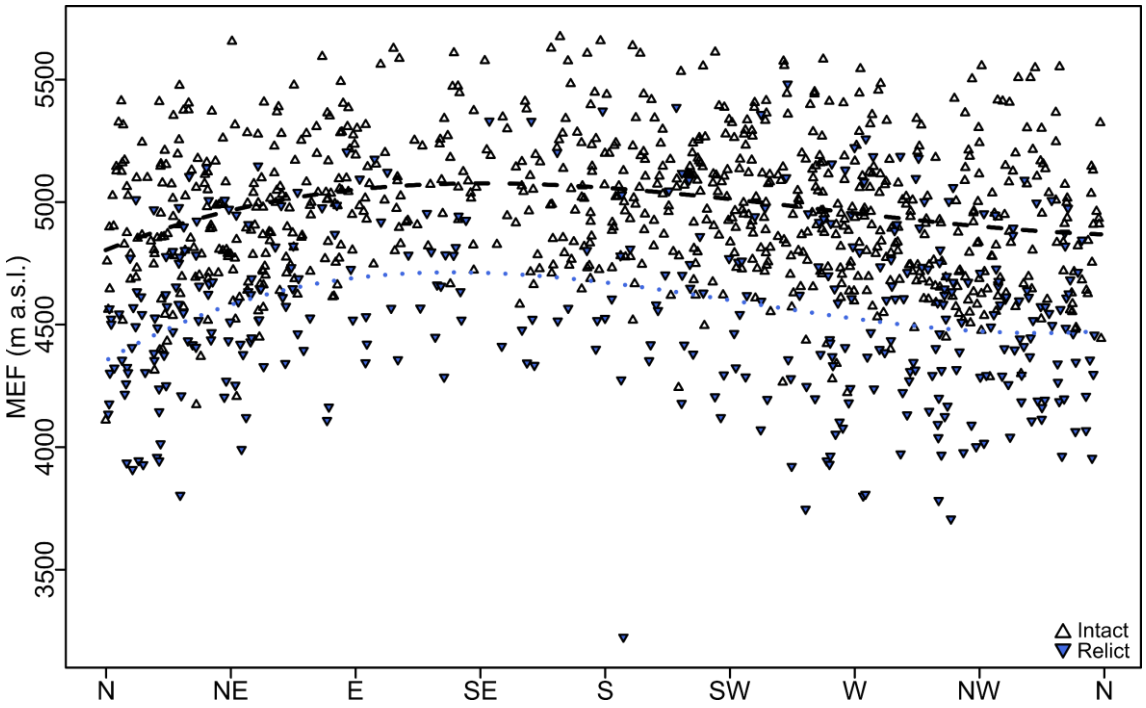

Figure 6.7. Scatterplot of mean aspect (°) against MEF showing the distribution of intact and relict landforms Nepal-wide. The two dashed lines are 3rd order polynomial fit (upper line: intact landforms; lower line: relict landforms).

Nationally, ANOVA showed statistically significant differences between aspect class and DDA/I-DL MEF (F-value = 17.94, *df* within groups = 7, between groups = 1,129, p = <0.001). Tukey post hoc testing confirms that DDAs/I-DLs situated within the northern aspect quadrant and western slope aspects occur at statistically lower MEFs than those found within the southern aspect quadrant and east slope aspects (**Figure 6.8**).

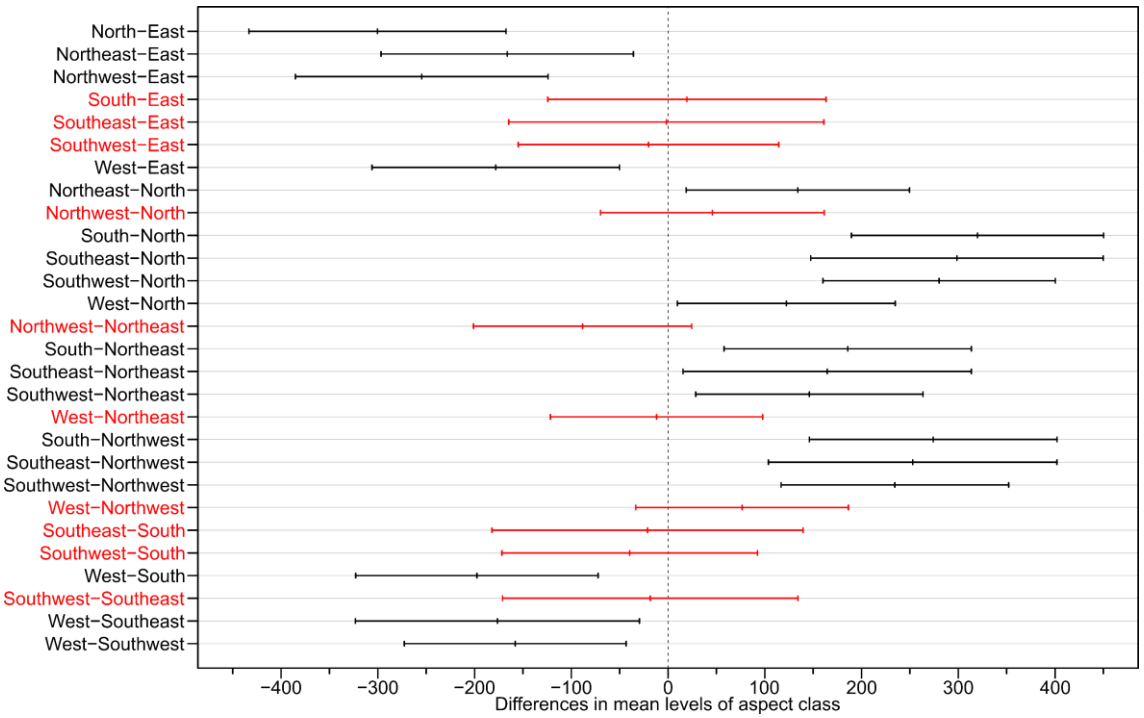

Figure 6.8. Tukey post hoc pairwise comparisons of landform MEF as a function of slope aspect class. The plotted lines represent the lower and upper level of the 95% confidence interval around the mean difference (black: statistically significant; red: non-statistically significant).

Slope aspect appears to have little influence on landform size (**Figure 6.9b**), and no significant difference was found (ANOVA: F-value = 0.79, *df* within groups = 7, between groups = 1,097, $p = 0.597$). Both DDA and I-DL mean size is largest on east-facing slopes. Indeed, the largest I-DL encompassing 3.55 km² is located on a south-facing slope ([4]NEP74_2_12-22-2011). Slope aspect appears to affect areal distribution (**Figure 6.9c**). DDA total area in the northern quadrant, ~30 km², is greater than that in the southern quadrant, ~10 km². In contrast, the pattern of I-DL total area is relatively homogenous across aspect classes, with two exceptions; the peak and trough in west and southeast aspect classes, respectively (**Figure 6.9c**). **Figure 6.10a** demonstrates that the frequency of hillslope aspects ≥3,225 m a.s.l. in the Nepalese Himalaya are relatively uniform, whereas **Figure 6.10b** reaffirms the relative dominance of the northern and west aspect classes.

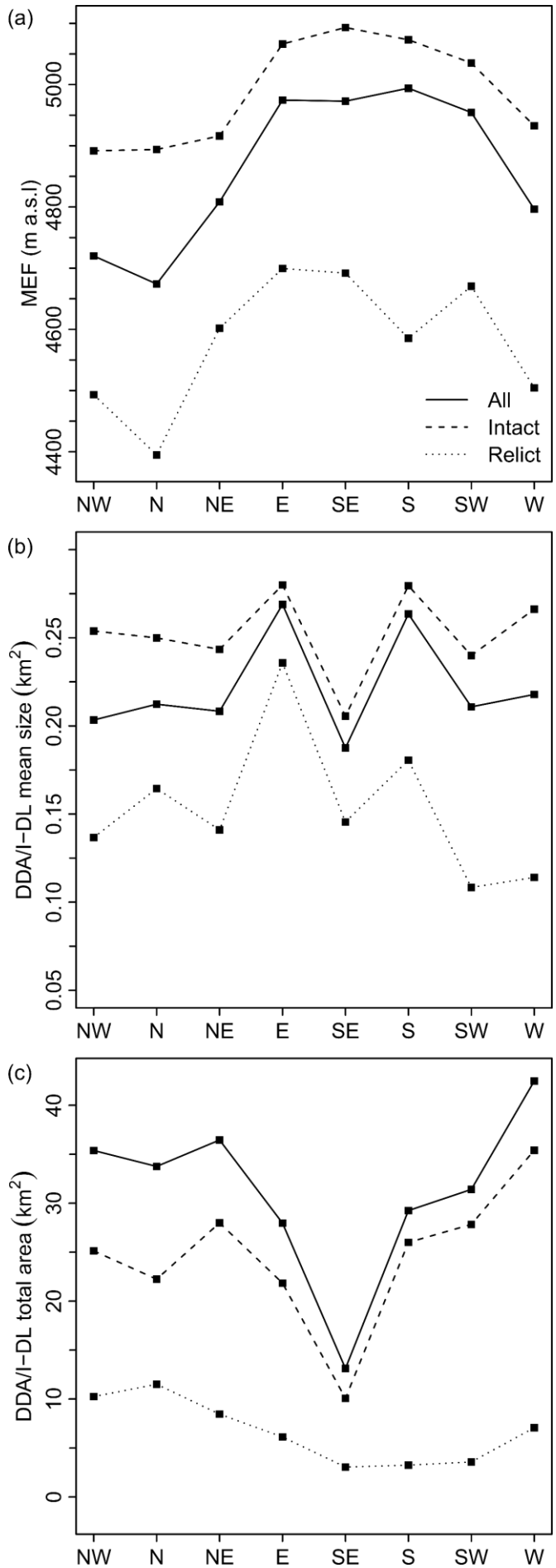

Figure 6.9. Analysis of: (a) MEF; (b) DDA/I-DL mean size; and (c) DDA/I-DL total area, as a function of slope aspect.

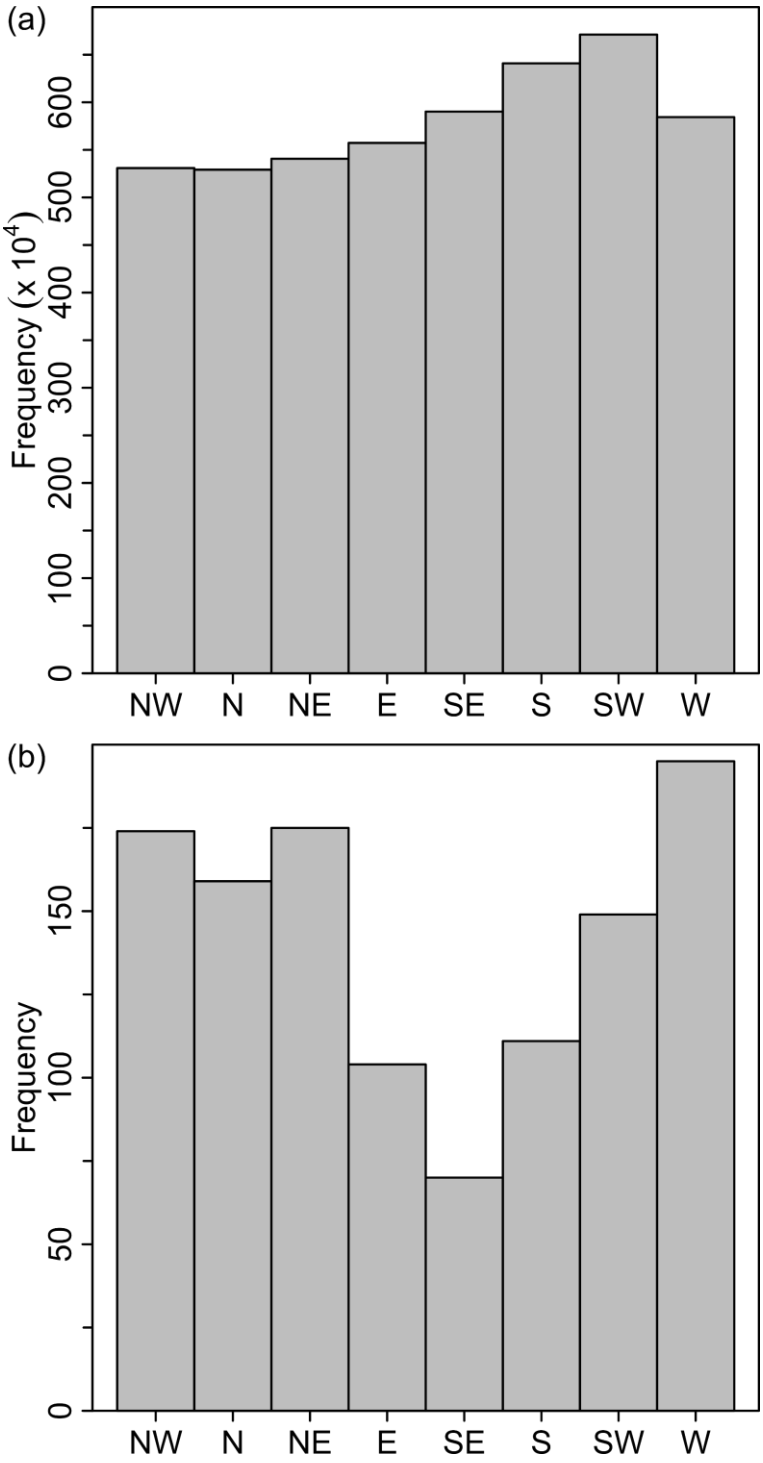

Figure 6.10. Analysis of hillslope aspect for landforms in the inventory: (a) frequency of hillslope aspects for all-mountain slopes (≥3,225 m a.s.l.) for each pixel in the Nepalese Himalaya; and (b) frequency of aspect classes for observed landforms in the Nepalese Himalaya.

6.5.1.3 LANDFORM MORPHOLOGY

The predominant geometry type (see **section 6.4.1.2**) of landforms in the inventory was tongue-shaped (91%), a proportion reflected by both DDAs and I-DLs (91% and 90%, respectively). Landforms >1 km in length form ~16% of the observed DDAs/I-DLs, examples of which are apparent in all five sub-regions. Remaining landforms were all <1 km long; overall mean

length was ~690 ± 519 m, while I-DL and DDA mean length was calculated to be 765 ± 569 and 531 ± 343 m respectively (**Table 6.4**). I-DL mean length was longest in the West region ($\bar{x}$ = 829 ± 610 m) and shortest in the Central region ($\bar{x}$ = 549 ± 264 m), while DDA mean length was longest in the Far-west region ($\bar{x}$ = 662 ± 359 m) and shortest in the East region at 413 ± 203 m (**Table 6.4**).

Median values (as opposed to means) are reported in order to analyse spatially the landform length since this variable is not normally distributed and exhibits large standard deviations. Across Nepal, the median landform length of I-DLs (615 m) is greater than that of DDAs (442 m); this pattern is reflected within all sub-regions (**Figure 6.11a**). Additionally, the median length of both I-DLs and DDAs generally increases from east to west (**Figure 6.11a**). Indeed, landform length differed statistically significantly between regions (ANOVA: F-value = 13.42, *df* within groups = 4, between groups = 1,132, p = <0.001).

Tukey post hoc testing of I-DL length (ANOVA: F-value = 5.61, *df* within groups = 4, between groups = 767, p = <0.001) showed that landforms in the western regions exhibit statistically greater lengths than those in the East region; the West region (p = <0.001) and Far-west region, p = 0.010). Similarly, DDAs (ANOVA: F-value = 6.33, *df* within groups = 4, between groups = 360, p = <0.001) towards western Nepal are also significantly longer than those situated in eastern Nepal; the Central-west- (p = 0.043), West- (p = 0.001) and Far-west-regions (p = 0.030) DDAs are statistically longer than in the Central region, while those situated in the West region (p = 0.001) and Far-west region (p = 0.037) are statistically longer than those of the East region. Indeed, the longest observed landform, measuring 4,686 m ([5]NEP207_1_11-18-2012), is situated within the Far-west region.

In total, the DDA/I-DL sample covers 249.83 km² of the Nepalese Himalaya. Furthermore, upscaled estimates total 1,371 km² throughout Nepal, with regional total upscaled estimates ranging between 43.86 and 731.82 km² in the Central- and West-region, respectively. Individually, digitised landform area varies between 0.005 and 3.54 km², with 719 (~63%) landforms ≥0.1 km² in area. Both the largest I-DL and DDA are situated within the West region (3.54 km² and 1.50 km², respectively). Nepal-wide mean landform area was reported at 0.22 ± 0.30 km² and median at 0.13 km². There are no DDAs/I-DLs >1 km² in the Central region.

Similar to landform length, regional mean DDA/I-DL area values exhibit large standard deviations and are not normally distributed, and thus median values are reported. Overall, median landform area ranges between 0.10 and 0.16 km² and generally increases for both DDAs and

I-DLs from east to west (**Figure 6.11b**). Furthermore, ANOVA showed statistically significant differences between regions and landform area (F-value = 12.21, *df* within groups = 4, between groups = 1,132, p = <0.001). Tukey post hoc testing of I-DL area (ANOVA: F-value = 6.13, *df* within groups = 4, between groups = 767, p = <0.001) showed that values in the Central-west- (p = 0.034), West- (p = <0.001) and Far-west-region (p = 0.013) were statistically larger than the East region. DDAs (ANOVA: F-value = 3.90, *df* within groups = 4, between groups = 360, p = 0.004) in the East region were also found to be statistically smaller than in other regions; the West region (p = 0.032) and Far-west region (p = 0.043). Conversely, previous work reported the opposite, with landform area in the Nepalese Himalaya decreasing from east to west (Regmi, 2008); however, this study focused on five relatively small-scale study areas across Nepal totalling 1,654 km².

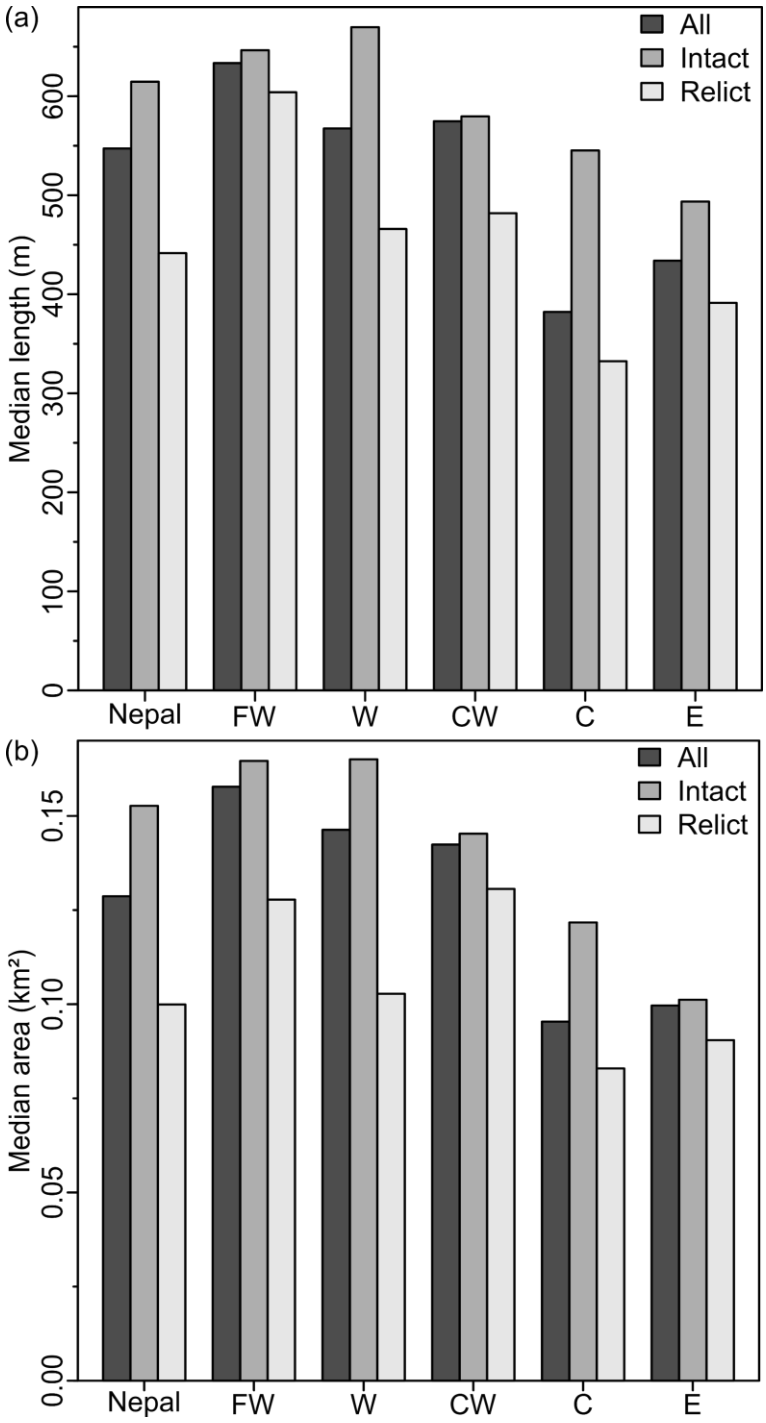

Figure 6.11. Nepal-wide- and regional-analysis of DDA/I-DL: (a) median landform length; and (b) median landform area.

6.5.2 WATER EQUIVALENT STORES

Sample I-DL thickness estimates ranged between ~19 and ~64 m (mean = ~35 m). Resulting sample I-DL ice content was estimated to be between 3.35 to 5.03 billion cubic metres; up-scaled I-DL ice content was estimated to be 22.99 ± 0.60 billion cubic metres (**Table 6.7**).

The results in **Table 6.7** show that the sample of I-DLs is estimated to contain a total WVEQ of 3.81 ± 0.84 km³ throughout Nepal. The reported upscaled estimates suggest total WVEQs of

20.90 ± 4.18 km³ could reasonably be stored within I-DLs throughout Nepal (see **Supplementary Figure 12.3**). Henceforth, I-DL volumetric results will reflect the format *sample result (upscaled result).* Regionally, I-DLs within the Central region have been estimated to contain the smallest WVEQs, storing between 0.04 and 0.06 km³ (0.23–0.35 km³) of water. The East- and Far-west-regions store 0.25 ± 0.05 km³ (1.31 ± 0.27 km³) and 0.58 ± 0.12 km³ (2.99 ± 1.60 km³) of water respectively, while I-DLs situated within the Central-west region contain frozen hydrological stores between 0.85 and 1.27 km³ (4.19–6.29 km³). In the West region, I-DLs contain the largest regional estimated WVEQ, 1.57 to 2.36 km³ (8.85–13.27 km³), more than double the stores within the Central-west region.

Table 6.7. Ice volume (km³) and corresponding WVEQs (km³) for both the sample and upscaled I-DLs, regionally and Nepal-wide (total). These calculations encompass a range of ice content by volume estimates with a lower (40%), average (50%) and upper (60%) bound. Values are reported to two decimal places.

Region	Ice content by volume		Sample I-DLs		Upscaled I-DLs	
			Ice volume (km³)	WVEQ (km³)	Ice volume (km³)	WVEQ (km³)
East (86°34'–88°12'E)	Lower	(40%)	0.22	0.20	1.16	1.05
	Average	(50%)	0.27	0.25	1.45	1.31
	Upper	(60%)	0.33	0.30	1.73	1.58
Central (84°56'–86°34'E)	Lower	(40%)	0.04	0.04	0.26	0.23
	Average	(50%)	0.05	0.05	0.32	0.29
	Upper	(60%)	0.07	0.06	0.38	0.35
Central-west (83°18'–84°56'E)	Lower	(40%)	0.85	0.77	4.61	4.19
	Average	(50%)	1.06	0.96	5.76	5.24
	Upper	(60%)	1.27	1.16	6.91	6.29
West (81°40'–83°18'E)	Lower	(40%)	1.73	1.57	9.73	8.85
	Average	(50%)	2.16	1.97	12.17	11.06
	Upper	(60%)	2.60	2.36	14.60	13.27
Far-west (80°02'–81°40'E)	Lower	(40%)	0.51	0.46	2.63	2.39
	Average	(50%)	0.64	0.58	3.29	2.99
	Upper	(60%)	0.76	0.69	3.95	3.59
Total	Lower	(40%)	3.35	3.05	18.39	16.72
	Average	(50%)	4.19	3.81	22.99	20.90
	Upper	(60%)	5.03	4.57	27.59	25.08

GlabTop2 provides estimated ice glacier thicknesses ranging between ~4 and ~454 m (mean = ~49 m) within Nepal, with total ice volume estimated to be ~219.59 billion cubic metres. On average, I-DLs within the Nepalese Himalaya contain 3.81 km³ (20.90 km³) of water, whereas ice glaciers store 197.63 km³ (**Table 6.7**; **Table 6.8**). This translates to a ratio of I-DL to ice glacier WVEQ of 1:52, indicating that ice glaciers store a volume of water ~52 times larger than I-DLs. This ratio reduces to 1:9, where upscaled I-DL WVEQs are considered. Regionally, the I-

DL to ice glacier WVEQ ratio is lowest within the West region, 1:17 (1:3), where I-DLs contain 1.97 km³ (11.06 km³) of water compared to 33.67 km³ stored within ice glaciers. Furthermore, regions west of 84°56'E have lower ratios (Central-west, 1:73 [1:13]; Far-west, 1:26 [1:5]) than those in the East- and Central-regions of Nepal. In the East region, I-DLs contain 0.25 km³ (1.31 km³) of water, yet 53.17 km³ resides within ice glaciers, resulting in an I-DL to ice glacier WVEQ ratio of 1:214 (1:40). The highest I-DL to ice glacier WVEQ ratio, 1:517 (1:89), aligns with the region containing the fewest number of I-DLs and smallest WVEQ – the Central region (0.05 km³ [0.29 km³]); ice glacier WVEQ in this region is estimated to be 25.86 km³.

Table 6.8. Regional and Nepal-wide area (km²) and associated WVEQs (km³) for I-DLs (sample and upscaled) and ice glaciers. Additionally, the I-DL to ice glacier ratios are directly compared. I-DL WVEQs assume the 50% (average) ice content by volume. Values are reported to two decimal places.

Region	Regional area (km²)	Ice-debris landform		Ice glacier		Ratio: I-DL: Ice glacier WVEQ	
		Sample WVEQ (km³)	Upscaled WVEQ (km³)	Area (km²)	WVEQ (km³)	Sample ratio	Upscaled ratio
East	~26,000	0.25	1.31	1,013.82	53.17	1:214	1:40
Central	~40,000	0.05	0.29	589.63	25.86	1:517	1:89
Central-west	~30,000	0.96	5.24	1,585.47	69.98	1:73	1:13
West	~26,500	1.97	11.06	850.14	33.67	1:17	1:3
Far-west	~25,000	0.58	2.99	386.89	14.95	1:26	1:5
Total	~147,500	3.81	20.90	4,425.96	197.63	1:52	1:9

6.5.3 INVENTORY VALIDATION

Certainty Index scores, listed in order of occurrence, for the sample are *high certainty* (~82%), *virtual certainty* (~11%) and *medium certainty* (~6%). I-DLs dominate the 'virtual certainty' category (96%), while DDAs have a proportionally larger presence in the 'medium certainty' category (63%). This is to be expected. As the geomorphic indicators used to identify DDAs/I-DLs are a surficial expression of the presence of abundant ice (**Table 6.1**), relict features (DDAs) or those transitioning towards relict activity status exhibit less well-defined morphological characteristics, and thus increased uncertainty with regards to: (i) clear external boundaries (i.e. outline); (ii) distinct longitudinal flow structure; (iii) distinct transverse flow structure; and (iv) steepness of the frontal slope. To better understand inventory uncertainty, there is a need for further inventory validation beyond those measures (i.e. Certainty Index) already in place.

6.5.3.1 COMPARISON WITH THE PERMAFROST ZONATION INDEX

Rock glaciers, as the most conspicuous morphological manifestation of permafrost in high mountain systems (Barsch, 1996), have previously been utilised for the estimation of permafrost distribution (Janke, 2005b; Sattler et al., 2016; Deluigi et al., 2017; Esper Angillieri, 2017). The Global Permafrost Zonation Index (PZI), based on a simple global model with a spatial resolution of ~1 km, is an index that helps to consistently constrain and visualise areas of likely permafrost occurrence (Gruber, 2012). In the HKH region, Schmid et al. (2015) reported good agreement between the PZI and mapped rock glaciers; therefore, here we compare the spatial distribution of the sample within Nepal to the PZI.

Overall, only ~4% of the DDA/I-DL sample reaches areas outside of the PZI boundary; thirty-one relict landforms and 13 intact landforms (**Figure 6.12**). PZI values ≥0.1 form the *permafrost region* (PR), with PZI <0.1 attributed to the *PZI fringe of uncertainty* – "the zone of uncertainty over which PZI could extend under conservative estimates" (cf. Table 1 in Gruber, 2012). Here, ninety-nine landforms, predominantly DDAs (82%), are situated within the PZI fringe of uncertainty. Thus, 87% of the DDA/I-DL sample was situated within the PR; 96% and 69% of I-DLs and DDAs, respectively. Additionally, with increasing 'habitat suitability' for I-DL development and sustainability, i.e. towards PZI = 1, we report largely concurrent increases in I-DL frequency and vice versa for DDAs (**Figure 6.12a**). Furthermore, **Figure 6.12b** reflects the spatial distribution of total landform area as a function of PZI values; this suggests a strong relationship between DDA/I-DL habitat suitability and total landform area. Regarding Certainty Index scores, those landforms categorised as high certainty and virtual certainty cluster

around PZI values ≥0.6 (~56% and ~71%, respectively). DDAs/I-DLs categorised as medium certainty cluster around PZI values ≤0.3 (59%), which may reflect the less well-defined morphological characteristics of landforms – relict features or those transitioning towards relict activity status – containing lower ice volumes. Based on this summary evaluation, both the DDA/I-DL identification and mapping and classification of activity status are in good agreement with the PZI. Additionally, several rock glaciers in the Khumbu region were also validated in the field.

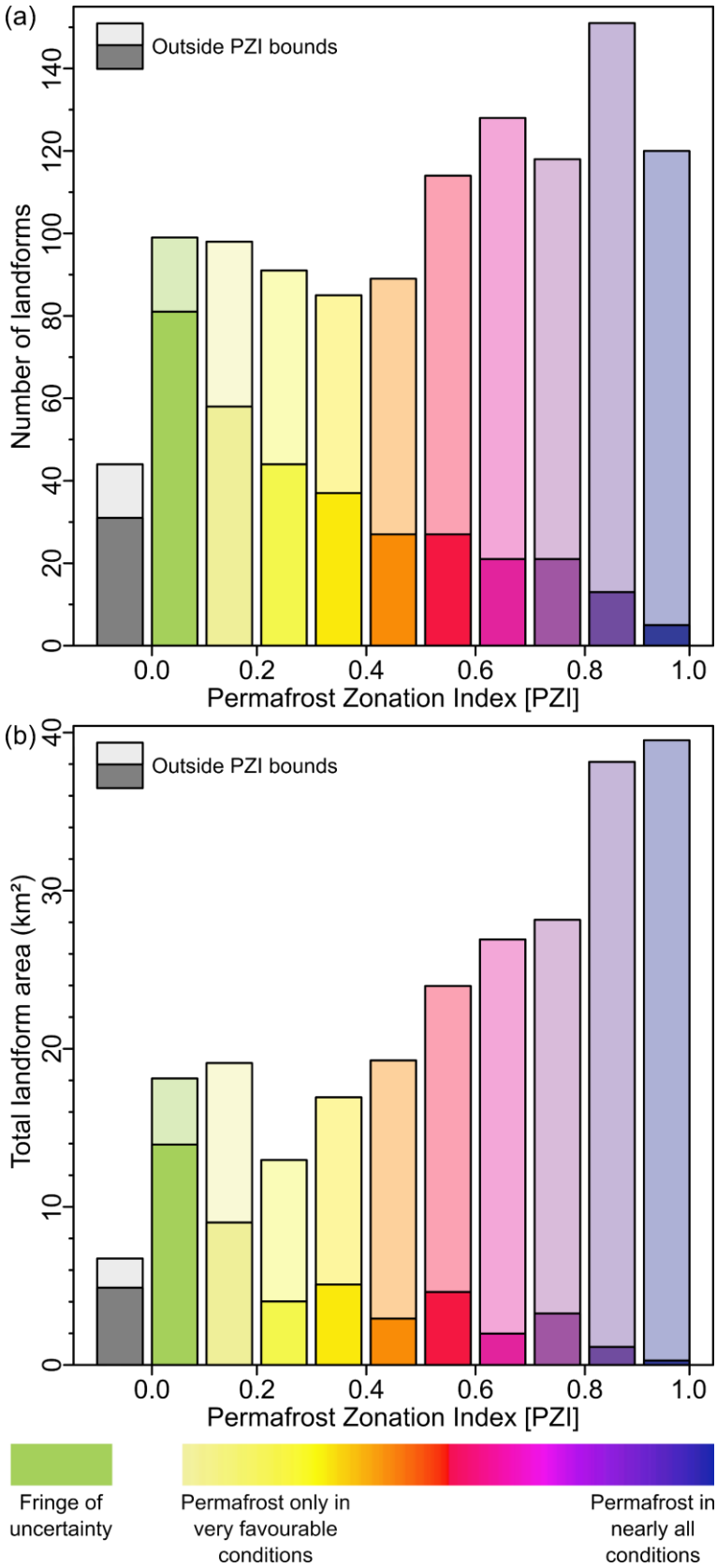

Figure 6.12. Analysis of the DDA/I-DL sample in relation to the PZI for: (a) the number of landforms; and (b) the total landform area. Pale colours represent intact (I-DL) landforms and intense colours indicate relict (DDA) landforms; bars are stacked. Regarding the PZI, see Gruber (2012) for further information.

6.6 DISCUSSION

6.6.1 LANDFORM DISTRIBUTION AND MORPHOLOGY

This Nepalese rock glacier inventory identified >6,000 landforms, from which a randomly selected ~20% sample (*n* = 1,137) was digitised, 772 intact and 365 relict landforms. The inter-regional MEF of observed landforms was rather inhomogeneous (**Figure 6.4**). Digitised DDAs and I-DLs were situated within an elevation range of 3,225–5,675 m a.s.l., broadly consistent with that reported for the HKH (3,500–5,500 m a.s.l.) (Schmid et al., 2015). Onaca et al. (2017) report that rock glaciers in the highest mountain ranges are comparatively larger than those in lower mountain ranges, as the duration of their activity lasted longer in the former. In the Nepalese Himalaya, many landform lengths are similar to the largest examples of rock glaciers found elsewhere, including the Karakoram Himalaya where many exceed 2 km, and some as much as 4 km (Hewitt, 2014, p. 276). The Chon-Aksu (Kalgan Tash, Tien Shan) and Karakoram rock glaciers, for example, are reported to be 3.2 and 3.7 km in length respectively (Bolch and Gorbunov, 2014). Additionally, rock glacier area ($\bar{x}$ = 0.22 km²) exceeds that of rock glaciers in other mountain ranges (see Jones et al., 2018a). Direct conversion of specific landform area (ha km^{-2}) to specific landform density (%) enables comparison with previous studies. At 3.40%, specific landform density within Nepal is higher than other studies in Central Asia; for example, ~1.50% in the Northern Tien Shan (Kazakhstan/Kyrgyzstan) (Bolch and Gorbunov, 2014) and 2.65% in the Zailyiskiy and Kungey Alatau (Kazakhstan/Kyrgyzstan) (Bolch and Marchenko, 2006). However, even higher densities have been reported in the Andes of Santiago (6.70%) and Andes of Mendoza, Chile (5.00%, Brenning, 2005a), and Turtmanntal, Swiss Alps (4.00%, Nyenhuis et al., 2005).

Rock glacier 'habitats' are typically situated in regions with high elevation, low MAAT and mainly low precipitation (Barsch, 1977; Haeberli, 1983; Baroni et al., 2004); conditions characteristic of the Nepalese Himalaya. At the regional-scale, precipitation and temperature climatically control rock glacier distribution; the former is dependent on elevation and aspect (Rangecroft et al., 2014).

The 0°C isotherm of MAAT and the equilibrium line altitude form the lower- and upper-bounds respectively, of I-DL development (Humlum, 1988; Brenning, 2005a; Rangecroft et al., 2014; Rangecroft et al., 2016). The mean MEF difference between intact and relict landforms, therefore, reflects an upward shift (~436 m) of the 0°C isotherm of MAAT over time. Across the Nepalese Himalaya, precipitation contributions decrease from east to west and from

south to north (Kansakar et al., 2004), for instance, regions north of high mountains are particularly arid (<500 mm yr^{-1}) compared to regions located on the windward side (Böhner et al., 2015 as cited in Karki et al., 2017). Furthermore, the lowest precipitation amounts are reported in Mustang, Manang and Dolpa (<150 mm yr^{-1}), situated in the leeward side of the Annapurna Range (Karki et al., 2017). In response to increasing continentality, the equilibrium line altitude increases, expanding the rock glacier niche (e.g., Rangecroft et al., 2014). Barsch and Jakob (1998) note that rock glaciers occur less frequently in subtropical mountain ranges associated with monsoon-dominated climates. In these zones, low snow lines and low equilibrium line altitudes result in extensive glaciation and thus restrict the niche appropriate for rock glacier development. Indeed, the largest and smallest range of DDA/I-DL MEFs occur in the West and Central regions respectively (**Figure 6.4**), and DDA/I-DL spatial density reflects this trend, with higher values towards the west of Nepal (**Table 6.5**). An inverse relationship is apparent between DDA/I-DL occurrence and precipitation, where high DDA/I-DL spatial densities are coupled with drier conditions. Similar assertions have been made for the European Alps (Boeckli et al., 2012). It should be noted, however, that under future warming the 0°C isotherm may move closer to, or above, mountain summits (Azócar and Brenning, 2010). The resulting smaller rock glacier niche, therefore, potentially leads to a decreased frequency in intact landforms and vice versa regarding relict landforms (Krainer and Ribis, 2012).

In the Nepalese Himalaya, analysis of observed landforms as a function of slope aspect confirms that DDAs/I-DLs situated within the north- to west-aspect classes, occur at lower MEFs than those found within the south- to east-aspect classes (**Figure 6.8**), corroborating findings from prior northern hemispheric studies which have found similar relationships (e.g., Seppi et al., 2012; Scotti et al., 2013). Furthermore, this finding is in agreement with previous work in the Kangchenjunga Himal, eastern Nepal, where the lowermost occurrences of rock glaciers were reported to vary from 4,800 m a.s.l. on northern slope aspects to 5,300 m a.s.l. on south- to east-facing slopes (Ishikawa et al., 2001). Therefore, northerly- and westerly-aspects with their reduced insolation, enable rock glacier formation and preservation at lower MEFs than other aspects (**Figure 6.7**). Furthermore, northerly aspects favour DDA/I-DL occurrence (**Table 6.6**), although there was no significant difference in landform frequency between aspects. Indeed, our results differ from previous inventories in the northern hemisphere (e.g., Barsch, 1996; Guglielmin and Smiraglia, 1997; Baroni et al., 2004) in which observed landforms cluster within the northern quadrant, with <10% situated in the remaining aspect classes; here, south-facing slopes account for 29% (SW, 13%; S, 10%; SE, 6%) of observed landforms.

Although elevation [temperature] is important in determining landform area, no correlation was observed between MEF and DDA/I-DL length (r = -0.04) or area (r = -0.09). Climatic controls, therefore, only partially explain DDA/I-DL characteristics and distribution.

In addition to climatic conditions, key controls on rock glacier characteristics and distribution include (i) glacial history (past- and modern-glaciations) and (ii) talus supply (Brenning, 2005a; Johnson et al., 2007). Topographic controls influence rock glacier form and distribution as local terrain, topoclimates and avalanche dynamics may override large-scale climatic- or altitudinal-drivers (Humlum, 1998; Janke, 2007). In the high and deeply incised Himalayas (Scherler et al., 2011), an abundance of steep rock walls associated with glacier-cirques (melted out) and over-deepened valley sides, provides suitable catchment areas for rock glacier development and, combined with intense monsoonal precipitation and tectonic activity, drives sediment transport processes (Barsch and Jakob, 1998). For example, within Central Asia, suggested explanations for rock glacier presence and absence in adjacent valleys of the northern Tien Shan, relate to large earthquake-driven rock avalanches or other mass movements (Gorbunov, 1983 as cited in Bolch and Gorbunov, 2014). It is important that lithology, a critical control for talus supply to ice- and rock-glacier surfaces (Haeberli et al., 2006), is evaluated with respect to the above. Unfortunately, high-quality lithological data for the Nepalese Himalaya was not available for use in this study.

6.6.2 ICE-DEBRIS LANDFORM WATER CONTENT

Results from the Nepalese Himalaya indicate that I-DLs may act as hydrologically valuable long-term water stores. Studies that consider rock glacier WVEQs are limited in number, particularly in Central Asia (Jones et al., 2018a); therefore, our estimates are compared to study regions further afield. I-DLs forming the sample in the Nepalese Himalaya are estimated to store the WVEQ of 3.05 to 5.03 km³, and between 16.72 and 25.08 km³ when considering upscaled estimates; significantly greater than estimates for other regions, for instance, the Chilean Andes (Azócar and Brenning, 2010), Bolivian Andes (Rangecroft et al., 2015), and Argentinean Andes (Perucca and Esper Angillieri, 2011). In Chile (27°–33°S), Azócar and Brenning (2010) found 147.5 km² of rock glaciers, estimated to store the water equivalent of 2.37 km³ – exclusive of our estimates, the largest WVEQ estimation to date. Overall, the upscaled national ratio of I-DL to ice glacier WVEQ is 1:9 (**Table 6.8**), suggesting that as water stores I-DLs in the Nepalese Himalaya are of relatively greater importance than those of the Bolivian Andes, 1:33 (Rangecroft et al., 2015) and the European (Swiss) Alps, ~1:83 (Brenning, 2005a).

However, evaluating the relative hydrological significance of I-DL WVEQs with respect to other water stores (e.g., ice glaciers) at the regional-scale vs the national-scale, provides important information for effective water resource management, particularly in terms of climate change adaptation strategies. **Table 6.8**, for instance, shows large inter-regional variability of I-DL WVEQs. In the Nepalese Himalaya, both the estimated volumetric ice content and spatial landform density (4.69%) were greatest within the West region, and therefore I-DLs situated in this region have the most potential as water sources. Conversely, volumetric ice content of I-DLs found in the Central region was the lowest in the Nepalese Himalaya. Rangecroft et al. (2015) suggest that through investigating these inter-regional differences in the context of both natural- and anthropogenic-external factors (e.g., population levels and alternate water sources), the hydrological significance of I-DL frozen water storage can be better understood.

6.6.3 ICE-DEBRIS LANDFORM HYDROLOGICAL SIGNIFICANCE

Across the Nepalese Himalaya, upscaled estimates of I-DL frozen water stores range between 0.29 and 11.06 km³ (**Table 6.7**; **Table 6.8**), with greater volumes found towards the west. I-DLs of the East- and Central-regions stored the lowest amounts of water (1.4% and 6.3% of total estimated I-DL WVEQ, respectively), yet with a combined population of ~15.5 million people (~58% of the Nepalese population), these regions are the most densely populated in Nepal (Central Bureau of Statistics, 2014)[4]. Within these regions, I-DL to ice glacier WVEQ ratios in **Table 6.8** show clearly that I-DLs contribute significantly less to regional water supply than ice glaciers. Central region estimated I-DL water storage is comparable to rock glaciers of the Chilean Andes (27°–29°S), which contain 0.35 km³ (Azócar and Brenning, 2010), although the relative abundance of other water sources in the Central region, Nepal, suggests I-DLs have lower relative importance than their counterparts in the Chilean Andes (ratio = 1:2.7 [Azócar and Brenning, 2010]). However, we hypothesise that I-DLs will become relatively more important compared to ice glaciers, with continued ice- and debris-covered-glacier mass loss in response to climate change in this region (e.g., Bolch et al., 2012; Kääb et al., 2012; Nuimura et al., 2012; Gardelle et al., 2013; King et al., 2017).

I-DLs are thermally decoupled from external micro- and meso-climates due to the insulative effect of the AL (Humlum, 1997; Bonnaventure and Lamoureux, 2013; Gruber et al., 2016). Consequently, the response of I-DLs to climate change occurs at decadal time scales,

[4] The five geographic sectors used within this study approximately align with the *development regions* used by the Central Bureau of Statistics (2014).

comparatively longer than ice glaciers (Haeberli et al., 2006). Therefore, I-DLs are more climatically resilient than ice glaciers (Millar and Westfall, 2008). Indeed, while I-DL MEFs are often strongly associated with the 0°C isotherm of MAAT (e.g., Sorg et al., 2015; Rangecroft et al., 2016), examples of I-DLs with positive MAATs have been reported (e.g., Baroni et al., 2004).

Climate-driven deglaciation resulting in the transition from glacial- to paraglacial-dominated process regimes in high mountain systems, for instance, the High Himalaya (Harrison, 2009), may subsequently increase ice glacier surface insulation through enhanced debris-supply (e.g., enhanced RSFs), preserving frozen water stores as ice glaciers transition to rock glacier forms (Knight and Harrison, 2014a). While few studies have reported the ice- to rock-glacier transition, Monnier and Kinnard (2015b) report an example in the Juncal Massif, Chilean central Andes, where the lower-section of the Presenteseracae debris-covered glacier has developed distinctive rock glacier morphology during the previous 60 years. Hillslope-erosion rates and hillslope angle usually increase concomitantly (Ouimet et al., 2009), with increased debris flux to glacier surfaces and therefore the formation of debris-covered glaciers linked to steep (>25°) accumulation areas; topographic characteristics typical within the high and deeply incised Himalayas (Scherler et al., 2011). Indeed, Himalayan debris-covered glaciers commonly have thick debris cover (>1 m) (Shroder et al., 2000; Nicholson and Benn, 2013). Steady-state talus-nourishment rates to (i) feature rooting zones encourage rock glacier growth (Bolch and Gorbunov, 2014) and restrict rock glacier starvation (Kellerer-Pirklbauer and Rieckh, 2016); and (ii) glacier surfaces encourages ice- to rock-glacier transition.

I-DLs situated in the Central-west- and West-regions contained the highest amounts of water (25.1% and 52.9% of total estimated I-DL WVEQ, respectively) according to our modelling results. In the West region, I-DLs have the highest relative importance as water stores compared to ice glaciers of all regions within the Nepalese Himalaya, with an I-DL to ice glacier WVEQ ratio of 1:3 (**Table 6.8**). This ratio is larger than that of the Sajama region, Bolivia (17°–18°S) (Rangecroft et al., 2015) and the Andes of Santiago, Chile (Brenning, 2005a), both with a ratio of 1:7, but of lower importance than in the Semi-arid Chilean Andes (29°–32°S) where rock glaciers are dominant with a ratio of 3:1 (Azócar and Brenning, 2010). Monsoonal precipitation (June–September) dominates annual precipitation (Shrestha et al., 2000; Karki et al., 2016), with contributions decreasing from east to west and from south to north (Kansakar et al., 2004). Consequently, as a result of substantial projected long-term glacial mass losses in response to climate warming (Bolch et al., 2012; Jiménez Cisneros et al., 2014; Huss and Hock,

2015; Shrestha et al., 2015), very low precipitation amounts, and limited investment in water resources infrastructure in mountainous regions (Bartlett et al., 2010, p. 18), we hypothesise that the hydrological value of I-DL water stores towards the west of Nepal, including the Central-west region (1:13), may be of greater importance than the I-DL to ice glacier WVEQ ratio initially suggests.

6.6.4 FURTHER CONSIDERATIONS AND FUTURE RESEARCH

Whereas much has been written on the role of ice glaciers in maintaining water supplies (Bradley et al., 2006; Vuille et al., 2008), that of rock glaciers has received comparatively little attention (Duguay et al., 2015). Rock glacier hydrology, however, is highly complex given: "various possible inputs and outputs; phase changes and movement of water associated with the AL; irregular distribution of frozen matrix that allows convoluted pathways for water flow; and deep crevices into which water disappears, among other complicating factors" (Burger et al., 1999). As a "porous medium that functions as an aquifer having recharge, discharge, throughflow characteristics, and storage" (Burger et al., 1999), 'storage' in rock glaciers occurs at *long-term*, *intermediate-term*, and *short-term* timescales (**Figure 4.3**). Within the Nepalese Himalaya, we have shown that I-DLs form long-term stores of frozen water of significant hydrological value; however, the total I-DL WVEQs calculated here may not be fully representative of readily available water for human consumption (Duguay et al., 2015; Rangecroft et al., 2015). Importantly, rock glacier hydrological significance relates not solely to the long-term storage of frozen water, but also to: (i) the seasonal storage and release of water; and (ii) the interaction of water flowing through or beneath rock glaciers.

Regarding (i), comparative studies focused on rock glacier- vs ice glacier-discharge are particularly few in number (Geiger et al., 2014). Within this small body of literature, contrasting perspectives have emerged with regards to the relative significance of rock glacier-derived hydrological contributions, particularly compared to other water sources. Previous studies have reported more consistent discharge from rock glaciers in comparison with ice glaciers (Potter, 1972; Corte, 1987; Gardner and Bajewsky, 1987; Bajewsky and Gardner, 1989). Additionally, rock glacier discharge patterns 'mimic' those of ice glaciers (Krainer and Mostler, 2002; Geiger et al., 2014), although at significantly lower magnitude (Geiger et al., 2014). Others (e.g., Falaschi et al., 2014) report rock glacier hydrological contributions to downstream-runoff are significant; however, these conclusions are based on non-quantitative data (Duguay et al., 2015). The discharge may originate from a single source or

multiple sources (e.g., ground ice degradation, groundwater discharge near the toe, precipitation events, through-flow of upstream ice- and/or snowpack-derived meltwater) (Burger et al., 1999). Indeed, a negligible or non-measurable contribution of ground ice degradation to discharge has been reported (Cecil et al., 1998; Croce and Milana, 2002; Krainer and Mostler, 2002; Krainer et al., 2007), corroborated by the predominant absence of springs near to the rock glacier toe (i.e. the base of the front slope) in semi-arid regions (Pourrier et al., 2014). However, it is plausible that rock glacier waters may drain directly underground (Pourrier et al., 2014). Discharge-related studies are predominantly focused on the present as opposed to potential future rock glacier-derived hydrological contributions; therefore, the hydrological significance of rock glaciers is defined according to a limited time-scale. At decadal and longer time-scales, under future climate warming, thawing of ground ice within rock glaciers may represent an increasing hydrological contribution to downstream regions (Thies et al., 2013). Therefore, we support previous studies (e.g., Duguay et al., 2015) and suggest further quantitative data is required, while field methodologies enabling separation of rock glacier-derived discharge from adjacent water sources are necessary.

Regarding (ii), rock glaciers can strongly influence catchment hydrology. Following precipitation events, total basin hydrographs indicate increased surface runoff within alpine catchments containing rock glaciers, which suggests rock glaciers form impervious surfaces (i.e. the perennially frozen layer at the base of the AL acts as an aquiclude) (Brenning, 2005b; Geiger et al., 2014). This may increase the likelihood of flooding (Krainer and Mostler, 2002; Geiger et al., 2014). Additionally, rock glaciers are characterised by high storage capacity (linked to high hydraulic conductivity) and low transmissive function in comparison to ice- and debris-covered-glaciers (Pourrier et al., 2014), particularly features with lower ground ice content. Therefore, rock glaciers can exhibit: (i) a strong buffering effect on the daily-to-monthly variability of transferring glacial- and snowpack-meltwater interflows to downstream areas; and (ii) a high storage capacity that partially delays glacier- and snowpack-meltwater transfer to downstream areas (Pourrier et al., 2014). Consequently, relict rock glaciers may strongly influence catchment hydrology by means of runoff interruption. For example, within the Niedere Tauern Range, Austria, Winkler et al. (2016b) report that following recharge events (i.e. precipitation events), relict rock glaciers rapidly (within hours) release ~20% of their recharge, however, the remaining ~80% is considerably delayed; calculated mean residence time is ~0.6 years (≅ 7 months). Furthermore, exceptionally high discharge rates reported from springs at the toe of relict rock glaciers (Kellerer-Pirklbauer et al., 2013),

emphasise the strong influence of this rock glacier type both on the water storage capabilities and discharge behaviour of these catchments. Therefore, relict rock glaciers potentially form 'temporary aquifers' of significant hydrological value; however, they are regularly neglected in the context of rock glacier hydrological significance. Indeed, as yet no scientific investigation has "quantitatively established the complete hydrological role of the periglacial environment within a given watershed or region" (Duguay et al., 2015). Their number, spatial distribution, and morphometric characteristics are defined within this inventory; however, much further research is required to better understand their hydrological role.

With further regards to (ii), given the potential of rock glaciers as potable water sources (Burger et al., 1999), understanding rock glacier outflow water quality characteristics is of critical importance. With slower recessional rates compared to ice glaciers, rock glaciers may influence the biogeochemistry of outflow over comparatively longer time-scales (Fegel et al., 2016). Despite this, the biogeochemistry of rock glacier outflow has been the focus of few scientific investigations. Generally, lower SSC and higher TDS relative to glacier-derived meltwater, have resulted in rock glacier outflow being described as 'clear' (Gardner and Bajewsky, 1987). However, given the greater debris fraction in rock glaciers compared to ice glaciers, mineral surface area-ground ice contact is greater, and thus undergoes active chemical weathering (Ilyashuk et al., 2014). Indeed, TDS analysis indicates that interflowing waters are chemically influenced with outflows becoming solute-enriched (Ilyashuk et al., 2014, 2018). Examples of rock glacier outflow are reported where abnormally high concentrations of certain elements exceed EU limit values for drinking water (e.g., sulphate, manganese, aluminium, nickel [Ilyashuk et al., 2014]). Furthermore, reported outflow pH levels (7.3–8.4) and interflow pH levels (6.4–6.9) (Ilyashuk et al., 2014), further illustrate the 'solute-concentrating effect' of rock glaciers. Others have reported similar findings (Williams et al., 2006; Thies et al., 2007; Thies et al., 2013; Nickus et al., 2015). Therefore, while rock glaciers may form reliable potable water sources, further research into water quality is necessary.

Lastly, in the adaptation context, "adaption needs are highly diverse, dynamic, and context-specific" (Regmi and Pandit, 2016), particularly in high mountain systems, therefore basin-scale knowledge is critically important. Additionally, research on the impacts of past environmental conditions of the hydrological function of rock glaciers is largely understudied (Sorg et al., 2015); research required to fully understand the applicability of the inventory presented in this study, to future contexts. Finally, under continued climate change, many ice glaciers

will potentially transition to rock glaciers; however, further research is required to understand this process.

6.7 CONCLUSION

In this study, the first complete inventory of DDAs/I-DLs in the Nepalese Himalaya has identified >6,000 features, covering an estimated 1,371 km². A ~20% sample (*n* = 1,137) of landforms were digitised, the majority (68%) of which were classified as intact and the remaining as relict. An inverse relationship between precipitation and DDA/I-DL occurrence, elevation and morphometric characteristics (i.e. length and area), with increasing values from east to west associated with drier conditions, was identified. Both DDAs and I-DLs situated within north- to west-aspect classes, reside at statistically significantly lower elevations than those within south- to east-aspects. Additionally, the majority (56%) of DDAs and I-DLs had a northerly aspect (NE, N, NW), suggesting that temperature (i.e. solar insolation) is an important control on DDA/I-DL characteristics and distribution. Climatic controls, however, only partially explain DDA/I-DL characteristics and distribution, and thus other controls such as debris supply, glacial history, competition with ice glaciers and lithology should be considered. Indeed, under future climate warming, the hydrological value of I-DL frozen water stores in mountain regions is likely to become increasingly important; therefore, improved understanding of the controls upon I-DL development is critical. Prior to this study, knowledge of Nepalese I-DL frozen water stores and their hydrological significance at local, regional, and national scales was limited. This study, for the first time, estimates I-DL WVEQs and evaluates their relative hydrological importance in comparison to ice glaciers. Across the Nepalese Himalaya, I-DLs stored ~21 trillion litres of frozen water, and their comparative hydrological importance increased westwards (e.g., ratio = 1:3, West region). With continued climatically-driven ice glacier recession, the relative importance of I-DLs in the Nepalese Himalaya will potentially increase.

6.8 ACKNOWLEDGEMENTS

This work was supported by the Natural Environment Research Council (grant number: NE/L002434/1 to DBJ); the Royal Geographical Society (with IBG) with a Dudley Stamp Memorial Award (awarded to DBJ); the European Union Seventh Framework Programme FP7/2007-2013 (grant number: 603864 to SH and RAB [HELIX: High-End cLimate Impacts and eXtremes; www.helixclimate.eu]). The work of RAB forms part of the BEIS/Defra Met Office Hadley Centre Climate Programme GA01101. The authors would like to thank Himalayan Research Expeditions (P) Ltd., who provided valuable organizational support with regards to the

field campaign. We would also like to acknowledge and thank the anonymous reviewers for their constructive comments and suggestions, which improved the manuscript greatly.

7 THE STATE OF HIMALAYAN ROCK GLACIERS

7.1 ABSTRACT

In HMA, human-induced climate warming threatens the high-mountain cryosphere. The consequential changes in future runoff raise major concerns regarding the sustainability of these natural 'water towers' and the implications of reduced water availability for human systems in mountains and the surrounding lowlands. I-DLs, including rock glaciers, are reportedly climatically more resilient than debris-covered and debris-free glaciers. Moreover, studies have shown that rock glaciers contain potentially hydrologically valuable WVEQs. Yet, in HMA information describing their number, spatial distribution, morphometric characteristics and WVEQ are scarce. In the present study, we present the first systematic inventory of DDAs/I-DLs for the Himalaya. This database encompasses ~25,000 landforms, with an estimated areal coverage of 3,747 km². A sample (n = 2,070) of the identified landforms were digitised, and their quantitative and qualitative characteristics analysed regionally (West Himalaya, Central Himalaya, East Himalaya) and across the Himalaya. The majority of these landforms (~65%) were categorised as I-DLs (i.e. containing ice) and the remainder as DDAs (i.e. not containing ice). Using the digitised landforms and a statistical upscaling procedure, we estimated I-DL WVEQ for the first time and evaluated their relative hydrological value vs glaciers within the Himalaya. I-DLs are estimated to contain 51.80 ± 10.36 km³ of water; equivalent to between 41 and 62 trillion litres. The comparative importance of I-DLs vs glaciers (I-DL: glacier WVEQ ratio) in the Himalaya was 1:24, ranging from 1:42 to 1:17 in the East and Central Himalaya, respectively. Additionally, for the first time we evaluate the influence of glacier volume methodology choice on I-DL: glacier WVEQ ratios. Across the Himalaya I-DL: glacier WVEQ ratios ranged between 1:23 and 1:36 depending on the chosen method of glacier volume calculation. Regardless, I-DLs within the Himalaya constitute hydrologically valuable long-term water stores. Indeed, with continued climatically-driven glacier recession and mass loss the relative hydrological value of I-DLs in mountain regions is likely to become increasingly important.

7.2 INTRODUCTION

In HMA, the high-mountain cryosphere forms natural water towers that are integral for ecosystem services provision, supplying multiple societal needs to ~800 million people living in the mountains and surrounding lowlands (Pritchard, 2019); e.g., potable water resources and water for irrigation, industry and agriculture (Immerzeel et al., 2010). However, considerable continued glacier mass loss is projected throughout the twenty-first century under multiple

RCPs (Kraaijenbrink et al., 2017; Hock et al., 2019a; Shannon et al., 2019). For instance, under high-end climate change scenarios,[5] glacier volume in HMA is projected to decrease by ~95% towards 2100, relative to the present-day. In this simulation, the volume losses are driven by an average temperature change of +5.9 °C over glaciated regions in combination with an average precipitation increase of 20.9%. Regarding the latter, an increased rain-to-snow fraction is projected (**Figure 7.1**). Linked to this, an overall decrease in snow water equivalent has been reported for a number of catchments in HMA, particularly during spring (MAM) and summer (JJA) (Smith and Bookhagen, 2018). The continued decline of the HMA high-mountain cryosphere raises major concerns for the future sustainability of cryospheric water resources, particularly following peak water. Indeed, under RCP4.5 most basins fed by HMA glaciers are projected to reach peak water by ~2050; 2045 ± 17 years (Indus), 2044 ± 21 years (Ganges) and 2049 ± 18 years (Brahmaputra), for example (Huss and Hock, 2018).

[5] High-end climate change is defined as warming that exceeds 2 °C global average warming during the twenty-first century (RCP8.5), relative to the pre-industrial period (Shannon et al., 2019).

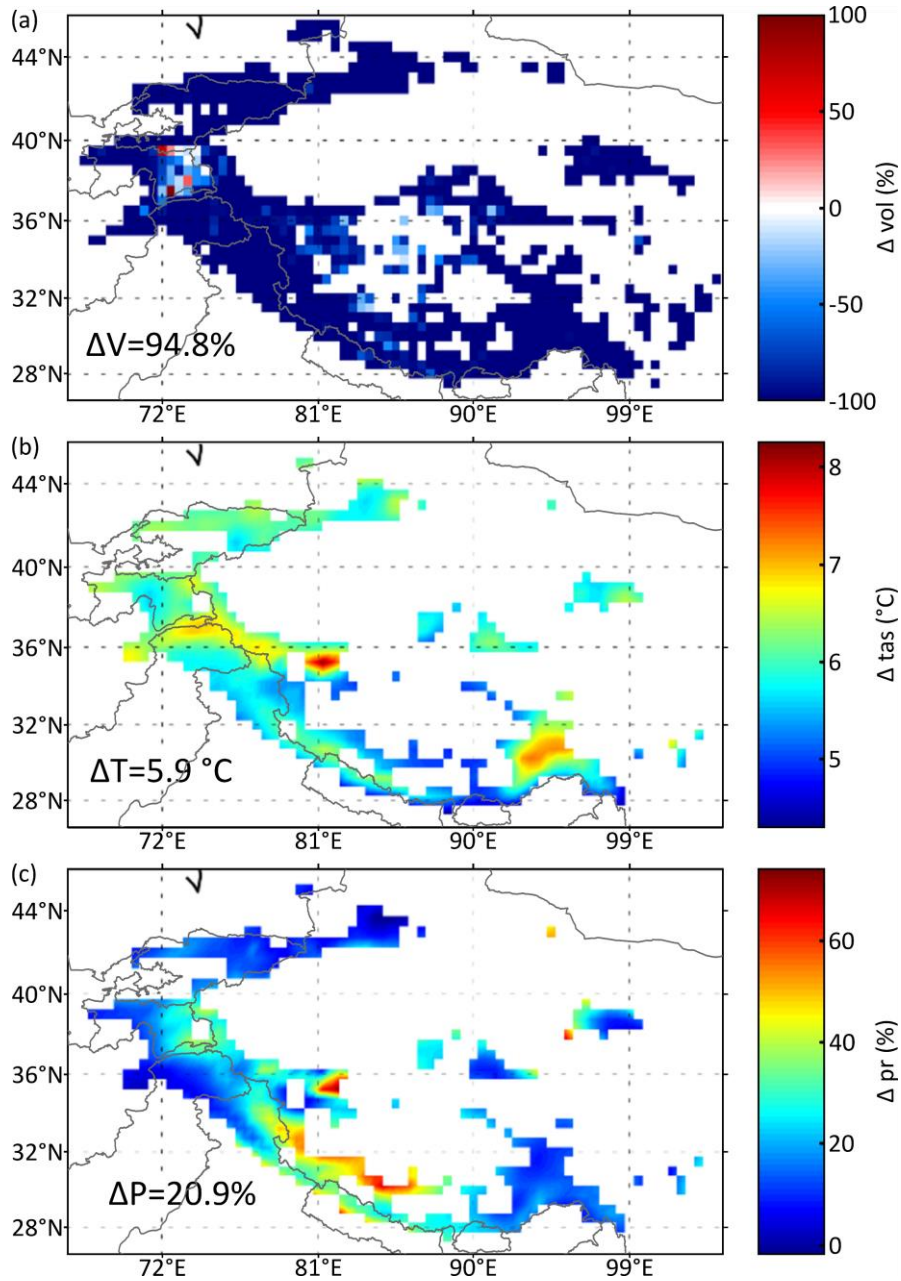

Figure 7.1. (a) Ensemble mean glacier volume loss, (b) air temperature change, and (c) precipitation change between the historical period (1980–2010) and the end of this century (2067–2097) over glaciated grid points. Glacier volume loss projections were derived from simulations made using an elevation-dependent mass balance scheme in the JULES land surface model under high-end climate change scenarios. JULES has been forced with seven Coupled Model Intercomparison Project Phase 5 (CMIP5) models downscaled using the HadGEM3-A atmosphere-only model. N.B. The anomaly ('hot spot') present in (b) represents an air temperature change of +8.26 °C, form -6.69 °C (historical period mean 1980–2010) to +1.57 °C (end of century mean 2067–2097). This large air temperature change is presumed to result from the pixel being snow-covered during the historical period, but land-covered in the future period. Land-covered pixel temperatures are higher due to lower albedo (Shannon, pers. comm.). Figure provided by Sarah Shannon.

Given the need for strong climate adaptation in HMA, it is clear that a more comprehensive understanding of all components of the hydrological cycle in the high-mountain cryosphere is required (Jones et al., 2019). Existing research suggests that rock glaciers – lobate or tongue

shaped landforms comprising a continuous and thick AL covering ice-supersaturated debris and/or pure ice, which slowly creep downslope (see Martin and Whalley, 1987; Barsch, 1996; Haeberli et al., 2006; Berthling, 2011) – may constitute increasingly important long-term water stores (Jones et al., 2018a). Owing to the insulating and damping properties of the AL, rock glaciers are thought to be climatically more resilient than glaciers; consequently, their relative hydrological importance vs glaciers may increase under future climate warming (ibid.) (**Figure 7.2**). Yet, to date, with a few notable exceptions (e.g., Jones et al., 2019; Schaffer et al., 2019), the hydrological role of rock glaciers has been afforded relatively scant consideration compared to both debris-free glaciers (see Fountain and Walder, 1998; Jansson et al., 2003; Irvine-Fynn et al., 2011) and debris-covered glaciers (Fyffe et al., 2019, and references therein). Indeed, in their recent book chapter, "Status and Change of the Cryosphere in the Extended Hindu Kush Himalayan Region", Bolch et al. (2019b) synthesised and evaluated the state of current scientific knowledge regarding changes in the high-mountain cryosphere; however, rock glaciers are only mentioned briefly. Furthermore, while systematic rock glacier inventory[6] coverage has increased globally, HMA is comparatively data-deficient (Jones et al., 2018a). Across HMA, with few exceptions (Jones et al., 2018b; Blöthe et al., 2019; Baral et al., in press), rock glacier inventories have been conducted at relatively small spatial scales or are not spatially explicit (e.g., Regmi, 2008; Bolch and Gorbunov, 2014; Schmid et al., 2015); therefore, rock glacier distribution and hydrological value are generally unknown.

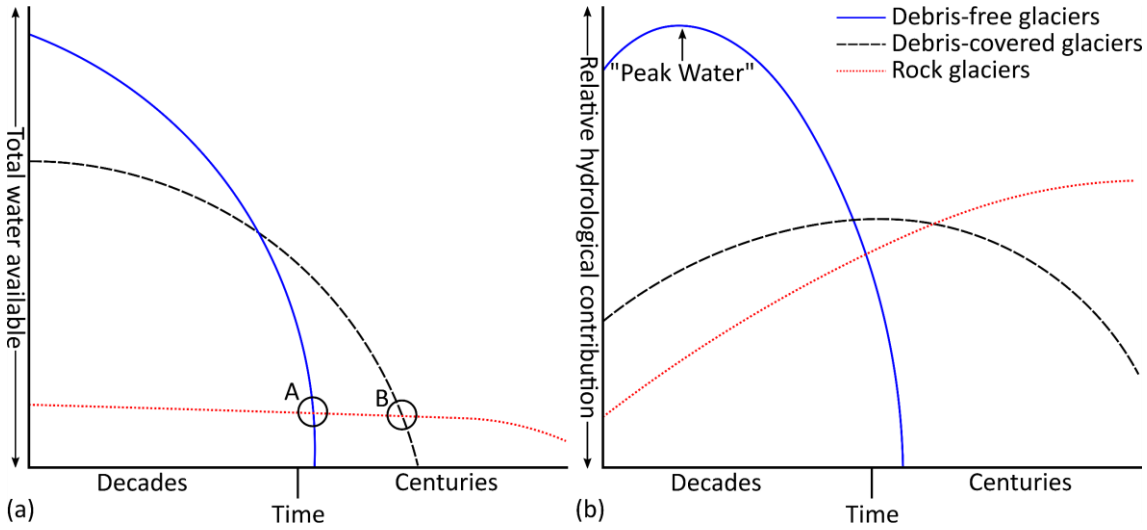

Figure 7.2. A conceptual diagram showing (a) the total water available, and (b) the relative hydrological contribution of debris-free glaciers, debris-covered glaciers and rock glaciers over time. [A] and [B] reflect the point where rock glaciers replace debris-free glaciers and debris-covered glaciers in terms of water storage, respectively.

[6] In this study, 'systematic inventory studies' refer to the strategic and complete mapping of rock glaciers within a study area.

Rock glacier genesis is the focus of a long-standing academic debate (see Barsch, 1977, 1987, 1996; Whalley and Martin, 1992; Hamilton and Whalley, 1995; Clark et al., 1998; Whalley and Azizi, 2003; Haeberli et al., 2006; Berthling, 2011). Here, we adopt the dispassionate view that rock glaciers can be derived through either the permafrost model or the glacier ice core model (as per Berthling, 2011). Therefore, in this study, we adopt the inclusive, and non-genetic terms DDAs and I-DLs to incorporate rock glaciers, protalus lobes and protalus ramparts (*sensu lato* Harrison et al., 2008; Jarman et al., 2013).

7.3 BRIEF METHODS

In this study, the primary objective was to compile the first systematic rock glacier inventory for the Himalaya (**Figure 1.2**); this forms an extension of the existing systematic rock glacier inventory for the Nepalese Himalaya (Jones et al., 2018b). The inventory presented in this study was generated using freely available, fine spatial resolution satellite image data (Google Earth Pro) and a 30 m DEM. A ~5% sample, excluding the Nepalese Himalaya, of the identified landforms from the W-Himalaya, C-Himalaya and E-Himalaya was randomly selected and digitised. The dynamic status of landforms was determined considering their presumed ice content and movement, according to the morphological classification by Barsch (1996), established using geomorphic indicators (**Table 6.1**). The sampled landforms were classified as: (i) active landforms, contain ice and display movement; (ii) inactive landforms, contain ice and no longer display movement; or (iii) relict landforms, do not contain ice nor display movement (Haeberli, 1985; Barsch, 1996). For simplicity, active and inactive landforms are often collectively termed intact landforms. In this study, DDAs and I-DLs represent relict and intact landforms, respectively.

The secondary objective was to calculate I-DL WVEQ and assess I-DL vs glacier WVEQ across a range of spatial scales. As a consequence of the paucity of detailed sub-surface information for I-DLs, particularly in HMA, 2-D-area-related statistics (i.e. empirical *H-S relations*) using data from the digitised sample were applied to estimate I-DL thickness and volume. Empirical H-S relations can be expressed as $\bar{h} = c \cdot S^{\beta}$, where mean feature thickness $\bar{h}$ (m) is calculated as a function of surface area *S* (km²) and a scaling parameter *c* (50) and scaling exponent *β* (0.2) (Brenning, 2005a). Feature volumes were determined by $V = \bar{h} \cdot S$. WVEQ was subsequently estimated through the multiplication of *V* and estimated ice content (% by vol.) and assuming an ice density conversion factor of 900 kg m^{-3} (Paterson, 1994). Volumetric I-DL ice content is assumed to be 40–60% vol. (i.e. lower [40%], mean [50%] and upper bounds [60%])

in accordance with previous studies (Brenning, 2005a; Bodin et al., 2010; Rangecroft et al., 2015; Jones et al., 2018a; Jones et al., 2018b) – consistent with *in situ* data derived from different climatic regions worldwide (e.g., Elconin and LaChapelle, 1997: >50%; Arenson et al., 2002: 40–70%; Croce and Milana, 2002: ~55%; Hausmann et al., 2007: 45–60%; Hausmann et al., 2012: 40–60%). In order to estimate total landform area and WVEQ for the Himalaya, (i) the database presented here was amalgamated with the existing systematic rock glacier inventory for the Nepalese Himalaya (Jones et al., 2018b), creating the first comprehensive systematic rock glacier inventory for the Himalaya; and (ii) the digitised sample (*n* = 2,070 [this study, *n* = 933; Jones et al., 2018, *n* = 1,137]) was extended to the entire population on a regional basis through the upscaling procedure outlined in **Supplementary Figure 12.3**. Glacier area and volume data for the Himalaya were derived from Frey et al. (2014). The estimated glacier ice volumes that the WVEQs are based upon were calculated using the GlabTop2 ice-thickness distribution model (ibid.). A full description of our methods and uncertainty assessment is provided in the Supplementary Information (see **section 12.3.1**).

7.4 RESULTS AND DISCUSSION

In the present study, we identified 24,968 DDAs/I-DLs across the Himalaya. I-DLs and DDAs accounted for ~65% (*n* = 16,334) and ~35% (*n* = 8,634) of the total identified landforms, respectively, based on upscaled estimates (**Table 7.1**). Approximately 40% (*n* = 10,060) of the identified landforms are located in the Central Himalaya, ~30% (*n* = 7,573) in the East Himalaya and ~29% (*n* = 7,335) in the West Himalaya (**Figure 7.3**; **Table 7.1**). The mean density (*n* km^{-2}) of DDAs/I-DLs, when considering terrain ≥3,225 m a.s.l. (i.e. the lowest MEF of sampled landforms), ranges from 0.06 (West Himalaya) and 0.08 (East Himalaya/Central Himalaya). Across the Himalaya, I-DL mean density is 0.05 and DDA mean density is 0.02 (**Supplementary Table 12.3**). Direct conversion of specific DDA/I-DL area (ha km^{-2}) to specific DDA/I-DL density (%) enables comparison with previous studies. At 1.05%, specific landform density in the Himalaya is lower than other studies in HMA (**Supplementary Table 12.3**); for example, ~1.50% in the Northern Tien Shan (Kazakhstan/Kyrgyzstan) (Bolch and Gorbunov, 2014), 2.65% in the Zailyiskiy and Kungey Alatau (Kazakhstan/Kyrgyzstan) (Bolch and Marchenko, 2006) and 3.40% in the Nepalese Himalaya (Jones et al., 2018b). However, as the Tibetan Plateau constitutes a significant proportion of the terrain ≥3,225 m a.s.l., this may suppress the specific landform density values presented here.

Table 7.1. Key mean characteristics for intact (I-DLs) and relict (DDAs) landforms

Region	Activity	No. of landforms	(%)	MEF (m a.s.l)	MaxE (m a.s.l)	Length (m)	Width (m)	Area (km²)	Aspect	No. of landforms (upscaled)
E – Himalaya	Intact	199	53%	5,036	5,158	413	172	0.08	Northwest	3,987
	Relict	179	47%	4,852	4,956	343	145	0.06	Northwest	3,586
	All	378	-	4,949	5,062	380	159	0.07	Northwest	7,573
C – Himalaya	Intact	897	67%	4,989	5,220	748	261	0.24	Northwest	6,790
	Relict	432	33%	4,599	4,785	518	219	0.14	Northwest	3,270
	All	1,329	-	4,863	5,078	673	248	0.21	Northwest	10,060
W – Himalaya	Intact	275	76%	4,564	4,729	587	223	0.15	Northwest	5,557
	Relict	88	24%	4,312	4,470	546	188	0.13	North	1,778
	All	363	-	4,503	4,666	577	215	0.15	Northwest	7,335
Total	Intact	1,371	66%	4,911	5,112	667	241	0.20	Northwest	16,334
	Relict	699	34%	4,628	4,789	477	196	0.12	Northwest	8,634
	All	2,070	-	4,815	5,003	603	226	0.17	Northwest	24,968

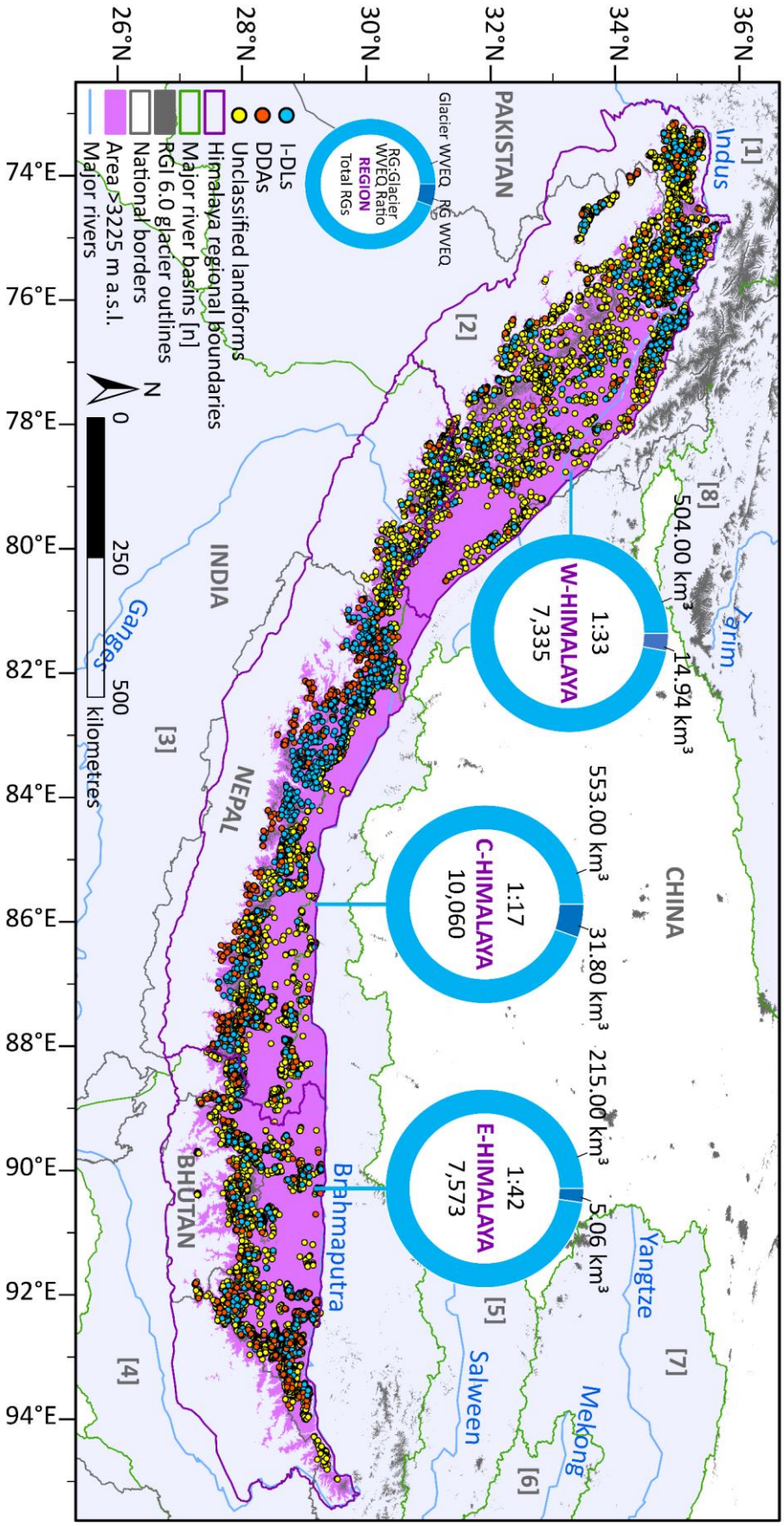

Figure 7.3. Map of the Himalaya showing the distribution of I-DLs and DDAs. I-DLs/DDAs with unclassified dynamic status (i.e. landforms that were not digitised) are included here for completeness. The total I-DL/DDA number, I-DL and glacier WVEQ and I-DL to glacier WVEQ ratios for the West, Central and East Himalaya regions are shown. These regions are derived from Bolch et al. (2012). Note that I-DL WVEQ assumes the 50% (average) ice content by volume. The area >3,225 m a.s.l. represents the lowermost MEF of I-DLs/DDAs across the Himalaya. Lastly, the major river basin boundaries are shown: [1] Amu Darya, [2] Indus, [3] Ganges, [4] Brahmaputra, [5] Salween, [6] Mekong, [7] Yangtze and [8] Tarim.

Across the Himalaya, the sampled DDAs and I-DLs (*n* = 2,070) are situated within an elevation range of 3,225 to 5,766 m a.s.l. (MEF), with 87% found between 4,200 and 5,400 m a.s.l. This is broadly consistent with that previously reported for the HKH (3,554–5,735 m a.s.l.) (Schmid et al., 2015). At the regional-scale, mean MEFs for the East (4,949 ± 256 m a.s.l.), Central (4,863 ± 372 m a.s.l.) and West Himalaya (4,503 ± 422 m a.s.l.) demonstrate a decreasing westward trend in DDA/I-DL elevation across the Himalaya (**Figure 7.4**; **Table 7.1**). This trend remains consistent when considering DDAs and I-DLs separately (**Table 7.1**). Furthermore, similar to Schmid et al. (2015), we report a pronounced south-to-north increase in DDA/I-DL MEF across the Himalaya, with DDAs/I-DLs found several hundreds of metres higher on the northern slopes (**Figure 7.4**). As expected, across the Himalaya I-DLs are located at statistically higher elevations than DDAs when considering DDA/I-DL MEFs (ANOVA: F-value [2, 2064] = 16.19, p = <0.001); Tukey post hoc testing shows that this finding translates to the regional-scale (West Himalaya: Diff = 252, p = <0.001; Central Himalaya: Diff: 390, p = <0.001; East Himalaya: Diff = 184, p = <0.001). Across the Himalaya, I-DLs are predominantly found above 4,800 m a.s.l. (65%) and DDAs below 4,800 m a.s.l. (67%). Furthermore, I-DLs are clustered between 4,400–5,400 m a.s.l. (84%) and DDAs between 4,200–5,200 m a.s.l. (79%). This result provides validation for the dynamic status classification, given the expected vertical progression of suitable habitats for I-DL development and persistence linked to climatic warming since the LIA.

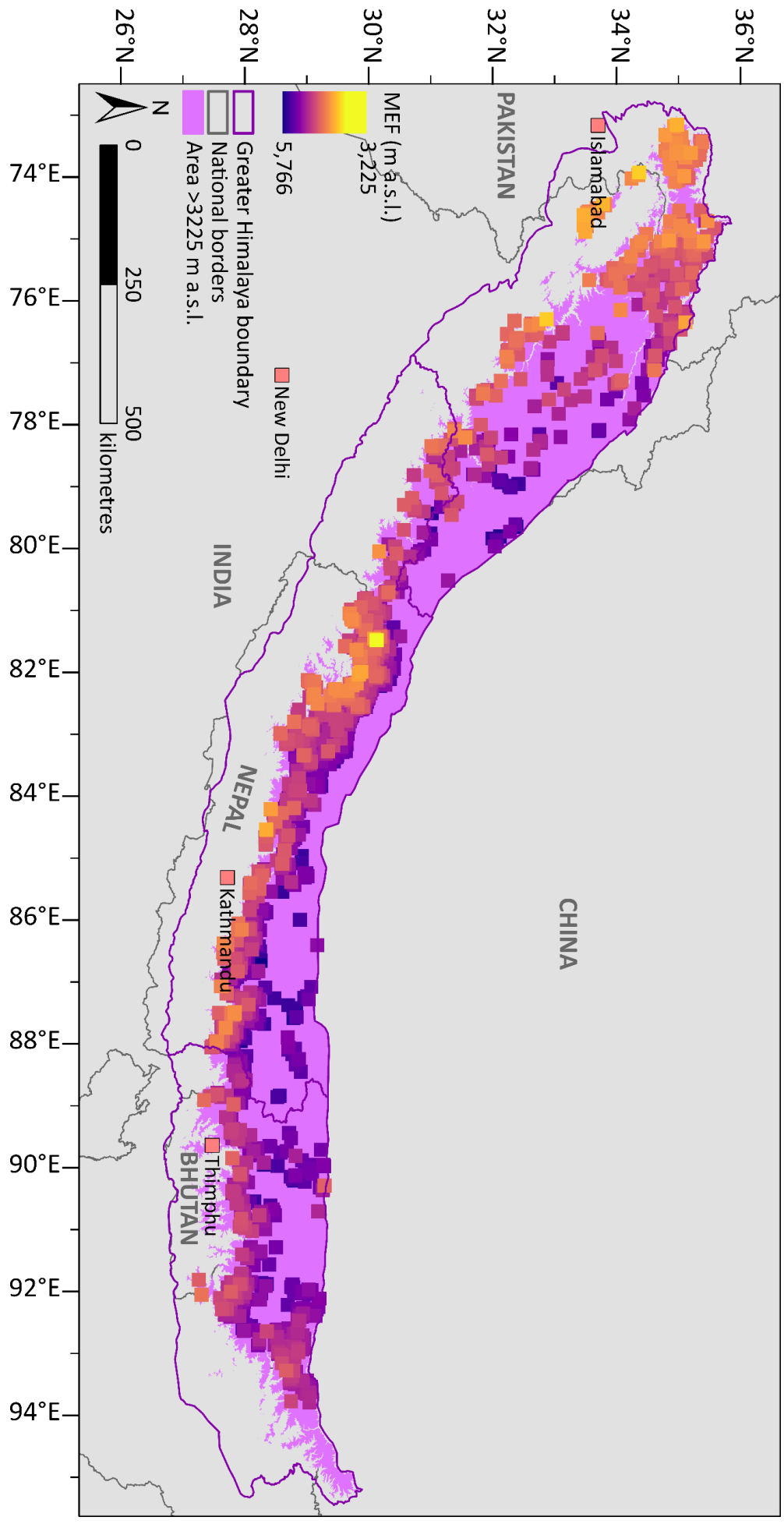

Figure 7.4. MEF of the sampled DDAs/I-DLs across the Himalaya.

Across the Himalaya, DDAs/I-DLs are primarily situated on north-facing slopes (NW, 17%; NE, 16%; N, 16%). Furthermore, the mean aspect of DDAs/I-DLs shows that they cluster around north-western slopes ($\bar{x}$ = 321°). Regionally, a greater proportion of I-DLs are situated within the northern (40–57%) compared to the southern quadrant (20–32%). Similarly, DDAs are also predominantly located within the northern (57–62%) compared to the southern quadrant (13–19%) (**Supplementary Table 12.4**). Circular variance indicates that DDAs have lower dispersal (0.39) than I-DLs (0.20), with proportionally more DDAs located on northerly slopes compared to I-DLs. In addition, across the Himalaya I-DLs/DDAs situated within the northern aspect quadrant occur at lower elevations than those found within the southern aspect quadrant (**Figure 7.5**). **Figure 7.5** also illustrates the clustering of DDAs/I-DLs around northerly aspects. The results presented here corroborate the findings of other northern hemispheric studies, which have detailed similar relationships (e.g., Ishikawa et al., 2001; Seppi et al., 2012; Scotti et al., 2013; Baral et al., in press). Therefore, it is reasonable to assume that northerly aspects with their reduced solar insolation, enable I-DL formation and preservation at lower elevations than other aspects, in particular, southerly aspects.

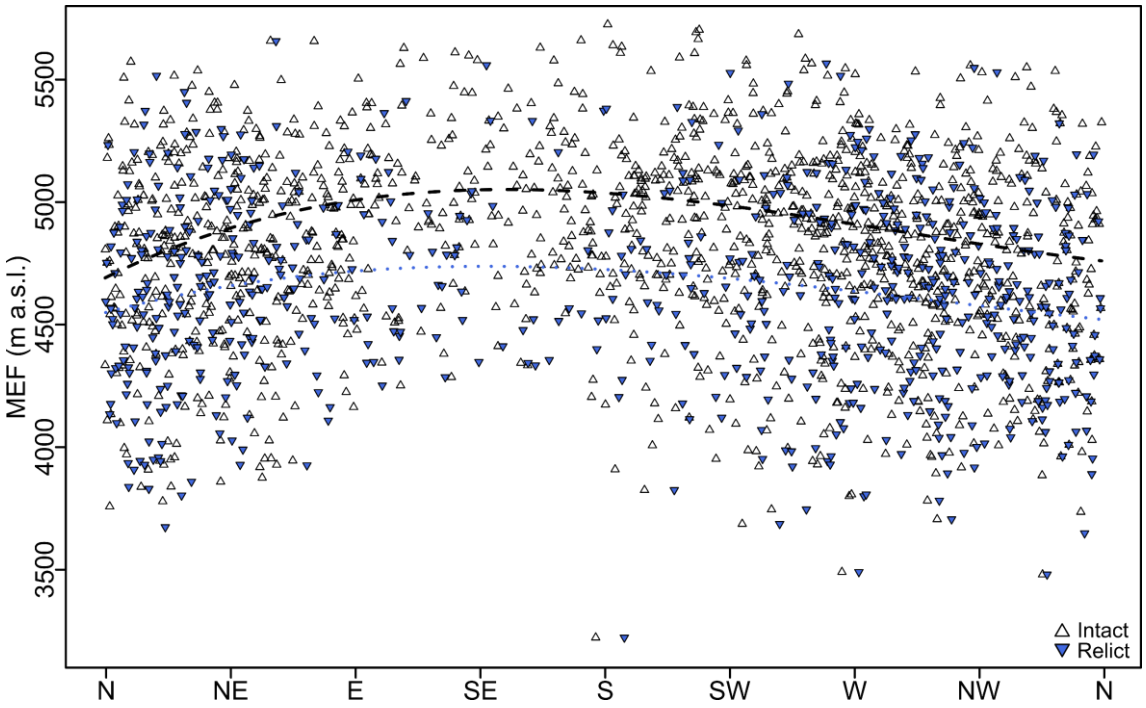

Figure 7.5. Scatterplot of mean aspect (°) against MEF showing the distribution of intact (I-DLs) and relict (DDAs) landforms across the Himalaya. The two dashed lines are 3rd order polynomial fit (upper line: intact landforms; lower line: relict landforms).

The sampled landforms (*n* = 2,070) across the Himalaya cover a total surface area of 359.95 km² with I-DLs constituting 277.78 km² and DDAs 82.18 km², ~77% and ~23% of the total coverage, respectively. Total DDA/I-DL surface coverage is largest in the Central Himalaya (278.70

km²), succeeded by the West Himalaya (53.76 km²) and East Himalaya (27.50 km²). Here, when reporting DDA/I-DL sample totals, it is important to note the proportionally larger sample size for the Central Himalaya, which is the result of the amalgamation of the database presented here with the existing systematic rock glacier inventory for the Nepalese Himalaya (Jones et al., 2018b) (see **section 12.3.1**). Correspondingly, the mean and median surface area is greatest in the Central Himalaya ($\bar{x}$ = 0.21 km² and $\tilde{x}$ = 0.12 km²) followed by the West and East Himalaya (**Table 7.1**). Considered individually, the largest I-DL (3.54 km²) and DDA (1.50 km²) are both located in the Central Himalaya. Across the Himalaya, the area of individual sampled landforms varies between 3.54 km² and 0.004 km², with 1,069 landforms ≥0.1 km² in area. Onaca et al. (2017) speculate that rock glaciers in the highest mountain ranges are comparatively larger than those situated in lower mountain ranges, linked to the longevity of active dynamic status. Additionally, given the importance of debris-supply to rock glacier development and persistence, Hewitt (2014, p. 276) notes that as interfluve height increases, more and larger rock glaciers are likely below it. In the high and deeply incised ranges of the Himalaya (Scherler et al., 2011), it is reasonable to assume that these topographic factors have considerable influence on DDA/I-DL size. Here, we report that several DDAs/I-DLs have similar areal coverage to the largest examples found elsewhere; for example, 1.95 km² (Bolch and Gorbunov, 2014) and 3.60 km² (Blöthe et al., 2019) in Central Asia. Furthermore, DDA/I-DL area ($\bar{x}$ = 0.17 km²) exceeds that of rock glaciers found in other mountain ranges globally (cf. Jones et al., 2018a). In the Himalaya, estimated total upscaled DDA/I-DL area is 3,747 km², representing ~16% of the area covered by glaciers in the same region (22,829 km²). At the regional-scale, DDA/I-DL coverage ranged between 550.87 km² and 2,109.63 km² in the East and Central Himalaya, respectively.

The results presented in **Supplementary Table 12.5** show that the sampled I-DLs contain an estimated WVEQ of 5.19 ± 1.04 km³ throughout the Himalaya. The reported upscaled estimates suggest that total WVEQs of 51.80 ± 10.36 km³ could reasonably be stored within I-DLs in our study area (**Supplementary Table 12.5**; **Figure 7.3**). Henceforth, I-DL volumetric results will reflect the format *sample result (upscaled result)*. Regionally, the WVEQ of I-DLs ranges from 0.25 ± 0.05 km³ *(5.06 ± 1.01 km³)* in the East Himalaya to 4.20 ± 0.84 km³ *(31.80 ± 6.36 km³)* in the Central Himalaya.

Across the Himalaya, glacier WVEQ is estimated to be 1,272 km³ (Frey et al., 2014; **Table 7.2**). This translates to a ratio of I-DL to glacier WVEQ of 1:244, indicating that glaciers store a

volume of water ~244 times larger than I-DLs. However, this ratio decreases to 1:24, where upscaled I-DL WVEQs are considered. Regionally, the I-DL to glacier WVEQ ratios range from 1:851 *(1:42)* in the East Himalaya to 1:131 *(1:17)* in the Central Himalaya.

Table 7.2. WVEQs (km³) for I-DLs (sampled and upscaled) and ice glaciers, regionally and across the Himalaya (total). Additionally, the I-DL to ice glacier ratios are directly compared. I-DL WVEQs assume the 50% (average) ice content by volume. Values are reported to two decimal places. Ice glacier WVEQ data are derived from Frey et al. (2014)

Region	Ice-debris landform		Ice glacier		Ratio: I-DL: Ice glacier WVEQ	
	Sample WVEQ (km³)	Upscaled WVEQ (km³)	Area (km²)	WVEQ (km³)	Sample ratio	Upscaled ratio
E – Himalaya	0.25	5.06	3,946.00	215.00	1:851	1:42
C – Himalaya	4.20	31.80	9,940.00	553.00	1:131	1:17
W – Himalaya	0.74	14.94	8,943.00	504.00	1:681	1:33
Total	**5.19**	**51.80**	**22,829.00**	**1,272.00**	**1:244**	**1:24**

The estimated glacier ice volumes that the WVEQ are based upon were calculated using the GlabTop2 ice-thickness distribution model (Frey et al., 2014). However, in the Himalaya glacier WVEQ ranges between 1,237 and 1,909 km³ depending on the choice of method used to estimate glacier volume (ibid.). For the different methods I-DL to glacier WVEQ ratios for the Himalaya varied between 1:23 and 1:36 (**Table 7.3**). Regardless of the method chosen, across the Himalaya I-DLs constitute hydrologically valuable long-term water stores.

Table 7.3. WVEQs (km³) for ice glaciers derived using different methodologies, regionally and across the Himalaya (total). The upscaled I-DL to ice glacier ratios are directly compared for each methodology. I-DL WVEQs used in the ratio calculations assume the 50% (average) ice content by volume. Values are reported to two decimal places. Ice glacier WVEQ data are derived from Frey et al. (2014).

Region	Chen & Ohmura (1990)		Bahr et al. (1997)		LIGG/WECS/NEA (1988)		Slope-dep. thick-ness est.		GlabTop2		HF-model	
	WVEQ (km³)	I-DL:IG WVEQ	WVEQ (km³)	I-DL:IG WVEQ	WVEQ (km³)	I-DL:IG WVEQ	WVEQ (km³)	I-DL:IG WVEQ	WVEQ (km³)	I-DL:IG WVEQ	WVEQ (km³)	I-DL:IG WVEQ
E – Himalaya	235	1:46	278	1:54	322	1:63	198	1:39	215	1:42	194	1:38
C – Himalaya	647	1:20	770	1:24	883	1:27	512	1:16	553	1:17	560	1:17
W – Himalaya	515	1:34	610	1:40	704	1:47	527	1:35	504	1:33	543	1:36
Total	**1,397**	**1:26**	**1,658**	**1:32**	**1,909**	**1:36**	**1,237**	**1:23**	**1,272**	**1:24**	**1,297**	**1:25**

7.5 CONCLUSIONS

We have presented the first systematic inventory of DDAs/I-DLs for the Himalaya and shown that there are approximately 25,000 DDAs/I-DLs, with an areal coverage of ~3,747 km². This is the most extensive systematic inventory (in terms of total DDA/I-DL number and areal coverage), conducted globally to date. A sample (*n* = 2,070) of the identified landforms analysed regionally (West Himalaya, Central Himalaya, East Himalaya) and across the Himalaya showed that the majority of these landforms (~65%) were I-DLs (i.e. intact) and the remainder as DDAs (i.e. relict). Upscaling to the wider region, I-DLs were estimated to contain a WVEQ of 51.80 ± 10.36 km³ of water; equivalent to between 41 and 62 trillion litres. The comparative importance of I-DLs vs glaciers (I-DL to glacier WVEQ ratio) in the Himalaya was 1:24, ranging from 1:42 to 1:17 in the East and Central Himalaya, respectively. Additionally, for the first time we evaluate the influence of glacier model choice on I-DL to glacier WVEQ ratios. Across the Himalaya I-DL to glacier WVEQ ratios ranged between 1:23 (slope-dependent thickness estimation) and 1:36 (V-S scaling relation [LIGG et al., 1988]). We conclude that I-DLs within the Himalaya constitute hydrologically valuable long-term water stores and given continued climatically-driven glacier recession and mass loss the relative hydrological value of I-DLs in mountain regions will likely become increasingly important. Prior to this study, knowledge of Himalayan-wide DDA/I-DL characteristics were missing, and so our work provides the first scientific baseline from which Himalayan-wide I-DL response to climate change can be assessed. Furthermore, this knowledge is important given the potential influence of DDAs/I-DLs upon mountain hydrology (see Jones et al., 2019).

8 ROCK GLACIERS AND THE GEOMORPHOLOGICAL EVOLUTION OF DEGLACIERIZING MOUNTAINS

8.1 ABSTRACT

Rock glaciers are an important geomorphic element of glaciated mountain landscapes, but our understanding of their distribution and ages, controls on their development, and their importance in regional mountain hydrology and mountain geomorphic evolution is incomplete. In part, this incomplete knowledge arises through problems associated with identifying rock glaciers on a morphological basis alone, amplified by the multiple ways in which rock glaciers can form in different glacial, periglacial, and paraglacial settings. This study focuses on rock glaciers as a paraglacial mountain landscape element and considers the relationships between rock glaciers and glacial, periglacial, and paraglacial processes. New geomorphic and sedimentary data on different rock glaciers from the Khumbu region of Nepal are presented. These data show that even within a single region, rock glaciers may have varied origins and thus likely ages and different climatic and environmental controls. We argue that rock glaciers in deglacierizing mountains may have a long residence time in the landscape, unlike many other glacially influenced mountain landforms, and can undergo significant morphodynamic changes as glaciated landscapes transition into paraglacial landscapes.

8.2 INTRODUCTION

Despite much recent research (e.g., Brenning, 2005b; Rangecroft et al., 2015; Jones et al., 2018b), the role of rock glaciers in the hydrology and morphological evolution of deglacierizing mountains remains poorly known. In part, this arises from limitations of the different ways in which rock glaciers have been identified, measured, and monitored (Hamilton and Whalley, 1995; Roer and Nyenhuis, 2007; Dall'Asta et al., 2017; Deluigi et al., 2017; Kenner et al., 2018). Remote sensing-based methods are not always able to clearly resolve differences between rock glaciers, debris accumulations such as rockfalls, and glacial moraines (Kenner, 2014; Wang et al., 2017); and the issue of mimicry and equifinality applies, especially in the case of rock glaciers (Jarman et al., 2013). In addition, individual studies have not always used consistent methodologies, thus making it difficult to compare results between different areas. Any remote sensing methodology largely depends on the data sets used and their resolutions (spectral and temporal), and this has hindered comparability between studies. Field-based methods of quantifying rock glacier properties, their morphometry, and spatial patterns (e.g., Martin and Whalley, 1987; Humlum, 1996; Ikeda and Matsuoka, 2006) are time-consuming

and expensive; and many mountain regions globally have not been examined in the field by geomorphologists, although numerous inventories from individual mountain blocks have been produced (e.g., Lilleøren and Etzelmüller, 2011; Krainer and Ribis, 2012; Scotti et al., 2013; Rangecroft et al., 2014; Falaschi et al., 2015; Onaca et al., 2017). As a result, rock glaciers remain one of the most poorly understood mountain landforms (Berthling, 2011). This is particularly the case for relict rock glaciers whose age, controls, and longevity are difficult to evaluate and whose evolution is difficult to reconstruct. Recent work has discussed the relationship of rock glaciers to paraglacial (landscape relaxation) processes following deglaciation (Knight and Harrison, 2018) and calculated the water balance and water mass budgets of rock glaciers (Krainer and Mostler, 2002). Other recent work has examined the morphometry, internal properties (Roer and Nyenhuis, 2007; Onaca et al., 2013; Emmert and Kneisel, 2017) and dynamic behaviour of rock glaciers (Konrad et al., 1999; Ødegård et al., 2003; Janke, 2005a; Jansen and Hergarten, 2006; Serrano et al., 2010; Müller et al., 2016; Anderson et al., 2018), their sediment sources and transport capacity (Barsch and Jakob, 1998; Humlum, 2000; Humlum et al., 2007), and hydrology (Schrott, 1996; Krainer and Mostler, 2002; Geiger et al., 2014; Rangecroft et al., 2015). Despite these varied foci of rock glacier research, the relationships of rock glaciers to other mountain landforms, and their evolution over time and space are still poorly known, conceptually and in field contexts (Johnson, 1983; Janke et al., 2015; Knight and Harrison, 2018). This study contributes to this emerging debate on rock glaciers and their morphodynamic significance in deglacierizing mountains by considering (i) the relationships of rock glaciers to glacial, periglacial, and paraglacial environments and processes and (ii) specific examples of rock glaciers in the Nepalese Himalaya that illustrate the varied geomorphic settings in which they can develop and with implications for long-term mountain landscape evolution. A key conclusion of this study is that not all rock glaciers exhibit the same sensitivity to climate forcing, depending on their genetic origin(s), and that glaciological vs slope vs climatic controls on rock glacier evolution vary through the rock glacier life cycle. This means that different rock glaciers cannot be compared uncritically to one another or used as equivalent sources of information when it comes to comparing the geomorphology or climatic evolution of different mountain regions worldwide.

8.3 METHODOLOGY AND APPROACH

The first part of this study is conceptual and is based upon a critical analysis of previous work on rock glaciers, supplemented by observations by the authors from active and relict rock

glaciers worldwide, including in Europe, South America, and the Himalayas. The second part of this study is based on new remote sensing and field evidence from the Khumbu area of the Nepalese Himalaya, which focuses on mapping the distribution and extent of rock glaciers in the region and on understanding the relationship between debris-covered glaciers and rock glaciers based on their formational setting and geomorphic and sedimentary properties. Rock glacier mapping was achieved using fine spatial resolution satellite image data accessed through Google Earth. Platforms used were SPOT, QuickBird, Worldview-1, Worldview-2, and IKONOS. Geomorphic mapping was done mainly by onscreen digitising and verified during fieldwork (Jones et al., 2018b). The context for the second part of this study is the critical interplay between glacial, periglacial, and paraglacial (rockfall sediment supply) processes in the development and dynamics of rock glaciers in this region (e.g., Scherler et al., 2011; Jones et al., 2018b), which are in turn critical for regional water supply and geohazard risk (Immerzeel et al., 2010; Kraaijenbrink et al., 2017).

8.4 ROCK GLACIERS: ENVIRONMENTAL DOMAINS AND EVOLUTIONARY RELATIONSHIPS

The different origins of rock glaciers have been debated for several decades (e.g., Barsch, 1977; Martin and Whalley, 1987; Berthling, 2011). Many rock glaciers can be viewed as polygenic landforms formed mainly during ice retreat (deglacial) phases in deglacierizing mountains, although they are also known to form in nonglacial, periglacial environments (Hamilton and Whalley, 1995). As a result, several different classification schemes of rock glaciers have been identified based on their morphology, dynamic behaviour, geomorphic setting, or some combination of these properties (Martin and Whalley, 1987; Hamilton and Whalley, 1995). For example, Johnson (1984) classified rock glaciers into simple glacial and nonglacial types, influenced by high magnitude geomorphic events. Giardino and Vitek (1988) identified rock glaciers as transitional landforms of glacial or periglacial types, evolving from debris from glaciers or slopes, and evolving to moraines and slope deposits, respectively. Janke et al. (2015) classified rock glaciers into three types, derived from variations in ice content evaluated using remote sensing methods. In summary, different rock glacier classification schemes exist, but these are usually mutually exclusive, applied to only a single area or region, and examine different combinations of physical or dynamical properties. To better integrate these ideas together, **Table 8.1** shows examples of rock glaciers formed in different environmental domains or formed or controlled by a set of processes associated with that particular environmental domain. Although largely polygenic, most rock glaciers reported in the literature are

dominated by certain sets of processes, which may reflect their evolutionary history or dominant regional climate regime (Giardino and Vitek, 1988). The classification scheme adopted here builds from Humlum (1988), who distinguished between rock glaciers of dominantly glacial origin (controlled by snow accumulation) and periglacial origin (controlled by ground temperature) (e.g., Ishikawa et al., 2001). Here, we add a further category, which describes rock glaciers of dominantly paraglacial origin, controlled by increased slope sediment supply during regional deglaciation. Rock glacier development in these three different environmental domains is now examined.

Table 8.1. Examples of rock glaciers that have formed from a certain dominant overall environmental domain or set of processes associated with that environmental domain.

Dominant genesis	Example location	Reference
Glacial (by debris burial of glacial ice)	Yukon, USA	(Johnson, 1980)
	Stubai Alps, Austria	(Krainer and Mostler, 2000)
	Upper Valtellina, Italian Alps	(Guglielmin et al., 2004)
	Tröllaskagi, Iceland	(Lilleøren et al., 2013)
	Andes, central Chile	(Monnier and Kinnard, 2015b)
	Andes, central Chile	(Janke et al., 2015)
Periglacial (by development of permafrost)	Vanoise Massif, French Alps	(Monnier et al., 2013)
	Ötztal Alps, Italian Alps	(Krainer et al., 2015)
Paraglacial (by development of talus slope deposits)	Yukon, USA	(Johnson, 1984)
	West Greenland	(Humlum, 2000)
	Sierra Nevada, USA	(Millar et al., 2013)
	Svalbard	(Hartvich et al., 2017)

8.4.1 GLACIAL ORIGINS

Rock glaciers can be formed at a valley glacier terminus by upward shearing of subglacial sediments followed by ice stagnation; coverage of the ice surface by supraglacial debris derived from valley sides; ice stagnation and downwasting leading to increased sediment concentration within the remaining ice; and by transformation of ice-cored moraines by mass movements or melting of internal ice, resulting in increased sediment concentration. Rock glaciers therefore usually develop at the onset of glacier retreat or stagnation, and at the front of valley glaciers, and are thus found in particular temporal and spatial contexts. In this environmental setting, rock glaciers mimic a valley glacier terminal moraine. Notably, rock glaciers do not develop at the termini of larger ice caps or ice sheets, largely because of a lack of adequate sediment supply. In the NW European Alps, glacier-derived rock glaciers have developed as a result of rockfalls onto steep glacier surfaces, and this is confirmed by ERT profiles (Bosson and Lambiel, 2016). Here, ablation rates beneath the debris cover are around 40 times lower

than on adjacent debris-free areas of the glacier surface, amplifying rock glacier response under conditions of climate warming and glacier thinning. Similar patterns are observed in eastern Nepal, where rock glaciers have evolved from inactive glaciers, particularly at the transition zone to discontinuous permafrost (Ishikawa et al., 2001). In the Andes of central Chile, the transition from glaciers to rock glaciers is dependent on supraglacial debris thickness, and thus the morphodynamic distinction between these types is related to whether surface debris has vertical and horizontal velocities different to those of the underlying glacier (Janke et al., 2015). This definition of a glacial ice-derived rock glacier also holds for examples in the Yukon, USA (Johnson, 1980).

8.4.2 PERIGLACIAL ORIGINS

The most common genetic origin reported for rock glaciers globally is in association with the periglacial environmental domain and linked to the development, maintenance, and seasonal dynamics of permafrost and the AL. Many studies suggest that the lowermost altitudinal limit of rock glaciers coincides with the lowermost altitude of permafrost within that mountain massif (e.g., Krainer and Ribis, 2012; Bolch and Gorbunov, 2014; Rangecroft et al., 2014; Sattler et al., 2016; Esper Angillieri, 2017) and that this is a deterministic relationship whereby rock glacier distribution can be used as a proxy for permafrost distribution and vice versa (e.g., Uxa and Mida, 2017). Although not helpful as an approach and based on circular reasoning, this relationship also alludes to the role of seasonal development of the AL in the dynamics of rock surface features, including the development and flow velocities of furrows and lobes (Kääb and Weber, 2004; Haeberli et al., 2006; Frehner et al., 2015). These features have been used as a diagnostic indicator of the presence of ice-rich permafrost within the rock glacier body. GPR and ERT methods have also been used to image and map subsurface permafrost bodies within the rock glacier. These methods can highlight the internal permafrost surface, variations in permafrost/snow temperatures and moisture, and debris concentrations (e.g., Isaksen et al., 2000; Hausmann et al., 2012; Monnier et al., 2013). Radiocarbon dating of plant macrofossils within the permafrost core of a rock glacier in the Ötztal Alps, Italy, shows that at 23.5 m depth, the permafrost is 8,960 years old; whereas, at 2.8 m depth it is 2,240 years old (Krainer et al., 2015). However, the presence of variable ice fabrics and shear planes within rock glacier bodies (e.g., Isaksen et al., 2000; Bucki and Echelmeyer, 2004; Krainer and Mostler, 2006) means that such chronologies cannot be used uncritically in this instance to infer that the rock glacier is of early Holocene age or that it has existed in the same state during this time period. Changes in the position of fixed points on the rock glacier surface have been

used as a method to track horizontal and vertical displacements of the rock glacier over time (e.g., Whalley et al., 1995; García et al., 2017). Depending on the sampling interval, this method can show seasonal variations in rock glacier surface morphologies that can inform on permafrost AL dynamics (Kellerer-Pirklbauer and Kaufmann, 2012). In addition to rates of surface flow determined by internal deformation of permafrost ice, slower or faster surface rates can be described based on compression and extension respectively within the rock glacier body (Kääb and Weber, 2004). Bucki and Echelmeyer (2004) suggested that higher and more variable rates of rock glacier surface velocities may be caused by the ice-rock mixture present. The reason for this is that ice and rock have different thermal and compressive strength properties and thus can become disaggregated during differential three-dimensional flow that promotes internal deformation of the rock glacier body (Humlum, 1997). There is also differential movement within and between snow/ice units of different origins and rheologies (Haeberli et al., 2006).

8.4.3 PARAGLACIAL ORIGINS

Rock glaciers can develop in a paraglacial context where rockfalls, rockslides, and other mass movement processes taking place on bedrock outcrops or on steep slopes can contribute material to debris piles located at the outcrop foot. This debris can also be detached by periglacial frost wedging. The debris can be included within snowbanks or onto dead glacier ice or permafrost located at the slope foot, which can ultimately lead to the formation of a rock glacier of dominantly paraglacial origin. The role of rockfalls and other mass movements to rock glacier formation has been identified in particular high-relief mountains with narrow valleys (e.g., Johnson, 1984; Hartvich et al., 2017) and where constricted valley glaciers are undergoing rapid downwasting in response to climate change. The relative timing of rockfall and other mass movement events in such settings has commonly been reconstructed using Schmidt hammer exposure dating (Hedding, 2016; Hartvich et al., 2017) or cosmogenic dating methods (Çiner et al., 2017; Winkler and Lambiel, 2018). In some regions, sediment supply rates by mass movements are strongly affected by slope aspect, in which slopes with a greater diurnal temperature regime result in higher weathering and sediment supply rates (Johnson et al., 2007; Nagai et al., 2013). In turn, this should result in distinctive spatial patterns of rock glacier distributions that correspond to paraglacial slope sediment supply – Nagai et al. (2013) reported that southwest-facing slopes in the Bhutan Himalaya are most strongly associated with glaciers with high frost shattering-derived debris accumulations. In other sites where paraglacial rockfalls dominate debris supply to valley bottoms, rock glacier distribution reflects the

orientation of steep rock walls that are shedding rock debris. The large size and angularity of much debris derived from slope processes mean that paraglacial rock glaciers have surface debris that is potentially coarser when compared to rock glaciers that have other origins. Here, the paraglacial rock glaciers have a steeper frontal slope and exhibit lower velocities of movement when compared to other rock glacier types. Further, as paraglacial rock glaciers are usually backed by a steep backwall sediment source, they may evolve over time by forward movement of the rock glacier front (rock glacier thinning) or by increased sediment supply (rock glacier thickening). Several studies have been concerned with the processes of *in situ* water/ice accumulation in the pore spaces of coarse rockfall/talus debris. This can take place by spring-fed water supply at the talus slope base, infiltration by snowfall, or advective cooling and associated moisture freezing within the debris body (Krainer and Mostler, 2002, 2006; Millar et al., 2013; Kellerer-Pirklbauer et al., 2015; Popescu et al., 2017).

8.4.4 DEVELOPING A MODEL FOR ROCK GLACIER EVOLUTION

Rock glaciers are equifinal landforms inasmuch as they can develop as a consequence of glacial, periglacial, and paraglacial processes, individually or in combination. Based on the foregoing discussion of different rock glacier types and their properties, a genetic classification model can be proposed to describe the corelationships between different controls on rock glacier origin and evolution (**Figure 8.1**). This typological model shows that rock glaciers of glacial origin are mainly controlled by water availability, those of periglacial origin by temperature and those of paraglacial origin by sediment supply. Although this is a nonexclusive classification and links exist between these process domains, the model can also show the different evolutionary pathways undertaken by individual rock glaciers described in the literature (**Figure 8.1**). For example, pathway 1 corresponds to rock glacier development by increased debris content at a stagnating glacier margin, by subglacial thrusting or supraglacial debris accumulation, or by transformation of an ice-cored moraine. Pathway 2 corresponds to a situation where the footslope of a talus cone or scree increases its water content over time by water percolation and freezing or by interstitial snow accumulation. Pathway 3 corresponds to a situation where buried glacier ice transforms into a seasonal AL where there is high enough interstitial moisture content to allow for seasonal meltwater advection through the debris layer. In sum, several different evolutionary pathways are theoretically possible, and individual examples of rock glaciers of these types have been described from the literature from different mountain blocks and climatic/glaciological settings worldwide. What remains unclear, however, is whether rock glaciers from a single region display such evolutionary

diversity. It is important to answer this question because it is generally assumed that rock glaciers from a single region – displaying broadly the same climatic, geologic, and glacial conditions – will have the same controls on their development. We now test this assumption against field data from a single region of the Nepalese Himalaya where large numbers of rock glaciers of different shapes and sizes have been mapped from remote sensing and field observations.

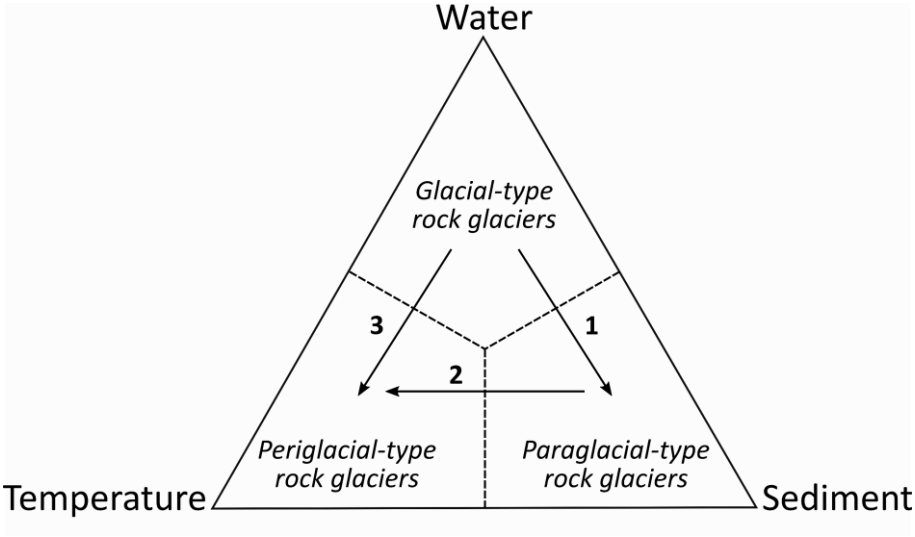

Figure 8.1. Ternary diagram illustrating a conceptual classification of different rock glacier types according to their dominant modes of origin. Evolutionary pathways 1–3 are discussed in the text.

8.5 ROCK GLACIERS IN THE HIMALAYAS: THEIR CLASSIFICATION AND EVOLUTION

In the Himalayas, rock glaciers have been widely observed; and their physical characteristics can be used to test a model of formation in dominant glacial, periglacial, or paraglacial settings. For example, Iwata et al. (2003) discussed a range of periglacial evidence from N and NW Bhutan that is related to the presence of permafrost and rock glaciers. They identified rock glaciers that have glacial or periglacial origins, and that may be either active or relict. Of these, only 9% (3) had glacial origins, the majority being periglacial. Most were active, but 22% (7) were deemed inactive (relict). Several studies have produced rock glacier inventories in different sectors of the Himalayas (e.g., Shroder et al., 2000; Ishikawa et al., 2001; Jones et al., 2018b). These studies do not show a simple distinction by height or aridity gradient, suggesting that the distribution of rock glaciers as a whole is not controlled by the current climate regime but broadly reflects antecedent conditions (Sorg et al., 2015). Previously mapped rock glaciers in the region may also have been misinterpreted (Fort, 2003). The suggestion that active rock glaciers represent the lowermost limit of permafrost (e.g., Iwata et al., 2003) is a circular argument and must be discarded in terms of evaluating rock glacier origins.

Several phases of glaciation during the late Quaternary took place in the Khumbu Himal study area of eastern Nepal, with the most recent glacier retreat and moraine formation around the Khumbu Glacier and adjacent glaciers taking place around 1,000–1,200 y BP, known as the Lobuche Stage (Richards et al., 2000). Alluvial fans and terraces located <5 km down the Khumbu Glacier valley have been dated by the cosmogenic method to different intervals at 16, 12, 8, 4, and 1.5 ky BP, corresponding to different phases of ice retreat (Barnard et al., 2006). The precise age of development of rock glaciers in the region is uncertain due to lack of exposure dating (e.g., Benn and Owen, 2002; Zech et al., 2009), but they likely correspond to these periods of ice retreat and land surface exposure. The Khumbu Glacier has experienced an increase in debris content in recent years at the glacier terminus (Nakawo et al., 1999).

In the Khumbu Himal region, rock glaciers have been extensively mapped using a combination of remote sensing and field mapping. The major properties of these rock glaciers and their genetic origins have been examined in several studies (e.g., Barsch and Jakob, 1998; Iwata et al., 2003). Other studies have also been concerned with the surface debris content and distribution on valley glaciers in the region, with the purpose of identifying variations in spatial patterns of debris content over time (e.g., Nakawo et al., 1999; Hambrey et al., 2008; Rounce and McKinney, 2014; Rowan et al., 2015; Schauwecker et al., 2015). In summary, the Khumbu region contains many rock glaciers of different types (Jones et al., 2018b); however, there is a lack of information on their detailed geometric, morphological and sedimentary properties that can inform on rock glacier origin. New evidence of rock glacier distribution and properties in this region is now presented, based on original fieldwork and supplemented by spatial data analysis from remote sensing.

A number of rock glacier examples are found within the Khumbu Himal region (**Figure 8.2**). In the field, Pokalde rock glacier (PO), Lingten rock glacier (LI), and Chola debris-covered glacier were investigated in detail. The Lingten rock glacier is located at ~4,940 m asl and extends from talus slopes beneath a high (~400–500 m), steep headwall (**Figure 8.2d**). The rock glacier has a steep (>30–35°), high (>30–40 m) and sharp-crested frontal slope, light-coloured frontal slope that suggests little clast weathering, and no vegetation cover (**Figure 8.3a**). These characteristics suggest that the upper lobes contain frozen material and are seasonally active. Conversely, the lowermost lobe has extensive vegetation cover with boulders that are weathered and lichen-covered, indicating long-term stability (i.e., the rock glacier contains no ice). Lingten

rock glacier has an AL composed of blocky matrix-free boulders (**Figure 8.3b**) and thus can be termed a 'bouldery rock glacier' according to Ikeda and Matsuoka's (2006) classification. Additionally, large, angular rockfall debris (**Figure 8.3c**) and perched boulders are commonly present. Previously, Regmi (2008) classified Lingten rock glacier as a periglacial feature based on remote sensing data; however, its morphological and debris characteristics suggest that it has a paraglacial origin. Within this region, only Dughla rock glacier (DU) was classified as having a periglacial origin. Previous studies show that this rock glacier is active with an average velocity of 4.0 to 8.5 cm y^{-1} and this is reflected in its 35–40° steep frontal slope (Jakob, 1992; Barsch and Jakob, 1998).

Figure 8.2. Khumbu Himal, Nepalese Himalaya. (a) Google Earth satellite image (11 March 2009) of rock glaciers and other features situated in the Khumbu valley. Values (m a.s.l.) reflect the elevation of rock glacier termini. The dominant environmental domain is also detailed for each rock glacier. A transitional feature (Chola glacier) is also

delineated. For the distribution of moraines and alluvial fans around the Khumbu Glacier terminus, please refer to Barnard et al. (2006). Annotated photographs of (b) Chola glacier; (c) Pokalde rock glacier (PO); (d) Lingten rock glacier (LI); (e) examples of rock slope failure and LIA moraine collapse, likely resulting from debuttressing following Khumbu glacier downwasting. Kongma rock glacier is also depicted (photos: D.B. Jones)

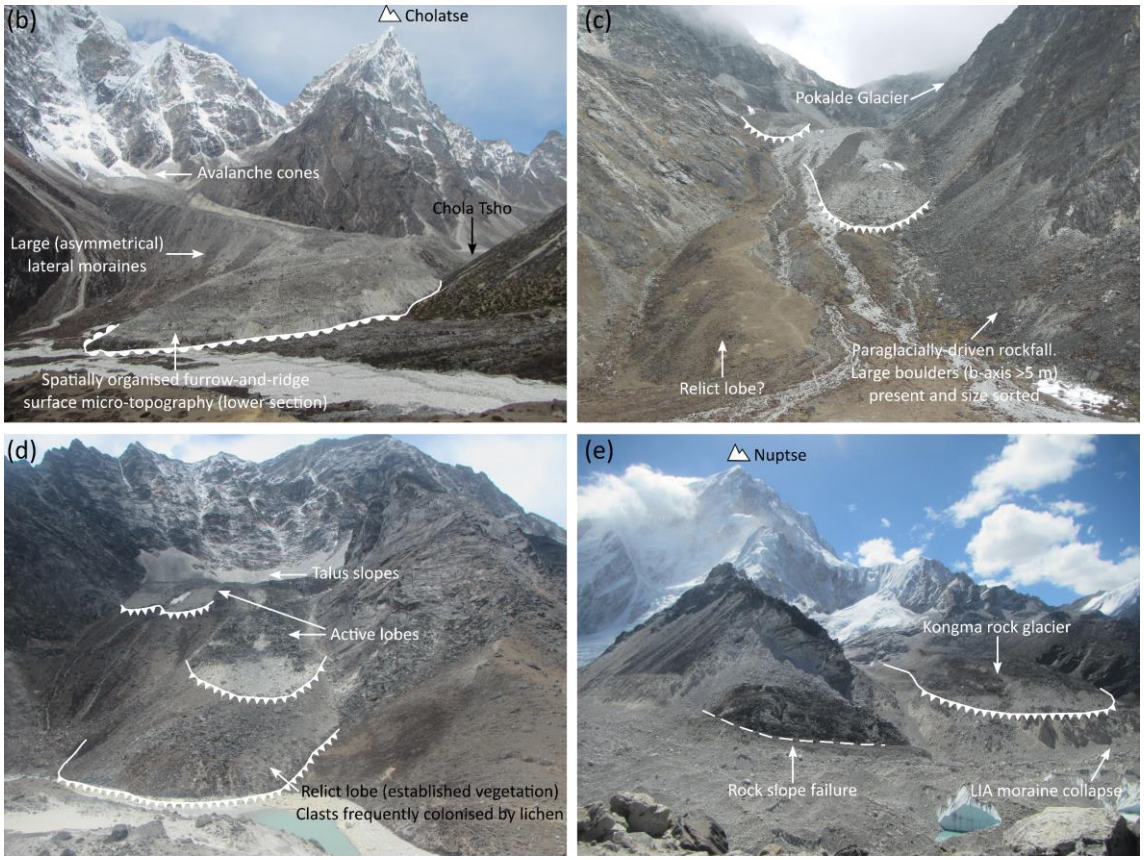

Figure 8.2. *(continued).*

The hitherto unnamed Pokalde rock glacier is a glacier-derived rock glacier, thus is of glacial origin, located at ~5,030 m a.s.l. with a west-facing aspect (**Figure 8.2c**). Rock glacier morphology (e.g., relatively flattened rock glacier body and gently sloping front of <30°) and minor vegetation cover suggests that the Pokalde rock glacier contains frozen material but displays no contemporary movement. The clean Pokalde Glacier is situated immediately upslope of this rock glacier and has receded considerably in recent years. Paraglacial processes are evident in the vicinity of the rock glacier (see **Figure 8.2c**) with angular (and occasionally large) perched boulders resulting from rockfall (**Figure 8.4**). While Pokalde rock glacier has developed in a glacial process domain, this evidence suggests paraglacial processes may have also sustained the rock glacier. Large scale rock slope failures, suggesting paraglacial relaxation of entire slopes (rather than the individual detachment of frost-wedged blocks), are also recorded nearby (**Figure 8.2e**).

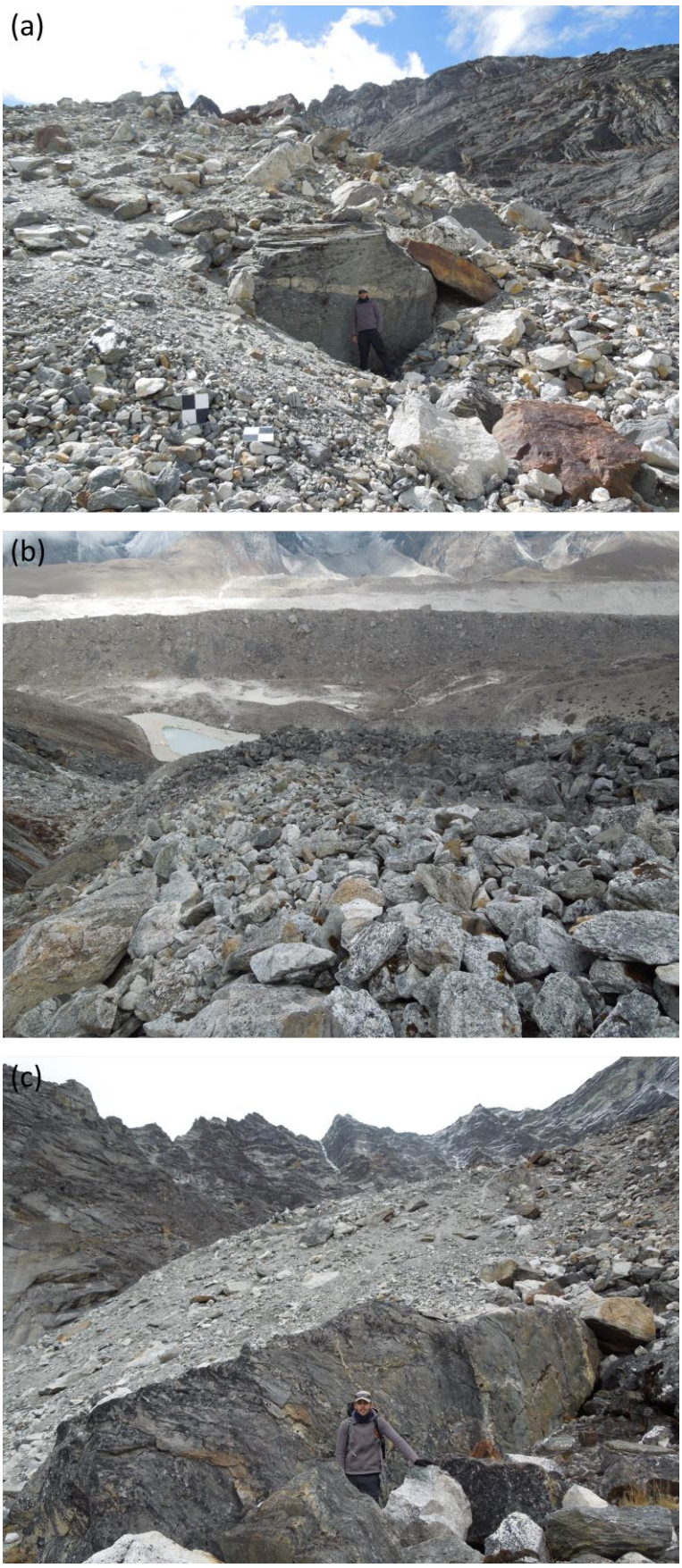

Figure 8.3. Ground views of Lingten rock glacier surficial characteristics including (a) the steep, high, sharp-crested and vegetation-free frontal slope indicating an active rock glacier; (b) the large blocky clasts forming the AL; (c) evidence of large rockfall-derived debris. Note also the high headwalls in the image background (photos: D.B. Jones).

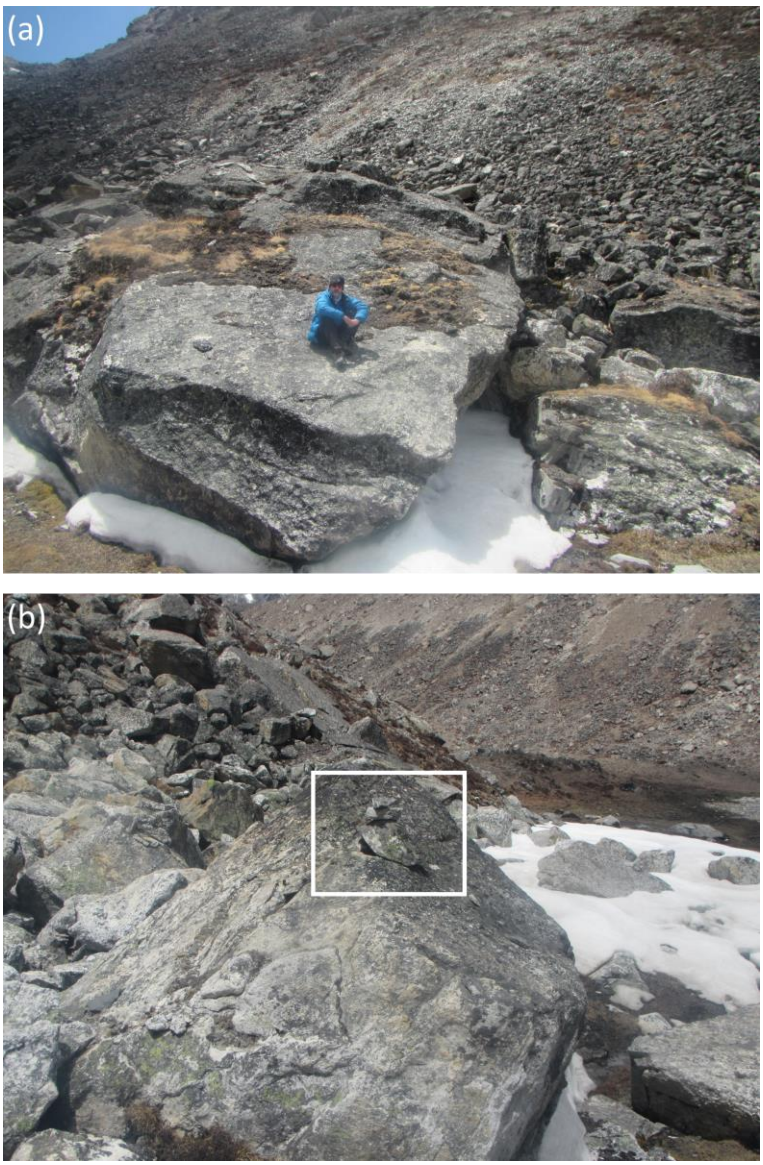

Figure 8.4. Paraglacially-driven rockfall evidence beneath Pokalde rock glacier. (a) Angular, large debris with smaller clasts in the background suggesting a degree of fall sorting; (b) perched boulders (photos: D.B. Jones).

The most conspicuous geomorphological expressions of glacier-rock glacier relationships are large composite landforms that form as debris-covered glaciers and then transition into rock glaciers (e.g., Ribolini et al., 2007; Emmer et al., 2015; Janke et al., 2015; Monnier and Kinnard, 2015b, 2017; Seppi et al., 2015). Geomorphological field surveys suggest that the tongue of Chola debris-covered glacier (**Figure 8.2b**) is transitioning to a glacier-derived rock glacier. Similar to the Presenteseracae debris-covered glacier in the Chilean Andes (Monnier and Kinnard, 2015b), the Chola debris-covered glacier has developed a characteristic rock glacier morphology (i.e., a spatially coherent furrow-and-ridge surface morphology) in its lowermost part. Additionally, the surface is characterised by very large (>4 m), angular boulders and a thick debris layer, indicating movement to the snout of rockfall-derived material (**Figure 8.5**). Such evidence of paraglacial processes suggests that glacier-rock glacier composite landforms in at

least part of the Himalayas are the product of glacial and paraglacial environmental domains (cf. Scherler et al., 2011; Nagai et al., 2013; Govindha Raj, 2017).

Figure 8.5. Ground-based view of the lowermost part of the Chola debris-covered glacier (photo: D.B. Jones).

Geomorphological mapping of rock glaciers in the Khumbu region can be supplemented by clast analysis of their constituent debris as a tool to discriminate between rock glacier types. This is a useful methodology because clast shape properties can identify their source areas in glaciated environments and specifically can distinguish between subglacial and supraglacial debris sources (Lukas et al., 2013). Measurements of individual clasts can be used to derive the RA ratio (the percentage of angular and very angular clasts in any sample) and the C_{40} index (the ratio of c/a-axis lengths ≤0.4). These are the two most useful parameters to distinguish clast source (Benn and Ballantyne, 1993). Results from the Khumbu region are presented in **Figure 8.6**. High RA and C_{40} values are typical of unmodified clasts formed by periglacial frost-shattering (Benn and Ballantyne, 1994). Notably, Pokalde rock glacier has significantly lower values than the other two sites examined, with no overlapping geometrical properties (**Figure 8.6e**), suggesting a different sediment source and a stronger geological control on sediment supply. These sedimentary data in combination with the geomorphic properties and landform associations of the rock glaciers discussed above suggest that debris making up Chola glacier and Lingten rock glacier is derived from steep, frost-shattered bedrock slopes; whereas debris making up Pokalde rock glacier is glacier-derived. Thus, despite both having cores of glacial ice, Chola and Pokalde have very different debris sources.

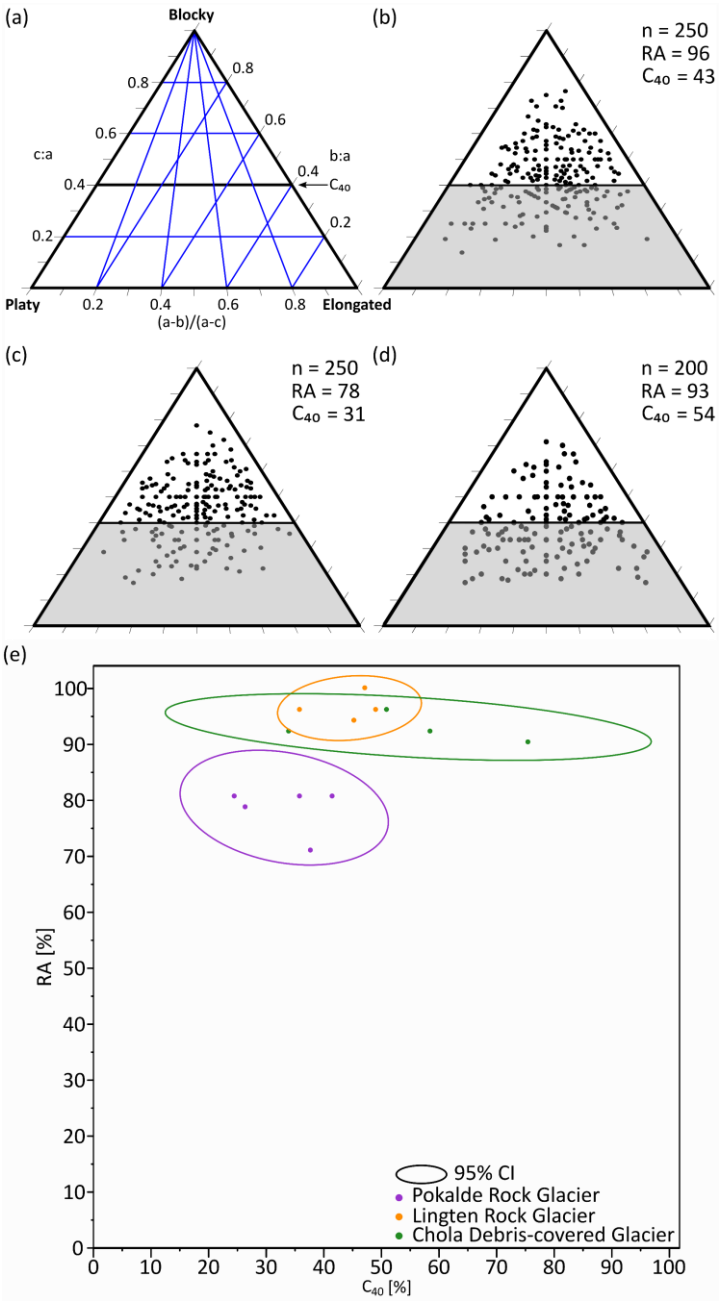

Figure 8.6. (a) Schematic ternary diagram, depicting axial ratios and clast end member states, and clast shape data from three sampled landforms: (b) Lingten rock glacier; (c) Pokalde rock glacier; and (d) Chola glacier. Abbreviations: n = number of clasts sampled; RA and C_{40} are defined in the text. (e) Summary RA-C_{40} bivariate scatterplot of the features sampled *in situ*. Envelopes (ellipses) reflect the 95% confidence interval of each data group.

This summary of different rock glacier properties from the Khumbu region shows that – even within a small area with uniform climatic, glacial, and geologic conditions – a variety of rock glacier types and origins can coexist. In detail, the reasons for such variability relates to micro-scale climatic variations caused by aspect; valley glacier width and bedrock slope (determining the likelihood of ice margin stagnation); antecedent conditions including whether glaciers or permafrost are growing or are in retreat; and proximity of the rock glacier to a potential rock-

slope sediment source (rock wall height and distance) (e.g., Shroder et al., 2000; Ishikawa et al., 2001; Fort, 2003; Nagai et al., 2013; Jones et al., 2018b).

8.6 DISCUSSION

Rock glaciers are equifinal polygenic landforms and are key elements of the geomorphology of cold mountains worldwide, but the different evolutionary pathways by which rock glaciers develop remain unclear. This is particularly the case where rock glaciers in the same area, such as the Khumbu region, show different geometries and physical properties. The proposed classification of rock glaciers globally into broad glacial, periglacial, and paraglacial process domains identifies three different rock glacier end-members (**Figure 8.1**). Within this, however, rock glaciers can evolve over time from one dominant process domain to another as a result of variations in sediment supply and climate (temperature and moisture availability) in combination. This means that there are limitations to the extent to which rock glaciers can inform on regional climate variability, or stages of regional glacier retreat, given that their geometry and morphodynamics may be more strongly controlled by other factors, such as aspect and antecedent conditions. This highlights that previous analyses of rock glacier inventories may have little scope for speaking to any single overarching theory for rock glacier formation because they may have limited applicability outside of their region of origin. This also means that the presence of relict rock glaciers in a region cannot be used uncritically in palaeoclimate reconstructions.

Studies of different rock glaciers from the Himalayas show their complex time evolution and morphological relationships to glacial and slope (paraglacial) landforms and processes (e.g., Owen and England, 1998; Shroder et al., 2000; Ishikawa et al., 2001; Fort, 2003; Iwata et al., 2003; Nagai et al., 2013; Sorg et al., 2015; Jones et al., 2018b). These varied controls mean that no one single evolutionary model applies to describe rock glaciers in this region. A better context for explaining their development is to consider them along the continua of variations in sediment supply and climate that drive their morphodynamic trajectory (**Figure 8.1**), and this approach can provide a classification and interpretative framework for all rock glaciers globally, irrespective of origin. By way of illustration, we have located on this model the examples described in the text from the Khumbu region (**Figure 8.7**). This suggested genetic classification of the different rock glaciers shows that they are of different types, that they do not have the same origins, drivers, and sensitivities and that this is of significance for evaluating the geomorphic evolution of deglacierizing mountains worldwide.

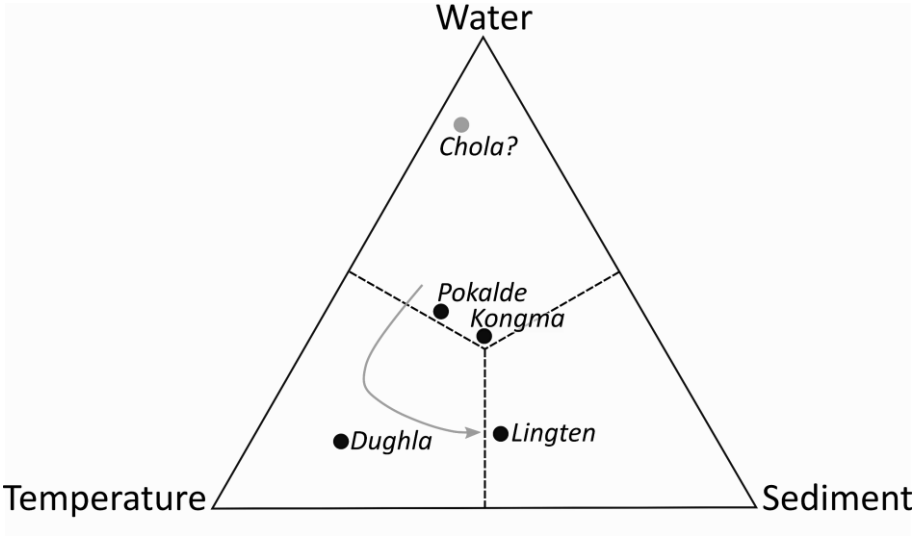

Figure 8.7. Rock glaciers in the studied Khumbu region, Nepal, and their suggested positioning on the schematic ternary diagram presented in **Figure 8.1**. The likely evolutionary trajectory of Lingten rock glacier discussed in the text is shown by the grey arrow.

The proposed evolutionary model of rock glacier development (**Figure 8.7**) also speaks to the evolution of rock glaciers through their varied life stages. This has not been adequately discussed in the literature. Although several studies identify rock glaciers as transient landforms found in deglacierizing terrain (e.g., Giardino and Vitek, 1988; Ballantyne, 2002a; Berthling, 2011; Monnier and Kinnard, 2017; Knight and Harrison, 2018), these rarely expand upon what this means in practice. Relationships between the three rock glacier types according to their dominant mode of origin (**Figure 8.1**) can change over time and space. Upon deglaciation, water availability within the interstices of rock glacier debris decreases, following the trajectory of the evolution of Chola debris-covered glacier illustrated in **Figure 8.7**. Thus, it may be that glacial- and periglacial-dominated rock glaciers transition to paraglacial types and that paraglacial rock glaciers can be considered as the final evolutionary stage of all rock glaciers in a deglacierizing mountain landscape. Despite these different rock glacier types, their temporal relationships, even within a single region, are uncertain; and there is no unidirectional trajectory from one type to another. Cosmogenic dating of clasts on rock glacier surfaces can be problematic because surficial clasts could be added by episodic rockfall at any time (producing young or inherited ages), and cryoturbation of clasts within the rock glacier body can take place during its movement, exhuming older clasts from below (producing anomalously old ages) (Çiner et al., 2017). Also, any determination of rock glacier age cannot unequivocally inform on rock glacier origin. This is because glacier ice can exist within the rock glacier body long after the glacier itself has melted away (Monnier et al., 2013; Krainer et al., 2015); glacial and periglacial (permafrost) processes can coexist during the rock glacier's life; and periglacial

and paraglacially enhanced slope sediment yield can exist for thousands of years after deglaciation (Ballantyne, 2002b).

8.6.1 GEOMORPHIC SENSITIVITY AND LANDSCAPE CHANGE IN DEGLACIERIZING MOUNTAINS

Paraglacial relaxation of unstable rock slopes is increasingly being recognized as an important component of deglacierizing mountains (e.g., Ballantyne, 2002a, 2002b; McColl, 2012; Knight and Harrison, 2014b; Beniston et al., 2018). Paraglacial processes include large-scale rock slope failures as well as more localized rockfalls, landslides and debris flows. These contribute to high slope sediment yields accompanying ice retreat. This paraglacial response is important because it affects first mountain glaciers and, then, mountain rock glaciers.

Studies show that Himalayan glaciers are experiencing increased debris cover and debris thickness as a result of increased recent slope sediment supply (Hambrey et al., 2008; Scherler et al., 2011; Rowan et al., 2015; Schauwecker et al., 2015; Lamsal et al., 2017). Surface debris can variously amplify or suppress glacier melting, leading to decreased or increased longevity of debris-covered glaciers respectively, and this affects the likelihood with which debris-covered glaciers can transition to glacial-derived rock glaciers and their resulting dynamics, including any seasonal variations in surface morphological change (Hausmann et al., 2012). Initial high rates of ice melting under a thin debris cover can rapidly switch to low rates of melting if the ratio of debris to ice changes (Ikeda and Matsuoka, 2002; Anderson and Anderson, 2018), and several studies have examined how surface debris thickness and grain size can influence the thermal regime of underlying ice (e.g., Humlum, 1997; Luethi et al., 2017; Anderson and Anderson, 2018). Changing spatial and temporal patterns of nonglacial (paraglacial) sediment supply can thus dramatically impact on glacier dynamics.

A key property in determining the dynamics of rock glaciers is the relative proportions of rock and ice. The former has the greatest potential for variability because it depends on the availability of a sediment source (bedrock cliffs located above the rock glacier surface) and the rate of sediment supply (weathering rates, degree of slope instability). In almost all known cases, debris content increases rather than decreases over time at the onset of deglaciation (e.g., Glasser et al., 2016) because debris has lower mobility than water and because of the positive feedback effects that debris has on glacier thermal regime. As a consequence of increased debris concentration, many mountain glaciers worldwide are likely to transition to rock glaciers, as is starting to happen at Chola debris-covered glacier (**Figure 8.2b**) and perhaps also at the snout of Khumbu glacier, which is becoming increasingly charged with debris (cf. Nakawo

et al., 1999). Rock glaciers are thus likely to become a more common mountain landform over coming decades/centuries, and their relative geomorphic stability as a latticework of angular debris means that they may have a long residence time in the landscape. Rock glaciers can, therefore, be viewed as an important extended paraglacial transient stage in mountain geomorphic evolution, between glacial and nonglacial endmembers (Cossart et al., 2017; Knight and Harrison, 2018). Notably, the key role of rock glaciers was not fully considered in previous models of paraglacial landscape change (e.g., Ballantyne, 2002a, 2002b).

8.7 CONCLUSIONS

This study shows that rock glaciers can develop under glacial, periglacial, and paraglacial environmental process domains. Interactions exist between these process domains as deglacierizing mountain landscapes change over time, leading to different evolutionary pathways for different rock glaciers, even within the same region, as shown by examples of rock glaciers from the Khumbu region of Nepal. The role of rock glaciers in mountain landscape evolution has hitherto not been fully recognized, and this is a critical research gap given that studies are now showing that mountain glaciers in the Himalayas and Andes, in particular, are now transitioning to rock glaciers. It is likely that rock glaciers will become more numerous and more significant in terms of water and sediment storage as climate change proceeds through the twenty-first century.

8.8 ACKNOWLEDGEMENTS

We thank two anonymous reviewers for their comments on a draft of this paper.

9 MOUNTAIN GLACIER-TO-ROCK GLACIER TRANSITION

9.1 ABSTRACT

In many of the world's high mountain systems, glacier recession in response to climate change is accompanied by a paraglacial response whereby glaciers are undergoing a transition to rock glaciers. We hypothesise that this transition has important implications for hydrological resources in high mountain systems and the surrounding lowlands given the insulating effects that debris cover can have on glacier ice. Despite this, however, little is known about how this transition occurs nor how quickly, which glaciers are liable to transition, the factors driving this process and the water supply implications that follow. This paper assesses the role of glacier and rock glacier textural properties from a deglaciating region of the Himalayas to begin to address some of these issues. We investigated six landsystems on the spectrum from glaciers-to-rock glaciers in the Khumbu Himal, Nepal, and sampled for clast shape and roundness during 2016 and 2017. KAP was additionally used to capture aerial images of an ongoing glacier-to-rock glacier transitional landform (Chola Glacier) to elucidate the surface geomorphic features of a fully transitioned landform. This image data, processed using a structure-from-motion multi-view stereo (SfM-MVS) photogrammetry approach, revealed the presence of a spatially coherent ridge-and-furrow surface morphology in the lower reaches of Chola Glacier, which is potentially indicative of an ongoing glacier-to-rock glacier transition. We show that glacier-derived and slope-derived clast roundness are significantly statistically different (Kolmogorov–Smirnov two-sample test: $D_{max} = 0.62$, two-tail $p < 0.001$; $n = 1{,}650$) and suggest that sediment connectivity (i.e. linkage between sediment sources and downslope landforms) is one of the drivers of the transition process. Consequently, we hypothesise that the presence of well-developed lateral moraines along glacier margins serves to reduce this connectivity, and thus the likelihood of glacier-to-rock glacier transition occurring. Understanding such processes has implications for predicting the geomorphological evolution of deglacierizing mountains under future climate warming and the water supply consequences that follow.

9.2 INTRODUCTION

In deglacierizing mountains, the importance of paraglacial (i.e. landscape relaxation) processes, e.g., large-scale rock slope failures and localised rockfalls, are increasingly recognised (Ballantyne, 2002b; Harrison, 2009; McColl, 2012; Knight and Harrison, 2014b; Beniston et al., 2018). In response to deglacial unloading or debuttressing following the exposure of glacially steepened rockwalls by glacier downwastage and/or retreat (Ballantyne, 2002b; Fischer et al.,

2006), rock slope modification may subsequently increase supraglacial debris coverage and thickness (e.g., Hambrey et al., 2008; Scherler et al., 2011; Rowan et al., 2015). Continuous and thick (i.e. decimetres to metres) supraglacial debris cover can suppress ablation of the underlying ice (Lambrecht et al., 2011; Pellicciotti et al., 2014) and also influence glacier dynamics significantly. One consequence of this is an increased likelihood that debris-covered glaciers will transform to rock glaciers (Shroder et al., 2000; Jones et al., 2018b; Knight et al., 2019). Given the potential WVEQ stored within rock glaciers around the world (Jones et al., 2018a), and that rock glaciers are reportedly more climatically resilient than debris-free and debris-covered glaciers (Anderson et al., 2018), glacier-rock glacier interactions – e.g., large glacier-rock glacier composite features, comprising debris-covered glaciers in their upper parts and rock glaciers in their lower parts – could enhance the resilience of the mountain cryosphere and preserve frozen water stores in the context of future climate change (Rangecroft et al., 2013; Monnier and Kinnard, 2017; Jones et al., 2018a; Jones et al., 2019). Importantly, the water supply implications associated with rock glacier hydrological contributions under climate change scenarios is yet to be established, with few existing studies investigating this issue (for reviews see: Duguay et al., 2015; Jones et al., 2019). Improved understanding of glacier-rock glacier interactions, therefore, is of critical importance if we are to better understand the response of high mountain glacial systems to climate change. In addition, there are considerable gaps in understanding whether glaciers will transition to rock glaciers (and develop climatically-resilient water stores) or recede and form lakes dammed by terminal moraines (and potentially produce damaging glacial lake outburst floods).

Found ubiquitously in high mountain systems around the world (see Jones et al., 2018a), rock glaciers are lobate or tongue-shaped assemblages of ice-supersaturated debris and/or pure ice, which slowly creep downslope (see Martin and Whalley, 1987; Barsch, 1996; Haeberli et al., 2006; Berthling, 2011). They typically display rates of movement in the order of centimetres-decimetres per year (see Table 3 in Janke et al., 2013); however, examples of rock glaciers with annual surface velocities of several metres have been reported (Gorbunov et al., 1992; Kääb et al., 2003; Krainer and Mostler, 2006; Delaloye et al., 2013; Sorg et al., 2015; Hartl et al., 2016b; Eriksen et al., 2018). They are characterised by distinctive flow-like morphometric features; e.g., spatially organised transverse and longitudinal ridge-and-furrow surface patterns, steep (~>30–35° – gradients of >40° have been observed [Krainer et al., 2012]) and sharp-crested frontal and lateral slopes etc. (Wahrhaftig and Cox, 1959; Baroni et al., 2004; Kääb and Weber, 2004). Recent research efforts have provided insights into the spatial

distribution of rock glaciers (e.g., Jones et al., 2018a, and references therein), internal structure (Hausmann et al., 2007, 2012; Maurer and Huack, 2007; Monnier and Kinnard, 2013, 2015a; Florentine et al., 2014; Emmert and Kneisel, 2017), dynamic behaviour (Kääb et al., 2007; Delaloye et al., 2008, 2010; Serrano et al., 2010; Müller et al., 2016; Wirz et al., 2016; Kenner et al., 2017a) and hydrological importance (Azócar and Brenning, 2010; Rangecroft et al., 2015; Janke et al., 2017; Jones et al., 2018a, 2018b). However, the temporal and spatial evolution of glacier-rock glacier interactions remains poorly understood (Monnier and Kinnard, 2015b).

Here, it is important to differentiate rock glaciers from debris-covered glaciers which, in spite of their semantic connection, constitute distinct landforms (Hambrey et al., 2008; Benn and Evans, 2010; Cogley et al., 2011; Kirkbride, 2011). The latter are glaciers partially or wholly covered with a thin (typically less than several-decimetres thick) debris mantle and characterised by a topographically complex, spatially-chaotic mosaic of surficial features, including hummocks, depressions, supraglacial melt ponds and frequent ice exposures (e.g., ice cliffs). Rock glaciers and debris-covered glaciers also have distinct flow dynamics; the former moves as a consequence of internal deformation, which predominantly occurs in a shear zone at depth within the feature (Arenson et al., 2002; Buchli et al., 2013, 2018; Krainer et al., 2015; Kenner et al., 2017a), whereas movement of the latter is governed by internal deformation, basal sliding and soft bed deformation (Bosson and Lambiel, 2016). It is worth noting that basal sliding is generally non-occurring or very limited for cold-based debris-covered glaciers (i.e. glaciers frozen to their beds), and only debris-covered glaciers underlain by a soft deformable substrate (i.e. unlithified sediments or poorly consolidated sedimentary rocks) experience soft bed deformation. Nevertheless, glacier-rock glacier interactions have defined the long-standing debate regarding rock glacier origin and evolution that abounds in the literature (see Barsch, 1977, 1987, 1996; Whalley and Martin, 1992; Hamilton and Whalley, 1995; Clark et al., 1998; Whalley and Azizi, 2003; Haeberli et al., 2006; Berthling, 2011). These divergent opinions, termed *the rock glacier controversy* by Berthling (2011), can be framed as the *permafrost model* vs the *glacier ice-core model*, whereby rock glacier internal ice is assumed to be of a dominantly periglacial/permafrost origin (Wahrhaftig and Cox, 1959; Barsch, 1977, 1987, 1988, 1996; Haeberli, 1985) or glacigenic origin (Outcalt and Benedict, 1965; Potter, 1972; Whalley, 1974; White, 1976; Humlum, 1996; Potter et al., 1998; Ishikawa et al., 2001; Monnier et al., 2013; Petersen et al., 2016; Guglielmin et al., 2018), respectively.

Monnier and Kinnard (2017) have identified three types of glacier-rock glacier interactions within the literature:

- *Type I:* glacier/debris-covered glacier re-advance and subsequent superimposition/embedding onto/into older permafrost bodies (Lugon et al., 2004; Haeberli, 2005; Ribolini et al., 2007, 2010; Monnier et al., 2013; Dusik et al., 2015; Bosson and Lambiel, 2016; Kellerer-Pirklbauer and Kaufmann, 2018; Kenner, 2019) – defined by the permafrost model.
- *Type II:* the continuous emergence of a rock glacier from a debris-covered glacier by evolution of the surface morphology, together with the creep of a massive and continuous ice body that has been buried and preserved (Potter, 1972; Potter et al., 1998; Humlum, 2000; Krainer and Mostler, 2000; Berger et al., 2004; Krainer et al., 2010; Krainer et al., 2012) – defined by the glacier ice-core model.
- *Type III:* debris-covered glacier-to-rock glacier evolution through the transformation of both the surface morphology and the internal structure, i.e. the development of a perennially frozen ice-debris mixture formed via incorporation of surface-derived debris and periglacial ice and fragmentation of the initial massive and continuous ice body (Monnier and Kinnard, 2015b; Seppi et al., 2015; Monnier and Kinnard, 2017). Numerical models of debris-covered glaciers have shown that (iii) forms a plausible end-member response for glacier-rock glacier interactions (Anderson et al., 2018). This has been described as an alternative to the dichotomous debate between a periglacial/permafrost origin or glacigenic origin for rock glaciers (Monnier and Kinnard, 2015b).

  Regarding Type II and III glacier-rock glacier interactions, continuity of the debris-covered glacier and emerging rock glacier morphology suggests a continuum between debris-free glaciers and rock glaciers where debris-covered glaciers form an intermediate stage (Giardino and Vitek, 1988). Striking examples of large, ongoing debris-covered glacier-rock glacier transitions are reported in the literature (Shroder et al., 2000; Monnier and Kinnard, 2015b; Monnier and Kinnard, 2017), and these real-world examples alongside numerical modelling simulations (Anderson et al., 2018) indicate that debris-covered glacier-to-rock glacier transitions can occur rapidly (<100 years). Yet, proponents of the permafrost model and glacier-ice core model have generally orientated studies towards already well-developed landforms (Monnier and Kinnard, 2015b).

Consequently, there exists an opportunity to conduct research that addresses questions about the processes governing *ongoing* debris-covered glacier-to-rock glacier transitions in order to elucidate the drivers that determine the likelihood that this transition will occur (Jones et al., 2019). Answering this question is of great importance if we wish to understand how glaciated mountains might evolve with future climate change and the hydrological and water supply implications that follow (ibid.). To illustrate this issue our study focuses upon an exemplar region where glaciers (clean and debris-covered) and rock glaciers co-exist to (i) investigate the sedimentological and geomorphological characteristics associated with a range of relevant landforms, and (ii) develop a hypothesis for glacier-to-rock glacier transition.

9.3 REGIONAL SETTING

9.3.1 CLIMATOLOGICAL AND GEOLOGICAL CONTEXT

The study area is located in the SNP, Khumbu Himal, north-eastern Nepal (**Figure 9.1a**). The climate of this area is dominated by the South Asian Summer Monsoon, with data from the PYRAMID Observatory Laboratory (hereafter: PYRAMID) near Lobuche (5,035 m a.s.l.) indicating that 90% of annual precipitation falls during June-September (Bollasina et al., 2002; Salerno et al., 2015). Also, instrumental records reflect a topographically-driven steep precipitation gradient, with pronounced south (Chaurikharka [~2,600 m a.s.l.]: 2,418 mm yr^{-1}) to north (PYRAMID: 449 mm yr^{-1}) reduction in precipitation within the SNP (Salerno et al., 2015). MAAT at the PYRAMID (1994–2012) was -2.4 °C, and mean temperature above 5,000 m a.s.l. is increasing by 0.044 °C yr^{-1} (ibid.). Seismic refraction studies conducted on four rock glaciers in the study region indicate that the regional lower limit of discontinuous permafrost is situated at ≃5,000–5,300 m a.s.l. (Jakob, 1992); however, ice preservation in openwork blocky debris accumulations (e.g., rock glaciers) several hundreds of metres below the regional limit of discontinuous permafrost have been reported (e.g., Delaloye and Lambiel, 2005). The detailed bedrock geology of the Everest Massif has been described (see Searle et al., 2003). Of significance for this study is that the features studied in this paper have surface debris consisting predominantly of granitic and gneissic debris, with some migmatitic debris. In the Khumbu region numerous landforms from across the spectrum of the glacial-paraglacial-periglacial landscape continuum occur within a relatively small spatial area. This means that climate conditions are relatively homogenous in the area and that we can, therefore, better isolate the non-climatic processes driving glacier-to-rock glacier transition.

9.3.2 GEOMORPHOLOGICAL CONTEXT OF DEBRIS-MANTLED LANDFORMS

The ~15.7 km long Khumbu Glacier (27°56'N, 86°49'E; **Figure 9.1a**) flows from the Western Cwm between Mt. Everest (8,848 m a.s.l.), Mt. Lhotse (8,516 m a.s.l.) and Mt. Nuptse (7,861 m a.s.l.) via the Khumbu Icefall, and terminates at ~4,900 m a.s.l. The lowermost ~8 km is debris-mantled, with debris thickness increasing towards the glacier terminus and reaching several metres (Nakawo et al., 1986). The debris-covered glacier tongue is characterised by a very low gradient, with the lowermost 3–4 km believed to be flowing at velocities <10 m a^{-1} (i.e. stagnant) (Hambrey et al., 2008; Quincey et al., 2009), and a pair of prominent lateral moraines (**Figure 9.1a** and **g**) dating from the LIA (Rowan, 2017). Lobuche Glacier (**Figure 9.1a** and **e**) on the western side of Khumbu Glacier is smaller and encompasses a relic debris-mantled ablation zone ~1 km in length that is disconnected from the clean-ice accumulation zone (Watson et al., 2018). Chola Glacier (**Figure 9.1a** and **b**), believed to be a glacier-rock glacier composite landform (Knight et al., 2019), is located beneath Mt. Taboche (6,542 m a.s.l.) and Mt. Cholatse (6,440 m a.s.l.) and flows ~3 km to ~4,400 m a.s.l. It is characterised by large, asymmetrical lateral moraines and has a near-continuous debris-mantle over the entirety of its length. Lastly, rock glaciers have been extensively mapped across the Khumbu Himal (Regmi, 2008; Jones et al., 2018b), including a number situated within the Pokalde Massif on the eastern side of Khumbu Glacier. In the field, Lingten and Pokalde rock glaciers were investigated in detail. Both of these are glacier-derived rock glaciers, and thus of glacigenic origin (Knight et al., 2019). The main properties of these rock glaciers, such as their sediment budget and general characteristics, have been examined in previous studies (Barsch and Jakob, 1998; Knight et al., 2019). Pokalde rock glacier is located at ~5,030 m a.s.l. with a west-facing aspect. It has a relatively flattened body and gently sloping front of <30°, with minor vegetation and lichen cover (**Figure 9.1c**). Knight et al. (2019) suggest that this rock glacier is inactive (i.e. containing ice but immobile). Pokalde Glacier, located immediately upslope of this rock glacier, has receded considerably in recent years. Lingten rock glacier is located at ~4,940 m a.s.l. and extends from talus slopes beneath a high (~400–500 m), steep headwall (**Figure 9.1d**). The rock glacier has a steep (>30–35°), high (>30–40 m) and sharp-crested frontal slope, light-coloured frontal slope, and no vegetation cover; characteristics that indicate the upper lobes contain frozen material and are seasonally active (Knight et al., 2019). Conversely, the lowermost lobe has extensive vegetation cover with boulders that are weathered and lichen-covered, indicating long-term stability (i.e. the rock glacier contains no ice and is immobile [relict activity status]) (ibid.).

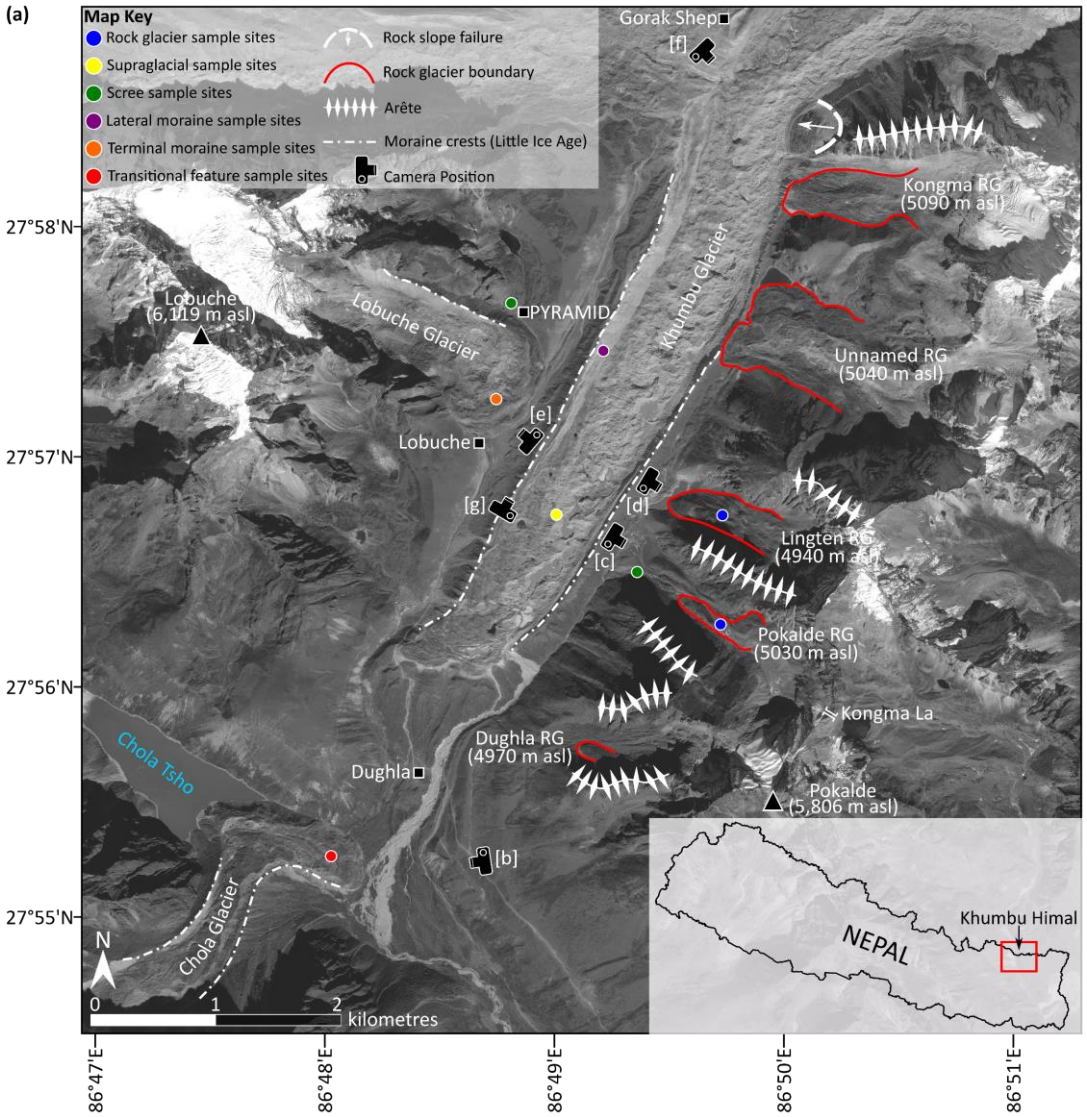

Figure 9.1. (a) The spatial distribution of relevant geomorphological landforms situated within the Khumbu valley and discussed in this paper. Sampling sites for clast characteristic analysis are indicated. Values (m asl) reflect the elevation of rock glacier (RG) termini. Background: orthorectified Pleiades panchromatic scene from November 2016. Inset: the location of the Khumbu Himal in Nepal. Annotated photographs of selected geomorphological elements examined in this paper are indicated: (b) Chola Glacier, probably undergoing contemporary glacier-rock glacier transition; (c) Pokalde rock glacier (glacier-derived); (d) Lingten rock glacier (glacier-derived); (e) debris-mantled surface and terminal moraine of Lobuche Glacier; (f) examples of rock slope failure, LIA moraine collapse and evidence for the degree of glacier downwasting below the LIA trimline; and (g) right-lateral moraine of Khumbu Glacier (photos: D.B. Jones [b-d, f] and O. King [e, g]).

Figure 9.1. *(continued).*

9.4 METHODS

9.4.1 CLAST MORPHOLOGY

Paraglacial landscapes represent highly dynamic systems; the adjustment from glacial- to paraglacial-dominated process regimes in high mountain systems occurs over a range of time-scales. Therefore, "[g]eoscientists [and geomorphologists] are generally unable to fully observe landscape forming processes because the time-scale of the observer and the time-scale of many geomorphic phenomena are different" (Micallef et al., 2014). Location-for-time substitution facilitates the inference of long-term landform development based upon the assumption that the modern landscape contains representative landforms at different stages of evolution, the comparison of which enables integration of long-term processes and short-

term investigations (field-based "snapshots") (see Paine, 1985) (e.g., Micallef et al., 2014; Klaar et al., 2015; Messenzehl et al., 2017). Previous research has indicated the utility of clast shape and roundness for distinguishing between different erosional, transportational and depositional clast histories in glaciated environments (e.g., Ballantyne, 1982; Benn and Ballantyne, 1993, 1994; Bennett et al., 1997; Hambrey and Ehrmann, 2004; Glasser et al., 2009; Brook and Lukas, 2012; Małecki et al., 2018), thus enabling the creation of hypotheses to test models of landscape development. Here, therefore, we substitute data collected through time with clast data from a range of landforms that span the glacier-rock glacier continuum to elucidate the nature of transitions along this evolutionary pathway.

During two field campaigns undertaken in May 2016 and 2017, 1,650 clasts from surface deposits were taken to determine clast shape (i.e. the relative dimensions of the clast) and roundness (i.e. the degree of curvature around the clast edges) characteristics following the method of Benn and Ballantyne (1993, 1994). Sedimentary facies were also described in the field on the basis of Hambrey and Glasser's (2003) modification of Moncrieff's (1989) textural classification of poorly sorted sediments. Field sampling was undertaken at 33 sites located across six distinct morphometric features on and in the vicinity of the Khumbu Glacier (**Figure 9.1a**; **Table 9.1**): supraglacial debris, terminal moraine debris, lateral moraine debris, rock glacier debris, possible glacier-rock glacier composite landform debris (termed: transitional feature) and rockfall debris (termed: scree). The clasts, in groups of fifty, were selected at random from 2 m^2 sample sites and the three orthogonal axes *a, b, c* (long, intermediate, short) were measured to the nearest 5 mm using a steel ruler. Clast roundness was determined visually for each clast on a modified Powers (1953) scale. Given the potential influence of lithology in determining clast shape (see Lukas et al., 2013), we confined our sampling strategy to clasts of similar lithology (granitic gneiss).

Table 9.1. Study sample site information. This information is also visualized in **Figure 9.1a**.

Feature Name	Latitude	Longitude	Elevation (m a.s.l.)	Facies sampled
Khumbu Glacier	27°56'30"N	86°48'54"E	4,950	Supraglacial debris
	27°57'16"N	86°49'07"E	4,990	Lateral moraine debris
Lobuche Glacier	27°57'06"N	86°48'42"E	5,010	Terminal moraine debris
Pokalde rock glacier	27°56'07"N	86°49'40"E	5,190	Rock glacier debris
Lingten rock glacier	27°56'35"N	86°49'44"E	5,130	Rock glacier debris
Chola Glacier	27°54'59"N	86°48'00"E	4,450	Transitional feature debris
Scree	27°56'18"N	86°49'14"E	4,920	Rockfall debris
	27°57'32"N	86°48'44"E	5,020	Rockfall debris

As advocated by Benn and Ballantyne (1993, 1994), ternary diagrams following Sneed and Folk (1958) were generated in the TRI-PLOT Excel spreadsheet (Graham and Midgley, 2000) and employed to visually and statistically interpret clast shape. The C_{40} index (percentage of clasts with a c/a axial ratio ≤ 0.4), was subsequently calculated for each sample site (i.e. 50 clasts). Clast roundness classifications were plotted as frequency distributions (%) and assessed visually. The RA index (percentage of angular and very angular clasts), was then determined for each sample site. Here, the C_{40} and RA indices are assumed to represent two contrasting modes of sediment transport: (i) active transport at or close to the ice-bed interface (i.e. subglacially modified); and (ii) passive transport at the feature surface (i.e. supraglacially transported) or within the ice (i.e. englacially transported) (Boulton, 1978; Benn, 2004). Boulton (1978) showed that dominantly edge-rounded, blocky and abraded clasts occurred in (i) and dominantly angular and platy clasts in (ii). To this end, the co-variance of the RA and C_{40} parameters for the six different morphometric features were plotted on a bivariate scatterplot as suggested by Benn and Ballantyne (1994). Landform associations were further statistically interrogated using the Kolmogorov-Smirnov two-sample test (McCarroll, 2016, p. 132).

9.4.2 STRUCTURE-FROM-MOTION MULTI-VIEW STEREO (SFM-MVS) PHOTOGRAMMETRY

In addition to sedimentological sampling, an experiment was undertaken to test the utility of emerging SfM-MVS photogrammetry approaches for modelling the surface features of a potentially ongoing glacier-to-rock glacier transition. Drones have emerged in geomorphological research as a *de-facto* platform for SfM-MVS data capture (Smith et al., 2016), but the use of drones in the study area was not feasible for a number of reasons. The SNP authority operates restrictions regarding the use of drones, which can make obtaining research permits more difficult (D. Regmi [Himalayan Research Expeditions], pers. comm.). Power supply issues, e.g., limited availability of solar power, device-type charging restrictions, high costs (~400 Rs./hr ≈ 3.5 USD) and low air mass – which results in poor flight efficiency and very short flight times – also restricts the use of drones here. In comparison to drones, KAP provides a number of advantages in high-altitude locations (Wigmore and Mark, 2018). These include: (1) KAP platforms are less affected by the lower air density of high-altitude regions; (2) KAP platforms are lighter and more compact than drones and thus simpler to transport to field sites; (3) powerful katabatic winds characteristic of high-altitude environments form conditions suitable for KAP, however, represent hazardous conditions for drones; (4) KAP platforms are less prone to

breakage than drones, an important consideration given the complex nature of mountainous terrain and the greater expense of the latter (ibid.).

Aerial images of the Chola Glacier were captured using KAP. A HQ KAP Foil 1.6 m² single-line kite was used for this purpose (**Figure 9.2a**); a KAP system previously demonstrated to provide a stable aerial platform (e.g., Duffy et al., 2018). This KAP system is suitable for wind conditions between 3.13 and 13.86 m s^{-1} (KAPshop, n.d.). PYRAMID Observatory Laboratory data indicates well-defined local circulatory systems with consistent south-southwest valley breezes (~4.5 m s^{-1}) peaking between 12:00 to 14:00 (Bollasina et al., 2002); therefore, the chosen kite platform was well-suited to these conditions. A ruggedized Canon PowerShot D30 12.1-megapixel compact digital camera was used to capture aerial photographs. The Canon Hack Development Kit firmware (CDHK; chdk.wikia.com/wiki/CHDK) was loaded onto the SD card, enabling fixed interval shooting; here, an interval of 5 s was used. The camera was mounted on a custom 3D printed lightweight mount (**Figure 9.2b**) and hung from a picavet suspension system ~10 m below the kite. The picavet system uses a system of twine and pulleys that serve to stabilize the KAP platform with the camera facing in the nadir position. In the field, 13 highly visible black and white chequered 250 mm x 250 mm plastic ground control points (GCPs) were distributed along the terminus of Chola Glacier. Laminated sheets with unique identifiers were positioned alongside each GCP to simplify maker identification within the images, and the GCP position was measured with a GARMIN eTrex® 10 Handheld GPS. Geospatial data collected from this device were recorded in the WGS-84 datum (ESPG: 4326) with an average horizontal error of ± 3 m. The kite was then walked around the Chola Glacier in a zig-zag fashion to ensure good image overlap and to gather images from various perspectives, both of which are important for the functioning of SfM-MVS algorithms (Westoby et al., 2012).

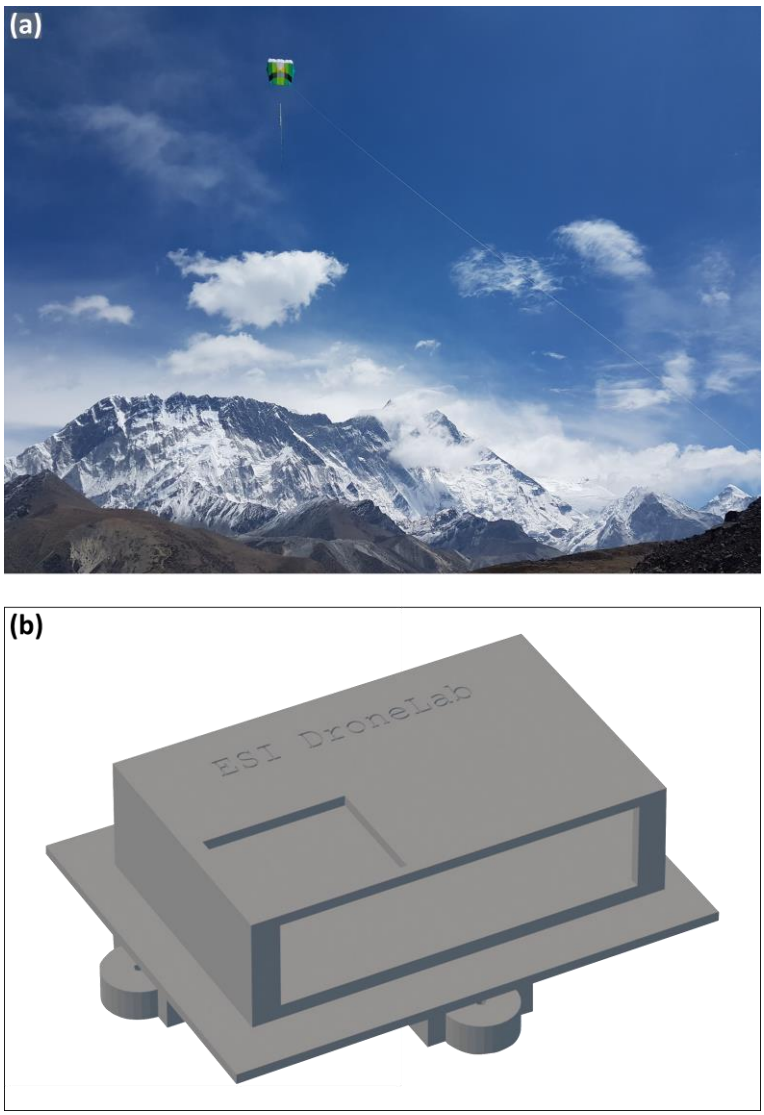

Figure 9.2. (a) The KAP system during a test flight on Duwo Glacier beneath Ama Dablam. The Nuptse-Lhotse ridge forms the backdrop. N.B. the larger HQ KAP Foil 5.0 m^2 single line kite is depicted. This KAP system, facilitating KAP in lower wind conditions (1.79–8.94 m s^{-1}) (KAPshop, n.d.), was also transported to the field sites but not used; and (b) 3D model representation of the picavet mount (photo: D.B. Jones).

Through manual inspection KAP-derived aerial images were filtered, removing those with visible motion blur, an excessively oblique angle, non-stationary occlusions such as people, and those captured during take-off and landing. This resulted in a subset of 282 images, which formed the input for a photogrammetric processing workflow. Subsequently, a dense point cloud, digital surface model (DSM) and orthomosaic were built using Agisoft PhotoScan Professional (v. 1.3.5) (Agisoft LLC, 2017). The sequential steps and the settings used within the photogrammetric workflow are available in the supplementary information (**section 12.4.1**). The specific algorithms implemented by PhotoScan are not detailed here; however, the SfM-MVS procedure is described by Westoby et al. (2012).

9.5 RESULTS AND DISCUSSION

9.5.1 ANALYSIS OF CLAST SEDIMENTOLOGY

Ternary diagrams and roundness histograms for the features sampled *in situ* are shown in **Figure 9.3**, and the RA-C_{40} (i.e. roundness vs shape) bivariate scatterplot in **Figure 9.4**.

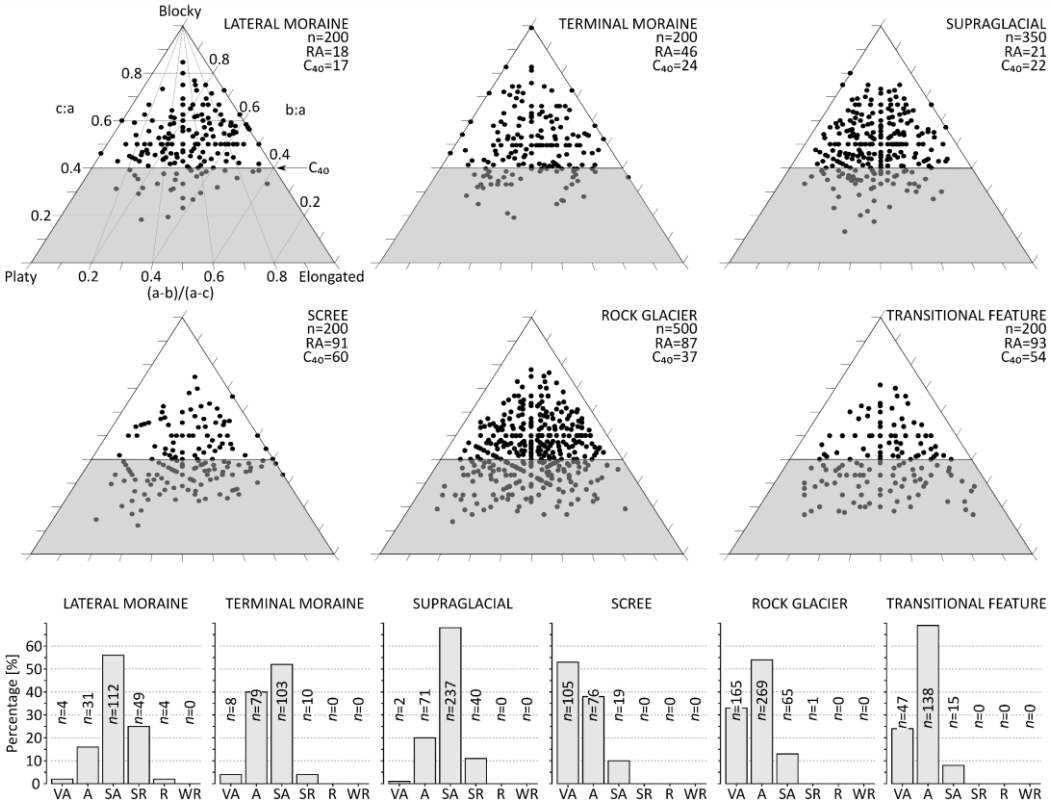

Figure 9.3. Aggregate clast shape data (ternary diagrams) and roundness data (histograms) for the six morphometric features. Abbreviations: n is the number of clasts sampled; RA and C_{40} are defined in the text; VA = very angular; A = angular; SA = sub-angular; SR = sub-rounded; R = rounded; and WR = well-rounded.

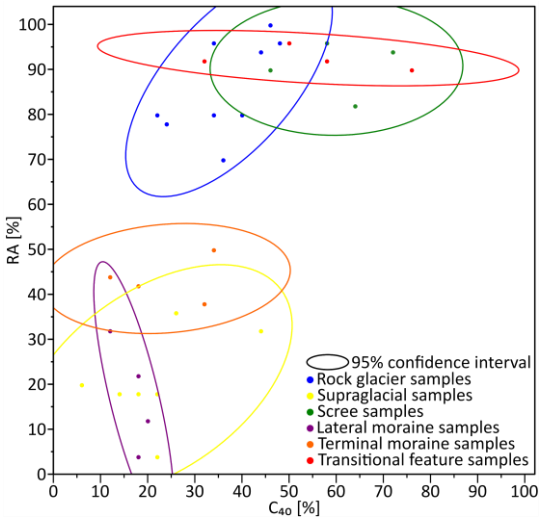

Figure 9.4. Summary RA-C_{40} bivariate scatterplot of the features sampled in situ. Envelopes (ellipses) reflect the 95% confidence interval of each data group. Abbreviations: RA and C_{40} are defined in the text. N.B. each plotted point represents a sample group of 50 clasts.

Sandy boulder-gravel, with minor cobbles and pebbles, dominates the near-continuous debris-mantle in the lower portions of Khumbu Glacier (**Figure 9.5a**). Supraglacial samples have moderate-high c:a ($\tilde{x}$ = 0.50) and b:a ($\tilde{x}$ = 0.78) axial ratios, and thus aggregate clast form is predominantly blocky (Ballantyne, 1982). Of note, C_{40} indices range considerably between 6% and 44%, indicating that supraglacial facies also contain smaller proportions of platy/elongate clasts. Typical clast roundness distribution of supraglacial facies reflects the predominance of sub-angular clasts (68%), with a lower occurrence of very angular (1%), angular (20%) and sub-rounded (11%) clasts. RA values are generally low (<20%), however two samples have more moderate values (32–36%). Generally, supraglacial samples are predominantly very angular and/or angular (e.g., Benn and Ballantyne, 1993; 1994; Bennett et al., 1997; Benn and Owen, 2002; Glasser et al., 2009; Brook and Lukas, 2012); thus, here, aggregate clast form attributes of supraglacial samples indicate that most debris has likely undergone active transportation at the ice-bed interface (Boulton, 1978) or fallen from collapsing lateral moraines (Hambrey et al., 2008) (**Figure 9.1f**). Additionally, the presence of large sub-angular/sub-rounded boulders up to 5 m (b-axis) at the surface (**Figure 9.5a**) and bullet-nosed clasts (Boulton, 1978; Benn et al., 2004, p. 362) suggests the importance of subglacial transport paths. Hambrey et al. (2008), report similar aggregate clast form results for supraglacial samples on Khumbu Glacier, lending credence to the findings presented above.

The LIA lateral moraines of Khumbu Glacier have unstable, non-vegetated inner faces dominated by sandy-boulder gravel (**Figure 9.5b**). Atop the lateral moraines, large, angular boulders several metres in diameter are present (**Figure 9.1g**). Clasts are blocky with moderate-high c:a ($\tilde{x}$ = 0.50) and b:a ($\tilde{x}$ = 0.75) axial ratios (Ballantyne, 1982). C_{40} (<20%) and RA indices (<32%) are both reasonably low (i.e. dominantly blocky shapes and very high percentages of edge-rounded clasts). Furthermore, clasts in lateral moraine facies are predominantly angular, sub-angular and sub-rounded, in which sub-angular and sub-rounded clasts are dominant with up to 64% and 38% in this category, respectively. The co-variant plot demonstrates a narrow distribution of RA/C_{40}, further suggesting a predominantly basal-origin for debris (i.e. actively transported).

Terminal moraine facies, sampled at Lobuche Glacier (**Figure 9.1a**), are predominantly blocky with moderate-high c:a ($\tilde{x}$ = 0.50) and b:a ($\tilde{x}$ = 0.75) axial ratios and few platy/elongate clasts (C_{40} = 24%) (Ballantyne, 1982). Clast roundness distribution is broad, with peaks in the angular (40%) and sub-angular (52%) categories. Additionally, the co-variant plot depicts

comparatively high RA indices (38–50%) vs supraglacial and lateral moraine facies, which combined with the presence of large, angular boulders (**Figure 9.5c**), infers a variable mixture of actively and passively transported sediment.

Scree facies, sampled at a number of locations (**Figure 9.1a**), are categorised as boulder-gravel, with minor proportions of cobbles and pebbles (**Figure 9.5d**). Additionally, angular boulders >5 m (b-axis) are common at the foot of rockwalls (**Figure 9.5d**). Sampled clasts have low-moderate c:a ($\tilde{x}$ = 0.38) and moderate-high b:a ($\tilde{x}$ = 0.67) axial ratios, and thus aggregate clast form is predominantly platy (Ballantyne, 1982). Relatively high C_{40} indices (60% [46–72%]) support this interpretation. Furthermore, clasts are predominantly very angular and angular (53% and 38%, respectively), with minor proportions of sub-angular debris. Intra-sample RA indices are all >82%. Combined, this indicates that scree facies have undergone predominantly passive transport.

Rock glacier facies are dominated by matrix-free, angular boulder-gravel (**Figure 9.5e**); thus, Pokalde and Lingten rock glaciers can be designated 'bouldery rock glaciers' according to Ikeda and Matsuoka's (2006) classification. In addition, paraglacially driven rockfall, e.g., large, angular rockfall debris several metres in diameter and perched boulders, characterise the rock glacier surface (**Figure 9.5e**). The frontal slope of the rock glaciers is dominated by sandy boulder-gravel, with minor cobbles and pebbles. Sampled clasts have moderate c:a ($\tilde{x}$ = 0.44) and moderate-high b:a ($\tilde{x}$ = 0.71) axial ratios and thus aggregate clast form is a variable mixture of blocky, platy and elongate forms. Moderate C_{40} indices of 37% indicate that platy/elongate clasts form a larger proportion of the total sample compared to the supraglacial, lateral moraine and terminal moraine facies. Rock glacier facies are dominated by very angular (33%) and angular (54%) debris and RA indices are consistently high (87% [70–100%]). Importantly, RA indices of Lingten rock glacier samples (94–100%) are considerably higher than those of Pokalde rock glacier (70–80%). This may indicate that Pokalde rock glacier likely formed via a Type I glacier-rock glacier dynamic relationship, whereas Lingten rock glacier represents a Type II or III glacier-rock glacier dynamic relationship. Therefore, while rock glacier facies data indicates predominantly passively transported sediment, that of Pokalde rock glacier is partially reworked subaerial debris (i.e. has undergone a degree of active transport) (Knight et al., 2019).

Transitional feature facies are classified as predominantly sandy boulder-gravel, with minor cobbles and pebbles. Transitional feature facies within the furrows, in particular, are

predominantly matrix-free boulder-gravel, with minor cobbles and pebbles and lacking significant sand. Similar to scree and rock glacier facies, transitional feature facies have low-moderate c:a ($\tilde{x}$ = 0.40) and moderate-high b:a ($\tilde{x}$ = 0.71) axial ratios, indicating that the aggregate clast form is predominantly platy (Ballantyne, 1982). Clast roundness distribution reflects the predominance of very angular (69%) and angular clasts (24%), with lower occurrence of subangular (8%) clasts. The co-variant plot show RA/C_{40} indices typically of 93/54 (%). Mean clast size (b-axis) of 30 boulders lying along an upslope transect was ~1.9 m, with several large, angular boulders >5 m (**Figure 9.5f**). This is indicative of the movement to the snout of rockfall-derived debris (Knight et al., 2019). Together, the above-described characteristics of transitional feature facies infer the dominance of passive transport processes.

The co-variant plot indicates that the sampled sedimentary facies form two groups with no overlapping geometrical properties (**Figure 9.4**): (i) glacier-derived sediment (i.e. predominantly active transport processes), including supraglacial, lateral moraine, and terminal moraine facies; and (ii) slope-derived sediment (i.e. predominantly passive transport processes), consisting of scree, rock glacier and transitional feature facies. A Kolmogorov–Smirnov two-sample test was applied to the data and showed that glacier-derived and slope-derived sediment were significantly statistically different with regard to clast roundness (D_{max} = 0.62, two-tail $p < 0.001$; n = 1,650).

Figure 9.5. Typical facies associated with the morphological units studied here: (a) sandy boulder-gravel on lower Khumbu Glacier; (b) general view of the right-lateral moraine showing sandy boulder-gravel, with large boulders atop the crest; (c) boulder-gravel, including large, angular boulders; note the GCP target for scale; (d) boulder-gravel, with minor proportions of cobbles and pebbles, characterising the scree slopes below Pokalde rock glacier. Large, angular debris in the foreground and smaller debris in the background suggesting a degree of fall sorting; (e) paraglacially driven rockfall (i.e. very large, angular debris) upon Lingten rock glacier; note the sandy boulder-gravel with minor cobbles and pebbles forming the frontal slope of the rock glacier in the background; and (f) matrix-free boulder-gravel at the surface of Chola Glacier. Large, angular boulders resulting from rockfall are evident at the surface (photos: D.B. Jones).

9.5.2 ANALYSIS OF KAP-DERIVED SFM-MVS PRODUCTS

On Chola Glacier which is a transitional feature, we used KAP to produce an SfM-MVS workflow, and this yielded a point cloud, DSM (**Figure 9.6a**) and orthomosaic (**Figure 9.6c**) covering ~0.04 km². The mean flying altitude was 33.2 m. The photogrammetric workflow produced a

point cloud with 27.6 points cm^{-2}, a DSM with a ground resolution of 19.00 mm $pixel^{-1}$ and an orthomosaic with a ground resolution of 9.52 mm $pixel^{-1}$. The reprojection error (calculated by the software) was ~0.6 pixels. Note that three of the original GCPs were omitted from the processing workflow for use as independent check points. Root mean square error (RMSE) calculated across x, y and z dimensions was ~5.8 m. The relatively large RMSE is to be expected when spatially variable overlap (typical of KAP surveys), and standard accuracy GPS (from a handheld system) is present. Please see the supplementary information for the full processing report of this model construction (**section 12.4.2**). Quantitative analysis of the DSM was not undertaken. Instead, the focus was on visual interpretation of the model surface, which exhibits the presence of a spatially coherent ridge-and-furrow surface morphology in the lower reaches of Chola Glacier (**Figure 9.6b**). Numerous large, angular boulders >5 m (b-axis) are present across the surface; further evidence of the movement to the snout of rockfall-derived debris (**Figure 9.6d**). Alongside the sedimentological analyses, this suggests that Chola Glacier potentially represents a contemporary transitional form.

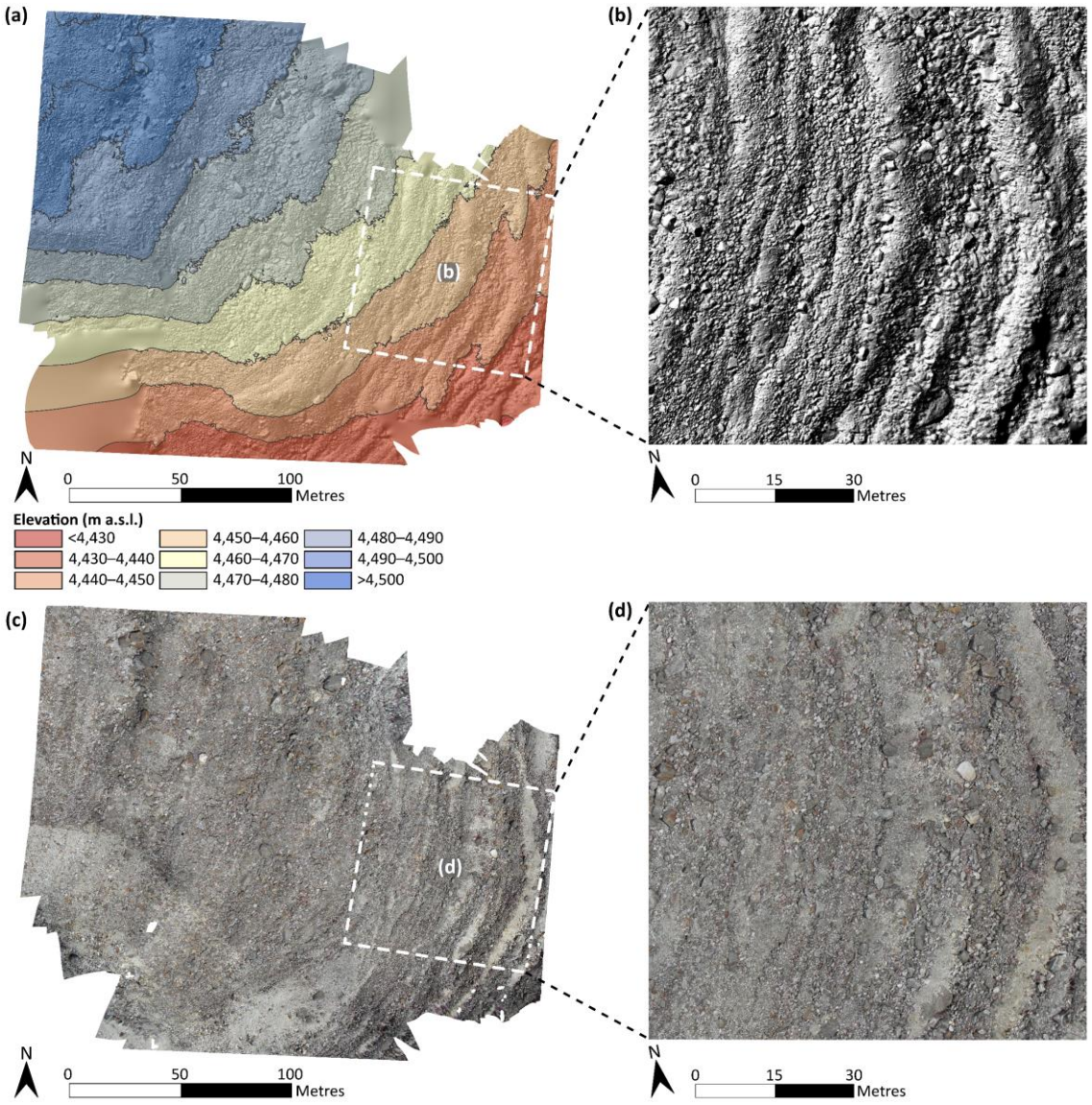

Figure 9.6. Products of the SfM-MVS workflow: (a) overview of the topography of Chola Glacier, as represented by a hillshaded DSM. Contours at 10 m intervals are also depicted; (b) finer spatial scale overview showing the ridge-and-furrow surface morphology, characteristic of rock glaciers, in the lower parts of the feature. Large boulders several metres in diameter (b-axis) are also visible; (c) overview of the sedimentological facies of Chola Glacier, visible in the orthomosaic. Debris banding reflects the aforementioned ridge-and-furrow surface morphology, with sandy boulder-gravel and boulder-gravel present on the distal and proximal slopes, respectively; and (d) finer spatial scale view of the transitional feature facies upon Chola Glacier. Large, angular boulders that reflect paraglacially driven rockfall evidence are common across the surface.

9.5.3 SYNTHESIS OF SITE-WIDE VARIATIONS

In spite of the long-standing debate regarding rock glacier origin and evolution (see section 4.3.2), the literature nevertheless consistently describes the requirement of continuous [thick] debris input for rock glacier formation and further development (e.g., Humlum et al., 2007; Kellerer-Pirklbauer and Rieckh, 2016). Frauenfelder et al. (2003) established correlations between rock glacier size and headwall extent in the Eastern Swiss Alps, findings

replicated for rock glaciers within the Front Range of Colorado (Janke and Frauenfelder, 2008). In addition to headwall extent, more recently Kenner and Magnusson (2017) found the *intensity* of headwall erosion strongly influenced rock glacier distribution and size, by partly controlling "(a) the formation time of an insulating debris layer superimposed on avalanche snow in the accumulation area, and (b) the accumulation mass that determines rock glacier length and long-term creep velocity". Indeed, they suggest that the combined effect of large headwall extents and high headwall erosion rates could have forced the presence of rock glacier fronts in elevation ranges otherwise unsuitable for long-term rock glacier existence (ibid.). While continuous debris supply is important, rock glacier formation has been associated with episodic high magnitude, low frequency rockfalls (i.e. catastrophic rockfalls following the failure of rock faces) (Johnson, 1984; Harrison et al., 2008; Monnier et al., 2008; Degenhardt Jr, 2009). Regarding glacier-rock glacier interactions, investigating large ice-debris complexes in Ak-Shiirak, Central Tien Shan, Bolch et al. (2019a) speculate that, in addition to continuous debris supply, a few large rockfall events, e.g., triggered by earthquakes, has buried and preserved former glacier ice. As previously described (see section 4.4), thick supraglacial debris cover (decimetres to metres) suppresses ablation of the underlying ice, particularly where the depth of the AL is exceeded, with significant influences upon glacier dynamics. Inefficient sediment evacuation processes encourage glacier-rock glacier interactions at short (a few decades) timescales (Shroder et al., 2000). The above-described examples underline the dependency of rock glaciers [and ice-debris complexes] on ongoing debris supply. Therefore, we argue that significant debris input forms the most efficient way for glacier-rock glacier transition to occur.

Here, the data suggest strongly that the surficial sediments in the lower reaches of Khumbu Glacier are linked to glacier-derived sediment and therefore we argue that the glacier is not transitioning. In contrast, the sediments associated with the lower reaches of Chola Glacier are slope-derived, and the glacier represents an ongoing glacier-to-rock glacier transition. Given the importance of debris-supply from bordering valley sides (Benn and Owen, 2002), this suggests a strong link between the delivery of sediment from the surrounding unstable mountain slopes to the glacier surface and the likelihood of glacier-to-rock glacier transition occurring. Indeed, Chola Glacier and the sampled rock glaciers are well connected to their debris source as they are in close proximity to rock-slopes where paraglacial processes occur with a high frequency (i.e. steep and tall rockwalls [amphitheatre-like]). Pokalde rock glacier, which represents a Type I glacier-to-rock glacier transition is less well-connected, and thus is

dynamically inactive (see Barsch, 1996, p. 8-10) and is transitioning towards relict activity status. It is clear from the data presented here and within other studies (see above) that sufficient sediment supply is critical to rock glacier development and persistence. Therefore, it is reasonable to assume that low sediment connectivity (i.e. linkage between sediment sources and downslope landforms) will reduce the likelihood with which glacier-to-rock glacier transition occurs.

As a result, we hypothesise that sediment delivery to the glacier surface is an important (and perhaps the primary) driver of glacier-to-rock glacier transition. The sedimentological facies of Khumbu Glacier vs Chola Glacier (and the rock glaciers) have undergone significantly different transport processes. The predominance of glacier-derived sediment (i.e. actively transported sediment) that characterises Khumbu Glacier indicates that the lower reaches of the glacier are not influenced by paraglacial processes. We have argued that significant rockfall input is the most efficient way for glacier-to-rock glacier transition to occur, and thus hypothesise that the large, well-developed lateral moraines of Khumbu Glacier, the trough-to-crest height of which is 75 m (left) and 60 m (right) in the vicinity of Lobuche (Hambrey et al., 2008) (**Figure 9.1a**), blocks the sediment from rockfalls reaching the glacier surface (**Figure 9.7a**). Furthermore, the Khumbu Valley widens with distance downslope, and the surrounding slopes are also elevationally lower. There is plentiful evidence of paraglacially driven rockfall at the base of slopes in the lateral morainic troughs alongside Khumbu Glacier; however, much of this debris becomes trapped here (**Figure 9.7b** and **c**). That is not to say that glaciers with large, well-developed lateral moraines will not undergo glacier-to-rock glacier transition, but they may require catastrophic events (e.g., sturzstrom) to facilitate this. Therefore, the ice-debris ratio (debris concentration) of Khumbu Glacier is such that while the terminus shows features (e.g., ridge-and-furrow surface morphology) characteristic of rock glaciers (Iwata, 1976) (**Figure 9.1a**), the lack of sufficient sediment delivery indicates that Khumbu Glacier is following a trajectory towards large supraglacial lake formation dammed by an ice-cored terminal moraine, in agreement with previous research (e.g., Hambrey et al., 2008; Watson et al., 2016). Furthermore, Monnier and Kinnard (2017) note that rock glaciers can develop upward at the expense of debris-covered glaciers, and this cannot occur on Khumbu Glacier if a large supraglacial lake forms.

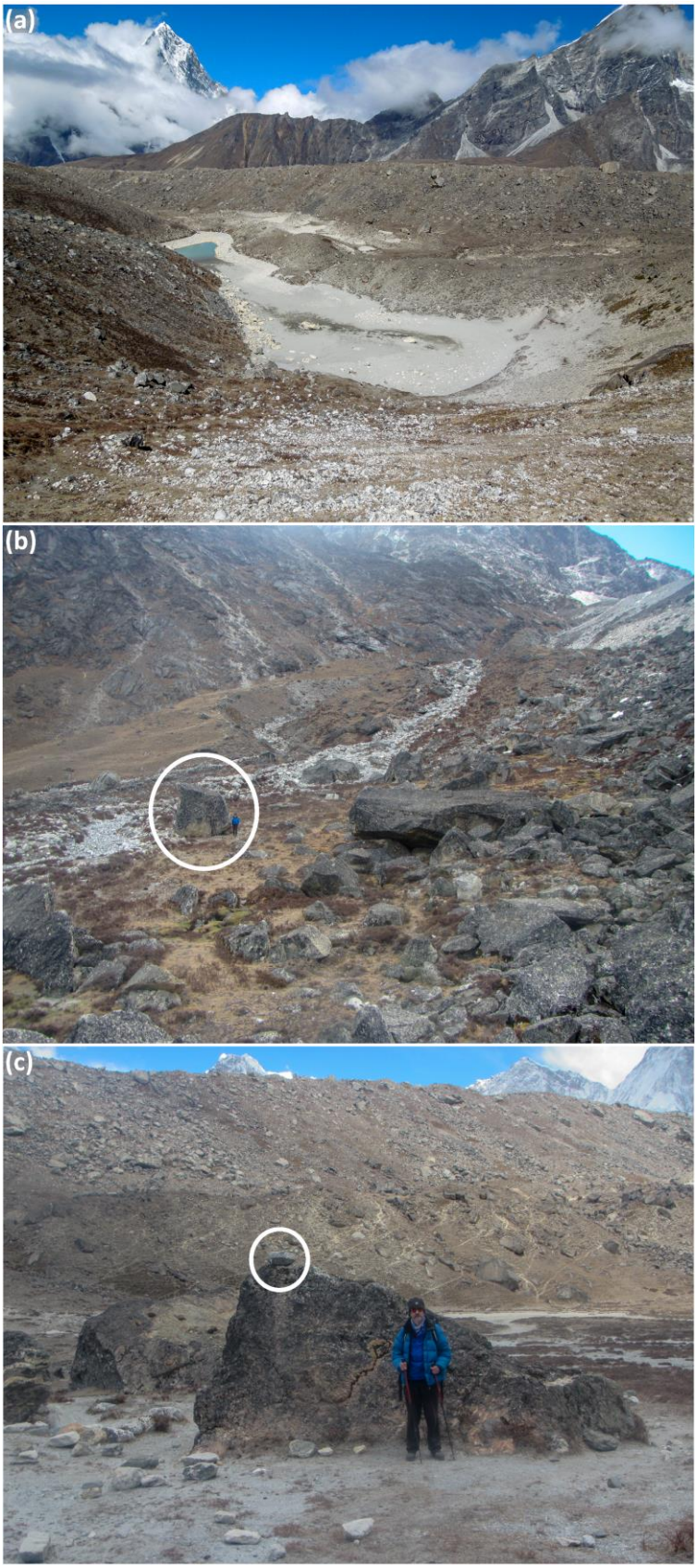

Figure 9.7. (a) the lateral morainic trough and LIA left-lateral moraine of Khumbu Glacier; (b) rockfall-derived large, angular boulders that are trapped in the lateral morainic trough; note the encircled person for scale; and (c) view of the LIA left-lateral moraine from within the lateral morainic trough. Further evidence of debris trapped within the lateral morainic trough is depicted; note the encircled perched boulders (photos: D.B. Jones).

9.6 CONCLUSION

Here we have used location-for-time substitution to investigate clast data from a range of landforms that span the glacier-rock glacier continuum in a high mountain setting to assess the ways in which glacier-to-rock glacier transition occurs. We can show clear sedimentological differences in these landforms and suggest that access to debris supply is one of the drivers of the transition process. As a result, the topographic connectivity between glacier surfaces and surrounding unstable mountain slopes is assumed to be a crucial component of this. We hypothesise that the presence of well-developed large lateral moraines along glacier margins serves to reduce this connectivity and therefore reduce the opportunity for glacier-to-rock glacier transition. Understanding these processes is of great importance if we are to better predict the geomorphological evolution of glaciated mountains under conditions of future climate change and the water supply implications that follow.

9.7 ACKNOWLEDGEMENTS

DBJ was funded by the Natural Environment Research Council (Grant No. NE/L002434/1) and the Royal Geographical Society (with IBG) through a Dudley Stamp Memorial Award. The authors wish to thank Dhananjay Regmi and Himalayan Research Expeditions Ltd. for providing organizational support with regards to the fieldwork campaign, and Mahesh Magar, Laxmi Kumar Kulung and Shankar Natshiring are thanked for their invaluable support during data collection. We thank James P. Duffy (University of Exeter) for providing the 3D printed KAP picavet mount, and for his guidance with data processing in Agisoft PhotoScan. The Pleiades image (**Figure 9.1**) was provided by the European Space Agency. Lastly, we acknowledge the detailed and constructive comments of the anonymous reviewers and the editor, which significantly improved the paper.

10 DISCUSSION

This PhD thesis presents an analysis regarding the role of rock glaciers in mountain hydrology and their future evolution. It uses a combination of remote and proximal sensing data and *in situ* data to investigate rock glaciers across a range of spatial scales. Accordingly, this thesis produces (i) the first comprehensive evaluation of the hydrological role of rock glaciers in mountains [Chapter 4]; (ii) the first [near] global-scale RGDB and approximation of their WVEQ vs glaciers [Chapter 5]; (iii) the first comprehensive rock glacier inventories for the Nepalese Himalaya and Himalaya [Chapter 6 and 7]; (iv) the first estimate of rock glacier vs glacier WVEQ in the Nepalese Himalaya and Himalaya [Chapter 6 and 7]; (v) an evaluation of the interactions between rock glaciers and glacial, periglacial and paraglacial environmental process domains, and the role of rock glaciers in mountain landscape evolution [Chapter 8]; and (vi) a new conceptual hypothesis for glacier-to-rock glacier transition in deglacierizing mountains [Chapter 9]. The rock glacier datasets (related to [ii], [iii] and [iv]) have been shared as open-source geodatabases to benefit the wider rock glacier research community[7]. Each of these chapters contains its own detailed discussion.

The overarching research aim of this thesis (as stated in Chapter 2) was **to review and extend scientific knowledge of the role of rock glaciers in mountain hydrology through advancing understanding of their frequency, spatial distribution, hydrological importance and evolutionary pathways.** This aim was primarily addressed through three key themes to which the chapters were aligned:

Theme 1. The hydrological role and importance of rock glaciers globally.

For high mountain systems at the global-scale, characterise

i. The hydrological role played by rock glaciers, and
ii. The water equivalent volume (WVEQ) stored in rock glaciers

Theme 2. Rock glacier distribution and hydrological significance in the Nepalese and Himalaya.

Address the paucity of data regarding the distribution and hydrological significance of rock glaciers at

[7] N.B. Chapter 7 is currently being prepared for publication; therefore, the systematic rock glacier inventory for the Himalaya will be made available after publication.

i. A national spatial scale – The Nepalese Himalaya, and

ii. A regional spatial scale – The Himalaya

Theme 3. Advancing rock glacier evolutionary theory.

Advance the understanding of rock glacier evolution, particularly in deglacierizing mountains by

i. Considering firstly the evolution of rock glaciers over time and space, and secondly their relationships with other mountain landforms, and

ii. Developing a conceptual hypothesis for glacier-to-rock glacier transition

In this chapter, I draw together new insights presented in this thesis, with respect to Themes 1–3 outlined above, and consider their implications for the broader understanding of the role of rock glaciers in mountain hydrology and landscape evolution (**sections 10.1–10.3**). Lastly, I signpost towards future research threads important for the progression of rock glacier-related research (**section 10.4**).

10.1 THE HYDROLOGICAL ROLE AND IMPORTANCE OF ROCK GLACIERS GLOBALLY

(i) For high mountain systems at the global-scale, characterise the hydrological role played by rock glaciers.

In Chapter 4, the state of current scientific knowledge regarding the hydrological role of rock glaciers in high mountain systems globally was critically assessed. The continued decline of the high-mountain cryosphere is anticipated to have severe implications for freshwater resources and their effective management (see Beniston, 2003; Bolch et al., 2012; Huss et al., 2017; Miller et al., 2017). Therefore, this chapter calls for a comprehensive understanding of all components of the mountain hydrological cycle, particularly rock glaciers. Yet, to date, with few notable exceptions (e.g., this thesis; Schaffer et al., 2019), the hydrological role of rock glaciers in mountains has been afforded relatively little consideration compared to debris-free and debris-covered glaciers. For instance, in their recent book chapter, "Status and Change of the Cryosphere in the Extended Hindu Kush Himalayan Region", Bolch et al. (2019b) synthesised and evaluated the state of current scientific knowledge regarding changes in the high-mountain cryosphere; however, rock glaciers are only mentioned briefly. Moreover, although rock glacier dynamics have received much attention, most prominently by the International Panel on Climate Change (IPCC) in the context of impacts of climate change upon high mountain permafrost (Vaughan et al., 2013), their potential hydrological importance has been

neglected by policymakers. It is reasonable to assume that this neglect may stem from a lack of awareness; consequently, this chapter provides a comprehensive understanding of the state-of-knowledge regarding the hydrological role of rock glaciers.

This chapter describes a general lack of consensus in the literature concerning the perceived hydrological significance of rock glaciers and highlights the pressing need for more research in this relatively young research field. Importantly, the "hydrological significance" of rock glaciers has been almost exclusively defined according to their ice volume/WVEQ and/or relative contribution to catchment runoff. In this chapter, the "hydrological significance" of rock glaciers is redefined as to also include for the first time (i) rock glacier-catchment interactions (i.e. total discharge volume, variability and timing), and (ii) rock glacier effects upon the physical characteristics of water (i.e. hydrochemistry, temperature). In addition, rock glacier hydrological significance has largely been considered according to a restricted timescale inasmuch as investigations generally focus on present opposed to potential future hydrological contributions. In this chapter, it is proposed that rock glacier water storage [and release] occurs over a range of timescales (see **Figure 4.3**); furthermore, it is recommended that future assessments of the hydrological significance of rock glaciers do so in this context. Lastly, this chapter notes a relative paucity of quantitative remote sensing (e.g., rock glacier number, spatial distribution, morphometric characteristics) and *in situ* data (e.g., discharge, internal structure [ice content by vol.]) that continues to restrict the assessment of their hydrological value. This chapter serves to frame the proceeding empirical chapters.

(ii) For high mountain systems at the global-scale, characterise the water volume equivalent (WVEQ) stored in rock glaciers.

While a small number of national-scale glacier inventories include rock glaciers, including the Inventario Nacional de Glaciares of Argentina (Zalazar et al., 2017; IANIGLA-CONICET, 2018), they are omitted from global-scale glacier databases (e.g., the GLIMS and RGI databases). Furthermore, although described as the most "pressing need" in rock glacier science, prior to this thesis no global-scale rock glacier inventory existed (Janke et al., 2013); thus, a full assessment of their global distribution and hydrological significance was prevented. This thesis argues that in the absence of this information, rock glaciers could be considered to be hydrologically insignificant by the rock glacier research community and policymakers. Therefore, Chapter 5 forms the first near-global scale RGDB.

The RGDB presented in this chapter includes in excess of 73,000 rock glaciers (intact = ~39,500 and relict = ~33,500). These are estimated to contain a total WVEQ of 83.7 ± 16.7 Gt [approximately 69–102 trillion litres of water]. Furthermore, the global-scale ratio of rock glacier: glacier WVEQ was estimated to be 1:456, ranging between 1:26 (North Asia) and 1:18,395 (Svalbard and Jan Mayen). The rock glacier: glacier WVEQ ratios presented in this chapter show that rock glaciers in certain regions constitute potentially important long-term water stores; however, these large-scale ratios are not representative at national- or regional-scale (e.g., 3:1 in the semi-arid Chilean Andes [29°–32°]) (Azócar and Brenning, 2010) and 1:3 in the Nepalese Himalaya (this thesis). The RGDB also served to identify underrepresented RGI regions (see Table 5.2). Indeed, only ~9% of the studies included in the RGDB cover HMA; therefore, HMA forms the focus for Theme 2 (see **section 10.2**). Although this chapter represents a first-order approximation of near-global rock glacier WVEQ due to considerable uncertainties (see **section 5.4.4**), this contribution is important for raising awareness of the potential hydrological significance of rock glaciers. The inclusion of this chapter [Jones et al., 2018a] in the latest IPCC report, entitled "IPCC Special Report on the Ocean and Cryosphere in a Changing Climate" (Hock et al., 2019b), reflects this.

10.2 ROCK GLACIER DISTRIBUTION AND HYDROLOGICAL SIGNIFICANCE IN THE NEPALESE AND HIMALAYA

Considerable recent research efforts have greatly elaborated systematic rock glacier inventory coverage (Chapter 1). Statistical analysis of these datasets, including the number, spatial distribution, morphometric characteristics and WVEQ, forms the first step in understanding their hydrological role in high mountain systems. This thesis recognises the role of spatial scale as being of great importance when considering rock glacier hydrological significance (see **section 10.1**), particularly in consideration of climate change adaptation strategies. Here, therefore, rock glaciers are investigated at global, regional, national and subnational spatial scales; much of the thesis novelty stems from this top-down approach. The RGDB (Chapter 5) shows that HMA – a region where severe water stress will likely result from future climate warming – is particularly data-scarce. Hence, Chapter 6 and 7 focus on the distribution and hydrological significance of rock glaciers in the Nepalese and Himalaya.

(i) Address the paucity of data regarding the distribution and hydrological significance of rock glaciers at a national spatial scale – The Nepalese Himalaya.

Chapter 6 describes the first systematic rock glacier inventory for the Nepalese Himalaya. This database includes in excess of 6,000 rock glaciers that cover an estimated area of 1,371 km². Of these, 4,226 landforms were classified as intact (i.e. containing ice) and are estimated to contain a WVEQ of 20.90 ± 4.18 km³ (19.16 ± 3.83 Gt). For the Nepalese Himalaya estimated I-DL: glacier WVEQ ratio is 1:9. This chapter argues that national-scale ratios mask the potential hydrological significance of rock glaciers at subnational-scales. Indeed, here, subnational ratios show that this ratio varies from 1:3 to 1:89 (**Table 6.8**). Importantly, intact landforms found in the Central-west and West regions (see **Figure 6.3**) contained the highest WVEQs, 25.1% and 52.9% of total estimated WVEQ, respectively. Monsoonal precipitation (JJAS) dominates annual precipitation (Shrestha et al., 2000; Karki et al., 2016) with contributions decreasing from east to west and south to north (Kansakar et al., 2004). Combined with substantial projected glacier recession and mass loss throughout the twenty-first century (e.g., Kraaijenbrink et al., 2017; Hock et al., 2019; Shannon et al., 2019) and limited investment in water resources infrastructure in mountainous regions (Bartlett et al., 2010, p. 18), this chapter hypothesises that the hydrological value of rock glaciers in the west-Nepalese Himalaya may be of increasingly greater importance than the ratio of I-DL: glacier WVEQ initially suggests.

(ii) Address the paucity of data regarding the distribution and hydrological significance of rock glaciers at a regional spatial scale – The Himalaya.

In Chapter 7, the first systematic rock glacier inventory for the Himalaya is presented. This database contains ~25,000 rock glaciers that have an estimated areal coverage of 3,747 km². Across the Himalaya, rock glaciers are estimated to contain a WVEQ of 51.80 ± 10.36 km³ (47.48 ± 9.50 Gt). This equates to a I-DL: glacier WVEQ ratio of 1:24, ranging from 1:42 to 1:17 in the East and Central Himalaya, respectively (**Figure 7.3**). Ice content [% by vol.] within rock glaciers is spatially heterogeneous (see **section 4.5.2.1**). In general, previous studies (including Chapter 5, 6 and 7) have adopted a volumetric ice content of 40–60% in order to account for uncertainty related to, for instance, dynamic status or landform origin (see **section 5.4.4**); however, this chapter is the first to evaluate the influence of glacier volume methodology choice on I-DL: glacier WVEQ ratios. Here, I-DL: glacier WVEQ ratios were shown to vary between 1:23 and 1:36 depending on the chosen method of glacier volume calculation (**Table 7.3**). Thus, this chapter recommends that uncertainties related to glacier volume calculation are more carefully considered in future studies. Importantly, this database forms the largest

systematic rock glacier inventory – in terms of rock glacier number, areal coverage and WVEQ – conducted to date.

The uncertainty associated with the systematic rock glacier inventories presented in Chapter 6 and 7 is thoroughly discussed within the respective chapters. Importantly, however, issues of polygenesis and mimicry/equifinality are absent from these discussions. Here, rock glaciers were identified, and their dynamic status determined using spaceborne remote sensing image data. Although several rock glaciers were ground-truthed in the Khumbu Valley (SNP), these form a very small proportion (0.02%) of the whole population. In previous studies, these issues have contributed to misidentifications of RSFs as rock glaciers (e.g., Jarman et al., 2013). This begs the question, therefore, *how do we know the landforms inventoried here are rock glaciers?* In HMA, the formidable logistical/financial challenges associated with rock glacier-related fieldwork prohibit large-scale ground-truthing. Furthermore, while kinematic data (e.g., SAR-derived movement rates) would facilitate validation of active rock glaciers, this method is unsuitable for intact and relict landforms. In practical terms, definitively answering this question is impossible; thus, issues of polygenesis and mimicry/equifinality form an unquantifiable uncertainty within these chapters.

10.3 ADVANCING ROCK GLACIER EVOLUTIONARY THEORY

(i) Advance the understanding of rock glacier evolution, particularly in deglacierizing mountains by considering firstly the evolution of rock glaciers over time and space, and secondly their relationships with other mountain landforms.

Chapter 8 shows that rock glaciers can develop under glacial, periglacial and paraglacial process domains. Here, therefore, rock glaciers are shown to be equifinal landforms inasmuch as they can develop from the abovementioned processes individually or in combination. Indeed, this chapter proposes a genetic classification model to describe the corelationships between glacial, periglacial and paraglacial process domains (**Figure 8.1**). Through this model, the evolutionary pathways undertaken by individual rock glaciers can be described. For instance, using geomorphic and sedimentological data derived from different rock glaciers in the Khumbu Valley (SNP), it is shown that even within a single region, rock glaciers may have varied origins. Furthermore, interactions between rock glaciers and the abovementioned process domains vary as deglacierizing mountain landscapes [including climatic and environmental controls] change over time, leading to different evolutionary pathways for different rock glaciers during

their lifecycle (**Figure 8.7**). This [equifinality] is important to consider when attempting to decipher the origin of rock glaciers, particularly relict forms (Jarman et al., 2013).

Importantly, here it is proposed that throughout the twenty-first century, continued climate-driven deglaciation and the associated shift from glacial- to paraglacial-dominated process regimes means glacier-to-rock glacier transition will likely become increasingly common. This will have significant implications for water and sediment storage in high mountain systems, particularly as rock glaciers in deglacierizing mountains may have a long residence time in the landscape. Indeed, this chapter suggests that rock glaciers can, therefore, be viewed as an important extended paraglacial transient stage in mountain geomorphic evolution, between glacial and nonglacial endmembers (Cossart et al., 2017; Knight and Harrison, 2018). Notably, the key role of rock glaciers was not fully considered in previous models of paraglacial landscape change (e.g., Ballantyne, 2002a, 2002b).

(ii) Advance the understanding of rock glacier evolution, particularly in deglacierizing mountains by developing a conceptual hypothesis for glacier-to-rock glacier transition.

In Chapter 9, location-for-time substitution was used to investigate clast data from a range of landforms that span the glacier-rock glacier continuum within the Khumbu Valley (SNP), and the ways in which glacier-to-rock glacier transition occurs were assessed. Here, KAP was additionally used to capture aerial images of an ongoing glacier-to-rock glacier transitional landform (Chola Glacier) to elucidate the surface geomorphic features of a fully transitioned landform. This image data, processed using a structure-from-motion multi-view stereo (SfM-MVS) photogrammetry approach, revealed the presence of a spatially coherent ridge-and-furrow surface morphology in the lower reaches of Chola Glacier, which is potentially indicative of an ongoing glacier-to-rock glacier transition. Glacier-derived and slope-derived clast roundness are significantly statistically different and suggest that sediment connectivity (i.e. linkage between sediment sources and downslope landforms) is one of the drivers of the transition process. It is, therefore, hypothesised that the presence of well-developed large lateral moraines along glacier margins serves to reduce sediment connectivity and thus reduce the opportunity for glacier-to-rock glacier transition. It is suggested that through sediment connectivity modelling (e.g., Micheletti and Lane, 2016), the conceptual hypothesis presented here could be tested in a variety of climatic and environmental settings. Indeed, the previous chapter suggests that a better context for explaining their development is to consider them along the continua of variations in sediment supply and climate that drive their morphodynamic

trajectory. Lastly, understanding which glaciers are likeliest to undergo transition to a rock glacier would improve glacio-hydrological predictions. In the context of this thesis, this would be highly beneficial for understanding the hydrological significance of rock glaciers and also enable more effective water resources management.

10.4 FUTURE WORK AND RECOMMENDATIONS

From this thesis, it is suggested that a relative paucity of quantitative *in situ* data continues to restrict the assessment of rock glacier hydrological significance, presumably owing to the formidable logistical challenges of rock glacier-related fieldwork globally (see **section 4.5.2.1**). Importantly, these data are needed from a range of locations and timescales; specifically, there is an urgent requirement for studies to deliver data that captures the full diversity of rock glacier characteristics and the environmental settings within which they are situated. This will require efforts within the research community to tackle sites that are less easily accessible (e.g., HMA) since much of the existing research has been conducted to date on the most accessible sites (e.g., within the European Alps), which may not adequately represent the whole population. As a consequence, this thesis identifies several candidate areas for future rock glacier-related research:

Rock glacier spatial distribution: Systematic rock glacier inventories are absent in many climatically vulnerable regions. In addition, relatively few studies share accessible open-source geodatabases (see Chapter 5). In order to improve the systematic rock glacier inventory coverage and accuracy, it is suggested that: (i) existing inventories are shared as open-source geodatabases; (ii) habitat suitability-type models are utilised, to encourage greater efficiency of systematic rock glacier inventory compilation in data-deficient regions; (iii) open-access platforms, such as Google Earth Pro, are used; (iv) updated satellite remote sensing is used to re-evaluate and update existing inventories (see **section 4.5.1**); and (v) further ground-truthing of developed inventories is undertaken. The recently established IPA Action Group (2018–2020), the primary objectives of which are "to sustain the first steps toward the organization and the management of a network dedicated to rock glacier mapping (inventorying) and monitoring all around the world and the definition of the necessary standards" support these suggestions (Delaloye et al., 2018).

Rock glacier ice content/WVEQ: Currently, rock glacier volumetric ice content and thus WVEQ are primarily estimated using an empirical H-S relation (**Equation 3**; Brenning, 2005a). Yet, few empirical studies have quantitative *in situ* datasets against which to test the rigour of this

relationship (see **section 4.5.2**). This thesis, therefore, calls for new experiments that (i) enable the physics (i.e. dynamics) of rock glaciers to be better understood, (ii) increase the sample size used to constrain the scaling parameter c and choose the value for β, and (iii) localise the scaling parameter c. Moreover, increased ground-truthing data is needed to deliver evidence-based science to test and review the suitability of the current empirical scaling relation. Lastly, a specific approach to estimate the ice content/WVEQ of *ongoing* glacier-rock glacier interactions, for which simple empirical power-law relationships are likely inappropriate (Bolch et al., 2019a), needs to be developed.

Rock glacier water storage and release: Quantitative *in situ* data describing the volume, variability and timing of rock glacier outflows is scarce. Available datasets are generally of short duration and are derived from a small number of predominantly intact rock glaciers. Consequently, this thesis calls for a long-term monitoring network to measure rock glacier discharge. As climate change progresses, rock glaciers will eventually transition from active to relict dynamic status; thus, quantitative *in situ* data are required that describe the effects of this upon rock glacier discharge. This requires a focus on space-for-time (or location-for-time) substitution experiments across the active-to-relict transition. Hitherto, very few attempts have been made to determine the proportional contribution to rock glacier discharge of different sources (see **section 4.6.1**); therefore, this thesis calls for methodological development to isolate rock glacier hydrological (i.e. icemelt) contributions. Lastly, geophysical methodologies, such as the 4-phase model (see **section 4.5.2**), provide opportunities to better understand the internal structure of rock glaciers and thus boost knowledge about subsurface hydrological processes (i.e. preferential subsurface flowpaths). Further, Cicoira et al. (2019) report that water, particularly at the shear horizon depth, rather than external air temperature, is the main driver of variations in rock glacier creep; therefore, subsurface data is highly important.

Rock glacier hydrochemistry: Based upon a limited number of studies, there is evidence that intact rock glaciers can adversely change the inorganic chemistry of water bodies and streams, downstream of outflows (see **section 4.7**). However, further scientific investigation of this is required, to extend research evidencing the suitability of water originating from rock glaciers for use as safe, potable water resources. Importantly, this thesis suggests that future studies should also assess outflows from relict rock glaciers, as hydrological storage capacity and residence time is greater than that of intact landforms (Colombo et al., 2018b). Lastly, this thesis

notes that to include hydrochemical sampling in the experimental design of future rock glacier studies would considerably advance this research field.

Rock glacier evolution: With few notable exceptions (e.g., Bolch et al., 2019a), *ongoing* glacier-rock glacier interactions are commonly not included in either glacier or rock glacier inventories. This thesis strongly suggests that the inclusion of these transitional landforms is important in the context of future water resource management. In Chapter 9, it is hypothesised that the presence of well-developed large lateral moraines along glacier margins serves to reduce sediment connectivity and therefore reduce the likelihood of glacier-to-rock glacier transition. This thesis suggests that the integration of sediment connectivity modelling (e.g., Micheletti and Lane, 2016) into glacier-to-rock glacier evolutionary studies could enable this hypothesis to be tested in a variety of settings. Key questions regarding glacier-to-rock glacier transition remain – *Which glaciers will undergo this transition? What are the drivers of this transition? What is the rate at which this transition occurs?*

Rock glacier climatic resilience: Research considering the effects of future climate warming on rock glaciers is in its infancy. Improved modelling of rock glacier thermal regimes (i.e. heat transport) is needed to study their response to different climate change scenarios (e.g., Pruessner et al., 2018). Long-term quantitative *in situ* temperature measurements, such as the PERMOS network (http://www.permos.ch/), are required for training and validating these models. This thesis notes that systematic rock glacier inventories provide a scientific baseline from which rock glacier response to climate change can be assessed. This thesis echoes the IPA Action Group (2018–2020)[8] and suggests that incorporation of kinematical data (using SAR-derived products, multi-temporal airborne LIDAR and multi-temporal fine spatial resolution satellite and aerial images, for example) will further enhance this assessment.

[8] For information see: https://www3.unifr.ch/geo/geomorphology/en/research/ipa-action-group-rock-glacier/

11 CONCLUSIONS

This thesis addresses the current and possible future role of rock glaciers in mountain hydrology across a range of spatial scales (global, regional, national and local), with a specific focus upon HMA. It produces a number of scientific advances. Firstly, I synthesise the available peer-reviewed literature and present the first comprehensive evaluation of the hydrological role of rock glaciers in deglacierizing mountains [Chapter 4]. Importantly, this synthesis reveals a general lack of consensus in the literature concerning the perceived hydrological significance of rock glaciers and highlights the pressing need for more research on this topic. Rock glacier-related research to date has almost exclusively defined their "hydrological significance" according to their WVEQ/ ice volume and/or relative contribution to runoff. In this thesis, I redefine the "hydrological significance" of rock glaciers to also include for the first time (i) rock glacier-catchment interactions (i.e. total discharge volume, variability and timing), and (ii) rock glacier effects on the physical characteristics of water (i.e. hydrochemistry, temperature). Additionally, I show that the hydrological significance of rock glaciers has been considered according to a restricted timescale inasmuch as investigations generally focus on present opposed to potential future hydrological contributions. Here, I propose that rock glacier water storage [and release] occurs over a range of timescales; further, I recommend that future studies assessing the hydrological significance of rock glaciers do so in this context. Lastly, the synthesis highlights a relative paucity of quantitative data (e.g., rock glacier number, distribution and morphometric characteristics) that continues to restrict the assessment of the hydrological significance of rock glaciers.

Consequently, I developed three key themes to which the empirical chapters were aligned: (1) the distribution and hydrological significance of rock glaciers at global scales [Chapter 5], (2) the distribution and hydrological significance of rock glaciers at regional and national spatial scales (Himalaya and Nepalese Himalaya) [Chapter 6 and 7], and (3) advancing rock glacier evolutionary theory [Chapter 8 and 9].

In Chapter 5, I created a meta-analysis of existing systematic rock glacier inventories and compiled the first near-global RGDB. The RGDB presented here includes >73,000 rock glaciers (intact = ~39,500, relict = ~33,500), which contain a WVEQ of 83.7 ± 16.7 Gt [~69–102 trillion litres]. Furthermore, the global-scale ratio of rock glacier: glacier WVEQ was estimated to be 1:456, with large variations at regional scales. Further interrogation of the RGDB revealed that

a paucity of information regarding the number, distribution, morphometric characteristics and WVEQ of rock glaciers in the HKH.

In Chapter 6 and 7, therefore, I produced the first systematic rock glacier inventory for the (i) Nepalese Himalaya (national-scale), and (ii) Himalaya (regional-scale). In the former (i) I inventoried >6,000 rock glaciers, and these are estimated to contain a WVEQ of 20.90 ± 4.18 km^3 (19.16 ± 3.83 Gt). For the Nepalese Himalaya estimated I-DL: glacier WVEQ ratio is 1:9. In the latter (ii) ~25,000 rock glaciers have been inventoried. The total WVEQ is 51.80 ± 10.36 km^3 (47.48 ± 9.50 Gt) with an estimated I-DL: glacier WVEQ ratio of 1:24. Importantly, this database (ii) forms the largest systematic rock glacier inventory – in terms of rock glacier number, areal coverage and WVEQ – conducted to date. The results of Chapter 5, 6 and 7 indicate that rock glaciers form considerable long-term water stores, which may become increasingly important as climatically-driven glacier recession and mass loss continues throughout the twenty-first century and beyond. The inventory data associated with Chapter 5 and 6 were shared as open-source geodatabases, in order to benefit the wider rock glacier research community.

Chapter 8 shows that rock glaciers can develop under glacial, periglacial and paraglacial process domains. Additionally, using examples from the Khumbu Valley, SNP, it is shown that interactions exist between these process domains as deglacierizing mountain landscapes change over time, leading to different evolutionary pathways for different rock glaciers during their lifecycle, even within the same region. I hypothesise that throughout the twenty-first century, moreover, continued climate-driven deglaciation and the associated shift from glacial- to paraglacial-dominated process regimes is likely to increase the frequency with which glacier-to-rock glacier transition occurs. This will have significant implications for water and sediment storage in high mountain systems, particularly as rock glaciers in deglacierizing mountains may have a long residence time in the landscape.

Lastly, in Chapter 9 location-for-time substitution was used to investigate clast data from a range of landforms that span the glacier-rock glacier continuum in a high mountain setting (Khumbu Valley, SNP) to assess the ways in which glacier-to-rock glacier transition occurs. I present clear sedimentological differences between these landforms and suggest that access to debris supply is one of the drivers of the transition process. As a result, the topographic connectivity between glacier surfaces and surrounding unstable mountain slopes is assumed to be a crucial component of this. It is hypothesised, therefore, that the presence of well-

developed large lateral moraines along glacier margins serves to reduce this connectivity and therefore reduce the opportunity for glacier-to-rock glacier transition. I argue that an improved understanding of these processes is of great importance if we are to better predict the geomorphological evolution of glaciated mountains under conditions of future climate change and the water supply implications that follow.

12 APPENDICES

12.1 CHAPTER 5: APPENDIX

12.1.1 SUPPLEMENTARY METHODS

12.1.1.1 ROCK GLACIER DATABASE (RGDB) COLLATION

Rock glacier studies published prior to October 2017 were identified by means of journal search tools (ISI Web of Science, Scopus, ProQuest Dissertations and Theses), online databases (NSIDC), and direct communication with academics involved in rock glacier research. We searched the ISI Web of Science for peer-reviewed journal papers published between 1900–2017 using topic searches for "rock glacier" OR "rockglacier" OR "rock glaciers" OR "rockglaciers". Scopus was searched for peer-reviewed journal papers with 'Document Type' restricted to 'Article', 'Conference Paper', 'Review', and 'Article in Press' and no time-period restriction, also using the search terms "rock glacier" OR "rockglacier" OR "rock glaciers" OR "rockglaciers". ProQuest Dissertations and Theses was searched for publications with full-text availability, using the search terms "rock glacier" OR "rockglacier" OR "rock glaciers" OR "rockglaciers". Note that dissertations and theses with research outcomes already published as journal papers were not included in the RGDB. Lastly, Google Scholar and NSIDC searches for "rock glacier" OR "rockglacier" OR "rock glaciers" OR "rockglaciers" were undertaken. Search results ISI Web of Science, Scopus and ProQuest Dissertations and Theses were categorised into (i) systematic inventory resources or (ii) not relevant.

Excluding duplicate studies, a total of 131 systematic rock glacier inventory studies resulted from the systematic meta-analysis. So as to avoid duplicate rock glacier data, i.e. overlapping study areas, 55 studies were excluded from the RGDB where more comprehensive and/or up-to-date inventories included the same rock glaciers. This process was undertaken through Google Earth (version 7.1.5.1557, Google Inc., California, USA) and ArcGIS (version 10.3.1, ESRI, Redlands, CA, USA). Partially overlapping study areas were partially excluded. For example, data from Cremonese et al. (2011) (European Alps) was partially excluded where the study area overlapped that of Winkler et al. (2016a) (Niedere Tauern Range, Austria).

The full RGDB structure required that the following fields be filled, where the data was available: (i) Source; (ii) Author(s) (including full citation); (iii) Study Location; (iv) Datasets Applied: (a) image dataset(s), (b) topographic dataset(s); (v) Inventory Validation: (a) Yes, (b) No, (c) NA (i.e. unknown); (vi) Number of Rock Glaciers: (a) total, (b) intact, (c) relict; (vii) Elevation (All, Intact, Relict): (a) mean(s), (b) minimum elevation at the front (MEF), (c) maximum elevation

of the landform (MaxE); (viii) Area (All, Intact, Relict): (a) total, (b) mean(s); (ix) Length (All, Intact, Relict): (a) mean(s), (b) maximum(s); (x) Width (All, Intact, Relict): (a) mean(s), (b) maximum(s); (xi) Planform-shape (tongue-shaped, lobate, spatulate, or coalescent); (xii) Dominant Aspect(s); (xiii) Water Volume Equivalent (WVEQ); (xiv) Specific Density; (xv) Ratio of Rock Glacier WVEQ to Glacier WVEQ; (xvi) Additional Information. Note that where inventory data is missing but calculable (e.g., dataset[s] provided as supplementary information files, requires unit conversion etc.), we reflect updated values in blue font within the full RGDB.

Supplementary Figure 12.2 and **Supplementary Table 12.2** illustrate the 19 first-order regions that form the spatial structure of the RGIv4.0 (Consortium, 2014). Further information is available from the GLIMS website (for access: http://www.glims.org/RGI/). In compiling the RGDB, a decision to merge consensus areas was taken for two key regions because the systematic rock glacier inventory studies could not be split easily to account for regional differences. Here, we combined the RGIv4.0 regions: (i) '01' (Alaska) and '02' (Western Canada and US) to create a new dataset for "North America"; and (ii) '16' (Low Latitudes) and '17' (Southern Andes) to create a new dataset for "South America", where there are high concentrations of both rock glaciers and glaciers. Regarding (ii), sites in Central America, Africa, and Southeast Asia, which contained relatively insignificant proportions of rock glaciers or glaciers, were grouped within the "South America" category. Systematic rock glacier inventories resulting from the meta-analysis were similarly divided into the 17 regions (**Supplementary Table 12.2**).

12.1.1.2 ESTIMATING ROCK GLACIER HYDROLOGICAL STORES

Estimations of rock glacier WVEQ were calculated based upon assumed ice volumes stored within intact rock glaciers. In order to place this work in the context of traditional glacier studies, the units of gigatons (Gt) are used. Here, H-S scaling relations, i.e. $\bar{h} = c \cdot S^{\beta}$ where mean rock glacier thickness in metres ($\bar{h}$) is calculated as a function of surface area (S) and two scaling parameters (c and β), were applied. Scaling parameters derived from the empirical rule established by Brenning (2005a) were used (**Equation 3**). Rock glacier volume was estimated through the multiplication of ($\bar{h}$) and (S). This approach has previously been applied in other studies (Azócar and Brenning, 2010; Rangecroft et al., 2015; Janke et al., 2017; Jones et al., 2018b). Importantly, it should be noted that further research is needed to improve area-thickness relationships.

Equation 3. $\bar{h} = 50 \times [km^{2(0.2)}]$

By definition, rock glaciers are ice-supersaturated accumulations of rock debris, and thus do not contain 100% ice. As such, ice content in rock glaciers is spatially heterogeneous. Additionally, establishing rock glacier genesis and the subsequent depth and distribution of ice is challenging (Seligman, 2009). Consequently, estimation of ice volume and thus WVEQ proves difficult. The genesis of rock glaciers remains contested; this controversy between the permafrost school (purely periglacial origin) vs the continuum school (glacigenic- and periglacial-origin) has previously been summarised and discussed in detail (Harrison et al., 2008; Berthling, 2011). Note that discussion of rock glacier genesis and evolution is beyond the scope of this study and is briefly highlighted here for completeness. Relatively few geophysical investigations of rock glacier internal structure have previously been conducted. Those studies that exist often focus on quantifying ice presence as opposed to ice content by volume. Therefore, here we assume estimated ice volume is 40–60% by volume (Barsch, 1996; Haeberli and Beniston, 1998; Haeberli et al., 1998; Hausmann et al., 2012), enabling lower (40%), average (50%), and upper (60%) estimates to be calculated. Finally, WVEQ was calculated assuming an ice density conversion factor of 900 kg m^{-3}.

Where complete rock glacier inventories were available, rock glacier surface area data were extracted for each individual feature for use in the abovementioned H-S relationship and subsequently WVEQ calculation. A three-step approach to determine rock glacier volume was applied where inventory data was incomplete or unknown (**Supplementary Figure 12.1**).

12.1.1.3 ESTIMATING GLACIER HYDROLOGICAL STORES

Regarding glaciers, volume-area (V-S) scaling relations, i.e. $V = c \cdot S^{\gamma}$ where glacier volume (V) is calculated as a function of surface area (S) and two scaling parameters (c and γ), are frequently used approaches for volume estimations (Frey et al., 2014). Indeed, previously, V-S approaches have been used in rock glacier-glacier comparative studies (Azócar and Brenning, 2010; Janke et al., 2017). Furthermore, V-S approaches have been applied to global-scale volume estimations of glaciers and ice caps (Grinsted, 2013). Reports indicate, however, the potential of V-S approaches to systematically overestimate ice volume, particularly for large and/or relatively steep glaciers (e.g., those within the Himalayan-Karakoram region [Frey et al., 2014]). Estimated ice volumes derived from ice-thickness distribution models, for instance, the HF-model (Huss and Farinotti, 2012), generally yield comparatively lower results than V-S approaches (Frey et al., 2014). Additionally, HF-model ice-thickness results have previously been validated, indicating good agreement with a comprehensive set of ice-thickness

observations from almost all glacierized mountain ranges globally (Huss and Farinotti, 2012; Frey et al., 2014; Huss and Hock, 2015). Direct validation cannot be undertaken for results derived from V-S relations (Frey et al., 2014). Therefore, here we use the results of Huss and Hock (2015). For each glacier of the RGIv4.0, Huss and Hock (2015) calculated glacier volume and ice thickness distribution through the application of the HF-model. Results within Huss and Hock (2015) were presented as SLE assuming an ice density of 900 km m^{-3} and an ocean area of 3.625 x 108 km^2. As such, conversion of SLE to ice volume was necessary. When converting from cubic kilometres to gigatons, we assumed that 1 Gt of nonporous ice equated to a volume of 1.091 km^3 (Kargel et al., 2014).

12.1.2 SUPPLEMENTARY FIGURES

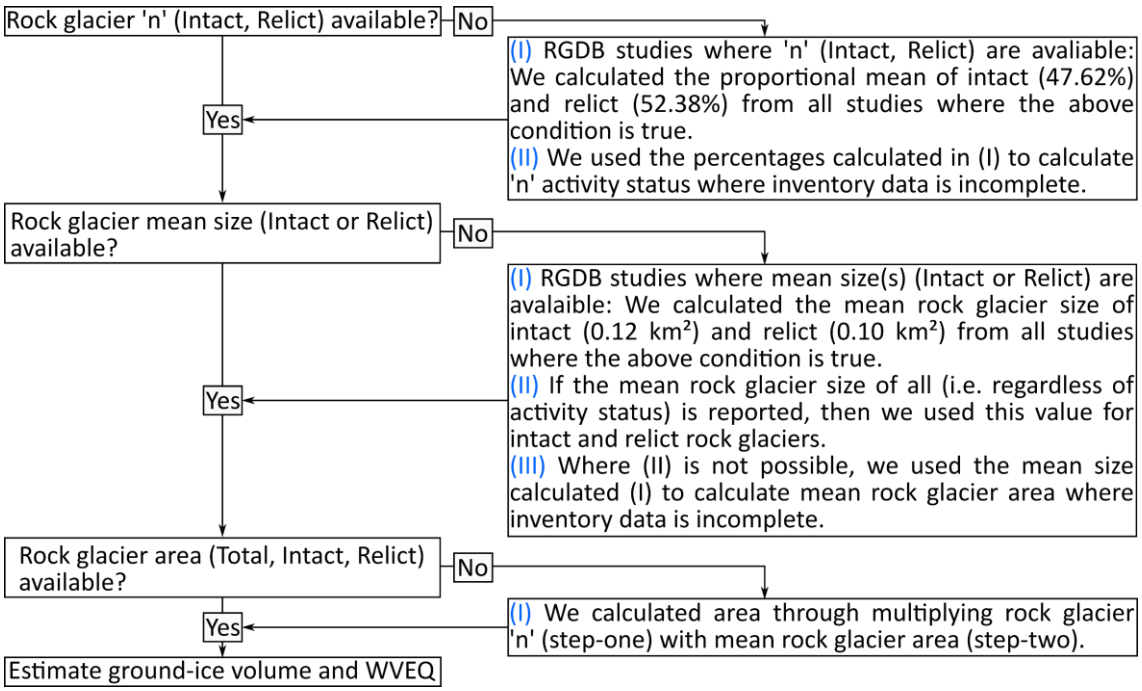

Supplementary Figure 12.1. Workflow to calculate incomplete systematic rock glacier inventory data, and subsequently ground-ice volume and WVEQ.

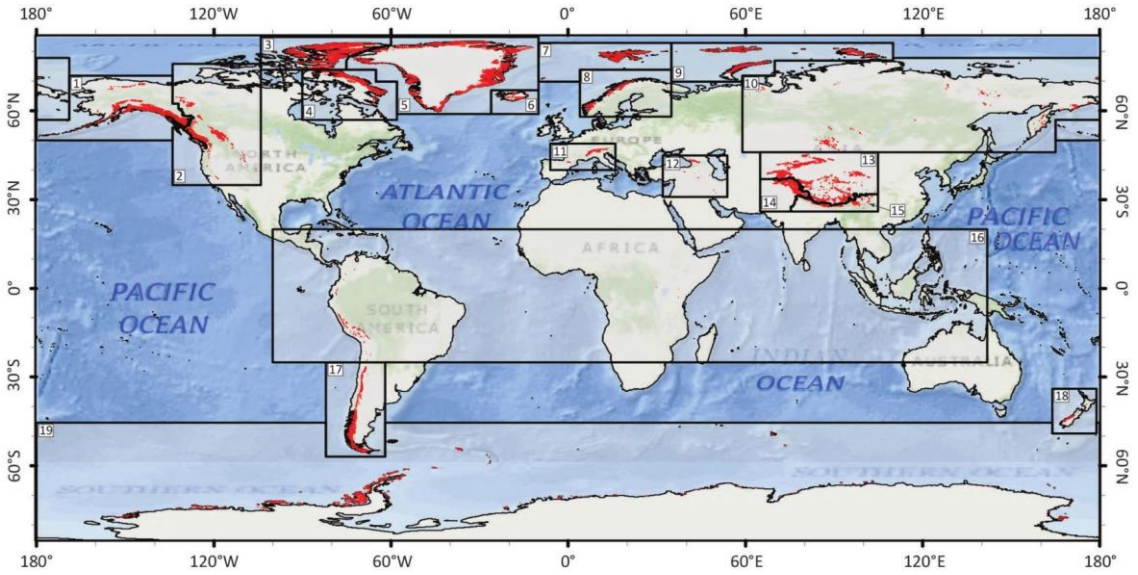

Supplementary Figure 12.2. First-order regions of the RGIv4.0, with glaciers shown in red. RGI region numbers are summarised in **Supplementary Table 12.2**. Figure reprinted from Pfeffer et al. (2014).

12.1.3 SUPPLEMENTARY TABLES

Supplementary Table 12.1. Results of RGDB searches. Note that duplicate studies in ISI Web of Science and Scopus (*n* = 579) are excluded from the latter.

Source	*n*	Category	
		(I)	(II)
ISI Web of Science	799	70	729
Scopus	1023	14	430
ProQuest Dissertations and Theses	357	4	353
Google Scholar	26	26	-
NSIDC	13	13	-
Personal Communication	4	4	-

I = Systematic inventory resource
II = Not relevant

Supplementary Table 12.2. Glacier ice volume (Gt) is converted from the SLE data of Huss and Hock (2015), assuming density of 900 kg m^{-3}, an ocean area of 3.625 * 10^8 km^2, and that 1 Gt of nonporous ice equates to 1.091 km^3 (Kargel et al., 2014). 'Years' reflects the average satellite acquisition date for each glacier outline in the region (±1 standard deviation). First-order regions of the RGIv4.0 are reflected here. This table has been adapted from Huss and Hock (2015).

RGI region		*n* (-)	Area (km^2)	SLE (mm)	Ice volume (Gt)	Years (-)
01	Alaska	26,944	86,715	45.28	16,716.57	2009 ± 2
02	Western Canada and US	15,215	14,559	2.47	911.88	2004 ± 5
	North America	42,159	101,274	47.75	17,628.45	-
03	Arctic Canada North	4538	104,873	67.02	24,742.59	1999 ± 0
04	Arctic Canada South	7347	40,894	19.70	7,272.89	2000 ± 6
05	Greenland Periphery	19,323	89,721	37.81	13,958.78	2001 ± 2
06	Iceland	568	11,060	8.13	3,001.45	2000 ± 1
07	Svalbard and Jan Mayen	1615	33,922	19.93	7,357.80	2007 ± 6
08	Scandinavia	2668	2851	0.36	132.91	2001 ± 2
09	Russian Arctic	1069	51,592	30.68	11,326.51	2002 ± 3
10	North Asia	4403	3430	0.40	147.67	1970 ± 19
11	Central Europe	3920	2063	0.28	103.37	2003 ± 5
12	Caucasus and Middle East	1386	1139	0.15	55.38	2000 ± 15
13	Central Asia	46,543	62,606	9.99	3,688.13	1970 ± 8
14	South Asia West	22,822	33,859	7.56	2,791.02	2000 ± 11
15	South Asia East	14,095	21,799	2.99	1,103.85	2000 ± 17
16	Low Latitudes	2863	2346	0.20	73.84	2002 ± 3
17	Southern Andes	16,046	29,333	13.00	4,799.37	2000 ± 0
	South America	18,909	31,679	13.20	4,873.21	-
18	New Zealand	3537	1162	0.15	55.38	1978 ± 0
19	Antarctic and Subantarctic	2752	132,867	107.90	39,834.76	1989 ± 15
GLOBAL		**197,654**	**726,792**	**374.00**	**138,074.14**	**-**

12.2 CHAPTER 6: APPENDIX

12.2.1 SUPPLEMENTARY FIGURES

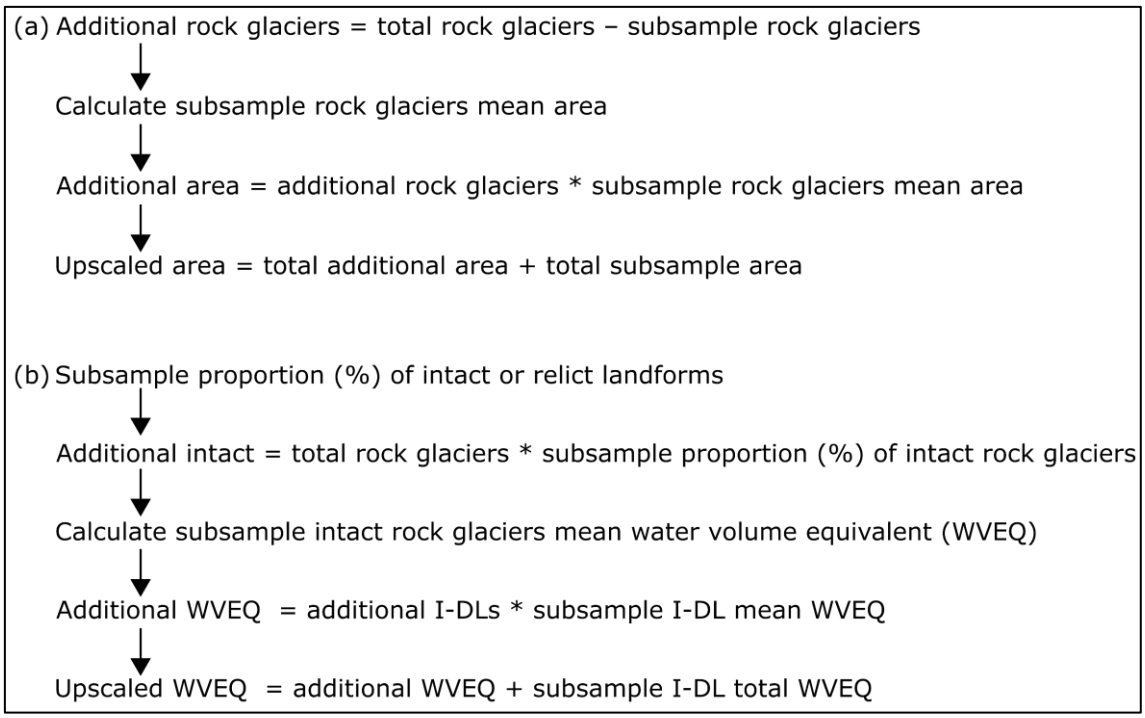

Supplementary Figure 12.3. Flow diagram detailing the process for (a) upscaling of DDA/I-DL surface area, and (b) upscaling of DDA/I-DL WVEQ. Both are derived from the digitised sample.

12.3 CHAPTER 7: APPENDIX

12.3.1 SUPPLEMENTARY METHODS

12.3.1.1 EARTH OBSERVATION DATA

In the Google Earth Pro platform (version 7.1.8.3036), we used publicly available current and archived satellite image data, including fine spatial resolution CNES/Airbus (e.g., SPOT and Pleiades) and DigitalGlobe-derived imagery (e.g., Worldview-1 and 2, and QuickBird), to compile the systematic rock glacier inventory for the Himalaya region. NASA SRTM Version 3.0 Global 1 arc second data (see https://lpdaac.usgs.gov/products/srtmgl1v003/) were used to generate a ~30 m resolution DEM of the topography of the study region (herein SRTM30 DEM).

12.3.1.2 ROCK GLACIER DATA

A gridded search methodology approach was employed to ensure inventory compilation was systematic and exhaustive. In ESRI ArcGIS (version 10.6.0.8321), a gridded overlay of 40 km² grid squares covering the study region was created. This shapefile was subsequently imported into Google Earth Pro, and each grid square was visually surveyed on an individual basis. Features of interest (DDAs and I-DLs) were identified according to geomorphic indicators (**Table 6.1**) and pinned within Google Earth Pro, and an initial point-based inventory was created for the Himalaya. In ArcGIS, the point-based inventory was split into the sub-regions (i.e. West Himalaya, Central Himalaya and East Himalaya) as defined by Bolch et al. (2012) (**Figure 1.2**). A ~5% sample of the identified landforms from each region (W-Himalaya, n = 363; C-Himalaya, n = 192; E-Himalaya, n = 378) were randomly selected within ArcGIS. Note that the Nepalese Himalaya, which constitutes a significant proportion of the C-Himalaya, has previously been inventoried by the current authors (Jones et al., 2018b); therefore, the above-described C-Himalaya sample was sourced from newly inventoried landforms only – i.e. excludes the existing Nepalese Himalaya inventory.

The geographic boundaries of the selected ~5% regional samples were digitised within Google Earth Pro, forming a polygonised inventory within which more detailed spatial attributes were measured. Multi-temporal satellite image data were used for this purpose (2000–2019), reducing mapping uncertainties associated with poor quality image data, affected by long-cast shadows on steep north-facing slopes, cloud cover and snow cover, for example (Jones et al., 2018b). For feature boundary digitisation, we adopted the approach of Scotti et al. (2013), as previously applied in Jones et al. (2018b). Here, the outline of the entire feature surface was

delineated, from the rooting zone (i.e. MaxE) to the base of the front slope (i.e. MEF) (**Figure 6.2**). Where multiple landforms coalesce into a single body, digitisation was challenging. In this study, "when the frontal lobes of two (or more) rock glaciers originating from distinct source basins join downslope, we consider the two components as separate bodies. Where the limits between lobes are unclear and the lobes share other morphological characteristics (e.g., dynamic status [i.e. degree of activity] and vegetation cover), we classify the whole system as a unique rock glacier" (Scotti et al., 2013). Further, where DDAs/I-DLs grade into upslope landforms, for instance where a rock glacier is gradually developing from a terminal or lateral moraine, "a clear distinction between the two landforms cannot be set and we delineated the whole body (i.e. moraine plus rock glacier)" (ibid.).

Both quantitative and qualitative attributes were extracted and recorded for each feature in the polygonised inventory (see **Supplementary Table 12.6**).

In ArcGIS, the present study used the Universal Transverse Mercator (UTM) WGS 84 projected coordinate system – UTM Zone 43N to 46N – in order to quantify the morphometric characteristics of all shapefiles (e.g., feature [DDA/I-DL] length, width, area [and thus WVEQ]). Digitised landforms were reprojected using the WGS 84 coordinate system for exportation to KML formatted files (see Supplementary Information). Feature lengths (parallel to the flow) were manually digitised within Google Earth Pro. Based upon an existing methodology (Frauenfelder et al., 2003), in order to account for width variation along the length of each feature widths (perpendicular to length) were digitised at ~50 m intervals and mean width calculated in ArcGIS (**Figure 6.2**). Landforms were categorised into tongue-shaped or lobate-shaped, where the length: width ratio is >1 or <1, respectfully (Guglielmin and Smiraglia, 1998).

Applying ArcGIS surface raster functions (*Zonal Statistics*) the digitised landforms were overlaid onto the SRTM30 DEM and the minimum, maximum, range and mean elevation extracted for each feature. In ArcGIS, an aspect raster surface was created using the SRTM DEM as the input and clipped to the digitised feature boundaries. As a circular parameter, feature mean aspect (i.e. the mean aspect of the raster pixels within each digitised feature) cannot be calculated using simple zonal statistics (i.e. the mean of 0° and 359° cannot be 180° [Davis, 1986 as cited in Janke, 2013]). The vector mean aspect ($\overline{\theta}$) was calculated in R (version 3.1.2, R Core Team, Vienna, Austria) using **Equation 1** and categorised into eight classes – N, NE, E, SE, S, SW, W and NW.

In Google Earth Pro the dynamic status of digitised landforms was determined considering their presumed ice content and movement, in accordance with the morphological classification by Barsch (1996), using the geomorphic indicators previously outlined (**Table 6.1**). In the present study, DDAs were categorised as *relict landforms* (no longer contain ice nor display movement) and I-DLs as *active landforms* (contain ice and display movement) and *inactive landforms* (contain ice but no longer display movement) (Haeberli, 1985; Barsch, 1996). Here, I-DLs refer to *intact landforms*, i.e. active and inactive landforms combined.

As a consequence of the paucity of detailed subsurface information for rock glaciers, 2-D-area-related statistics (i.e. *empirical thickness-area [H-S] relations*) were applied in this study to predict I-DL thickness and derive volume. Empirical H-S relations can be expressed as $\bar{h} = c \cdot S^{\beta}$, where mean feature thickness $\bar{h}$ (m) is calculated as a function of surface area *S* (km²) and a scaling parameter *c* (50) and scaling exponent *β* (0.2) (Brenning, 2005a). Feature volumes were determined by $V = \bar{h} \cdot S$. WVEQ was subsequently estimated through the multiplication of *V* and estimated ice content (% by vol.) and assuming an ice density conversion factor of 900 kg m^{-3} (Paterson, 1994). Here, a volumetric I-DL ice content of 40–60% vol. (i.e. lower [40%], mean [50%] and upper bounds [60%]) was assumed in accordance with previous studies (Brenning, 2005a; Bodin et al., 2010; Rangecroft et al., 2015; Jones et al., 2018a; Jones et al., 2018b) – consistent with *in situ* data derived from different climatic regions worldwide (e.g., Elconin and LaChapelle, 1997: >50%; Arenson et al., 2002: 40–70%; Croce and Milana, 2002: ~55%; Hausmann et al., 2007: 45–60%; Hausmann et al., 2012: 40–60%).

In the present study, the dataset generated through the application of the above-described methodology and pre-existing rock glacier inventory of the Nepalese Himalaya (Jones et al., 2018b) were amalgamated, creating the first systematic inventory of rock glaciers in the Himalaya. In order to estimate DDA/I-DL area and WVEQ in the Himalaya, the digitised sample (*n* = 2,070) was extended to the entire population (*n* = 24,968) on a regional basis through the upscaling procedure outlined in **Supplementary Figure 12.3**.

12.3.1.3 GLACIER DATA

Glacier data for the study region were derived from Frey et al. (2014). Figure 1 in Frey et al. (2014) describes the sources of the original glacier outlines. The estimated ice volumes, which the WVEQs are based upon, were calculated using the Glacier bed Topography (GlabTop2) ice-thickness distribution model (see Frey et al., 2014). Regional data are presented for the W-

Himalaya, C-Himalaya and E-Himalaya using the same geographic boundaries (i.e. Bolch et al., 2012) as in this study, enabling the direct comparison of rock glacier and glacier results.

12.3.1.4 UNCERTAINTY

In order to quantify the uncertainties associated with the identification, digitisation and classification of features of interest (see Brardinoni et al., 2019), we detailed the degree of 'uncertainty' through the application of a *Certainty Index* score, adapted from Schmid et al. (2015), for each digitised feature (**Table 6.3**). Additionally, as arguably the most conspicuous morphological manifestation of permafrost in high mountain systems (Barsch, 1996), I-DLs are often strongly associated with the lower limit of permafrost distribution. Consequently, here values were extracted from the PZI – a global index that helps to constrain and visualise areas of likely permafrost occurrence (Gruber, 2012) – for each digitised feature, and the agreement between I-DL spatial distribution and their associated PZI values was assessed. The uncertainty associated with the calculation of I-DL WVEQ using the above-described empirical H-S relation has previously been discussed at length (see Jones et al., 2019). Lastly, the influence of methodology selection upon glacier ice volume estimations (and thus WVEQs) was quantitatively assessed using I-DL to glacier WVEQ ratios related to a range of different approaches (Frey et al., 2014) (**Table 7.3**).

12.3.2 SUPPLEMENTARY TABLES

Supplementary Table 12.3. DDA/I-DL proportion, proportional area ≥3,225 m a.s.l., DDA/I-DL density and DDA/I-DL specific area for the sub-regions of the Himalaya. Where appropriate, values are reported to two decimal places.

	E – Himalaya	C – Himalaya	W – Himalaya
DDA/I-DL proportion	30%	30%	40%
Proportional area ≥ 3225 m a.s.l	26%	37%	37%
Density (n km^{-2})*	0.08	0.08	0.06
Specific area (ha km^{-2})†	0.59	1.60	0.82

*Density (n km^{-2}) was calculated by considering the regional area ≥3,225 m a.s.l. (MEF of lowest observed land-form).
†Specific area (ha km^{-2}) where 'ha' reflects DDA/I-DL area, was also calculated by considering the regional area ≥3,225 m a.s.l. The upscaled results were used within calculations of both density and specific area.

Supplementary Table 12.4. Regional aspect classification of DDAs and I-DLs into north- (292.5 to 67.5°) and south- (112.5 to 247.5°) facing aspect quadrants.

Activity	Aspect Quadrant	Region		
		E – Himalaya	C – Himalaya	W – Himalaya
Intact	North (NW, N, NE)	46%	40%	57%
	South (SW, S, SE)	24%	32%	20%
Relict	North (NW, N, NE)	62%	58%	57%
	South (SW, S, SE)	13%	19%	18%

Supplementary Table 12.5. Ice volume (km^3) and corresponding WVEQs (km^3) for both the sampled and upscaled I-DLs, regionally and across the Himalaya (total). These calculations encompass a range of ice content by volume estimates with a lower (40%), average (50%) and upper (60%) bound. Values are reported to two decimal places.

Region	Ice content by volume		Sample I-DLs		Upscaled I-DLs	
			Ice volume (km^3)	WVEQ (km^3)	Ice volume (km^3)	WVEQ (km^3)
E – Himalaya	Lower	40%	0.22	0.20	4.50	4.05
	Average	50%	0.28	0.25	5.62	5.06
	Upper	60%	0.34	0.30	6.74	6.07
C – Himalaya	Lower	40%	3.73	3.36	28.27	25.44
	Average	50%	4.67	4.20	35.33	31.80
	Upper	60%	5.60	5.04	42.40	38.16
W – Himalaya	Lower	40%	0.66	0.59	13.28	11.95
	Average	50%	0.82	0.74	16.60	14.94
	Upper	60%	0.99	0.89	19.92	17.93
Total	**Lower**	**40%**	**4.62**	**4.15**	**46.04**	**41.44**
	Average	**50%**	**5.77**	**5.19**	**57.55**	**51.80**
	Upper	**60%**	**6.92**	**6.23**	**69.07**	**62.16**

Supplementary Table 12.6. Attributes recorded for each feature in the polygonised inventory, with attribute explanation. This table has been adapted from Jones et al. (2018b).

Attribute	Attribute Explanation
Name	Region_Feature No._MM/DD/YYYY* (e.g., WH_1_10/07/2013)
Region	[EH] East Himalaya, [CH] Central Himalaya, [WH] West Himalaya
DMSLon	Longitudinal coordinate of polygon centroid (DDD°MM'SS.sss [N|S])
DMSLat	Latitudinal coordinate of polygon centroid (DDD°MM'SS.sss [W|E])
MEF (m a.s.l.)	Minimum elevation at the front
MaxE (m a.s.l.)	Maximum elevation of the feature
Elevation (m a.s.l.)	Range | Mean
Area (km²)	/
Mean Aspect (°)	0-359
Aspect Class	N, NE, E, SE, S, SW, W, NW (e.g., 90° = E, 180° = S)
Max Length (m)	/
Mean Width (m)	/
L:W Ratio	Length: width ratio
Geometry Type	Tongue-shaped, Lobate-shaped
Dynamic Type	Active, Inactive, Relict
WVEQ (km³)	40% | 50% | 60%
Index Code	See **Table 6.3**
Certainty Index	Medium_Certainty, High_Certainty, Virtual_Certainty

* MM/DD/YYYY refers to the satellite image date.

12.4 CHAPTER 9: APPENDIX

12.4.1 AGISOFT PHOTOSCAN WORKFLOW

Hardware and software

- Windows 7, Intel Core i5-4690 CPU, 24 GB (RAM), 64-bit.
- Agisoft PhotoScan Professional Version: 1.3.5 64-bit.

Foreword

Note that the procedure followed within this study reflects that found in the supplementary information of Duffy et al. (2018).

Photogrammetric workflow

1. Manually inspect KAP-derived aerial photos, removing unsuitable images from the dataset.
2. Add the image subset to Agisoft PhotoScan
3. Run Align Photos (Accuracy: [High] | Generic preselection: [x] | Reference preselection: [x] | Key point limit: [125,000] | Tie point limit: [0] | Constrain features by mask: [x] | Adaptive camera model fitting: [x])
4. Run Build Mesh (Surface type: [Height field] | Source data: [Sparse cloud] | Face count: [Medium] | Interpolation: [Enabled]
5. Manually locate and position GCPs across all relevant images
6. Import the coordinates from the GARMIN eTrex® 10 Handheld GPS on which the position of GCPs were recorded
7. Uncheck images and a subset of the GCPs. This GCP subset will be used as validation/check points. Ensure the remaining GCPs are checked
8. Run Align Photos (Accuracy: [High] | Generic preselection: [x] | Reference preselection: [x] | Key point limit: [125,000] | Tie point limit: [0] | Adaptive camera model fitting: [x])
9. In Reference Settings: (i) set the (Image coord accuracy: [Marker accuracy (pix)] to the chunks RMS re-projection error (see James et al., 2017). The RMS re-projection error is found via R-click chunk > Show Info; and (ii) set the (Measurement accuracy: [Marker accuracy (m)] to that of the GARMIN eTrex® 10 Handheld GPS on which the position of GCPs were recorded (± 3 m)
10. Run Optimise Cameras (wand symbol)

11. Run Build Dense Cloud (Quality: [High] | Depth filtering: [Aggressive])
12. Use Gradual Selection to remove points within the dense point cloud with re-projection errors ≥0.8 pix
13. Run Build DEM (Source data: [Dense cloud] | Interpolation: [Enabled])
14. Run Build Orthomosaic (Surface: [DEM] | Blending mode: [Mosaic] | Enable hole filling: [x])

12.4.2 AGISOFT PHOTOSCAN REPORT

Chola Glacier Survey

Processing Report
23 November 2018

Supplementary Figure 12.4. Agisoft PhotoScan processing report: The Chola Glacier.

Survey Data

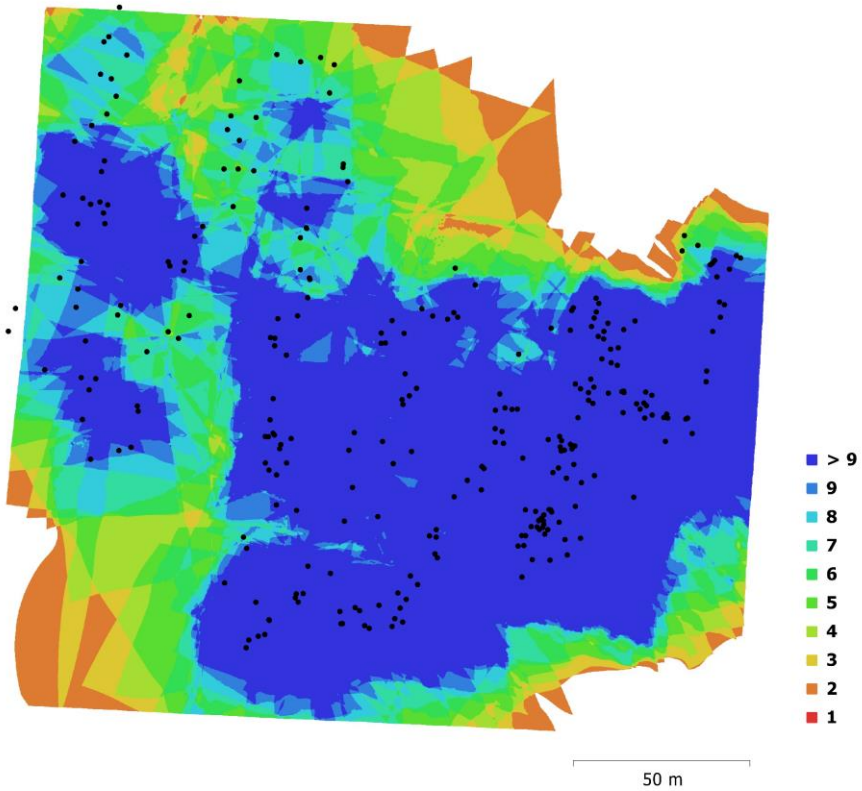

Fig. 1. Camera locations and image overlap.

Number of images:	282	Camera stations:	282
Flying altitude:	33.2 m	Tie points:	1,560,502
Ground resolution:	9.52 mm/pix	Projections:	4,524,222
Coverage area:	0.0358 km²	Reprojection error:	0.644 pix

Camera Model	Resolution	Focal Length	Pixel Size	Precalibrated
Canon PowerShot D30 (5mm)	4000 x 3000	5 mm	1.55 x 1.55 µm	No

Table 1. Cameras.

Supplementary Figure 12.4. *(continued).*

Camera Calibration

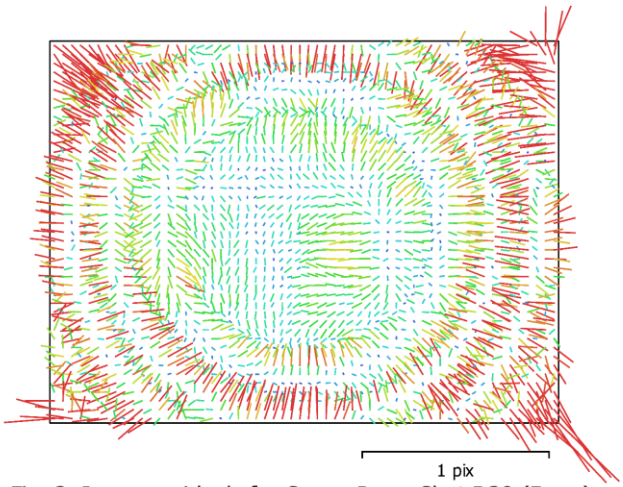

Fig. 2. Image residuals for Canon PowerShot D30 (5mm).

Canon PowerShot D30 (5mm)
282 images

Type	Resolution	Focal Length	Pixel Size
Frame	**4000 x 3000**	**5 mm**	**1.55 x 1.55 µm**

	Value	Error	F	Cx	Cy	B1	B2	K1	K2	K3	K4	P1	P2
F	**3296.04**	0.037	1.00	-0.39	-0.06	-0.00	0.01	-0.07	0.16	-0.15	0.14	-0.46	-0.14
Cx	**-35.3242**	0.046		1.00	0.02	-0.36	-0.29	-0.04	0.00	-0.01	0.01	0.92	0.07
Cy	**3.86249**	0.045			1.00	0.31	-0.47	0.02	-0.01	0.01	-0.01	-0.02	0.91
B1	**-1.03341**	0.0079				1.00	0.03	0.04	-0.01	0.01	-0.01	-0.44	0.19
B2	**-1.1666**	0.0076					1.00	0.00	-0.00	0.00	-0.00	-0.16	-0.53
K1	**-0.00983077**	4.7e-05						1.00	-0.97	0.92	-0.86	-0.05	0.01
K2	**0.0569401**	0.00034							1.00	-0.99	0.96	0.01	-0.01
K3	**-0.173755**	0.00095								1.00	-0.99	-0.01	0.01
K4	**0.16216**	0.00091									1.00	0.01	-0.01
P1	**-0.0040034**	3.7e-06										1.00	0.06
P2	**-0.000811491**	3.4e-06											1.00

Table 2. Calibration coefficients and correlation matrix.

Supplementary Figure 12.4. *(continued).*

Ground Control Points

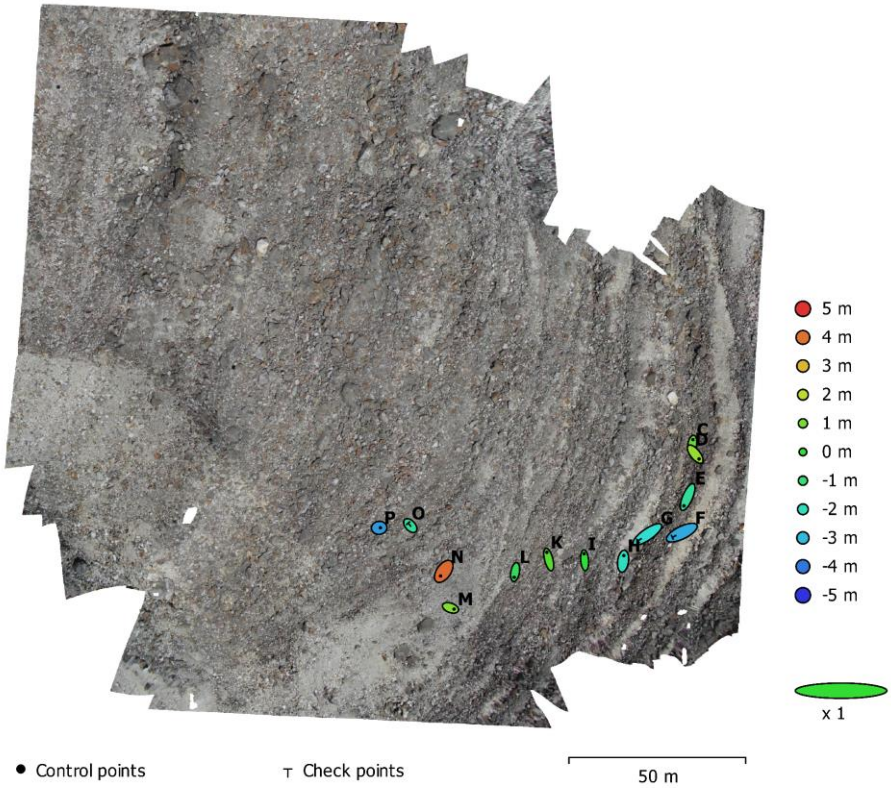

Fig. 3. GCP locations and error estimates.
Z error is represented by ellipse color. X,Y errors are represented by ellipse shape.
Estimated GCP locations are marked with a dot or crossing.

Count	X error (m)	Y error (m)	Z error (m)	XY error (m)	Total (m)
10	1.37316	3.09268	2.03357	3.38382	3.94786

Table 3. Control points RMSE.
X - Longitude, Y - Latitude, Z - Altitude.

Count	X error (m)	Y error (m)	Z error (m)	XY error (m)	Total (m)
3	4.4382	2.7163	2.48591	5.20345	5.76677

Table 4. Check points RMSE.
X - Longitude, Y - Latitude, Z - Altitude.

Supplementary Figure 12.4. *(continued).*

Label	X error (m)	Y error (m)	Z error (m)	Total (m)	Image (pix)
C	0.467902	2.75588	0.740929	2.89185	0.655 (15)
D	2.17228	-2.71893	1.41688	3.75752	0.526 (11)
E	-2.11754	-4.93129	-1.53087	5.58079	0.436 (2)
H	0.424292	3.18048	-2.11213	3.84143	0.548 (12)
K	-1.03808	4.11198	0.450586	4.26486	1.126 (17)
I	-0.289043	3.70959	-0.145529	3.72368	0.276 (3)
L	-0.515631	-2.92877	-0.604748	3.03468	0.798 (7)
N	-1.8209	-2.54249	4.18644	5.22553	0.879 (9)
P	0.71759	0.0767092	-3.54522	3.61793	2.314 (4)
M	1.99909	-0.713201	1.14365	2.411	0.518 (3)
Total	**1.37316**	**3.09268**	**2.03357**	**3.94786**	**0.911**

Table 5. Control points.
X - Longitude, Y - Latitude, Z - Altitude.

Label	X error (m)	Y error (m)	Z error (m)	Total (m)	Image (pix)
F	-5.39572	-2.62858	-3.2518	6.82623	1.129 (5)
G	-5.33718	-3.65869	-2.36033	6.88786	0.423 (9)
O	-1.22211	1.35625	-1.5472	2.39307	1.128 (7)
Total	**4.4382**	**2.7163**	**2.48591**	**5.76677**	**0.897**

Table 6. Check points.
X - Longitude, Y - Latitude, Z - Altitude.

Supplementary Figure 12.4. *(continued).*

Digital Elevation Model

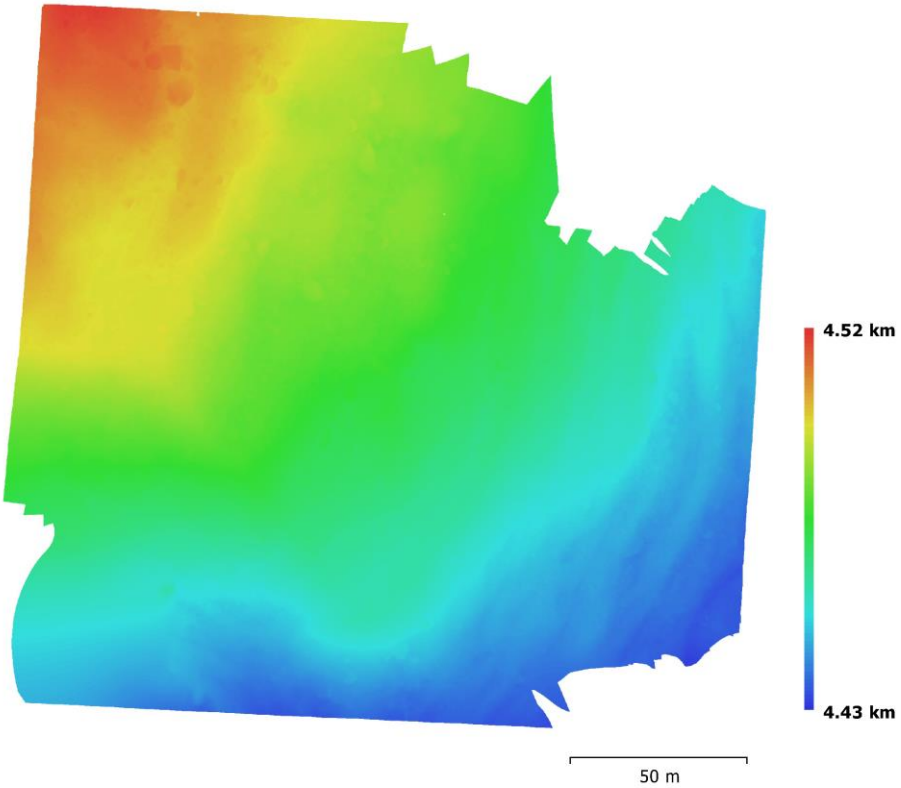

Fig. 4. Reconstructed digital elevation model.

Resolution:	1.9 cm/pix
Point density:	27.6 points/cm²

Supplementary Figure 12.4. *(continued).*

Processing Parameters

General	
Cameras	282
Aligned cameras	282
Markers	13
Coordinate system	WGS 84 (EPSG::4326)
Rotation angles	Yaw, Pitch, Roll
Point Cloud	
Points	1,560,502 of 1,682,013
RMS reprojection error	0.131817 (0.643824 pix)
Max reprojection error	0.473659 (33.6035 pix)
Mean key point size	4.52645 pix
Effective overlap	3.19666
Alignment parameters	
Accuracy	High
Generic preselection	Yes
Reference preselection	Yes
Key point limit	125,000
Tie point limit	0
Constrain features by mask	Yes
Adaptive camera model fitting	Yes
Matching time	41 minutes 22 seconds
Alignment time	10 minutes 5 seconds
Optimization parameters	
Parameters	f, b1, b2, cx, cy, k1-k4, p1, p2
Fit rolling shutter	No
Optimization time	32 seconds
Dense Point Cloud	
Points	122,552,137
Reconstruction parameters	
Quality	High
Depth filtering	Aggressive
Depth maps generation time	2 hours 0 minutes
Dense cloud generation time	2 hours 49 minutes
DEM	
Size	12,128 x 10,929
Coordinate system	WGS 84 (EPSG::4326)
Reconstruction parameters	
Source data	Dense cloud
Interpolation	Enabled
Processing time	1 minutes 49 seconds
Orthomosaic	
Size	22,698 x 21,522
Coordinate system	WGS 84 (EPSG::4326)
Channels	3, uint8
Reconstruction parameters	
Blending mode	Mosaic
Surface	DEM
Enable color correction	No
Enable hole filling	Yes
Processing time	8 minutes 33 seconds
Software	
Version	1.3.5 build 5649
Platform	Windows 64

Supplementary Figure 12.4. *(continued).*

BIBLIOGRAPHY

Ackert, R.P., 1998. A rock glacier/debris-covered glacier system at Galena Creek, Absaroka Mountains, Wyoming. Geografiska Annaler: Series A, Physical Geography, 80(3/4): 267-276.

Alifu, H., Tateishi, R. and Johnson, B., 2015. A new band ratio technique for mapping debris-covered glaciers using Landsat imagery and a digital elevation model. International Journal of Remote Sensing, 36(8): 2063-2075.

Allen, S.K., Owens, I. and Huggel, C., 2008. A first estimate of mountain permafrost distribution in the Mount Cook region of New Zealand's southern alps, 9th International Conference on Permafrost, Fairbanks, Alaska, pp. 37-42.

Anderson, K., Fawcett, D., Cugulliere, A., Benford, S., Jones, D. and Leng, R., 2019. Vegetation expansion in the subnival Hindu Kush Himalaya. Global Change Biology: 1-18.

Anderson, L.S. and Anderson, R.S., 2018. Debris thickness patterns on debris-covered glaciers. Geomorphology, 311: 1-12.

Anderson, R.S., Anderson, L.S., Armstrong, W.H., Rossi, M.W. and Crump, S.E., 2018. Glaciation of alpine valleys: The glacier – debris-covered glacier – rock glacier continuum. Geomorphology, 311: 127-142.

Andreassen, L.M., Huss, M., Melvold, K., Elvehøy, H. and Winsvold, S.H., 2015. Ice thickness measurements and volume estimates for glaciers in Norway. Journal of Glaciology, 61(228): 763-775.

Arenson, L., Hoelzle, M. and Springman, S., 2002. Borehole deformation measurements and internal structure of some rock glaciers in Switzerland. Permafrost and Periglacial Processes, 13(2): 117-135.

Arenson, L.U., Hauck, C., Hilbich, C., Seward, L., Yamamoto, Y. and Springman, S.M., 2010. Sub-surface heterogeneities in the Murtèl-Corvatsch rock glacier, Switzerland, Proceedings of the joint 63rd Canadian Geotechnical Conference and the 6th Canadian Permafrost Conference. Canadian Geotechnical Society, pp. 1494-1500.

Arenson, L.U. and Jakob, M., 2010. The significance of rock glaciers in the dry Andes – A discussion of Azócar and Brenning (2010) and Brenning and Azócar (2010). Permafrost and Periglacial Processes, 21(3): 282-285.

Arenson, L.U. and Springman, S.M., 2005. Mathematical descriptions for the behaviour of ice-rich frozen soils at temperatures close to 0 °C. Canadian Geotechnical Journal, 42(2): 431-442.

Azócar, G.F. and Brenning, A., 2010. Hydrological and geomorphological significance of rock glaciers in the dry Andes, Chile (27°-33°S). Permafrost and Periglacial Processes, 21(1): 42-53.

Azócar, G.F., Brenning, A. and Bodin, X., 2017. Permafrost distribution modelling in the semi-arid Chilean Andes. The Cryosphere, 11(2): 877-890.

Bahr, D.B., Meier, M.F. and Peckham, S.D., 1997. The physical basis of glacier volume-area scaling. Journal of Geophysical Research: Solid Earth, 102(B9): 20355-20362.

Bahr, D.B., Pfeffer, W.T. and Kaser, G., 2015. A review of volume-area scaling of glaciers. Reviews of Geophysics, 53(1): 95-140.

Bajewsky, I. and Gardner, J.S., 1989. Discharge and sediment-load characteristics of the Hilda rock-glacier stream, Canadian Rocky Mountains, Alberta. Physical Geography, 10(4): 295-306.

Bajracharya, S.R., Maharjan, S.B., Shrestha, F., Guo, W., Liu, S., Immerzeel, W. and Shrestha, B., 2015. The glaciers of the Hindu Kush Himalayas: Current status and observed changes from the 1980s to 2010. International Journal of Water Resources Development, 31(2): 161-173.

Bajracharya, S.R. and Shrestha, B., 2011. The Status of Glaciers in the Hindu Kush-Himalayan Region. ICIMOD, Kathmandu.

Ballantyne, C.K., 1982. Aggregate clast form characteristics of deposits near the margins of four glaciers in the Jotunheimen Massif, Norway. Norsk Geografisk Tidsskrift - Norwegian Journal of Geography, 36(2): 103-113.

Ballantyne, C.K., 2002a. A general model of paraglacial landscape response. The Holocene, 12(3): 371-376.

Ballantyne, C.K., 2002b. Paraglacial geomorphology. Quaternary Science Reviews, 21(18): 1935-2017.

Ballantyne, C.K., 2018. Periglacial Geomorphology. Wiley Blackwell, Hoboken, NJ, 454 pp.

Ballantyne, C.K., Sandeman, G.F., Stone, J.O. and Wilson, P., 2014. Rock-slope failure following late Pleistocene deglaciation on tectonically stable mountainous terrain. Quaternary Science Reviews, 86(Supplement C): 144-157.

Baraer, M., Mark, B.G., McKenzie, J.M., Condom, T., Bury, J., Huh, K.-I., Portocarrero, C., Gómez, J. and Rathay, S., 2012. Glacier recession and water resources in Peru's Cordillera Blanca. Journal of Glaciology, 58(207): 134-150.

Baral, P., Haq, M.A. and Yaragal, S., in press. Assessment of rock glaciers and permafrost distribution in Uttarakhand, India. Permafrost and Periglacial Processes.

Barboux, C., Delaloye, R. and Lambiel, C., 2014. Inventorying slope movements in an Alpine environment using DInSAR. Earth Surface Processes and Landforms, 39(15): 2087-2099.

Barcaza, G., Nussbaumer, S.U., Tapia, G., Valdés, J., García, J.-L., Videla, Y., Albornoz, A. and Arias, V., 2017. Glacier inventory and recent glacier variations in the Andes of Chile, South America. Annals of Glaciology, 58(75pt2): 166-180.

Barlow, M., Wheeler, M., Lyon, B. and Cullen, H., 2005. Modulation of daily precipitation over Southwest Asia by the Madden–Julian Oscillation. Monthly Weather Review, 133(12): 3579-3594.

Barnard, P.L., Owen, L.A. and Finkel, R.C., 2006. Quaternary fans and terraces in the Khumbu Himal south of Mount Everest: Their characteristics, age and formation. Journal of the Geological Society, 163(2): 383.

Barnett, T.P., Adam, J.C. and Lettenmaier, D.P., 2005. Potential impacts of a warming climate on water availability in snow-dominated regions. Nature, 438(7066): 303-309.

Baron, J.S., Schmidt, T.M. and Hartman, M.D., 2009. Climate-induced changes in high elevation stream nitrate dynamics. Global Change Biology, 15(7): 1777-1789.

Baroni, C., Carton, A. and Seppi, R., 2004. Distribution and behaviour of rock glaciers in the Adamello–Presanella Massif (Italian Alps). Permafrost and Periglacial Processes, 15(3): 243-259.

Barsch, D., 1977. Nature and importance of mass-wasting by rock glaciers in alpine permafrost environments. Earth Surface Processes, 2(2-3): 231-245.

Barsch, D., 1987. The problem of the ice-cored rock glacier. In: J.R. Giardino, J.F. Shroder and J.D. Vitek (Editors), Rock Glaciers Allen and Unwin, London, pp. 45-54.

Barsch, D., 1988. Rockglaciers. In: M.J. Clark (Editor), Advances in Periglacial Geomorphology. Wiley, Chichester, pp. 69-90.

Barsch, D., 1992. Permafrost creep and rockglaciers. Permafrost and Periglacial Processes, 3(3): 175-188.

Barsch, D., 1996. Rockglaciers: Indicators for the Present and Former Geoecology in High Mountain Environments. Springer-Verlag Berlin Heidelberg, Berlin, Germany, 331 pp.

Barsch, D. and Jakob, M., 1998. Mass transport by active rockglaciers in the Khumbu Himalaya. Geomorphology, 26(1–3): 215-222.

Bartlett, R., Bharati, L., Pant, D., Hosterman, H. and McCornick, P., 2010. Climate change impacts and adaptation in Nepal. International Water Management Institute (IWMI Working Paper 139), Colombo, Sri Lanka, pp. 35.

Bavay, M., Grünewald, T. and Lehning, M., 2013. Response of snow cover and runoff to climate change in high Alpine catchments of Eastern Switzerland. Advances in Water Resources, 55: 4-16.

Bellisario, A., Ferrando, F. and Janke, J., 2013. Water resources in Chile: The critical relation between glaciers and mining for sustainable water management. Investigaciones Geográficas, 46: 3-24.

Beniston, M., 2003. Climatic change in mountain regions: A review of possible impacts. Climatic Change, 59(1-2): 5-31.

Beniston, M., Farinotti, D., Stoffel, M., Andreassen, L.M., Coppola, E., Eckert, N., Fantini, A., Giacona, F., Hauck, C., Huss, M., Huwald, H., Lehning, M., López-Moreno, J.I., Magnusson, J., Marty, C., Moran-Tejéda, E., Morin, S., Naaim, M., Provenzale, A., Rabatel, A., Six, D., Stötter, J., Strasser, U., Terzago, S. and Vincent, C., 2018. The European mountain cryosphere: A review of its current state, trends, and future challenges. The Cryosphere, 12(2): 759-794.

Beniston, M., Stoffel, M., Hill Clarvis, M. and Quevauviller, P., 2014. Assessing climate change impacts on the quantity of water in Alpine regions: Foreword to the adaptation and policy implications of the EU/FP7 “ACQWA” project. Environmental Science & Policy, 43: 1-4.

Benn, D.I., 2004. Clast morphology. In: D.J.A. Evans and D.I. Benn (Editors), A Practical Guide to the Study of Glacial Sediments. Arnold, London, pp. 77-92.

Benn, D.I. and Ballantyne, C.K., 1993. The description and representation of particle shape. Earth Surface Processes and Landforms, 18(7): 665-672.

Benn, D.I. and Ballantyne, C.K., 1994. Reconstructing the transport history of glacigenic sediments: A new approach based on the co-variance of clast form indices. Sedimentary Geology, 91: 215-227.

Benn, D.I. and Evans, D.J.A., 2010. Glaciers and Glaciation. Hodder Education, London, 802 pp.

Benn, D.I., Kirkbride, M.P., Owen, L.A. and Brazier, V., 2004. Glaciated valley landsystems. In: D.J.A. Evans (Editor), Glacial Landsystems. Arnold, London, pp. 372-406.

Benn, D.I. and Owen, L.A., 2002. Himalayan glacial sedimentary environments: A framework for reconstructing and dating the former extent of glaciers in high mountains. Quaternary International, 97-98: 3-25.

Bennett, M.R., Hambrey, M.J. and Huddart, D., 1997. Modification of clast shape in high-Arctic glacial environments. Journal of Sedimentary Research, 67(3): 550-559.

Berger, J., Krainer, K. and Mostler, W., 2004. Dynamics of an active rock glacier (Ötztal Alps, Austria). Quaternary Research, 62(3): 233-242.

Berghuijs, W.R., Woods, R.A. and Hrachowitz, M., 2014. A precipitation shift from snow towards rain leads to a decrease in streamflow. Nature Climate Change, 4(7): 583-586.

Berthling, I., 2011. Beyond confusion: Rock glaciers as cryo-conditioned landforms. Geomorphology, 131(3-4): 98-106.

Bhambri, R. and Bolch, T., 2009. Glacier mapping: A review with special reference to the Indian Himalayas. Progress in Physical Geography, 33(5): 672-704.

Bishop, M.P., Shroder, J.F., Ali, G., Bush, A.B.G., Haritashya, U.K., Roohi, R., Sarikaya, M.A. and Weihs, B.J., 2014. Remote Sensing of Glaciers in Afghanistan and Pakistan. In: S.J. Kargel, J.G. Leonard, P.M. Bishop, A. Kääb and H.B. Raup (Editors), Global Land Ice Measurements from Space. Springer Berlin Heidelberg, Berlin, Heidelberg, pp. 509-548.

Biskaborn, B.K., Smith, S.L., Noetzli, J., Matthes, H., Vieira, G., Streletskiy, D.A., Schoeneich, P., Romanovsky, V.E., Lewkowicz, A.G., Abramov, A., Allard, M., Boike, J., Cable, W.L., Christiansen, H.H., Delaloye, R., Diekmann, B., Drozdov, D., Etzelmüller, B., Grosse, G., Guglielmin, M., Ingeman-Nielsen, T., Isaksen, K., Ishikawa, M., Johansson, M., Johannsson, H., Joo, A., Kaverin, D., Kholodov, A., Konstantinov, P., Kröger, T., Lambiel, C., Lanckman, J.-P., Luo, D., Malkova, G., Meiklejohn, I., Moskalenko, N., Oliva, M., Phillips, M., Ramos, M., Sannel, A.B.K., Sergeev, D., Seybold, C., Skryabin, P., Vasiliev, A., Wu, Q., Yoshikawa, K., Zheleznyak, M. and Lantuit, H., 2019. Permafrost is warming at a global scale. Nature Communications, 10(1): 264.

Blöthe, J.H., Rosenwinkel, S., Höser, T. and Korup, O., 2019. Rock-glacier dams in High Asia. Earth Surface Processes and Landforms, 44: 808-824.

Blumstengel, W. and Harris, S.A., 1988. Observations on an active lobate rock glacier, Slims River valley, St. Elias Range, Canada, Proceedings of the Fifth International Conference on Permafrost. Tapir Press, Trondheim, Norway, pp. 689-694.

Boccali, C., Žebre, M. and Colucci, R.R., 2019. Geometry and paleo-ice content of rock glaciers in the southeastern Alps (NE Italy – NW Slovenia). Journal of Maps, 15(2): 346-355.

Bodin, X., 2013. Present status and development of rock glacier complexes in south-faced valleys (45°N, French Alps). Geografia Fisica e Dinamica Quaternaria, 36(2): 27-28.

Bodin, X., Krysiecki, J.-M., Schoeneich, P., Le Roux, O., Lorier, L., Echelard, T., Peyron, M. and Walpersdorf, A., 2017. The 2006 collapse of the Bérard rock glacier (Southern French Alps). Permafrost and Periglacial Processes, 28(1): 209-223.

Bodin, X., Rojas, F. and Brenning, A., 2010. Status and evolution of the cryosphere in the Andes of Santiago (Chile, 33.5°S.). Geomorphology, 118(3-4): 453-464.

Bodin, X., Thibert, E., Fabre, D., Ribolini, A., Schoeneich, P., Francou, B., Reynaud, L. and Fort, M., 2009. Two decades of responses (1986–2006) to climate by the Laurichard rock glacier, French Alps. Permafrost and Periglacial Processes, 20(4): 331-344.

Boeckli, L., Brenning, A., Gruber, S. and Noetzli, J., 2012. A statistical approach to modelling permafrost distribution in the European Alps or similar mountain ranges. The Cryosphere, 6(1): 125-140.

Bolch, T., 2017. Asian glaciers are a reliable water source. Nature, 545: 161.

Bolch, T. and Gorbunov, A.P., 2014. Characteristics and origin of rock glaciers in Northern Tien Shan (Kazakhstan/Kyrgyzstan). Permafrost and Periglacial Processes, 25(4): 320-332.

Bolch, T. and Kamp, U., 2006. Glacier mapping in high mountains using DEMs, Landsat and ASTER data, Grazer Schriften der Geographie und Raumforschung (Proceedings of the 8th International Symposium on High Mountain Remote Sensing Cartography), La Paz, Bolivia, pp. 13-24.

Bolch, T., Kulkarni, A., Kääb, A., Huggel, C., Paul, F., Cogley, J.G., Frey, H., Kargel, J.S., Fujita, K., Scheel, M., Bajracharya, S. and Stoffel, M., 2012. The state and fate of Himalayan glaciers. Science, 336(6079): 310-314.

Bolch, T. and Marchenko, S.S., 2006. Significance of glaciers, rockglaciers and ice-rich permafrost in the Northern Tien Shan as water towers under climate change conditions. In: L. Braun, W. Hagg, I.V. Severskiy and G.J. Young (Editors), Proceedings of the Workshop Assessment of Snow-Glacier and Water Resources in Asia. IHP/HWRP-Berichte, Almaty, Kazakhstan, pp. 132-144.

Bolch, T., Menounos, B. and Wheate, R., 2010. Landsat-based inventory of glaciers in western Canada, 1985–2005. Remote Sensing of Environment, 114(1): 127-137.

Bolch, T., Rohrbach, N., Kutuzov, S., Robson, B.A. and Osmonov, A., 2019a. Occurrence, evolution and ice content of ice-debris complexes in the Ak-Shiirak, Central Tien Shan revealed by geophysical and remotely-sensed investigations. Earth Surface Processes and Landforms, 44: 129-143.

Bolch, T., Shea, J.M., Liu, S., Azam, F.M., Gao, Y., Gruber, S., Immerzeel, W.W., Kulkarni, A., Li, H., Tahir, A.A., Zhang, G. and Zhang, Y., 2019b. Status and Change of the Cryosphere in the Extended Hindu Kush Himalaya Region. In: P. Wester, A. Mishra, A. Mukherji and A.B. Shrestha (Editors), The Hindu Kush Himalaya Assessment: Mountains, Climate Change, Sustainability and People. Springer International Publishing, Cham, pp. 209-255.

Bollasina, M., Bertolani, L. and Tartari, G., 2002. Meteorological observations at high altitude in the Khumbu Valley, Nepal Himalayas, 1994-1999. Bulletin of Glaciological Research, 19: 1-11.

Bonnaventure, P.P. and Lamoureux, S.F., 2013. The active layer: A conceptual review of monitoring, modelling techniques and changes in a warming climate. Progress in Physical Geography, 37(3): 352-376.

Bookhagen, B. and Burbank, D.W., 2006. Topography, relief, and TRMM-derived rainfall variations along the Himalaya. Geophysical Research Letters, 33(8).

Bookhagen, B. and Burbank, D.W., 2010. Toward a complete Himalayan hydrological budget: Spatiotemporal distribution of snowmelt and rainfall and their impact on river discharge. Journal of Geophysical Research: Earth Surface, 115(F3).

Bosson, J.-B. and Lambiel, C., 2016. Internal structure and current evolution of very small debris-covered glacier systems located in alpine permafrost environments. Frontiers in Earth Science, 4(39).

Boulton, G.S., 1978. Boulder shapes and grain-size distributions of debris as indicators of transport paths through a glacier and till genesis. Sedimentology, 25(6): 773-799.

Bradley, R.S., Vuille, M., Diaz, H.F. and Vergara, W., 2006. Threats to water supplies in the tropical Andes. Science, 312(5781): 1755-1756.

Brardinoni, F., Scotti, R., Sailer, R. and Mair, V., 2019. Evaluating sources of uncertainty and variability in rock glacier inventories. Earth Surface Processes and Landforms, 44(12): 2450-2466.

Brazier, V., Kirkbride, M.P. and Owens, I.F., 1998. The relationship between climate and rock glacier distribution in the Ben Ohau Range, New Zealand. Geografiska Annaler: Series A, Physical Geography, 80(3-4): 193-207.

Brenning, A., 2005a. Climatic and Geomorphological Controls of Rock Glaciers in the Andes of Central Chile: Combining Statistical Modelling and Field Mapping, Humboldt-Universität zu Berlin, Berlin, Germany, 153 pp.

Brenning, A., 2005b. Geomorphological, hydrological and climatic significance of rock glaciers in the Andes of Central Chile (33-35°S). Permafrost and Periglacial Processes, 16(3): 231-240.

Brenning, A., 2008. The impact of mining on rock glaciers and glaciers: Examples from Central Chile. In: B. Orlove, E. Wiegandt and B.H. Luckman (Editors), Darkening Peaks. Glacier Retreat, Science, and Society. University of California Press, Berkeley, CA, pp. 196-205.

Brenning, A., 2009. Benchmarking classifiers to optimally integrate terrain analysis and multispectral remote sensing in automatic rock glacier detection. Remote Sensing of Environment, 113(1): 239-247.

Brenning, A., 2010. The significance of rock glaciers in the dry Andes – reply to L. Arenson and M. Jakob. Permafrost and Periglacial Processes, 21(3): 286-288.

Brenning, A. and Azócar, G.F., 2010. Statistical analysis of topographic and climatic controls and multispectral signatures of rock glaciers in the dry Andes, Chile (27°–33°S). Permafrost and Periglacial Processes, 21(1): 54-66.

Brenning, A., Grasser, M. and Friend, D.A., 2007. Statistical estimation and generalized additive modeling of rock glacier distribution in the San Juan Mountains, Colorado, United States. Journal of Geophysical Research: Earth Surface, 112(F02S15).

Brighenti, S., Tolotti, M., Bruno, M.C., Wharton, G., Pusch, M.T. and Bertoldi, W., 2019. Ecosystem shifts in Alpine streams under glacier retreat and rock glacier thaw: A review. Science of The Total Environment, 675: 542-559.

Brook, M.S. and Lukas, S., 2012. A revised approach to discriminating sediment transport histories in glacigenic sediments in a temperate alpine environment: A case study from Fox Glacier, New Zealand. Earth Surface Processes and Landforms, 37(8): 895-900.

Brown, R.D. and Mote, P.W., 2009. The response of northern hemisphere snow cover to a changing climate. Journal of Climate, 22(8): 2124-2145.

Buchli, T., Kos, A., Limpach, P., Merz, K., Zhou, X. and Springman Sarah, M., 2018. Kinematic investigations on the Furggwanghorn rock glacier, Switzerland. Permafrost and Periglacial Processes, 29(1): 3-20.

Buchli, T., Merz, K., Zhou, X., Kinzelbach, W. and Springman, S.M., 2013. Characterization and monitoring of the Furggwanghorn Rock Glacier, Turtmann Valley, Switzerland: Results from 2010 to 2012. Vadose Zone Journal, 12(1).

Bucki, A.K. and Echelmeyer, K.A., 2004. The flow of Fireweed rock glacier, Alaska, USA. Journal of Glaciology, 50(168): 76-86.

Burger, K.C., Degenhardt Jr, J.J. and Giardino, J.R., 1999. Engineering geomorphology of rock glaciers. Geomorphology, 31(1–4): 93-132.

Cannon, F., Carvalho, L.M.V., Jones, C. and Bookhagen, B., 2015. Multi-annual variations in winter westerly disturbance activity affecting the Himalaya. Climate Dynamics, 44(1): 441-455.

Cecil, L.D., Green, J.R., Vogt, S., Michel, R. and Cottrell, G., 1998. Isotopic composition of ice cores and meltwater from Upper Fremont Glacier and Galena Creek rock glacier, Wyoming. Geografiska Annaler: Series A, Physical Geography, 80(3/4): 287-292.

Center for International Earth Science Information Network - CIESIN - Columbia University, 2018. Gridded Population of the World, Version 4 (GPWv4): Population Count Adjusted to Match 2015 Revision of UN WPP Country Totals, Revision 11. NASA Socioeconomic Data and Applications Center (SEDAC), Palisades, NY.

Central Bureau of Statistics, 2014. Population Monograph of Nepal, Volume I - Population Dynamics. National Planning Commission Secretariat. Government of Nepal Kathmandu: Nepal.

Charbonneau, A.A., 2015. Rock glacier activity and distribution in the southeastern British Columbia Coast Mountains, University of Victoria.

Charbonneau, A.A. and Smith, D.J., 2018. An inventory of rock glaciers in the Central British Columbia Coast Mountains, Canada, from high resolution Google Earth imagery. Arctic, Antarctic, and Alpine Research, 50(1): e1489026.

Chen, J. and Ohmura, A., 1990. Estimation of Alpine glacier water resources and their change since the 1870s. In: H. Lang and A. Musy (Editors), Hydrology in Mountainous Regions. I-Hydrological Measurements. IAHS Press Publications, Oxfordshire, UK, pp. 127-135.

Chueca, J., 1992. A statistical analysis of the spatial distribution of rock glaciers, Spanish Central Pyrenees. Permafrost and Periglacial Processes, 3(3): 261-265.

Cicoira, A., Beutel, J., Faillettaz, J. and Vieli, A., 2019. Water controls the seasonal rhythm of rock glacier flow. Earth and Planetary Science Letters, 528: 115844.

Çiner, A., Sarıkaya, M.A. and Yıldırım, C., 2017. Misleading old age on a young landform? The dilemma of cosmogenic inheritance in surface exposure dating: Moraines vs. rock glaciers. Quaternary Geochronology, 42: 76-88.

Clark, D.H., Steig, E.J., Potter, J.N. and Gillespie, A.R., 1998. Genetic variability of rock glaciers. Geografiska Annaler: Series A, Physical Geography, 80(3-4): 175-182.

Clark, D.H., Steig, E.J., Potter, N., Updike, A., Fitzpatrick, J. and Clark, G.M., 1996. Old ice in rock glaciers may provide long-term climate records. Eos, Transactions American Geophysical Union, 77(23): 217-222.

Clow, D.W., Schrott, L., Webb, R., Campbell, D.H., Torizzo, A. and Dornblaser, M., 2003. Ground water occurrence and contributions to streamflow in an alpine catchment, Colorado Front Range. Groundwater, 41(7): 937-950.

Cogley, J.G., 2011. Present and future states of Himalaya and Karakoram glaciers. Annals of Glaciology, 52(59): 69-73.

Cogley, J.G., Hock, R., Rasmussen, L.A., Arendt, A.A., Bauder, A., Braithwaite, R.J., Jansson, P., Kaser, G., Möller, M., Nicholson, L. and Zemp, M., 2011. Glossary of Glacier Mass Balance and Related Terms. UNESCO-IHP, Paris.

Colombo, N., Gruber, S., Martin, M., Malandrino, M., Magnani, A., Godone, D., Freppaz, M., Fratianni, S. and Salerno, F., 2018a. Rainfall as primary driver of discharge and solute export from rock glaciers: The Col d'Olen rock glacier in the NW Italian Alps. Science of The Total Environment, 639: 316-330.

Colombo, N., Salerno, F., Gruber, S., Freppaz, M., Williams, M., Fratianni, S. and Giardino, M., 2018b. Review: Impacts of permafrost degradation on inorganic chemistry of surface fresh water. Global and Planetary Change, 162: 69-83.

Colombo, N., Sambuelli, L., Comina, C., Colombero, C., Giardino, M., Gruber, S., Viviano, G., Vittori Antisari, L. and Salerno, F., 2018c. Mechanisms linking active rock glaciers and impounded surface water formation in high-mountain areas. Earth Surface Processes and Landforms, 43(2): 417-431.

Colucci, R.R., Boccali, C., Žebre, M. and Guglielmin, M., 2016. Rock glaciers, protalus ramparts and pronival ramparts in the South-Eastern Alps. Geomorphology, 269: 112-121.

Colucci, R.R., Forte, E., Žebre, M., Maset, E., Zanettini, C. and Guglielmin, M., 2019. Is that a relict rock glacier? Geomorphology, 330: 177-189.

Consortium, R., 2014. Randolph Glacier Inventory – A Dataset of Global Glacier Outlines: Version 4.0: Technical Report, Global Land Ice Measurements from Space. Digital Media, Colorado, USA.

Consortium, R., 2017. Randolph Glacier Inventory – A Dataset of Global Glacier Outlines: Version 6.0: Technical Report, Global Land Ice Measurements from Space. Digital Media, Colorado, USA.

Corte, A.E., 1976. The hydrological significance of rock glaciers. Journal of Glaciology, 17: 157-158.

Corte, A.E., 1987. Central Andes rock glaciers: Applied aspects. In: J.R. Giardino, J.F. Shroder Jr and J.D. Vitek (Editors), Rock Glaciers. Allen and Unwin, London, pp. 289-304.

Cossart, E., Mercier, D., Coquin, J., Decaulne, A., Feuillet, T., Jónsson, H.P. and Sæmundsson, Þ., 2017. Denudation rates during a postglacial sequence in Northern Iceland: Example of Laxárdalur valley in the Skagafjörður area. Geografiska Annaler: Series A, Physical Geography, 99(3): 240-261.

Cremonese, E., Gruber, S., Phillips, M., Pogliotti, P., Boeckli, L., Noetzli, J., Suter, C., Bodin, X., Crepaz, A., Kellerer-Pirklbauer, A., Lang, K., Letey, S., Mair, V., Morra di Cella, U., Ravanel, L., Scapozza, C., Seppi, R. and Zischg, A., 2011. Brief communication: "An inventory of permafrost evidence for the European Alps". The Cryosphere, 5(3): 651-657.

Crespo, S., Aranibar, J., Gomez, L., Schwikowski, M., Bruetsch, S., Cara, L. and Villalba, R., 2017. Ionic and stable isotope chemistry as indicators of water sources to the Upper Mendoza River basin, Central Andes of Argentina. Hydrological Sciences Journal, 62(4): 588-605.

Croce, F.A. and Milana, J.P., 2002. Internal structure and behaviour of a rock glacier in the arid Andes of Argentina. Permafrost and Periglacial Processes, 13(4): 289-299.

Dall'Asta, E., Forlani, G., Roncella, R., Santise, M., Diotri, F. and Morra di Cella, U., 2017. Unmanned Aerial Systems and DSM matching for rock glacier monitoring. ISPRS Journal of Photogrammetry and Remote Sensing, 127: 102-114.

Davis, J.C., 2002. Statistics and Data Analysis in Geology. John Wiley & Sons, USA.

Degenhardt Jr, J.J., 2009. Development of tongue-shaped and multilobate rock glaciers in alpine environments – Interpretations from ground penetrating radar surveys. Geomorphology, 109(3–4): 94-107.

Degenhardt Jr, J.J. and Giardino, J.R., 2003. Subsurface investigation of a rock glacier using ground-penetrating radar: Implications for locating stored water on Mars. Journal of Geophysical Research: Planets, 108(E4).

Delaloye, R., Barboux, C., Bodin, X., Brenning, A., Hartl, L., Hu, Y., Ikeda, A., Kaufmann, V., Kellerer-Pirklbauer, A., Lambiel, C., Liu, L., Marcer, M., Rick, B., Scotti, R., Takadema, H., Trombotto, D., Vivero, S. and Winterberger, M., 2018. Rock Glacier Inventories and Kinematics: A New IPA Action Group, 5th European Conference On Permafrost. Edytem, Chamonix, France.

Delaloye, R. and Lambiel, C., 2005. Evidence of winter ascending air circulation throughout talus slopes and rock glaciers situated in the lower belt of alpine discontinuous permafrost (Swiss Alps). Norsk Geografisk Tidsskrift-Norwegian Journal of Geography, 59(2): 194-203.

Delaloye, R., Lambiel, C. and Gärtner-Roer, I., 2010. Overview of rock glacier kinematics research in the Swiss Alps. Geographica Helvetica, 65(2): 135-145.

Delaloye, R., Morard, S., Barboux, C., Abbet, D., Gruber, V., Riedo, M. and Gachet, S., 2013. Rapidly moving rock glaciers in Mattertal. In: C. Graf (Editor), Jahrestagung der Schweizerischen Geomorphologischen Gesellschaft. Eidg. Forschungsanstalt WSL, St. Niklaus, pp. 21-31.

Delaloye, R., Perruchoud, E., Avian, M., Kaufmann, V., Bodin, X., Hausmann, H., Ikeda, A., Kääb, A., Kellerer-Pirklbauer, A., Krainer, K., Lambiel, C., Mihajiovic, D., Staub, B., Roer, I. and Thibert, E., 2008. Recent interannual variations of rock glacier creep in the European Alps. In: D.L. Kane and K.M. Hinkel (Editors), 9th International Conference on Permafrost, Fairbanks, Alaska, pp. 343-348.

Deluigi, N., Lambiel, C. and Kanevski, M., 2017. Data-driven mapping of the potential mountain permafrost distribution. Science of The Total Environment, 590–591: 370-380.

Dhar, O.N. and Nandargi, S., 2004. Rainfall distribution over the Arunachal Pradesh Himalayas. Weather, 59(6): 155-157.

Dimri, A.P., Niyogi, D., Barros, A.P., Ridley, J., Mohanty, U.C., Yasunari, T. and Sikka, D.R., 2015. Western disturbances: A review. Reviews of Geophysics, 53(2): 225-246.

Drewes, J., Moreiras, S. and Korup, O., 2018. Permafrost activity and atmospheric warming in the Argentinian Andes. Geomorphology, 323: 13-24.

Duffy, J., Shutler, J., Witt, M., DeBell, L. and Anderson, K., 2018. Tracking fine-scale structural changes in coastal dune morphology using kite aerial photography and uncertainty-assessed structure-from-motion photogrammetry. Remote Sensing, 10(9): 1494.

Duguay, M.A., Edmunds, A., Arenson, L.U. and Wainstein, P.A., 2015. Quantifying the Significance of the Hydrological Contribution of a Rock Glacier - A Review, GEOQuébec 2015: Challenges from North to South, 68th Canadian Geotechnical Conference and 7th Canadian Permafrost Conference, Québec, Canada.

Dusik, J.-M., Leopold, M., Heckmann, T., Haas, F., Hilger, L., Morche, D., Neugirg, F. and Becht, M., 2015. Influence of glacier advance on the development of the multipart Riffeltal rock glacier, Central Austrian Alps. Earth Surface Processes and Landforms, 40(7): 965-980.

Echelard, T., Krysiecki, J.M., Gay, M. and Schoeneich, P., 2013. Détection des mouvements de glaciers rocheux dans les Alpes françaises par interférométrie radar différentielle (D-InSAR) dérivée des archives satellitaires ERS (European Remote Sensing). Geomorphologie-Relief Processus Environnement, 19(3): 231-242.

Elconin, R.F. and LaChapelle, E.R., 1997. Flow and internal structure of a rock glacier. Journal of Glaciology, 43(144): 238-244.

Ellis, J.M. and Calkin, P.E., 1979. Nature and Distribution of Glaciers, Neoglacial Moraines, and Rock Glaciers, East-Central Brooks Range, Alaska. Arctic and Alpine Research, 11(4): 403-420.

Emmer, A., Loarte, E.C., Klimeš, J. and Vilímek, V., 2015. Recent evolution and degradation of the bent Jatunraju glacier (Cordillera Blanca, Peru). Geomorphology, 228: 345-355.

Emmert, A. and Kneisel, C., 2017. Internal structure of two alpine rock glaciers investigated by quasi-3-D electrical resistivity imaging. The Cryosphere, 11(2): 841-855.

Eriksen, H.Ø., Rouyet, L., Lauknes, T.R., Berthling, I., Isaksen, K., Hindberg, H., Larsen, Y. and Corner, G.D., 2018. Recent acceleration of a rock glacier complex, Ádjet, Norway, documented by 62 years of remote sensing observations. Geophysical Research Letters, 45: 8314–8323.

Esper Angillieri, M.Y., 2009. A preliminary inventory of rock glaciers at 30°S latitude, Cordillera Frontal of San Juan, Argentina. Quaternary International, 195(1–2): 151-157.

Esper Angillieri, M.Y., 2017. Permafrost distribution map of San Juan Dry Andes (Argentina) based on rock glacier sites. Journal of South American Earth Sciences, 73(Supplement C): 42-49.

Etzelmüller, B., Farbrot, H., Guðmundsson, Á., Humlum, O., Tveito, O.E. and Björnsson, H., 2007. The regional distribution of mountain permafrost in Iceland. Permafrost and Periglacial Processes, 18(2): 185-199.

Fabrot, H., Isaksen, K., Eiken, T., Kääb, A. and Sollid, J.L., 2005. Composition and internal structures of a rock glacier on the strandflat of western Spitsbergen, Svalbard. Norsk Geografisk Tidsskrift - Norwegian Journal of Geography, 59(2): 139-148.

Falaschi, D., Castro, M., Masiokas, M., Tadono, T. and Ahumada, A.L., 2014. Rock glacier inventory of the Valles Calchaquíes region (~ 25°S), Salta, Argentina, derived from ALOS data. Permafrost and Periglacial Processes, 25(1): 69-75.

Falaschi, D., Masiokas, M., Tadono, T. and Couvreux, F., 2016. ALOS-derived glacier and rock glacier inventory of the Volcán Domuyo region (~36° S), southernmost Central Andes, Argentina. Zeitschrift für Geomorphologie, 60(3): 195-208.

Falaschi, D., Tadono, T. and Masiokas, M., 2015. Rock glaciers in the Patagonian Andes: An inventory for the Monte San Lorenzo (Cerro Cochrane) Massif, 47° S. Geografiska Annaler: Series A, Physical Geography, 97(4): 769-777.

Fegel, T.S., Baron, J.S., Fountain, A.G., Johnson, G.F. and Hall, E.K., 2016. The differing biogeochemical and microbial signatures of glaciers and rock glaciers. Journal of Geophysical Research: Biogeosciences, 121(3): 919-932.

Fernandes, M., Palma, P., Lopes, L., Ruiz-Fernández, J., Pereira, P. and Oliva, M., 2018. Spatial distribution and morphometry of permafrost-related landforms in the Central Pyrenees and associated paleoclimatic implications. Quaternary International, 470: 96-108.

Fischer, L., Kääb, A., Huggel, C. and Noetzli, J., 2006. Geology, glacier retreat and permafrost degradation as controlling factors of slope instabilities in a high-mountain rock wall: The Monte Rosa east face. Natural Hazards and Earth System Sciences, 6(5): 761-772.

Florentine, C., Skidmore, M., Speece, M., Link, C. and Shaw, C.A., 2014. Geophysical analysis of transverse ridges and internal structure at Lone Peak rock glacier, Big Sky, Montana, USA. Journal of Glaciology, 60(221): 453-462.

Fort, M., 2003. Are high altitude, lava stream-like, debris mixtures all rock glaciers? A perspective from the Western Himalaya. Zeitschrift fur Geomorphologie, Supplementband, 130: 11-29.

Forte, A.P., Villarroel, C.D. and Esper Angillieri, M.Y., 2016. Impact of natural parameters on rock glacier development and conservation in subtropical mountain ranges. Northern sector of the Argentine Central Andes. The Cryosphere Discuss., 2016: 1-24.

Fountain, A.G. and Walder, J.S., 1998. Water flow through temperate glaciers. Reviews of Geophysics, 36(3): 299-328.

Francou, B., Ribstein, P., Wagnon, P., Ramirez, E. and Pouyaud, B., 2005. Glaciers of the Tropical Andes: Indicators of Global Climate Variability. In: U.M. Huber, H.K.M. Bugmann and M.A. Reasoner (Editors), Global Change and Mountain Regions: An Overview of Current Knowledge. Springer Netherlands, Dordrecht, pp. 197-204.

Frans, C., Istanbulluoglu, E., Lettenmaier, D.P., Clarke, G., Bohn, T.J. and Stumbaugh, M., 2016. Implications of decadal to century scale glacio-hydrological change for water resources of the Hood River basin, OR, USA. Hydrological Processes, 30(23): 4314-4329.

Frauenfelder, R., Haeberli, W. and Hoelzle, M., 2003. Rockglacier occurrence and related terrain parameters in a study area of the Eastern Swiss Alps, Proceedings 8th International Conference on Permafrost. Swets and Zeitlinger, Lisse, pp. 253-258.

Frehner, M., Ling, A.H.M. and Gärtner-Roer, I., 2015. Furrow-and-ridge morphology on rockglaciers explained by gravity-driven buckle folding: A case study from the Murtèl Rockglacier (Switzerland). Permafrost and Periglacial Processes, 26(1): 57-66.

Frey, H., Machguth, H., Huss, M., Huggel, C., Bajracharya, S., Bolch, T., Kulkarni, A., Linsbauer, A., Salzmann, N. and Stoffel, M., 2014. Estimating the volume of glaciers in the Himalayan-Karakoram region using different methods. The Cryosphere, 8(6): 2313-2333.

Fyffe, C.L., Brock, B.W., Kirkbride, M.P., Mair, D.W.F., Arnold, N.S., Smiraglia, C., Diolaiuti, G. and Diotri, F., 2019. Do debris-covered glaciers demonstrate distinctive hydrological behaviour compared to clean glaciers? Journal of Hydrology, 570: 584-597.

Galanin, A.A., 2017. Rock glaciers in the Southern Chukchi Peninsula. Geomorphology RAS(1): 66-79 (in Russ.).

García, A., Ulloa, C., Amigo, G., Milana, J.P. and Medina, C., 2017. An inventory of cryospheric landforms in the arid diagonal of South America (high Central Andes, Atacama region, Chile). Quaternary International, 438(part A): 4-19.

Gardelle, J., Berthier, E., Arnaud, Y. and Kääb, A., 2013. Region-wide glacier mass balances over the Pamir-Karakoram-Himalaya during 1999-2011. The Cryosphere, 7: 1263-1286.

Gardner, A.S., Moholdt, G., Cogley, J.G., Wouters, B., Arendt, A.A., Wahr, J., Berthier, E., Hock, R., Pfeffer, W.T., Kaser, G., Ligtenberg, S.R.M., Bolch, T., Sharp, M.J., Hagen, J.O., van den Broeke, M.R. and Paul, F., 2013. A reconciled estimate of glacier contributions to sea level rise: 2003 to 2009. Science, 340(6134): 852-857.

Gardner, J.S. and Bajewsky, I., 1987. Hilda rock glacier stream discharge and sediment load characteristics, Sunwapta Pass area, Canadian Rocky Mountains. In: J.R. Giardino, J.F. Shroder Jr and J.D. Vitek (Editors), Rock Glaciers. Allen and Unwin, London, pp. 161-174.

Geiger, S.T., Daniels, J.M., Miller, S.N. and Nicholas, J.W., 2014. Influence of rock glaciers on stream hydrology in the La Sal Mountains, Utah. Arctic, Antarctic, and Alpine Research, 46(3): 645-658.

Giardino, J.R., Regmi, N.R. and Vitek, J.D., 2011. Rock Glaciers. In: V.P. Singh, P. Singh and U.K. Haritashya (Editors), Encyclopedia of Snow, Ice and Glaciers. Springer Netherlands, Dordrecht, pp. 943-948.

Giardino, J.R. and Vick, S.G., 1987. Geologic engineering aspects of rock glaciers In: J.R. Giardino, J.F. Shroder and J.D. Vitek (Editors), Rock Glaciers. Allen and Unwin, London, pp. 265-288.

Giardino, J.R. and Vitek, J.D., 1988. The significance of rock glaciers in the glacial-periglacial landscape continuum. Journal of Quaternary Science, 3(1): 97-103.

Giardino, J.R., Vitek, J.D. and Demorett, J.L., 1992. A model of water movement in rock glaciers and associated water characteristics. In: J.C. Dixon and A.D. Abrahams (Editors), Periglacial geomorphology: proceedings of the 22nd Annual Binghamton Symposium in Geomorphology. Wiley, Chichester; New York, pp. 159-184.

Glasser, N.F., Harrison, S. and Jansson, K.N., 2009. Topographic controls on glacier sediment–landform associations around the temperate North Patagonian Icefield. Quaternary Science Reviews, 28(25): 2817-2832.

Glasser, N.F., Holt, T.O., Evans, Z.D., Davies, B.J., Pelto, M. and Harrison, S., 2016. Recent spatial and temporal variations in debris cover on Patagonian glaciers. Geomorphology, 273: 202-216.

Gleick, P.H. and Palaniappan, M., 2010. Peak water limits to freshwater withdrawal and use. Proceedings of the National Academy of Sciences of the United States of America, 107(25): 11155-11162.

Gorbunov, A.P., Marchenko, S.S. and Seversky, E.V., 2004. The thermal environment of blocky materials in the mountains of Central Asia. Permafrost and Periglacial Processes, 15(1): 95-98.

Gorbunov, A.P., Seversky, E.V., Titkov, S.N., Marchenko, S.S. and Popov, M., 1998. Rock glaciers, Zailiysiky Range, Kungei Ranges, Tienshan, Kazakhstan. . In: NSIDC (Editor). Digital media, Boulder, CO.

Gorbunov, A.P., Titkov, S.N. and Polyakov, V.G., 1992. Dynamics of rock glaciers of the Northern Tien Shan and the Djungar Ala Tau, Kazakhstan. Permafrost and Periglacial Processes, 3(1): 29-39.

Gorelick, N., Hancher, M., Dixon, M., Ilyushchenko, S., Thau, D. and Moore, R., 2017. Google Earth Engine: Planetary-scale geospatial analysis for everyone. Remote Sensing of Environment, 202: 18-27.

Govindha Raj, K.B., 2017. A birds eye view of debris-avalanche on Miyar Glacier, Chenab Basin, India. Journal of the Indian Society of Remote Sensing, 45(6): 1031-1038.

Graham, D.J. and Midgley, N.G., 2000. Graphical representation of particle shape using triangular diagrams: An Excel spreadsheet method. Earth Surface Processes and Landforms, 25(13): 1473-1477.

Grêt-Regamey, A., Brunner, S.H. and Kienast, F., 2012. Mountain ecosystem services: Who cares? Mountain Research and Development, 32(S1): S23-S34.

Grinsted, A., 2013. An estimate of global glacier volume. The Cryosphere, 7(1): 141-151.

Gruber, S., 2012. Derivation and analysis of a high-resolution estimate of global permafrost zonation. The Cryosphere, 6(1): 221-233.

Gruber, S., Fleiner, R., Guegan, E., Panday, P., Schmid, M.O., Stumm, D., Wester, P., Zhang, Y. and Zhao, L., 2016. Review article: Inferring permafrost and permafrost thaw in the mountains of the Hindu Kush Himalaya region. The Cryosphere Discuss., 2016: 1-29.

Gruber, S. and Hoelzle, M., 2008. The Cooling Effect of Coarse Blocks Revisited: A Modeling Study of a Purely Conductive Mechanism, 9th International Conference on Permafrost, Fairbanks, Alaska, pp. 557-561.

Guglielmin, M., Camusso, M., Polesello, S. and Valsecchi, S., 2004. An old relict glacier body preserved in permafrost environment: The Foscagno rock glacier ice core (Upper Valtellina, Italian central Alps). Arctic Antarctic and Alpine Research, 36(1): 108-116.

Guglielmin, M., Ponti, S. and Forte, E., 2018. The origins of Antarctic rock glaciers: Periglacial or glacial features? Earth Surface Processes and Landforms, 43(7): 1390-1402.

Guglielmin, M. and Smiraglia, C., 1997. Rock glacier inventory of the Italian Alps. Italian Glaciological Committee Archives, 3: 117.

Guglielmin, M. and Smiraglia, C., 1998. The Rock Glacier Inventory of the Italian Alps, Permafrost - Seventh International Conference (Proceedings). Collection Nordicana, Yellowknife (Canada).

Guo, W., Liu, S., Xu, J., Wu, L., Shangguan, D., Yao, X., Wei, J., Bao, W., Yu, P., Liu, Q. and Jiang, Z., 2015. The second Chinese glacier inventory: Data, methods and results. Journal of Glaciology, 61(226): 357-372.

Haeberli, W., 1983. Permafrost-glacier relationships in the Swiss Alps - today and in the past, Permafrost Fourth International Conference, NAP/Washington D.C., pp. 415-420.

Haeberli, W., 1985. Creep of mountain permafrost: Internal structure and flow of alpine rock glaciers. Mitteilungen der Versuchsanstalt für Wasserbau, Hydrologie und Glaziologie an der Eidgenössischen Technischen Hochschule Zürich, 77, Zürich, 142 pp.

Haeberli, W., 1989. Glacier ice-cored rock glaciers in the Yukon Territory, Canada? Journal of Glaciology, 35(120): 294-295.

Haeberli, W., 2000. Modern research perspectives relating to permafrost creep and rock glaciers: A discussion. Permafrost and Periglacial Processes, 11(4): 290-293.

Haeberli, W., 2005. Investigating glacier-permafrost relationships in high-mountain areas: Historical background, selected examples and research needs. In: C. Harris and J.B. Murton (Editors), Cryospheric Systems: Glaciers and Permafrost. Geological Society, London, Special Publications, pp. 29-37.

Haeberli, W., 2013. Mountain permafrost — research frontiers and a special long-term challenge. Cold Regions Science and Technology, 96: 71-76.

Haeberli, W. and Beniston, M., 1998. Climate change and its impacts on glaciers and permafrost in the Alps. Ambio, 27(4): 258-265.

Haeberli, W., Hallet, B., Arenson, L., Elconin, R.F., Humlum, O., Kääb, A., Kaufmann, V., Ladanyi, B., Matsuoka, N., Springman, S. and Mühll, D.V., 2006. Permafrost creep and rock glacier dynamics. Permafrost and Periglacial Processes, 17(3): 189-214.

Haeberli, W., Hoelzle, M., Kääb, A., Keller, F., Vonder Mühll, D. and Wagner, S., 1998. Ten years after drilling through the permafrost of the active rock glacier Murtèl, eastern Swiss Alps: Answered questions and new perspectives. In: A.G. Lewkowicz and M. Allard (Editors), Proceedings of the Seventh International Conference on Permafrost. Proceedings. Collection Nordicana, Yellowknife (Canada), pp. 403-410.

Haeberli, W., Kääb, A., Vonder Mühll, D. and Teysseire, P., 2001. Prevention of outburst floods from periglacial lakes at Grubengletscher, Valais, Swiss Alps. Journal of Glaciology, 47(156): 111-122.

Haeberli, W., Noetzli, J., Arenson, L., Delaloye, R., Gärtner-Roer, I., Gruber, S., Isaksen, K., Kneisel, C., Krautblatter, M. and Phillips, M., 2010. Mountain permafrost: Development and challenges of a young research field. Journal of Glaciology, 56(200): 1043-1058.

Haeberli, W. and Vonder Mühll, D., 1996. On the characteristics and possible origins of ice in rock glacier permafrost. Zeitschrift für Geomorphologie, Supplementband, 104: 43-57.

Hambrey, M.J. and Ehrmann, W., 2004. Modification of sediment characteristics during glacial transport in high-alpine catchments: Mount Cook area, New Zealand. Boreas, 33(4): 300-318.

Hambrey, M.J. and Glasser, N.F., 2003. Glacial sediments: Processes, environments and facies. In: G.V. Middleton (Editor), Encyclopedia of Sediments and Sedimentary Rocks. Springer Netherlands, Kluwer, Dordrecht, pp. 316-331.

Hambrey, M.J., Quincey, D.J., Glasser, N.F., Reynolds, J.M., Richardson, S.J. and Clemmens, S., 2008. Sedimentological, geomorphological and dynamic context of debris-mantled glaciers, Mount Everest (Sagarmatha) region, Nepal. Quaternary Science Reviews, 27(25–26): 2361-2389.

Hamilton, S.J. and Whalley, W.B., 1995. Rock glacier nomenclature: A re-assessment. Geomorphology, 14(1): 73-80.

Hanson, S. and Hoelzle, M., 2004. The thermal regime of the active layer at the Murtèl rock glacier based on data from 2002. Permafrost and Periglacial Processes, 15(3): 273-282.

Hanzer, F., Förster, K., Nemec, J. and Strasser, U., 2018. Projected cryospheric and hydrological impacts of 21st century climate change in the Ötztal Alps (Austria) simulated using a physically based approach. Hydrology and Earth System Sciences, 22: 1593-1614.

Harrington, J.S., Mozil, A., Hayashi, M. and Bentley, L.R., 2018. Groundwater flow and storage processes in an inactive rock glacier. Hydrological Processes, 32: 3070-3088.

Harris, C. and Murton, J.B., 2005. Interactions between glaciers and permafrost: An introduction. Geological Society, London, Special Publications, 242(1): 1-9.

Harris, S.A., Blumstengel, W.K., Cook, D., Krouse, H.R. and Whitley, G., 1994. Comparison of the water drainage from an active near-slope rock glacier and a glacier, St. Elias Mountains, Yukon Territory Erdkunde, 48(2): 81-91.

Harris, S.A. and Pedersen, D.E., 1998. Thermal regimes beneath coarse blocky materials. Permafrost and Periglacial Processes, 9(2): 107-120.

Harrison, S., 2009. Climate sensitivity: Implications for the response of geomorphological systems to future climate change. In: J. Knight and S. Harrison (Editors), Periglacial and Paraglacial Processes and Environments. Geological Society of London, London, pp. 257-265.

Harrison, S., Whalley, B. and Anderson, E., 2008. Relict rock glaciers and protalus lobes in the British Isles: Implications for late Pleistocene mountain geomorphology and palaeoclimate. Journal of Quaternary Science, 23(3): 287-304.

Hartl, L., Fischer, A., Klug, C. and Nicholson, L., 2016a. Can a simple numerical model help to fine-tune the analysis of ground-penetrating radar data? Hochebenkar rock glacier as a case study. Arctic, Antarctic, and Alpine Research, 48(2): 377-393.

Hartl, L., Fischer, A., Stocker-Waldhuber, M. and Abermann, J., 2016b. Recent speed-up of an alpine rock glacier: An updated chronology of the kinematics of Outer Hochebenkar rock glacier based on geodetic measurements. Geografiska Annaler: Series A, Physical Geography, 98(2): 129-141.

Hartvich, F., Blahut, J. and Stemberk, J., 2017. Rock avalanche and rock glacier: A compound landform study from Hornsund, Svalbard. Geomorphology, 276: 244-256.

Hauck, C., 2013. New concepts in geophysical surveying and data interpretation for permafrost terrain. Permafrost and Periglacial Processes, 24(2): 131-137.

Hauck, C., Boettcher, M. and Maurer, H., 2011. A new model for estimating subsurface ice content based on combined electrical and seismic data sets. Cryosphere, 5(2): 453-468.

Hauck, C. and Kneisel, C., 2008. Introduction. In: C. Hauck and C. Kneisel (Editors), Applied Geophysics in Periglacial Environments. Cambridge University Press, Cambridge, pp. xiii-xvi.

Hausmann, H., Krainer, K., Brückl, E. and Mostler, W., 2007. Internal structure and ice content of Reichenkar rock glacier (Stubai Alps, Austria) assessed by geophysical investigations. Permafrost and Periglacial Processes, 18(4): 351-367.

Hausmann, H., Krainer, K., Brückl, E. and Ullrich, C., 2012. Internal structure, ice content and dynamics of Ölgrube and Kaiserberg rock glaciers (Ötztal Alps, Austria) determined from geophysical surveys. Austrian Journal of Earth Sciences, 105(2): 12-31.

Hedding, D.W., 2016. Pronival ramparts: A review. Progress in Physical Geography: Earth and Environment, 40(6): 835-855.

Hewitt, K., 2014. Rock glaciers and related phenomena. In: K. Hewitt (Editor), Glaciers of the Karakoram Himalaya: Glacial Environments, Processes, Hazards and Resources. Springer Netherlands, Dordrecht, pp. 267-289.

Hock, R., Bliss, A., Marzeion, B.E.N., Giesen, R.H., Hirabayashi, Y., Huss, M., RadiĆ, V. and Slangen, A.B.A., 2019a. GlacierMIP – A model intercomparison of global-scale glacier mass-balance models and projections. Journal of Glaciology, 65(251): 453-467.

Hock, R., Rasul, G., Adler, C., Cáceres, B., Gruber, S., Hirabayashi, Y., Jackson, M., Kääb, A., Kang, S., Kutuzov, S., Milner, A., Molau, U., Morin, S., Orlove, B. and H., S., 2019b. High Mountain Areas. In: H.-O. Pörtner, D.C. Roberts, V. Masson-Delmotte, P. Zhai, M. Tignor, E. Poloczanska, K. Mintenbeck, M. Nicolai, A. Okem, J. Petzold, B. Rama and N. Weyer (Editors), IPCC Special Report on the Ocean and Cryosphere in a Changing Climate, In Press.

Humlum, O., 1988. Rock glacier appearance level and rock glacier initiation line altitude: A methodological approach to the study of rock glaciers. Arctic and Alpine Research, 20(2): 160-178.

Humlum, O., 1996. Origin of rock glaciers: Observations from Mellemfjord, Disko Island, Central West Greenland. Permafrost and Periglacial Processes, 7(4): 361-380.

Humlum, O., 1997. Active layer thermal regime at three rock glaciers in Greenland. Permafrost and Periglacial Processes, 8(4): 383-408.

Humlum, O., 1998. The climatic significance of rock glaciers. Permafrost and Periglacial Processes, 9(4): 375-395.

Humlum, O., 2000. The geomorphic significance of rock glaciers: Estimates of rock glacier debris volumes and headwall recession rates in West Greenland. Geomorphology, 35(1–2): 41-67.

Humlum, O., Christiansen, H.H. and Juliussen, H., 2007. Avalanche-derived rock glaciers in Svalbard. Permafrost and Periglacial Processes, 18(1): 75-88.

Huss, M., Bookhagen, B., Huggel, C., Jacobsen, D., Bradley, R.S., Clague, J.J., Vuille, M., Buytaert, W., Cayan, D.R., Greenwood, G., Mark, B.G., Milner, A.M., Weingartner, R. and Winder, M., 2017. Toward mountains without permanent snow and ice. Earth's Future, 5(5): 418-435.

Huss, M. and Farinotti, D., 2012. Distributed ice thickness and volume of all glaciers around the globe. Journal of Geophysical Research: Earth Surface, 117(F4).

Huss, M. and Hock, R., 2015. A new model for global glacier change and sea-level rise. Frontiers in Earth Science, 3(54).

Huss, M. and Hock, R., 2018. Global-scale hydrological response to future glacier mass loss. Nature Climate Change, 8(2): 135-140.

IANIGLA-CONICET, 2018. Inventario Nacional de Glaciares: Informe de la cuenca de los lagos Buenos Aires y Pueyrredón. IANIGLA-CONICET, Ministerio de Ambiente y Desarrollo Sustentable de la Nación, 69 pp.

Ikeda, A. and Matsuoka, N., 2002. Degradation of talus-derived rock glaciers in the Upper Engadin, Swiss Alps. Permafrost and Periglacial Processes, 13(2): 145-161.

Ikeda, A. and Matsuoka, N., 2006. Pebbly versus bouldery rock glaciers: Morphology, structure and processes. Geomorphology, 73(3–4): 279-296.

Ikeda, A., Matsuoka, N. and Kaab, A., 2008. Fast deformation of perennially frozen debris in a warm rock glacier in the Swiss Alps: An effect of liquid water. Journal of Geophysical Research-Earth Surface, 113(F1).

Ilyashuk, B.P., Ilyashuk, E.A., Psenner, R., Tessadri, R. and Koinig, K.A., 2014. Rock glacier outflows may adversely affect lakes: Lessons from the past and present of two neighboring water bodies in a crystalline-rock watershed. Environmental Science & Technology, 48(11): 6192-6200.

Ilyashuk, B.P., Ilyashuk, E.A., Psenner, R., Tessadri, R. and Koinig, K.A., 2018. Rock glaciers in crystalline catchments: Hidden permafrost-related threats to alpine headwater lakes. Global Change Biology, 24(4): 1548-1562.

Imaizumi, F., Nishiguchi, T., Matsuoka, N., Trappmann, D. and Stoffel, M., 2018. Interpretation of recent alpine landscape system evolution using geomorphic mapping and L-band InSAR analyses. Geomorphology, 310: 125-137.

Imhof, M., 1996. Modelling and verification of the permafrost distribution in the Bernese Alps (Western Switzerland). Permafrost and Periglacial Processes, 7(3): 267-280.

Immerzeel, W.W., van Beek, L.P.H. and Bierkens, M.F.P., 2010. Climate change will affect the Asian Water Towers. Science, 328(5984): 1382-1385.

Irvine-Fynn, T.D.L., Hodson, A.J., Moorman, B.J., Vatne, G. and Hubbard, A.L., 2011. Polythermal glacier hydrology: A review. Reviews of Geophysics, 49(4).

Isaksen, K., Odegard, R.S., Eiken, T. and Sollid, J.L., 2000. Composition, flow and development of two tongue-shaped rock glaciers in the permafrost of Svalbard. Permafrost and Periglacial Processes, 11(3): 241-257.

Ishikawa, M., Watanabe, T. and Nakamura, N., 2001. Genetic differences of rock glaciers and the discontinuous mountain permafrost zone in Kanchanjunga Himal, Eastern Nepal. Permafrost and Periglacial Processes, 12(3): 243-253.

Iwata, S., 1976. Late Pleistocene and Holocene moraines in the Sagarmatha (Everest) Region, Khumbu Himal: Glaciological expedition to Nepal, contribution no. 23. Journal of the Japanese Society of Snow and Ice, 38(Special): 109-114.

Iwata, S., Naito, N., Narama, C. and Karma, T., 2003. Rock glaciers and the lower limit of mountain permafrost in the Bhutan Himalayas. Zeitschrift für Geomorphologie, Supplementband, 130: 129-143.

Jacob, T., Wahr, J., Pfeffer, W.T. and Swenson, S., 2012. Recent contributions of glaciers and ice caps to sea level rise. Nature, 482: 514-518.

Jakob, M., 1992. Active rock glaciers and the lower limit of discontinuous alpine permafrost, Khumbu Himalaya, Nepal. Permafrost and Periglacial Processes, 3(3): 253-256.

James, M.R., Robson, S. and Smith, M.W., 2017. 3-D uncertainty-based topographic change detection with structure-from-motion photogrammetry: Precision maps for ground control and directly georeferenced surveys. Earth Surface Processes and Landforms, 42(12): 1769-1788.

Janke, J. and Frauenfelder, R., 2008. The relationship between rock glacier and contributing area parameters in the Front Range of Colorado. Journal of Quaternary Science, 23(2): 153-163.

Janke, J.R., 2005a. Long-term flow measurements (1961-2002) of the Arapaho, Taylor, and Fair rock glaciers, Front Range, Colorado. Physical Geography, 26(4): 313-336.

Janke, J.R., 2005b. Modeling past and future alpine permafrost distribution in the Colorado Front Range. Earth Surface Processes and Landforms, 30(12): 1495-1508.

Janke, J.R., 2007. Colorado Front Range rock glaciers: Distribution and topographic characteristics. Arctic, Antarctic, and Alpine Research, 39(1): 74-83.

Janke, J.R., 2013. Using airborne LiDAR and USGS DEM data for assessing rock glaciers and glaciers. Geomorphology, 195: 118-130.

Janke, J.R., Bellisario, A.C. and Ferrando, F.A., 2015. Classification of debris-covered glaciers and rock glaciers in the Andes of Central Chile. Geomorphology, 241: 98-121.

Janke, J.R., Ng, S. and Bellisario, A., 2017. An inventory and estimate of water stored in firn fields, glaciers, debris-covered glaciers, and rock glaciers in the Aconcagua River Basin, Chile. Geomorphology, 296: 142-152.

Janke, J.R., Regmi, N.R., Giardino, J.R. and Vitek, J.D., 2013. Rock glaciers. In: J. Shroder, R. Giardino and J. Harbor (Editors), Treatise on Geomorphology. Academic Press, San Diego, CA, pp. 238-273.

Jansen, F. and Hergarten, S., 2006. Rock glacier dynamics: Stick-slip motion coupled to hydrology. Geophysical Research Letters, 33(10): L10502.

Jansson, P., Hock, R. and Schneider, T., 2003. The concept of glacier storage: A review. Journal of Hydrology, 282(1–4): 116-129.

Jarman, D., Wilson, P. and Harrison, S., 2013. Are there any relict rock glaciers in the British mountains? Journal of Quaternary Science, 28(2): 131-143.

Jiménez Cisneros, B.E., Oki, T., Arnell, N.W., Benito, B., Cogley, J.G., Döll, P., Jiang, T. and Mwakalila, S.S., 2014. Freshwater resources. In: C.B. Field, V.R. Barros, D.J. Dokken, K.J. Mach, M.D. Mastrandrea, T.E. Bilir, M. Chatterjee, K.L. Ebi, Y.O. Estrada, R.C. Genova, B. Girma, E.S. Kissel, A.N. Levy, S. MacCracken, P.R. Mastrandrea and L.L. White (Editors), Climate Change 2014: Impacts, Adaptation, and Vulnerability. Part A: Global and Sectoral Aspects. Contribution of Working Group II to the Fifth Assessment Report of the Intergovernmental Panel on Climate Change. Cambridge University Press, Cambridge, United Kingdom and New York, NY, USA, pp. 229-269.

Jiskoot, H., 2011. Dynamics of Glaciers. In: V.P. Singh, P. Singh and U.K. Haritashya (Editors), Encyclopedia of Snow, Ice and Glaciers. Springer Netherlands, Dordrecht, pp. 245-256.

Johnson, B.G., Thackray, G.D. and Van Kirk, R., 2007. The effect of topography, latitude, and lithology on rock glacier distribution in the Lemhi Range, Central Idaho, USA. Geomorphology, 91(1–2): 38-50.

Johnson, P.G., 1978. Rock glacier types and their drainage systems, Grizzly Creek, Yukon Territory. Canadian Journal of Earth Sciences, 15(9): 1496-1507.

Johnson, P.G., 1980. Glacier-rock glacier transition in the Southwest Yukon Territory, Canada. Arctic and Alpine Research, 12(2): 195-204.

Johnson, P.G., 1981. The structure of a talus-derived rock glacier deduced from its hydrology. Canadian Journal of Earth Sciences, 18(9): 1422-1430.

Johnson, P.G., 1983. Rock glaciers. A case for a change in nomenclature. Geografiska Annaler: Series A, Physical Geography, 65(1/2): 27-34.

Johnson, P.G., 1984. Rock glacier formation by high-magnitude low-frequency slope processes in the Southwest Yukon. Annals of the Association of American Geographers, 74(3): 408-419.

Jones, D.B., Harrison, S., Anderson, K. and Betts, R.A., 2018a. Mountain rock glaciers contain globally significant water stores. Scientific Reports, 8(1): 2834.

Jones, D.B., Harrison, S., Anderson, K., Selley, H.L., Wood, J.L. and Betts, R.A., 2018b. The distribution and hydrological significance of rock glaciers in the Nepalese Himalaya. Global and Planetary Change, 160(Supplement C): 123-142.

Jones, D.B., Harrison, S., Anderson, K. and Whalley, W.B., 2019. Rock glaciers and mountain hydrology: A review. Earth-Science Reviews, 193: 66-90.

Juliussen, H. and Humlum, O., 2008. Thermal regime of openwork block fields on the mountains Elgåhogna and Sølen, Central-Eastern Norway. Permafrost and Periglacial Processes, 19(1): 1-18.

Kääb, A., 2013. Periglacial landforms, rock forms | rock glaciers and protalus forms. In: S.A. Elias (Editor), Encyclopedia of Quaternary Science. Elsevier, Oxford, pp. 2236-2242.

Kääb, A., Berthier, E., Nuth, C., Gardelle, J. and Arnaud, Y., 2012. Contrasting patterns of early twenty-first-century glacier mass change in the Himalayas. Nature, 488(7412): 495-498.

Kääb, A., Frauenfelder, R. and Roer, I., 2007. On the response of rockglacier creep to surface temperature increase. Global and Planetary Change, 56: 172-187.

Kääb, A. and Haeberli, W., 2001. Evolution of a high-mountain thermokarst lake in the Swiss Alps. Arctic, Antarctic, and Alpine Research, 33(4): 385-390.

Kääb, A., Haeberli, W. and Gudmundsson, G.H., 1997. Analysing the creep of mountain permafrost using high precision aerial photogrammetry: 25 years of monitoring Gruben rock glacier, Swiss Alps. Permafrost and Periglacial Processes, 8(4): 409-426.

Kääb, A., Kaufmann, V., Ladstädter, R. and Eiken, T., 2003. Rock glacier dynamics: Implications from high-resolution measurements of surface velocity fields. In: M. Phillips, S.M. Springman and L.U. Arenson (Editors), Permafrost, Vols 1 and 2, pp. 501-506.

Kääb, A. and Weber, M., 2004. Development of transverse ridges on rock glaciers: Field measurements and laboratory experiments. Permafrost and Periglacial Processes, 15(4): 379-391.

Kansakar, S.R., Hannah, D.M., Gerrard, J. and Rees, G., 2004. Spatial pattern in the precipitation regime of Nepal. International Journal of Climatology, 24(13): 1645-1659.

KAPshop, n.d. http://www.kapshop.com/, Accessed 4th December 2018.

Kargel, J.S., Leonard, G.J., Bishop, M.P., Kaab, A. and Raup, B.H., 2014. A world of changing glaciers: Summary and climatic context. In: J.S. Kargel, G.J. Leonard, M.P. Bishop, A. Kaab and B.H. Raup (Editors), Global Land Ice Measurements from Space Springer-Verlag Berlin Heidelberg, pp. 781-840.

Karki, R., Hasson, S., Schickhoff, U., Scholten, T. and Böhner, J., 2017. Rising Precipitation Extremes across Nepal. Climate, 5(1): 4.

Karki, R., Talchabhadel, R., Aalto, J. and Baidya, S.K., 2016. New climatic classification of Nepal. Theoretical and Applied Climatology, 125(3): 799-808.

Kaser, G., Großhauser, M. and Marzeion, B., 2010. Contribution potential of glaciers to water availability in different climate regimes. Proceedings of the National Academy of Sciences of the United States of America, 107(47): 20223-20227.

Kaufmann, V. and Ladstädter, R., 2007. Mapping of the 3D surface motion field of Doesen rock glacier (Ankogel group, Austria) and its spatio-temporal change (1954-1998) by means of digital photogrammetry, Proceedings of the 9th International Symposium of High Mountain Remote Sensing Cartography. Grazer Schriften der Geographie und Raumforschung, pp. 127-144.

Kellerer-Pirklbauer, A., Delaloye, R., Lambiel, C., Gärtner-Roer, I., Kaufmann, V., Scapozza, C., Krainer, K., Staub, B., Thibert, E., Bodin, X., Fischer, A., Hartl, L., Morra di Cella, U., Mair, V., Marcer, M. and Schoeneich, P., 2018. Interannual Variability of Rock Glacier Flow Velocities in the European Alps, 5th European Conference on Permafrost (EUCOP5), Chamonix, Mont-Blanc (France).

Kellerer-Pirklbauer, A. and Kaufmann, V., 2012. About the relationship between rock glacier velocity and climate parameters in Central Austria. Austrian Journal of Earth Sciences, 105(2): 94-112.

Kellerer-Pirklbauer, A. and Kaufmann, V., 2018. Deglaciation and its impact on permafrost and rock glacier evolution: New insight from two adjacent cirques in Austria. Science of The Total Environment, 621: 1397-1414.

Kellerer-Pirklbauer, A., Lieb, G.K. and Kleinferchner, H., 2012. A new rock glacier inventory of the eastern European Alps. Austrian Journal of Earth Sciences, 105(2): 78-93.

Kellerer-Pirklbauer, A., Pauritsch, M. and Winkler, G., 2013. Relict rock glaciers in alpine catchments: A regional study in Central Austria, EGU General Assembly 2013, Vienna, Austria.

Kellerer-Pirklbauer, A., Pauritsch, M. and Winkler, G., 2015. Widespread occurrence of ephemeral funnel hoarfrost and related air ventilation in coarse-grained sediments of a relict rock glacier in the Seckauer Tauern Range, Austria. Geografiska Annaler: Series A, Physical Geography, 97(3): 453-471.

Kellerer-Pirklbauer, A. and Rieckh, M., 2016. Monitoring nourishment processes in the rooting zone of an active rock glacier in an alpine environment. Zeitschrift für Geomorphologie, Supplementband, 60(3): 99-121.

Kellerer-Pirklbauer, A., Wagner, T. and Winkler, G., 2016. Inventorying rock glacier-suspected landforms and their hydrological catchments in the Styrian part of the Niedere Tauern Range using high-resolution digital elevation models. Joannea - Geologie und Palaontologie, 12: 53-62.

Kenner, R., 2019. Geomorphological analysis on the interaction of Alpine glaciers and rock glaciers since the Little Ice Age. Land Degradation & Development, 30(5): 580-591.

Kenner, R. and Magnusson, J., 2017. Estimating the effect of different influencing factors on rock glacier development in two regions in the Swiss Alps. Permafrost and Periglacial Processes, 28(1): 195-208.

Kenner, R., Phillips, M., Beutel, J., Hiller, M., Limpach, P., Pointner, E. and Volken, M., 2017a. Factors controlling velocity variations at short-term, seasonal and multiyear time scales, Ritigraben rock glacier, Western Swiss Alps. Permafrost and Periglacial Processes, 28(4): 675-684.

Kenner, R., Phillips, M., Hauck, C., Hilbich, C., Mulsow, C., Bühler, Y., Stoffel, A. and Buchroithner, M., 2017b. New insights on permafrost genesis and conservation in

talus slopes based on observations at Flüelapass, Eastern Switzerland. Geomorphology, 290: 101-113.

Kenner, R., Phillips, M., Limpach, P., Beutel, J. and Hiller, M., 2018. Monitoring mass movements using georeferenced time-lapse photography: Ritigraben rock glacier, western Swiss Alps. Cold Regions Science and Technology, 145: 127-134.

Kenner, R.B., Y.;Delaloye, R.;Ginzler, C.;Phillips, M., 2014. Monitoring of high alpine mass movements combining laser scanning with digital airborne photogrammetry. Geomorphology, 206: 492-504.

Kenyi, L.W. and Kaufmann, V., 2003. Estimation of rock glacier surface deformation using SAR interferometry data. IEEE Transactions on Geoscience and Remote Sensing, 41(6): 1512-1515.

King, O., Quincey, D.J., Carrivick, J.L. and Rowan, A.V., 2017. Spatial variability in mass loss of glaciers in the Everest region, central Himalayas, between 2000 and 2015. The Cryosphere, 11(1): 407-426.

Kirkbride, M.P., 2011. Debris-covered glaciers. In: V.P. Singh, P. Singh and U.K. Haritashya (Editors), Encyclopedia of Snow, Ice and Glaciers. Springer Netherlands, Dordrecht, pp. 180-182.

Klaar, M.J., Kidd, C., Malone, E., Bartlett, R., Pinay, G., Chapin, F.S. and Milner, A., 2015. Vegetation succession in deglaciated landscapes: Implications for sediment and landscape stability. Earth Surface Processes and Landforms, 40(8): 1088-1100.

Kneisel, C., Hauck, C., Fortier, R. and Moorman, B., 2008. Advances in geophysical methods for permafrost investigations. Permafrost and Periglacial Processes, 19(2): 157-178.

Knight, J. and Harrison, S., 2012. The impacts of climate change on terrestrial Earth surface systems. Nature Climate Change, 3(1): 24-29.

Knight, J. and Harrison, S., 2014a. Glacial and Paraglacial Environments. Geografiska Annaler: Series A, Physical Geography, 96(3): 241-244.

Knight, J. and Harrison, S., 2014b. Mountain glacial and paraglacial environments under global climate change: Lessons from the past, future directions and policy implications. Geografiska Annaler: Series A, Physical Geography, 96(3): 245-264.

Knight, J. and Harrison, S., 2018. Transience in cascading paraglacial systems. Land Degradation & Development, 29(6): 1991-2001.

Knight, J., Harrison, S. and Jones, D.B., 2019. Rock glaciers and the geomorphological evolution of deglacierizing mountains. Geomorphology, 324: 14-24.

Kohler, T., Wehrli, A. and Jurek, M., 2014. Mountains and climate change: A global concern. Sustainable Mountain Development Series. Centre for Development and Environment (CDE), Swiss Agency for Development and Cooperation (SDC) and Geographica Bernensia, Bern, Switzerland, 136 pp.

Konrad, S.K., Humphrey, N.F., Steig, E.J., Clark, D.H., Potter, N. and Pfeffer, W.T., 1999. Rock glacier dynamics and paleoclimatic implications. Geology, 27(12): 1131-1134.

Kraaijenbrink, P.D.A., Bierkens, M.F.P., Lutz, A.F. and Immerzeel, W.W., 2017. Impact of a global temperature rise of 1.5 degrees Celsius on Asia's glaciers. Nature, 549: 257-260.

Krainer, K., 2014. Permafrost and climate change in north and south Tyrol. permAfrost, Austrian Permafrost Research Initiative, Final Report: 51-67.

Krainer, K., Bressan, D., Dietre, B., Haas, J.N., Hajdas, I., Lang, K., Mair, V., Nickus, U., Reidl, D., Thies, H. and Tonidandel, D., 2015. A 10,300-year-old permafrost core from the active rock glacier Lazaun, southern Ötztal Alps (South Tyrol, northern Italy). Quaternary Research, 83(2): 324-335.

Krainer, K., Lang, K. and Hausmann, H., 2010. Active rock glaciers at Croda Rossa/Hohe Gaisl, Eastern Dolomites (Alto Adige/South Tyrol, Northern Italy). Geografia Fisica e Dinamica Quaternaria, 33(1): 25-36.

Krainer, K. and Mostler, W., 2000. Reichenkar rock glacier: A glacier derived debris-ice system in the western Stubai Alps, Austria. Permafrost and Periglacial Processes, 11(3): 267-275.

Krainer, K. and Mostler, W., 2002. Hydrology of active rock glaciers: Examples from the Austrian Alps. Arctic, Antarctic, and Alpine Research, 34(2): 142-149.

Krainer, K. and Mostler, W., 2006. Flow velocities of active rock glaciers in the Austrian Alps. Geografiska Annaler: Series A, Physical Geography, 88(4): 267-280.

Krainer, K., Mostler, W. and Spötl, C., 2007. Discharge from active rock glaciers, Austrian Alps: A stable isotope approach. Austrian Journal of Earth Sciences, 100: 102-112.

Krainer, K., Mussner, L., Behm, M. and Hausmann, H., 2012. Multi-disciplinary investigation of an active rock glacier in the Sella Group (Dolomites; northern Italy). Austrian Journal of Earth Sciences, 105(2): 48-62.

Krainer, K. and Ribis, M., 2012. A rock glacier inventory of the Tyrolean Alps (Austria). Austrian Journal of Earth Sciences, 105(2): 32-47.

Lambiel, C., Delaloye, R., Strozzi, T., Lugon, R. and Raetzo, H., 2008. ERS InSAR for assessing rock glacier activity. In: D.L. Kane and K.M. Hinkel (Editors), Proceedings of the 9th International Conference on Permafrost, Fairbanks, Alaska, pp. 1019–1024.

Lambrecht, A., Mayer, C., Hagg, W., Popovnin, V., Rezepkin, A., Lomidze, N. and Svanadze, D., 2011. A comparison of glacier melt on debris-covered glaciers in the northern and southern Caucasus. The Cryosphere, 5(3): 525-538.

Lamsal, D., Fujita, K. and Sakai, A., 2017. Surface lowering of the debris-covered area of Kanchenjunga Glacier in the eastern Nepal Himalaya since 1975, as revealed by Hexagon KH-9 and ALOS satellite observations. The Cryosphere, 11(6): 2815-2827.

Lang, T.J. and Barros, A.P., 2004. Winter storms in the Central Himalayas. Journal of the Meteorological Society of Japan. Ser. II, 82(3): 829-844.

Lardeux, P., Glasser, N., Holt, T. and Hubbard, B., 2016. Debris-covered glaciers extend the lifespan of water supplies in the European Alps. Geophysical Research Abstracts, 18: EGU2016-427.

Legg, B.N., 2016. Rock glacier morphology and morphometry in Glacier National Park, Northwest Montana, USA. Masters Thesis Thesis, Texas State University, 77 pp.

Lilleøren, K.S. and Etzelmüller, B., 2011. A regional inventory of rock glaciers and ice-cored moraines in Norway. Geografiska Annaler: Series A, Physical Geography, 93(3): 175-191.

Lilleøren, K.S., Etzelmüller, B., Gärtner-Roer, I., Kääb, A., Westermann, S. and Guðmundsson, Á., 2013. The Distribution, Thermal Characteristics and Dynamics of Permafrost in Tröllaskagi, Northern Iceland, as Inferred from the Distribution of Rock Glaciers and Ice-Cored Moraines. Permafrost and Periglacial Processes, 24(4): 322-335.

Linsbauer, A., Paul, F., Hoelzle, M., Frey, H. and Haeberli, W., 2009. The Swiss Alps without glaciers – a GIS-based modelling approach for reconstruction of glacier beds. In: R. Purves, S. Gruber, R. Straumann and T. Hengl (Editors), Proceedings of Geomorphometry 2009, University of Zurich, Zurich, Switzerland, pp. 243–247.

Liu, L., Millar, C.I., Westfall, R.D. and Zebker, H.A., 2013. Surface motion of active rock glaciers in the Sierra Nevada, California, USA: Inventory and a case study using InSAR. The Cryosphere, 7(4): 1109-1119.

LLC, A., 2017. Photoscan Professional (1.3.5).

Luckman, B.H. and Crockett, K.J., 1978. Distribution and characteristics of rock glaciers in the southern part of Jasper National Park, Alberta. Canadian Journal of Earth Sciences, 15(4): 540-550.

Luethi, R., Phillips, M. and Lehning, M., 2017. Estimating non-conductive heat flow leading to intra-permafrost talik formation at the Ritigraben Rock Glacier (Western Swiss Alps). Permafrost and Periglacial Processes, 28(1): 183-194.

Lugon, R., Delaloye, R., Serrano, E., Reynard, E., Lambiel, C. and González-Trueba, J.J., 2004. Permafrost and Little Ice Age glacier relationships, Posets Massif, Central Pyrenees, Spain. Permafrost and Periglacial Processes, 15(3): 207-220.

Lukas, S., Benn, D.I., Boston, C.M., Brook, M., Coray, S., Evans, D.J.A., Graf, A., Kellerer-Pirklbauer, A., Kirkbride, M.P., Krabbendam, M., Lovell, H., Machiedo, M., Mills, S.C., Nye, K., Reinardy, B.T.I., Ross, F.H. and Signer, M., 2013. Clast shape analysis and clast transport paths in glacial environments: A critical review of methods and the role of lithology. Earth-Science Reviews, 121: 96-116.

Lutz, A.F., Immerzeel, W.W., Shrestha, A.B. and Bierkens, M.F.P., 2014. Consistent increase in High Asia's runoff due to increasing glacier melt and precipitation. Nature Climate Change, 4: 587.

Lytkin, V.M. and Galanin, A.A., 2016. Rock glaciers in the Suntar-Khayata Range. Ice and Snow, 56(4): 511-524.

Małecki, J., Lovell, H., Ewertowski, W., Górski, Ł., Kurczaba, T., Latos, B., Miara, M., Piniarska, D., Płocieniczak, J., Sowada, T., Spiralski, M., Warczachowska, A. and Rabatel, A., 2018. The glacial landsystem of a tropical glacier: Charquini Sur, Bolivian Andes. Earth Surface Processes and Landforms, 43(12): 2584-2602.

Marcer, M., Serrano, C., Brenning, A., Bodin, X., Goetz, J. and Schoeneich, P., 2019. Evaluating the destabilization susceptibility of active rock glaciers in the French Alps. The Cryosphere, 13(1): 141-155.

Martin, H.E. and Whalley, W.B., 1987. Rock glaciers. Part 1: Rock glacier morphology: Classification and distribution. Progress in Physical Geography, 11(2): 260-282.

Marzeion, B., Cogley, J.G., Richter, K. and Parkes, D., 2014. Attribution of global glacier mass loss to anthropogenic and natural causes. Science, 345(6199): 919-921.

Marzeion, B., Jarosch, A.H. and Hofer, M., 2012. Past and future sea-level change from the surface mass balance of glaciers. The Cryosphere, 6(6): 1295-1322.

Mateo, E.I. and Daniels, J.M., 2019. Surface hydrological processes of rock glaciated basins in the San Juan Mountains, Colorado. Physical Geography, 40(3): 275-293.

Maurer, H. and Huack, C., 2007. Instruments and methods: Geophysical imaging of alpine rock glaciers. Journal of Glaciology, 53(180).

McCarroll, D., 2016. Simple Statistical Tests for Geography. Chapman and Hall/CRC, Philadelphia, PA, USA, 336 pp.

McColl, S.T., 2012. Paraglacial rock-slope stability. Geomorphology, 153-154: 1-16.

Merz, K., Green, A.G., Buchli, T., Springman, S.M. and Maurer, H., 2015a. A new 3-D thin-skinned rock glacier model based on helicopter GPR results from the Swiss Alps. Geophysical Research Letters, 42(11): 4464-4472.

Merz, K., Maurer, H., Buchli, T., Horstmeyer, H., Green, A.G. and Springman, S.M., 2015b. Evaluation of ground-based and helicopter ground-penetrating radar data acquired across an alpine rock glacier. Permafrost and Periglacial Processes, 26(1): 13-27.

Messenzehl, K., Meyer, H., Otto, J.-C., Hoffmann, T. and Dikau, R., 2017. Regional-scale controls on the spatial activity of rockfalls (Turtmann Valley, Swiss Alps) — A multivariate modeling approach. Geomorphology, 287: 29-45.

Messerli, B., Viviroli, D. and Weingartner, R., 2004. Mountains of the world: Vulnerable water towers for the 21st Century. Ambio, 13: 29-34.

Mewes, B., Hilbich, C., Delaloye, R. and Hauck, C., 2017. Resolution capacity of geophysical monitoring regarding permafrost degradation induced by hydrological processes. The Cryosphere, 11(6): 2957-2974.

Micallef, A., Ribó, M., Canals, M., Puig, P., Lastras, G. and Tubau, X., 2014. Space-for-time substitution and the evolution of a submarine canyon–channel system in a passive progradational margin. Geomorphology, 221: 34-50.

Micheletti, N. and Lane, S.N., 2016. Water yield and sediment export in small, partially glaciated Alpine watersheds in a warming climate. Water Resources Research, 52(6): 4924-4943.

Millar, C.I. and Westfall, R.D., 2008. Rock glaciers and related periglacial landforms in the Sierra Nevada, CA, USA; Inventory, distribution and climatic relationships. Quaternary International, 188(1): 90-104.

Millar, C.I., Westfall, R.D. and Delany, D.L., 2013. Thermal and hydrologic attributes of rock glaciers and periglacial talus landforms: Sierra Nevada, California, USA. Quaternary International, 310: 169-180.

Milner, A.M., Khamis, K., Battin, T.J., Brittain, J.E., Barrand, N.E., Füreder, L., Cauvy-Fraunié, S., Gíslason, G.M., Jacobsen, D., Hannah, D.M., Hodson, A.J., Hood, E., Lencioni, V., Ólafsson, J.S., Robinson, C.T., Tranter, M. and Brown, L.E., 2017. Glacier shrinkage driving global changes in downstream systems. Proceedings of the National Academy of Sciences, 114(37): 9770-9778.

Mölg, N., Bolch, T., Rastner, P., Strozzi, T. and Paul, F., 2018. A consistent glacier inventory for Karakoram and Pamir derived from Landsat data: Distribution of debris cover and mapping challenges. Earth System Science Data, 10(4): 1807-1827.

Moncrieff, A.C.M., 1989. Classification of poorly-sorted sedimentary rocks. Sedimentary Geology, 65(1): 191-194.

Monnier, S., Camerlynck, C. and Rejiba, F., 2008. Ground penetrating radar survey and stratigraphic interpretation of the Plan du Lac rock glaciers, Vanoise Massif, northern French Alps. Permafrost and Periglacial Processes, 19(1): 19-30.

Monnier, S., Camerlynck, C., Rejiba, F., Kinnard, C. and Galibert, P.-Y., 2013. Evidencing a large body of ice in a rock glacier, Vanoise Massif, Northern French Alps. Geografiska Annaler: Series A, Physical Geography, 95(2): 109-123.

Monnier, S. and Kinnard, C., 2013. Internal structure and composition of a rock glacier in the Andes (upper Choapa valley, Chile) using borehole information and ground-penetrating radar. Annals of Glaciology, 54(64): 61-72.

Monnier, S. and Kinnard, C., 2015a. Internal structure and composition of a rock glacier in the Dry Andes, inferred from ground-penetrating radar data and its artefacts. Permafrost and Periglacial Processes, 26(4): 335-346.

Monnier, S. and Kinnard, C., 2015b. Reconsidering the glacier to rock glacier transformation problem: New insights from the central Andes of Chile. Geomorphology, 238: 47-55.

Monnier, S. and Kinnard, C., 2017. Pluri-decadal (1955–2014) evolution of glacier–rock glacier transitional landforms in the central Andes of Chile (30–33 °S). Earth Surface Dynamics, 5(3): 493-509.

Mountain Research Initiative EDW Working Group, 2015. Elevation-dependent warming in mountain regions of the world. Nature Climate Change, 5(5): 424-430.

Mountain Research Initiative, E.D.W.W.G., 2015. Elevation-dependent warming in mountain regions of the world. Nature Climate Change, 5: 424.

Müller, J., Vieli, A. and Gärtner-Roer, I., 2016. Rock glaciers on the run – understanding rock glacier landform evolution and recent changes from numerical flow modeling. The Cryosphere, 10(6): 2865-2886.

Munroe, J.S., 2018. Distribution, evidence for internal ice, and possible hydrologic significance of rock glaciers in the Uinta Mountains, Utah, USA. Quaternary Research, 90(1): 50-65.

Nagai, H., Fujita, K., Nuimura, T. and Sakai, A., 2013. Southwest-facing slopes control the formation of debris-covered glaciers in the Bhutan Himalaya. The Cryosphere, 7(4): 1303-1314.

Nakawo, M., Iwata, S., Watanabe, O. and Yoshida, M., 1986. Processes which distribute supraglacial debris on the Khumbu Glacier, Nepal Himalaya. Annals of Glaciology, 8: 129-131.

Nakawo, M., Yabuki, H. and Sakai, A., 1999. Characteristics of Khumbu Glacier, Nepal Himalaya: Recent change in the debris-covered area. Annals of Glaciology, 28: 118-122.

Nicholson, L. and Benn, D.I., 2013. Properties of natural supraglacial debris in relation to modelling sub-debris ice ablation. Earth Surface Processes and Landforms, 38(5): 490-501.

Nickus, U., Abermann, J., Fischer, A., Krainer, K., Schneider, H., Span, N. and Thies, H., 2015. Rock glacier Äußeres Hochebenkar (Austria) – recent results of a monitoring network. Zeitschrift für Gletscherkunde und Glazialgeologie, 47/48: 43-62.

Nuimura, T., Fujita, K., Yamaguchi, S. and Sharma, R.R., 2012. Elevation changes of glaciers revealed by multitemporal digital elevation models calibrated by GPS survey in the Khumbu region, Nepal Himalaya, 1992–2008. Journal of Glaciology, 58(210): 648-656.

Nyenhuis, M., Hoelzle, M. and Dikau, R., 2005. Rock glacier mapping and permafrost distribution modelling in the Turtmanntal, Valais, Switzerland. Zeitschrift Fur Geomorphologie, 49(3): 275-292.

Ødegård, R.S., Isaksen, K., Eiken, T. and Sollid, J.L., 2003. Terrain analyses and surface velocity measurements of the Hiorthfjellet rock glacier, Svalbard. Permafrost and Periglacial Processes, 14(4): 359-365.

Onaca, A., Ardelean, F., Urdea, P. and Magori, B., 2017. Southern Carpathian rock glaciers: Inventory, distribution and environmental controlling factors. Geomorphology, 293(Part B): 391-404.

Onaca, A.L., Urdea, P. and Ardelean, A.C., 2013. Internal structure and permafrost characteristics of the rock glaciers of Southern Carpathians (Romania) assessed by geoelectrical soundings and thermal monitoring. Geografiska Annaler: Series A, Physical Geography, 95(3): 249-266.

Ouimet, W.B., Whipple, K.X. and Granger, D.E., 2009. Beyond threshold hillslopes: Channel adjustment to base-level fall in tectonically active mountain ranges. Geology, 37(7): 579-582.

Outcalt, S.I. and Benedict, J.B., 1965. Photo-interpretation of two types of rock glacier in the Colorado Front Range, U.S.A. Journal of Glaciology, 5(42): 849-856.

Owen, L.A. and England, J., 1998. Observations on rock glaciers in the Himalayas and Karakoram Mountains of northern Pakistan and India. Geomorphology, 26(1–3): 199-213.

Page, A., 2009. A topographic and photogrammetric study of rock glaciers in the southern Yukon Territory. M.Sc. Thesis, University of Ottawa (Canada), 160 pp.

Paine, A.D.M., 1985. 'Ergodic' reasoning in geomorphology: Time for a review of the term? Progress in Physical Geography: Earth and Environment, 9(1): 1-15.

Palma, P., Oliva, M., García-Hernández, C., Gómez Ortiz, A., Ruiz-Fernández, J., Salvador-Franch, F. and Catarineu, M., 2017. Spatial characterization of glacial and periglacial landforms in the highlands of Sierra Nevada (Spain). Science of The Total Environment, 584-585(Supplement C): 1256-1267.

Pandey, P., 2019. Inventory of rock glaciers in Himachal Himalaya, India using high-resolution Google Earth imagery. Geomorphology, 340: 103-115.

Parry, L., Harrison, S., Betts, R., Shannon, S., Jones, D.B. and Knight, J., 2020. Impacts of Climate Change on Himalayan Glaciers: Processes, Predictions and Uncertainties. In: A.P. Dimri, B. Bookhagen, M. Stoffel and T. Yasunari (Editors), Himalayan Weather and Climate and their Impact on the Environment. Springer International Publishing, Cham, pp. 331-349.

Paterson, W.S.B., 1994. The Physics of Glaciers. Butterworth-Heinemann, Oxford, 480 pp.

Paul, F., Barry, R.G., Cogley, J.G., Frey, H., Haeberli, W., Ohmura, A., Ommanney, C.S.L., Raup, B., Rivera, A. and Zemp, M., 2009. Recommendations for the compilation of glacier inventory data from digital sources. Annals of Glaciology, 50(53): 119-126.

Paul, F., Winsvold, S., Kääb, A., Nagler, T. and Schwaizer, G., 2016. Glacier remote sensing using Sentinel-2. Part II: Mapping glacier extents and surface facies, and comparison to Landsat 8. Remote Sensing, 8(7): 575.

Pellicciotti, F., Carenzo, M., Bordoy, R. and Stoffel, M., 2014. Changes in glaciers in the Swiss Alps and impact on basin hydrology: Current state of the art and future research. Science of The Total Environment, 493: 1152-1170.

PERMOS, 2016. Permafrost in Switzerland 2010/2011 to 2013/2014. In: J. Noetzli, R. Luethi and B. Staub (Editors), Glaciological Report (Permafrost) No. 12-15 of the Cryospheric Commission of the Swiss Academy of Sciences, pp. 85.

Perruchoud, E. and Delaloye, R., 2007. Short-Term Changes in Surface Velocities on the Becs-de-Bosson Rock Glacier (western Swiss Alps), 9th International Symposium on High Mountain Remote Sensing Cartography. Grazer Schriften der Geographie und Raumforschung, Graz, pp. 131-136.

Perucca, L. and Esper Angillieri, M., 2011. Glaciers and rock glaciers' distribution at 28° SL, Dry Andes of Argentina, and some considerations about their hydrological significance. Environmental Earth Sciences, 64(8): 2079-2089.

Perucca, L. and Esper Angillieri, Y., 2008. A preliminary inventory of periglacial landforms in the Andes of La Rioja and San Juan, Argentina, at about 28°S. Quaternary International, 190(1): 171-179.

Petersen, E., Holt, J., Stuurman, C., Levy, J., Nerozzi, S., Paine, J., Larsen, C. and Fahnestock, M., 2016. Sourdough Rock Glacier, Alaska: An Analog to Martian Debris-Covered Glaciers, 47th Lunar and Planetary Science Conference.

Pfeffer, W.T., Arendt, A.A., Bliss, A., Bolch, T., Cogley, J.G., Gardner, A.S., Hagen, J.-O., Hock, R., Kaser, G., Kienholz, C., Miles, E.S., Moholdt, G., Mölg, N., Paul, F., Radi, Valentina, Rastner, P., Raup, B.H., Rich, J. and Sharp, M.J., 2014. The Randolph Glacier Inventory: A globally complete inventory of glaciers. Journal of Glaciology, 60(221): 537-552.

Popescu, R., 2018. Permafrost investigations in Iezer Mountains, Southern Carpathians. Revista de Geomorfologie, 20: 102-122.

Popescu, R., Vespremeanu-Stroe, A., Onaca, A., Vasile, M., Cruceru, N. and Pop, O., 2017. Low-altitude permafrost research in an overcooled talus slope–rock glacier system in the Romanian Carpathians (Detunata Goală, Apuseni Mountains). Geomorphology, 295(Supplement C): 840-854.

Potter, J., N., Steig, E.J., Clark, D.H., Speece, M.A., Clark, G.M. and Updike, A.B., 1998. Galena Creek rock glacier revisited - new observations on an old controversy. Geografiska Annaler: Series A, Physical Geography, 80(3-4): 251-265.

Potter, N., 1972. Ice-cored rock glacier, Galena Creek, Northern Absaroka Mountains, Wyoming. Geological Society of America Bulletin, 83(10): 3025-3058.

Pourrier, J., Jourde, H., Kinnard, C., Gascoin, S. and Monnier, S., 2014. Glacier meltwater flow paths and storage in a geomorphologically complex glacial foreland: The case of the Tapado glacier, dry Andes of Chile (30°S). Journal of Hydrology, 519, Part A: 1068-1083.

Powers, M.C., 1953. A new roundness scale for sedimentary particles. Journal of Sedimentary Research, 23(2): 117-119.

Pritchard, H.D., 2017. Asia's glaciers are a regionally important buffer against drought. Nature, 545(7653): 169-174.

Pritchard, H.D., 2019. Asia's shrinking glaciers protect large populations from drought stress. Nature, 569(7758): 649-654.

Pruessner, L., Phillips, M., Farinotti, D., Hoelzle, M. and Lehning, M., 2018. Near-surface ventilation as a key for modeling the thermal regime of coarse blocky rock glaciers. Permafrost and Periglacial Processes, 29(3): 152-163.

Quincey, D.J., Luckman, A. and Benn, D., 2009. Quantification of Everest region glacier velocities between 1992 and 2002, using satellite radar interferometry and feature tracking. Journal of Glaciology, 55(192): 596-606.

Rabatel, A., Francou, B., Soruco, A., Gomez, J., Caceres, B., Ceballos, J.L., Basantes, R., Vuille, M., Sicart, J.-E., Huggel, C., Scheel, M., Lejeune, Y., Arnaud, Y., Collet, M., Condom, T., Consoli, G., Favier, V., Jomelli, V., Galarraga, R., Ginot, P., Maisincho, L., Mendoza, J., Menegoz, M., Ramirez, E., Ribstein, P., Suarez, W., Villacis, M. and Wagnon, P., 2013. Current state of glaciers in the tropical Andes: A multi-century perspective on glacier evolution and climate change. The Cryosphere, 7(1): 81-102.

Radić, V., Bliss, A., Beedlow, A.C., Hock, R., Miles, E. and Cogley, J.G., 2014. Regional and global projections of twenty-first century glacier mass changes in response to climate scenarios from global climate models. Climate Dynamics, 42(1): 37-58.

Radić, V. and Hock, R., 2010. Regional and global volumes of glaciers derived from statistical upscaling of glacier inventory data. Journal of Geophysical Research: Earth Surface, 115(F01010).

Ramírez, E., Francou, B., Ribstein, P., Descloitres, M., Guérin, R., Mendoza, J., Gallaire, R., Pouyaud, B. and Jordan, E., 2001. Small glaciers disappearing in the tropical Andes: A case-study in Bolivia: Glaciar Chacaltaya (16° S). Journal of Glaciology, 47(157): 187-194.

Ran, Z. and Liu, G., 2018. Rock glaciers in Daxue Shan, south-eastern Tibetan Plateau: An inventory, their distribution, and their environmental controls. The Cryosphere, 12(7): 2327-2340.

Rangecroft, S., Harrison, S. and Anderson, K., 2015. Rock glaciers as water stores in the Bolivian Andes: An assessment of their hydrological importance. Arctic, Antarctic, and Alpine Research, 47(1): 89-98.

Rangecroft, S., Harrison, S., Anderson, K., Magrath, J., Castel, A. and Pacheco, P., 2013. Climate change and water resources in arid mountains: An example from the Bolivian Andes. Ambio, 42(7): 852-863.

Rangecroft, S., Harrison, S., Anderson, K., Magrath, J., Castel, A.P. and Pacheco, P., 2014. A first rock glacier inventory for the Bolivian Andes. Permafrost and Periglacial Processes, 25(4): 333-343.

Rangecroft, S., Suggitt, A.J., Anderson, K. and Harrison, S., 2016. Future climate warming and changes to mountain permafrost in the Bolivian Andes. Climatic Change, 137(1): 231-243.

Regmi, B.R. and Pandit, A., 2016. Classification of adaptation measures in criteria for evaluation: Case studies in the Gandaki River Basin, HI-AWARE Working Paper 6. HI-AWARE, Kathmandu.

Regmi, D., 2008. Rock Glacier distribution and the lower limit of discontinuous mountain permafrost in the Nepal Himalaya, Proceedings of the Ninth International Conference on Permafrost, Fairbanks, Alaska, pp. 1475-1480.

Ribolini, A., Chelli, A., Guglielmin, M. and Pappalardo, M., 2007. Relationships between glacier and rock glacier in the Maritime Alps, Schiantala Valley, Italy. Quaternary Research, 68(3): 353-363.

Ribolini, A., Guglielmin, M., Fabre, D., Bodin, X., Marchisio, M., Sartini, S., Spagnolo, M. and Schoeneich, P., 2010. The internal structure of rock glaciers and recently deglaciated slopes as revealed by geoelectrical tomography: Insights on permafrost and recent glacial evolution in the Central and Western Alps (Italy-France). Quaternary Science Reviews, 29(3-4): 507-521.

Richards, B.W.M., Benn, D.I., Owen, L.A., Rhodes, E.J. and Spencer, J.Q., 2000. Timing of late Quaternary glaciations south of Mount Everest in the Khumbu Himal, Nepal. GSA Bulletin, 112(10): 1621-1632.

Roer, I., Haeberli, W., Avian, M., Kaufmann, V., Delaloye, R., Lambiel, C. and Kääb, A., 2008. Observations and Considerations on Destabilizing Active Rock Glaciers in the European Alps, Ninth International Conference on Permafrost, Fairbanks, Alaska, pp. 1505-1510.

Roer, I., Kääb, A. and Dikau, R., 2005. Rockglacier acceleration in the Turtmann valley (Swiss Alps): Probable controls. Norsk Geografisk Tidsskrift - Norwegian Journal of Geography, 59(2): 157-163.

Roer, I. and Nyenhuis, M., 2007. Rockglacier activity studies on a regional scale: Comparison of geomorphological mapping and photogrammetric monitoring. Earth Surface Processes and Landforms, 32(12): 1747-1758.

Rogger, M., Chirico, G.B., Hausmann, H., Krainer, K., Brückl, E., Stadler, P. and Blöschl, G., 2017. Impact of mountain permafrost on flow path and runoff response in a high alpine catchment. Water Resources Research, 53(2): 1288-1308.

Rosenwinkel, S., 2018. Rock Glaciers and Natural Dams in Central Asia, Universität Potsdam, 203 pp.

Roudnitska, S., Charvet, R., Ribeyre, C. and Favreaux, B.L., 2016. Les glaciers-rocheux De Savoie: Inventaire, cartographie et risques associés - rapport provisoire. In: Office National des Forets Service de Restauration des Terrains en Montagne, Chambery.

Rounce, D.R. and McKinney, D.C., 2014. Debris thickness of glaciers in the Everest area (Nepal Himalaya) derived from satellite imagery using a nonlinear energy balance model. The Cryosphere, 8(4): 1317-1329.

Rowan, A.V., 2017. The 'Little Ice Age' in the Himalaya: A review of glacier advance driven by Northern Hemisphere temperature change. The Holocene, 27(2): 292-308.

Rowan, A.V., Egholm, D.L., Quincey, D.J. and Glasser, N.F., 2015. Modelling the feedbacks between mass balance, ice flow and debris transport to predict the response to climate change of debris-covered glaciers in the Himalaya. Earth and Planetary Science Letters, 430: 427-438.

Rudolph, E.M., Meiklejohn, K.I., Hansen, C.D., Hedding, D.W. and Nel, W., 2018. Rock glaciers in the Jutulsessen, Dronning Maud Land, East Antarctica. Polish Polar Research, 39(1): 1-17.

Salerno, F., Guyennon, N., Thakuri, S., Viviano, G., Romano, E., Vuillermoz, E., Cristofanelli, P., Stocchi, P., Agrillo, G., Ma, Y. and Tartari, G., 2015. Weak precipitation, warm winters and springs impact glaciers of south slopes of Mt. Everest (central Himalaya) in the last 2 decades (1994-2013). Cryosphere, 9(3): 1229-1247.

Salvador-Franch, F., Pérez-Sánchez, J., Salvà-Catarineu, M. and Gómez-Ortiz, A., 2016. Inventory and spatial distribution of rock glaciers in the Eastern Pyrenees: Paleoenvironmental implications. Geophysical Research Abstracts, 18: EGU2016-16284.

Sasaki, O., Noguchi, O., Zhang, Y., Hirabayashi, Y. and Kanae, S., 2016. A global high-resolution map of debris on glaciers derived from multi-temporal ASTER images, The Cryosphere Discuss. Copernicus Publications, pp. 1-24.

Sattler, K., Anderson, B., Mackintosh, A., Norton, K. and de Róiste, M., 2016. Estimating permafrost distribution in the maritime Southern Alps, New Zealand, based on climatic conditions at rock glacier sites. Frontiers in Earth Science, 4.

Scapozza, C., Lambiel, C., Bozzini, C., Mari, S. and Conedera, M., 2014. Assessing the rock glacier kinematics on three different timescales: A case study from the southern Swiss Alps. Earth Surface Processes and Landforms, 39(15): 2056-2069.

Scapozza, C., Lambiel, C., Gex, P. and Reynard, E., 2011. Prospection géophysique multi-méthodes du pergélisol alpin dans le Sud des Alpes suisses (Multi-method geophysical prospecting of alpine permafrost in the southern Swiss Alps) (in French). Géomorphologie: relief, processus, environnement, 17(1): 15-32.

Schaffer, N., MacDonell, S., Réveillet, M., Yáñez, E. and Valois, R., 2019. Rock glaciers as a water resource in a changing climate in the semiarid Chilean Andes. Regional Environmental Change.

Schauwecker, S., Rohrer, M., Huggel, C., Kulkarni, A., Ramanathan, A.L., Salzmann, N., Stoffel, M. and Brock, B., 2015. Remotely sensed debris thickness mapping of Bara Shigri Glacier, Indian Himalaya. Journal of Glaciology, 61(228): 675-688.

Scherler, D., Bookhagen, B. and Strecker, M.R., 2011. Spatially variable response of Himalayan glaciers to climate change affected by debris cover. Nature Geoscience, 4(3): 156-159.

Schmid, M.O., Baral, P., Gruber, S., Shahi, S., Shrestha, T., Stumm, D. and Wester, P., 2015. Assessment of permafrost distribution maps in the Hindu Kush Himalayan region using rock glaciers mapped in Google Earth. The Cryosphere, 9(6): 2089-2099.

Schmidt, S. and Nüsser, M., 2012. Changes of high altitude glaciers from 1969 to 2010 in the Trans-Himalayan Kang Yatze Massif, Ladakh, Northwest India. Arctic, Antarctic, and Alpine Research, 44(1): 107-121.

Schneider, S., Daengeli, S., Hauck, C. and Hoelzle, M., 2013. A spatial and temporal analysis of different periglacial materials by using geoelectrical, seismic and borehole temperature data at Murtèl–Corvatsch, Upper Engadin, Swiss Alps. Geographica Helvetica, 68: 265-280.

Schoeneich, P., Bodin, X., Echelard, T., Kaufmann, V., Kellerer-Pirklbauer, A., Krysiecki, J.M. and Lieb, G.K., 2015. Velocity changes of rock glaciers and induced hazards. Engineering Geology for Society and Territory, Vol 1: Climate Change and Engineering Geology, 223-227 pp.

Schrott, L., 1996. Some geomorphological-hydrological aspects of rock glaciers in the Andes (San Juan, Argentina). Zeitschrift fur Geomorphologie, Supplementband, 104: 161-173.

Scott, C.A., Zhang, F., Mukherji, A., Immerzeel, W., Mustafa, D. and Bharati, L., 2019. Water in the Hindu Kush Himalaya. In: P. Wester, A. Mishra, A. Mukherji and A.B. Shrestha (Editors), The Hindu Kush Himalaya Assessment: Mountains, Climate Change, Sustainability and People. Springer International Publishing, Cham, pp. 257-299.

Scott, W.J., Sellmann, P.V. and Hunter, J.A., 1990. Geophysics in the study of permafrost. In: S. Ward (Editor), Geotechnical and Environmental Geophysics. Society of Exploration Geophysics, Tulsa, pp. 355-384.

Scotti, R., Brardinoni, F., Alberti, S., Frattini, P. and Crosta, G.B., 2013. A regional inventory of rock glaciers and protalus ramparts in the central Italian Alps. Geomorphology, 186: 136-149.

Scotti, R., Crosta, G.B. and Villa, A., 2017. Destabilisation of creeping permafrost: The Plator rock glacier case study (Central Italian Alps). Permafrost and Periglacial Processes, 28(1): 224-236.

Searle, M.P., Simpson, R.L., Law, R.D., Parrish, R.R. and Waters, D.J., 2003. The structural geometry, metamorphic and magmatic evolution of the Everest massif, High Himalaya of Nepal–South Tibet. Journal of the Geological Society, 160(3): 345.

Seligman, Z.M., 2009. Rock-glacier distribution, activity, and movement, northern Absaroka and Beartooth ranges, MT, USA, University of Montana, Missoula, MT, 63 pp.

Selley, H., Harrison, S., Glasser, N., Wündrich, O., Colson, D. and Hubbard, A., 2018. Rock glaciers in central Patagonia. Geografiska Annaler: Series A, Physical Geography: 1-15.

Seppi, R., Carton, A., Zumiani, M., Dall'Amico, M., Zampedri, G. and Rigon, R., 2012. Inventory, distribution and topographic features of rock glaciers in the southern region of the Eastern Italian Alps (Trentino). Geografia Fisica e Dinamica Quaternaria, 35(2): 185-197.

Seppi, R., Zanoner, T., Carton, A., Bondesan, A., Francese, R., Carturan, L., Zumiani, M., Giorgi, M. and Ninfo, A., 2015. Current transition from glacial to periglacial processes in the Dolomites (South-Eastern Alps). Geomorphology, 228: 71-86.

Serrano, E., Juan de Sanjose, J. and Jose Gonzalez-Trueba, J., 2010. Rock glacier dynamics in marginal periglacial environments. Earth Surface Processes and Landforms, 35(11): 1302-1314.

Shannon, S., Smith, R., Wiltshire, A., Payne, T., Huss, M., Betts, R., Caesar, J., Koutroulis, A., Jones, D. and Harrison, S., 2019. Global glacier volume projections under high-end climate change scenarios. The Cryosphere, 13(1): 325-350.

Sharma, E., Molden, D., Rahman, A., Khatiwada, Y.R., Zhang, L., Singh, S.P., Yao, T. and Wester, P., 2019. Introduction to the Hindu Kush Himalaya Assessment. In: P. Wester, A. Mishra, A. Mukherji and A.B. Shrestha (Editors), The Hindu Kush Himalaya Assessment: Mountains, Climate Change, Sustainability and People. Springer International Publishing, Cham, pp. 1-16.

Shrestha, A.B., Agrawal, N.K., Alfthan, B., Bajracharya, S.R., Maréchal, J. and van Oort, B., 2015. The Himalayan Climate and Water Atlas: Impact of climate change on water resources in five of Asia's major river basins. ICIMOD, GRID-Arendal and CICERO.

Shrestha, A.B. and Aryal, R., 2011. Climate change in Nepal and its impact on Himalayan glaciers. Regional Environmental Change, 11(1): 65-77.

Shrestha, A.B. and Joshi, S.P., 2011. Snow Cover and Glacier Change Study in Nepalese Himalaya Using Remote Sensing and Geographic Information System. Journal of Hydrology and Meteorology, 6(1): 11.

Shrestha, A.B., Wake, C.P., Dibb, J.E. and Mayewski, P.A., 2000. Precipitation fluctuations in the Nepal Himalaya and its vicinity and relationship with some large scale climatological parameters. International Journal of Climatology, 20(3): 317-327.

Shrestha, M.L., 2000. Interannual variation of summer monsoon rainfall over Nepal and its relation to Southern Oscillation Index. Meteorology and Atmospheric Physics, 75(1): 21-28.

Shroder, J.F., Bishop, M.P., Copland, L. and Sloan, V.F., 2000. Debris-covered glaciers and rock glaciers in the Nanga Parbat Himalaya, Pakistan. Geografiska Annaler: Series A, Physical Geography, 82(1): 17-31.

Shukla, A. and Ali, I., 2016. A hierarchical knowledge-based classification for glacier terrain mapping: A case study from Kolahoi Glacier, Kashmir Himalaya. Annals of Glaciology, 57(71): 1-10.

Shukla, A., Arora, M.K. and Gupta, R.P., 2010. Synergistic approach for mapping debris-covered glaciers using optical–thermal remote sensing data with inputs from geomorphometric parameters. Remote Sensing of Environment, 114(7): 1378-1387.

Smith, M.W., Carrivick, J.L. and Quincey, D.J., 2016. Structure from motion photogrammetry in physical geography. Progress in Physical Geography: Earth and Environment, 40(2): 247-275.

Smith, T. and Bookhagen, B., 2018. Changes in seasonal snow water equivalent distribution in High Mountain Asia (1987 to 2009). Science Advances, 4(1): e1701550.

Sneed, E.D. and Folk, R.L., 1958. Pebbles in the Lower Colorado River, Texas a study in particle morphogenesis. The Journal of Geology, 66(2): 114-150.

Sollid, J.L. and Sørbel, L., 1992. Rock glaciers in Svalbard and Norway. Permafrost and Periglacial Processes, 3(3): 215-220.

Sorg, A., Huss, M., Rohrer, M. and Stoffel, M., 2014a. The days of plenty might soon be over in glacierized Central Asian catchments. Environmental Research Letters, 9(10): 104018.

Sorg, A., Kääb, A., Roesch, A., Bigler, C. and Stoffel, M., 2015. Contrasting responses of Central Asian rock glaciers to global warming. Scientific Reports, 5: 8228.

Sorg, A., Mosello, B., Shalpykova, G., Allan, A., Hill Clarvis, M. and Stoffel, M., 2014b. Coping with changing water resources: The case of the Syr Darya river basin in Central Asia. Environmental Science & Policy, 43: 68-77.

Soruco, A., Vincent, C., Rabatel, A., Francou, B., Thibert, E., Sicart, J.E. and Condom, T., 2015. Contribution of glacier runoff to water resources of La Paz city, Bolivia (16° S). Annals of Glaciology, 56(70): 147-154.

Springman, S.M., Arenson, L.U., Yamamoto, Y., Maurer, H., Kos, A., Buchli, T. and Derungs, G., 2012. Multidisciplinary investigations on three rock glaciers in the swiss alps: Legacies and future perspectives. Geografiska Annaler: Series A, Physical Geography, 94(2): 215-243.

Stine, M., 2013. Clyde Wahrhaftig and Allan Cox (1959) Rock glaciers in the Alaska Range. Bulletin of the Geological Society of America 70(4): 383–436. Progress in Physical Geography, 37(1): 130-139.

Strozzi, T., Kääb, A. and Frauenfelder, R., 2004. Detecting and quantifying mountain permafrost creep from in situ inventory, space-borne radar interferometry and airborne digital photogrammetry. International Journal of Remote Sensing, 25(15): 2919-2931.

Tenthorey, G., 1992. Perennial névés and the hydrology of rock glaciers. Permafrost and Periglacial Processes, 3(3): 247-252.

Tenthorey, G., 1994. Hydrologie liee aux glaciers rocheux, Haut-Val De Réchy (Nax, VS). Bulletin de Murithienne, 112: 97-116.

Thies, H., Nickus, U., Mair, V., Tessadri, R., Tait, D., Thaler, B. and Psenner, R., 2007. Unexpected response of high alpine lake waters to climate warming. Environmental Science & Technology, 41(21): 7424-7429.

Thies, H., Nickus, U., Tolotti, M., Tessadri, R. and Krainer, K., 2013. Evidence of rock glacier melt impacts on water chemistry and diatoms in high mountain streams. Cold Regions Science and Technology, 96: 77-85.

Thompson, W.F., 1962. Preliminary Notes on the Nature and Distribution of Rock Glaciers Relative to True Glaciers and Other Effects of the Climate on the Ground in North America, Symposium at Obergurgl. International Association of Scientific Hydrology Publication Obergurgl, Austria, pp. 212-219.

Triglav-Čekada, M., Barkorič, B., Ferk, M. and Zorn, M., 2016. Nationwide aerial laser scanning reveals relict rock glaciers and protalus ramparts in Slovenia. The Cryosphere Discuss., 2016: 1-17.

Udmale, P., Ishidaira, H., Thapa, B. and Shakya, N., 2016. The Status of Domestic Water Demand: Supply Deficit in the Kathmandu Valley, Nepal. Water, 8(5): 196.

USGS, 2015. https://lpdaac.usgs.gov/sites/default/files/public/measures/docs/NASA_SRTM_V3.pdf, Accessed 25/08/2016.

Uxa, T. and Mida, P., 2017. Rock glaciers in the Western and High Tatra Mountains, Western Carpathians. Journal of Maps, 13(2): 844-857.

Vaughan, D.G., Comiso, J.C., Allison, I., Carrasco, J., Kaser, G., Kwok, R., Mote, P., Murray, T., Paul, F., Ren, J., Rignot, E., Solomina, O., Steffen, K. and Zhang, T., 2013. Observations: Cryosphere. In: T.F. Stocker, D. Qin, G.-K. Plattner, M. Tignor, S.K. Allen, J. Boschung, A. Nauels, Y. Xia, V. Bex and P.M. Midgley (Editors), Climate Change 2013: The Physical Science Basis. Contribution of Working Group I to the Fifth Assessment Report of the Intergovernmental Panel on Climate Change. Cambridge University Press, Cambridge, United Kingdom and New York, NY, USA, pp. 317–382.

Villarroel, C.D., Tamburini Beliveau, G., Forte, A.P., Monserrat, O. and Morvillo, M., 2018. DInSAR for a regional inventory of active rock glaciers in the Dry Andes Mountains of Argentina and Chile with Sentinel-1 data. Remote Sensing, 10(10): 1588.

Viviroli, D., Archer, D.R., Buytaert, W., Fowler, H.J., Greenwood, G.B., Hamlet, A.F., Huang, Y., Koboltschnig, G., Litaor, M.I., López-Moreno, J.I., Lorentz, S., Schädler, B., Schreier, H., Schwaiger, K., Vuille, M. and Woods, R., 2011. Climate change and mountain water resources: Overview and recommendations for research, management and policy. Hydrology and Earth System Sciences, 15(2): 471-504.

Viviroli, D., Dürr, H.H., Messerli, B., Meybeck, M. and Weingartner, R., 2007. Mountains of the world, water towers for humanity: Typology, mapping, and global significance. Water Resources Research, 43(7): 1-13.

Viviroli, D. and Weingartner, R., 2004. The hydrological significance of mountains: From regional to global scale. Hydrology and Earth System Sciences, 8(6): 1017-1030.

von Wakonigg, H., 1996. Unterkühlte schutthalden (Undercooled talus) (in German). Arbeiten aus dem Institut für Geographie der Karl-Franzens-Universität Graz, 33: 209-223.

Vuille, M., Francou, B., Wagnon, P., Juen, I., Kaser, G., Mark, B.G. and Bradley, R.S., 2008. Climate change and tropical Andean glaciers: Past, present and future. Earth-Science Reviews, 89(3–4): 79-96.

Wagner, T., Pauritsch, M. and Winkler, G., 2016. Impact of relict rock glaciers on spring and stream flow of alpine watersheds: Examples of the Niedere Tauern Range, Eastern Alps (Austria). Austrian Journal of Earth Sciences, 109(1): 84-98.

Wahrhaftig, C. and Cox, A., 1959. Rock glaciers in the Alaska range. Geological Society of America Bulletin, 70(4): 383-436.

Wang, X., Liu, L., Zhao, L., Wu, T., Li, Z. and Liu, G., 2016. Mapping and inventorying active rock glaciers in the Northern Tien Shan (China) using satellite SAR interferometry. The Cryosphere Discuss., 2016: 1-36.

Wang, X., Liu, L., Zhao, L., Wu, T., Li, Z. and Liu, G., 2017. Mapping and inventorying active rock glaciers in the northern Tien Shan of China using satellite SAR interferometry. The Cryosphere, 11(2): 997-1014.

Watson, C.S., Carrivick, J. and Quincey, D., 2015. An improved method to represent DEM uncertainty in glacial lake outburst flood propagation using stochastic simulations. Journal of Hydrology, 529, Part 3: 1373-1389.

Watson, C.S., Quincey, D.J., Carrivick, J.L. and Smith, M.W., 2016. The dynamics of supraglacial ponds in the Everest region, central Himalaya. Global and Planetary Change, 142: 14-27.

Watson, C.S., Quincey, D.J., Carrivick, J.L., Smith, M.W., Rowan, A.V. and Richardson, R., 2018. Heterogeneous water storage and thermal regime of supraglacial ponds on debris-covered glaciers. Earth Surface Processes and Landforms, 43(1): 229-241.

Wayne, W.J., 1981. Ice segregation as an origin for lenses of non-glacial ice in "ice-cemented" rock glaciers. Journal of Glaciology, 27(97): 506-510.

Weekes, A.A., Torgersen, C.E., Montgomery, D.R., Woodward, A. and Bolton, S.M., 2015. Hydrologic response to valley-scale structure in alpine headwaters. Hydrological Processes, 29(3): 356-372.

Westoby, M.J., Brasington, J., Glasser, N.F., Hambrey, M.J. and Reynolds, J.M., 2012. 'Structure-from-Motion' photogrammetry: A low-cost, effective tool for geoscience applications. Geomorphology, 179: 300-314.

Whalley, W.B., 1974. Origin of rock glaciers. Journal of Glaciology, 13(68): 323-324.

Whalley, W.B. and Azizi, F., 1994. Rheological models of active rock glaciers: Evaluation, critique and a possible test. Permafrost and Periglacial Processes, 5(1): 37-51.

Whalley, W.B. and Azizi, F., 2003. Rock glaciers and protalus landforms: Analogous forms and ice sources on Earth and Mars. Journal of Geophysical Research: Planets, 108(E4).

Whalley, W.B. and Martin, H.E., 1992. Rock glaciers: II models and mechanisms. Progress in Physical Geography, 16(2): 127-186.

Whalley, W.B., Martin, H.E. and Gellatly, A.F., 1986. The problem of "hidden" ice in glacier mapping. Annals of Glaciology, 8: 181-183.

Whalley, W.B., Palmer, C., Hamilton, S. and Gordon, J., 1994. Ice exposures in rock glaciers. Journal of Glaciology, 40(135): 427-429.

Whalley, W.B. and Palmer, C.F., 1998. A glacial interpretation for the origin and formation of the Marinet Rock Glacier, Alpes Maritimes, France. Geografiska Annaler: Series A, Physical Geography, 80(3-4): 221-236.

Whalley, W.B., Palmer, C.F., Hamilton, S.J. and Martin, H.E., 1995. An assessment of rock glacier sliding using seventeen years of velocity data: Nautardalur Rock Glacier, North Iceland. Arctic and Alpine Research, 27(4): 345-351.

White, S.E., 1976. Rock glaciers and block fields, review and new data. Quaternary Research, 6(1): 77-97.

Wicky, J. and Huack, C., 2017. Numerical modelling of convective heat transport by air flow in permafrost talus slopes. The Cryosphere, 11(3): 1311-1325.

Wigmore, O. and Mark, B., 2018. High altitude kite mapping: Evaluation of kite aerial photography (KAP) and structure from motion digital elevation models in the Peruvian Andes. International Journal of Remote Sensing, 39(15-16): 4995-5015.

Williams, M.W., Knauf, M., Caine, N., Liu, F. and Verplanck, P.L., 2006. Geochemistry and source waters of rock glacier outflow, Colorado Front Range. Permafrost and Periglacial Processes, 17(1): 13-33.

Winkler, G., Pauritsch, M., Wagner, T. and Kellerer-Pirklbauer, A., 2016a. Reliktische blockgletscher als grundwasserspeicher in alpinen einzugsgebieten der Niederen Tauern. Berichte der wasserwirtschaftlichen planung Steiermark. Band, 87: 134 (in German).

Winkler, G., Wagner, T., Pauritsch, M., Birk, S., Kellerer-Pirklbauer, A., Benischke, R., Leis, A., Morawetz, R., Schreilechner, M.G. and Hergarten, S., 2016b. Identification and assessment of groundwater flow and storage components of the relict Schoneben rock glacier, Niedere Tauern Range, Eastern Alps (Austria). Hydrogeology Journal, 24(4): 937-953.

Winkler, S. and Lambiel, C., 2018. Age constraints of rock glaciers in the Southern Alps/New Zealand – Exploring their palaeoclimatic potential. The Holocene, 28(5): 778-790.

Wirz, V., Gruber, S., Purves, R.S., Beutel, J., Gärtner-Roer, I., Gubler, S. and Vieli, A., 2016. Short-term velocity variations at three rock glaciers and their relationship with meteorological conditions. Earth Surface Dynamics, 4(1): 103-123.

Wouter, B., Simon, M., Luis, A., Bert De, B., Carlos, O., Marcos, V., Carolina, T. and Koen, M.J.V., 2017. Glacial melt content of water use in the tropical Andes. Environmental Research Letters, 12(11): 114014.

Yu, L. and Gong, P., 2012. Google Earth as a virtual globe tool for Earth science applications at the global scale: Progress and perspectives. International Journal of Remote Sensing, 33(12): 3966-3986.

Zalazar, L., Ferri, L., Castro, M., Gargantini, H., Giménez, M., Pitte, P., Ruiz, L., Masiokas, M. and Villalba, R., 2017. Glaciares de Argentina: Resultados preliminares del Inventario Nacional de Glaciares. Revista de Glaciares y Ecosistemas de Montaña, 2: 13-22.

Zech, R., Zech, M., Kubik, P.W., Kharki, K. and Zech, W., 2009. Deglaciation and landscape history around Annapurna, Nepal, based on 10Be surface exposure dating. Quaternary Science Reviews, 28(11): 1106-1118.

Zhou, H., Aizen, E. and Aizen, V., 2017. Seasonal snow cover regime and historical change in Central Asia from 1986 to 2008. Global and Planetary Change, 148: 192-216.